VOLUME: 18 NO: 4 YEAR: 2021

Indexed in PMC and Web of Science
ULAKBİM / TR Dizin, Scopus

ISSN: 1304-530X

TURKISH JOURNAL OF PHARMACEUTICAL SCIENCES

An Official Journal of the Turkish Pharmacists' Association, Academy of Pharmacy

TURKISH
JOURNAL OF PHARMACEUTICAL SCIENCES

TURKISH
JOURNAL OF PHARMACEUTICAL SCIENCES

TURKISH JOURNAL OF PHARMACEUTICAL SCIENCES

AIMS AND SCOPE

The Turkish Journal of Pharmaceutical Sciences is the only scientific periodical publication of the Turkish Pharmacists' Association and has been published since April 2004.
Turkish Journal of Pharmaceutical Sciences journal is regularly published 6 times in a year (February, April, June, August, October, December). The issuing body of the journal is Galenos Yayinevi/Publishing House level.
The aim of Turkish Journal of Pharmaceutical Sciences is to publish original research papers of the highest scientific and clinical value at an international level. The target audience includes specialists and professionals in all fields of pharmaceutical sciences.
The editorial policies are based on the "Recommendations for the Conduct, Reporting, Editing, and Publication of Scholarly Work in Medical Journals (ICMJE Recommendations)" by the International Committee of Medical Journal Editors (2013, archived at http://www.icmje.org/) rules.

Editorial Independence

Turkish Journal of Pharmaceutical Sciences is an independent journal with independent editors and principles and has no commerical relationship with the commercial product, drug or pharmaceutical company regarding decisions and review processes upon articles.

ABSTRACTED/INDEXED IN

PubMed Central
Web of Science-Emerging Sources Citation Index (ESCI)
SCOPUS SJR
TÜBİTAK/ULAKBİM TR Dizin
Directory of Open Access Journals (DOAJ)
ProQuest
Chemical Abstracts Service (CAS)
EBSCO
EMBASE
GALE
Index Copernicus
Analytical Abstracts
International Pharmaceutical Abstracts (IPA)
Medicinal & Aromatic Plants Abstracts (MAPA)
British Library
CSIR INDIA
GOALI
Hinari
OARE
ARDI
AGORA
Türkiye Atıf Dizini
Türk Medline
UDL-EDGE
J- Gate
Idealonline
CABI

OPEN ACCESS POLICY

This journal provides immediate open access to its content on the principle that making research freely available to the public supports a greater global exchange of knowledge.
Open Access Policy is based on the rules of the Budapest Open Access Initiative (BOAI) http://www.budapestopenaccessinitiative.org/. By "open access" to peer-reviewed research literature, we mean its free availability on the public internet, permitting any users to read, download, copy, distribute, print, search, or link to the full texts of these articles, crawl them for indexing, pass them as data to software, or use them for any other lawful purpose, without financial, legal, or technical barriers other than those inseparable from gaining access to the internet itself. The only constraint on reproduction and distribution, and the only role for copyright in this domain, should be to give authors control over the integrity of their work and the right to be properly acknowledged and cited.

CORRESPONDENCE ADDRESS

All correspondence should be directed to the Turkish Journal of Pharmaceutical Sciences Editorial Board

Post Address: Turkish Pharmacists' Association, Mustafa Kemal Mah 2147.Sok No:3 06510 Çankaya/Ankara, TURKEY
Phone: +90 (312) 409 81 00
Fax: +90 (312) 409 81 09
Web Page: http://turkjps.org
E-mail: teb@teb.org.tr

PERMISSIONS

Requests for permission to reproduce published material should be sent to the publisher.
Publisher: Erkan Mor
Adress: Molla Gürani Mah. Kaçamak Sok. 21/1 Fındıkzade, Fatih, Istanbul, Turkey
Telephone: +90 212 621 99 25
Fax: +90 212 621 99 27
Web page: http://www.galenos.com.tr/en
E-mail: info@galenos.com.tr

ISSUING BODY CORRESPONDING ADDRESS

Issuing Body : Galenos Yayınevi
Address: Molla Gürani Mah. Kaçamak Sk. No: 21/1, 34093 İstanbul, Turkey
Phone: +90 212 621 99 25 Fax: +90 212 621 99 27
E-mail: info@galenos.com.tr

MATERIAL DISCLAIMER

The author(s) is (are) responsible for the articles published in the JOURNAL.
The editor, editorial board and publisher do not accept any responsibility for the articles.

TURKISH
JOURNAL OF PHARMACEUTICAL SCIENCES

INSTRUCTIONS TO AUTHORS

Turkish Journal of Pharmaceutical Sciences journal is published 6 times (February, April, June, August, October, December) per year and publishes the following articles:

• Research articles

• Reviews (only upon the request or consent of the Editorial Board)

• Preliminary results/Short communications/Technical notes/Letters to the Editor in every field of pharmaceutical sciences.

The publication language of the journal is English.

The Turkish Journal of Pharmaceutical Sciences does not charge any article submission or processing charges.

A manuscript will be considered only with the understanding that it is an original contribution that has not been published elsewhere.

The Journal should be abbreviated as "Turk J Pharm Sci" when referenced.

The scientific and ethical liability of the manuscripts belongs to the authors and the copyright of the manuscripts belongs to the Journal. Authors are responsible for the contents of the manuscript and accuracy of the references. All manuscripts submitted for publication must be accompanied by the Copyright Transfer Form [copyright transfer]. Once this form, signed by all the authors, has been submitted, it is understood that neither the manuscript nor the data it contains have been submitted elsewhere or previously published and authors declare the statement of scientific contributions and responsibilities of all authors.

Experimental, clinical and drug studies requiring approval by an ethics committee must be submitted to the JOURNAL with an ethics committee approval report including approval number confirming that the study was conducted in accordance with international agreements and the Declaration of Helsinki (revised 2013) (http://www.wma.net/en/30publications/10policies/b3/). The approval of the ethics committee and the fact that informed consent was given by the patients should be indicated in the Materials and Methods section. In experimental animal studies, the authors should indicate that the procedures followed were in accordance with animal rights as per the Guide for the Care and Use of Laboratory Animals (http://oacu.od.nih.gov/regs/guide/guide.pdf) and they should obtain animal ethics committee approval.

Authors must provide disclosure/acknowledgment of financial or material support, if any was received, for the current study.

If the article includes any direct or indirect commercial links or if any institution provided material support to the study, authors must state in the cover letter that they have no relationship with the commercial product, drug, pharmaceutical company, etc. concerned; or specify the type of relationship (consultant, other agreements), if any.

Authors must provide a statement on the absence of conflicts of interest among the authors and provide authorship contributions.

All manuscripts submitted to the journal are screened for plagiarism using the 'iThenticate' software. Results indicating plagiarism may result in manuscripts being returned or rejected.

The Review Process

This is an independent international journal based on double-blind peer-review principles. The manuscript is assigned to the Editor-in-Chief, who reviews the manuscript and makes an initial decision based on manuscript quality and editorial priorities. Manuscripts that pass initial evaluation are sent for external peer review, and the Editor-in-Chief assigns an Associate Editor. The Associate Editor sends the manuscript to at least two reviewers (internal and/or external reviewers). The Associate Editor recommends a decision based on the reviewers' recommendations and returns the manuscript to the Editor-in-Chief. The Editor-in-Chief makes a final decision based on editorial priorities, manuscript quality, and reviewer recommendations. If there are any conflicting recommendations from reviewers, the Editor-in-Chief can assign a new reviewer.

The scientific board guiding the selection of the papers to be published in the Journal consists of elected experts of the Journal and if necessary, selected from national and international authorities. The Editor-in-Chief, Associate Editors may make minor corrections to accepted manuscripts that do not change the main text of the paper.

In case of any suspicion or claim regarding scientific shortcomings or ethical infringement, the Journal reserves the right to submit the manuscript to the supporting institutions or other authorities for investigation. The Journal accepts the responsibility of initiating action but does not undertake any responsibility for an actual investigation or any power of decision.

The Editorial Policies and General Guidelines for manuscript preparation specified below are based on "Recommendations for the Conduct, Reporting, Editing, and Publication of Scholarly Work in Medical Journals (ICMJE Recommendations)" by the International Committee of Medical Journal Editors (2013, archived at http://www.icmje.org/).

Preparation of research articles, systematic reviews and meta-analyses must comply with study design guidelines:

CONSORT statement for randomized controlled trials (Moher D, Schultz KF, Altman D, for the CONSORT Group. The CONSORT statement revised recommendations for improving the quality of reports of parallel group randomized trials. JAMA 2001; 285: 1987-91) (http://www.consort-statement.org/);

PRISMA statement of preferred reporting items for systematic reviews and meta-analyses (Moher D, Liberati A, Tetzlaff J, Altman DG, The PRISMA Group. Preferred Reporting Items for Systematic Reviews and Meta-Analyses: The PRISMA Statement. PLoS Med 2009; 6(7): e1000097.) (http://www.prisma-statement.org/);

STARD checklist for the reporting of studies of diagnostic accuracy (Bossuyt PM, Reitsma JB, Bruns DE, Gatsonis CA, Glasziou PP, Irwig LM, et al., for the STARD Group. Towards complete and accurate reporting of studies of diagnostic accuracy: the STARD initiative. Ann Intern Med 2003;138:40-4.) (http://www.stard-statement.org/);

STROBE statement, a checklist of items that should be included in reports of observational studies (http://www.strobe-statement.org/);

MOOSE guidelines for meta-analysis and systemic reviews of observational studies (Stroup DF, Berlin JA, Morton SC, et al. Meta-analysis of observational studies in epidemiology: a proposal for reporting Meta-analysis of observational Studies in Epidemiology (MOOSE) group. JAMA 2000; 283: 2008-12).

GENERAL GUIDELINES

Manuscripts can only be submitted electronically through the Journal Agent website (http://journalagent.com/tjps/) after creating an account. This system allows online submission and review.

TURKISH
JOURNAL OF PHARMACEUTICAL SCIENCES

INSTRUCTIONS TO AUTHORS

Format: Manuscripts should be prepared using Microsoft Word, size A4 with 2.5 cm margins on all sides, 12 pt Arial font and 1.5 line spacing.

Abbreviations: Abbreviations should be defined at first mention and used consistently thereafter. Internationally accepted abbreviations should be used; refer to scientific writing guides as necessary.

Cover letter: The cover letter should include statements about manuscript type, single-Journal submission affirmation, conflict of interest statement, sources of outside funding, equipment (if applicable), for original research articles.

ETHICS COMMITTEE APPROVAL

The editorial board and our reviewers systematically ask for ethics committee approval from every research manuscript submitted to the Turkish Journal of Pharmaceutical Sciences. If a submitted manuscript does not have ethical approval, which is necessary for every human or animal experiment as stated in international ethical guidelines, it must be rejected on the first evaluation.

Research involving animals should be conducted with the same rigor as research in humans; the Turkish Journal of Pharmaceutical Sciences asks original approval document to show implements the 3Rs principles. If a study does not have ethics committee approval or authors claim that their study does not need approval, the study is consulted to and evaluated by the editorial board for approval.

SIMILARITY

The Turkish Journal of Pharmaceutical Sciences is routinely looking for similarity index score from every manuscript submitted before evaluation by the editorial board and reviewers. The journal uses iThenticate plagiarism checker software to verify the originality of written work. There is no acceptable similarity index; but, exceptions are made for similarities less than 15 %.

REFERENCES

Authors are solely responsible for the accuracy of all references.

In-text citations: References should be indicated as a superscript immediately after the period/full stop of the relevant sentence. If the author(s) of a reference is/are indicated at the beginning of the sentence, this reference should be written as a superscript immediately after the author's name. If relevant research has been conducted in Turkey or by Turkish investigators, these studies should be given priority while citing the literature.

Presentations presented in congresses, unpublished manuscripts, theses, Internet addresses, and personal interviews or experiences should not be indicated as references. If such references are used, they should be indicated in parentheses at the end of the relevant sentence in the text, without reference number and written in full, in order to clarify their nature.

References section: References should be numbered consecutively in the order in which they are first mentioned in the text. All authors should be listed regardless of number. The titles of Journals should be abbreviated according to the style used in the Index Medicus.

Reference Format

Journal: Last name(s) of the author(s) and initials, article title, publication title and its original abbreviation, publication date, volume, the inclusive page numbers. Example: Collin JR, Rathbun JE. Involutional entropion: a review with evaluation of a procedure. Arch Ophthalmol. 1978;96:1058-1064.

Book: Last name(s) of the author(s) and initials, book title, edition, place of publication, date of publication and inclusive page numbers of the extract cited.

Example: Herbert L. The Infectious Diseases (1st ed). Philadelphia; Mosby Harcourt; 1999:11;1-8.

Book Chapter: Last name(s) of the author(s) and initials, chapter title, book editors, book title, edition, place of publication, date of publication and inclusive page numbers of the cited piece.

Example: O'Brien TP, Green WR. Periocular Infections. In: Feigin RD, Cherry JD, eds. Textbook of Pediatric Infectious Diseases (4th ed). Philadelphia; W.B. Saunders Company;1998:1273-1278.

Books in which the editor and author are the same person: Last name(s) of the author(s) and initials, chapter title, book editors, book title, edition, place of publication, date of publication and inclusive page numbers of the cited piece. Example: Solcia E, Capella C, Kloppel G. Tumors of the exocrine pancreas. In: Solcia E, Capella C, Kloppel G, eds. Tumors of the Pancreas. 2nd ed. Washington: Armed Forces Institute of Pathology; 1997:145-210.

TABLES, GRAPHICS, FIGURES, AND IMAGES

All visual materials together with their legends should be located on separate pages that follow the main text.

Images: Images (pictures) should be numbered and include a brief title. Permission to reproduce pictures that were published elsewhere must be included. All pictures should be of the highest quality possible, in

JPEG format, and at a minimum resolution of 300 dpi.

Tables, Graphics, Figures: All tables, graphics or figures should be enumerated according to their sequence within the text and a brief descriptive caption should be written. Any abbreviations used should be defined in the accompanying legend. Tables in particular should be explanatory and facilitate readers' understanding of the manuscript, and should not repeat data presented in the main text.

MANUSCRIPT TYPES

Original Articles

Clinical research should comprise clinical observation, new techniques or laboratories studies. Original research articles should include title, structured abstract, key words relevant to the content of the article, introduction, materials and methods, results, discussion, study limitations, conclusion references, tables/figures/images and acknowledgement sections. Title, abstract and key words should be written in both Turkish and English. The manuscript should be formatted in accordance with the above-mentioned guidelines and should not exceed 16 A4 pages.

Title Page: This page should include the title of the manuscript, short title, name(s) of the authors and author information. The following descriptions should be stated in the given order:

TURKISH
JOURNAL OF PHARMACEUTICAL SCIENCES

INSTRUCTIONS TO AUTHORS

1. Title of the manuscript (Turkish and English), as concise and explanatory as possible, including no abbreviations, up to 135 characters

2. Short title (Turkish and English), up to 60 characters

3. Name(s) and surname(s) of the author(s) (without abbreviations and academic titles) and affiliations

4. Name, address, e-mail, phone and fax number of the corresponding author

5. The place and date of scientific meeting in which the manuscript was presented and its abstract published in the abstract book, if applicable

Abstract: A summary of the manuscript should be written in both Turkish and English. References should not be cited in the abstract. Use of abbreviations should be avoided as much as possible; if any abbreviations are used, they must be taken into consideration independently of the abbreviations used in the text. For original articles, the structured abstract should include the following sub-headings:

Objectives: The aim of the study should be clearly stated.

Materials and Methods: The study and standard criteria used should be defined; it should also be indicated whether the study is randomized or not, whether it is retrospective or prospective, and the statistical methods applied should be indicated, if applicable.

Results: The detailed results of the study should be given and the statistical significance level should be indicated.

Conclusion: Should summarize the results of the study, the clinical applicability of the results should be defined, and the favorable and unfavorable aspects should be declared.

Keywords: A list of minimum 3, but no more than 5 key words must follow the abstract. Key words in English should be consistent with "Medical Subject Headings (MESH)" (www.nlm.nih.gov/mesh/MBrowser.html). Turkish key words should be direct translations of the terms in MESH.

Original research articles should have the following sections:

Introduction: Should consist of a brief explanation of the topic and indicate the objective of the study, supported by information from the literature.

Materials and Methods: The study plan should be clearly described, indicating whether the study is randomized or not, whether it is retrospective or prospective, the number of trials, the characteristics, and the statistical methods used.

Results: The results of the study should be stated, with tables/figures given in numerical order; the results should be evaluated according to the statistical analysis methods applied. See General Guidelines for details about the preparation of visual material.

Discussion: The study results should be discussed in terms of their favorable and unfavorable aspects and they should be compared with the literature. The conclusion of the study should be highlighted.

Study Limitations: Limitations of the study should be discussed. In addition, an evaluation of the implications of the obtained findings/results for future research should be outlined.

Conclusion: The conclusion of the study should be highlighted.

Acknowledgements: Any technical or financial support or editorial contributions (statistical analysis, English/Turkish evaluation) towards the study should appear at the end of the article.

References: Authors are responsible for the accuracy of the references. See General Guidelines for details about the usage and formatting required.

Review Articles

Review articles can address any aspect of clinical or laboratory pharmaceuticals. Review articles must provide critical analyses of contemporary evidence and provide directions of or future research. Most review articles are commissioned, but other review submissions are also welcome. Before sending a review, discussion with the editor is recommended.

Reviews articles analyze topics in depth, independently and objectively. The first chapter should include the title in Turkish and English, an unstructured summary and key words. Source of all citations should be indicated. The entire text should not exceed 25 pages (A4, formatted as specified above).

TURKISH
JOURNAL OF PHARMACEUTICAL SCIENCES

CONTENTS

TURKISH
JOURNAL OF PHARMACEUTICAL SCIENCES

CONTENTS

Turk J Pharm Sci 2021;18(4):385-387
DOI: 10.4274/tjps.galenos.2021.44389

LETTER TO EDITOR

Enthalpy-Entropy Compensation in the Gelatinization of *Cyperus* Starch

Cyperus Nişastasının Jelatinizasyonunda Entalpi-Entropi Kompensasyonu

Jonghoon KANG[1]*, Luz GREEN[2], Kwajalen HALL[3]

[1]Department of Biology, Valdosta State University, Valdosta, Georgia, USA
[2]Department of Psychology, Valdosta State University, Valdosta, Georgia, USA
[3]Department of Chemistry, Valdosta State University, Valdosta, Georgia, USA

Key words: Enthalpy, entropy, thermodynamics, starch, gelatinization
Anahtar kelimeler: Entalpi, entropi, termodinamik, nişasta, jelatinizasyon

Dear Editor,

A recent paper by Olayemi et al.[1] examined various properties of starch cross-linked with citric acid to improve its physicochemical characteristics. This modified starch has considerable applications in food and pharmaceutical industries. The citric acid used in the study was derived from fruit wastes (orange peels)-an approach followed in green chemistry. We agree with the authors that the green chemistry approach is valuable from an environmental perspective because of the various benefits it confers, such as safe operability, faster processing, easy scalability, and less energy consumption.[2]

Of the physicochemical characteristics of starch, the authors measured the thermodynamic parameters of gelatinization. These parameters are used to examine the effects of sampling time point of the liquid substrates of orange peels, which served as a source of citric acid for starch modification. The authors prepared four types of starch: TS0, TS1, TS2, and TS3. TS0 is native starch without any cross-linking, whereas TS1, TS2, and TS3 are starch types cross-linked with citric acid in the liquid substrates of orange peels, which were produced by natural solid-state fermentation on day 5, 10, and 15, respectively. The authors performed differential scanning calorimetry to characterize the gelatinization of the four sets of starch in terms of thermodynamics. They measured enthalpy (ΔH) and three characteristic temperatures, onset, peak, and conclusion, of gelatinization.

On the basis of their data, the value of ΔH was positive for all four samples, indicating that starch gelatinization is an endergonic process. Although ΔH provides valuable information about starch gelatinization, another major thermodynamic parameter, entropy (ΔS), was not discussed in their paper. In this letter, we present our analysis of their results to provide the numerical values of ΔS in the gelatinization of various types of starch.

Starch gelatinization is a type of phase transition,[3] and ΔS in a phase transition can be determined by the following equation:[4]

$$\Delta S = \frac{\Delta H}{T_m} \qquad \text{equation (1)}$$

Where T_m is the melting temperature, the mid-point temperature in phase transition.[3] Although information about T_m was not available in the original paper, the peak temperature in starch gelatinization was found to be in considerable agreement with T_m.[3] Therefore, we used the peak temperature reported in the original paper as a substitute for T_m in our analysis. Using the numerical values of ΔH and the peak temperature in the gelatinization of the four types of starch in equation (1), we obtained ΔS for each type.

*Correspondence: jkang@valdosta.edu, Phone: 1-229-333-7140, ORCID-ID: orcid.org/0000-0001-5594-6141
Received: 26.04.2021, Accepted: 05.05.2021

Figure 1 shows the resulting values of ΔS and ΔH for each type of starch. The graph clearly illustrates two features of starch gelatinization. First, both native and cross-linked types of starch had positive values of ΔS. This implies that starch gelatinization is an entropy-driven process ($\Delta S > 0$), regardless of the modification status. Second, ΔH exhibited a wide variation among the starch types. For instance, the difference of ΔH between TS1 and TS2 was >1500 J/g; however, the difference in their peak temperature was <20°C. This is a consequence of the compensatory behavior between enthalpy and entropy, which is referred to as enthalpy-entropy compensation.[5] Linear regression identified a numerical relationship between enthalpy and entropy (R^2: 0.9982):

$$\Delta S = \alpha \times \Delta H + \beta \qquad \text{equation (2)}$$

Where the values of α and β and their standard errors were $2.4\text{x}10^{-3}\pm7.3\text{x}10^{-5}$ and $4.7\text{x}10^{-2}\pm0.11$, respectively.

This phenomenon has been observed in various weakly coupled systems such as the melting of human hair, which is made of keratin proteins.[5] Our analysis elucidated that modification of starch through cross-linking with citric acid can result in a significant variation in both ΔH and ΔS in gelatinization (Figure 1). However, owing to the enthalpy-entropy compensation, the variation in the peak temperature was highly limited to 17°C.[1]

Another feature evident in the results of the original paper[1] is the inconsistency between the duration of fermentation of orange peels and the thermodynamic parameters (Figure 2). Although the authors proposed a plausible mechanism for the inconsistency, it clearly demonstrated a unique feature of green chemistry: minimum human intervention on a system results in unpredictable fluctuations in the physical and chemical variables of the system. One of the chemical variables of the orange peel substrates examined in the original paper[1] was the pH of the orange peel liquid substrates. Although the pH itself was inconsistent with fermentation duration (Figure 2), we recognized a significant correlation between the thermodynamic parameters of gelatinization and pH (Figure 3) as the R^2 value in both cases was 0.9951. The correlation of enthalpy and entropy with pH is shown in equations (3) and (4), respectively:

$$\Delta H = a_1 \exp\left(-b_1 \times pH\right) \qquad \text{equation (3)}$$

$$\Delta S = a_2 \exp\left(-b_2 \times pH\right) \qquad \text{equation (4)}$$

Where $a_1=11.6\times10^4\pm4.6\times10^4$, $b_1=2.0\pm0.2$, $a_2=243.9\pm92.5$, and $b_2=1.9\pm0.2$. Equations (3) and (4) together elucidate a mathematical reason for the enthalpy-entropy compensation in starch gelatinization (Figure 1). Normalized enthalpy and entropy showed a similar pH dependency: The decreasing factors were 2 and 1.9 for enthalpy and entropy, respectively. The t-test indicated that the difference between b_1 and b_2

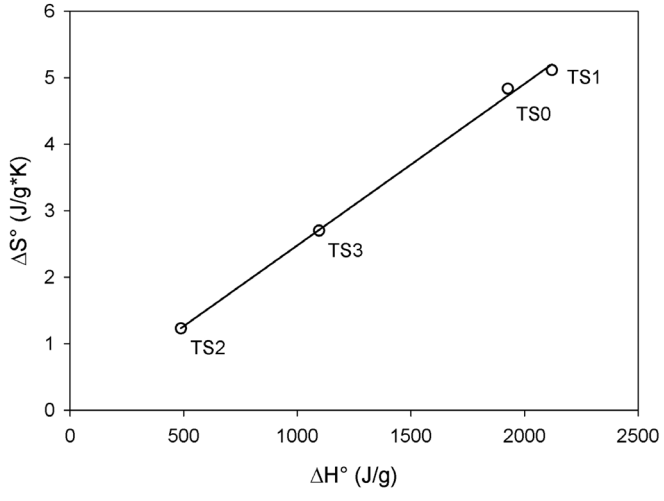

Figure 1. Enthalpy-entropy compensation in starch gelatinization. Solid line is a plot of equation (2). Linear regression was performed using SigmaPlot (Systat Software, San Jose, CA)

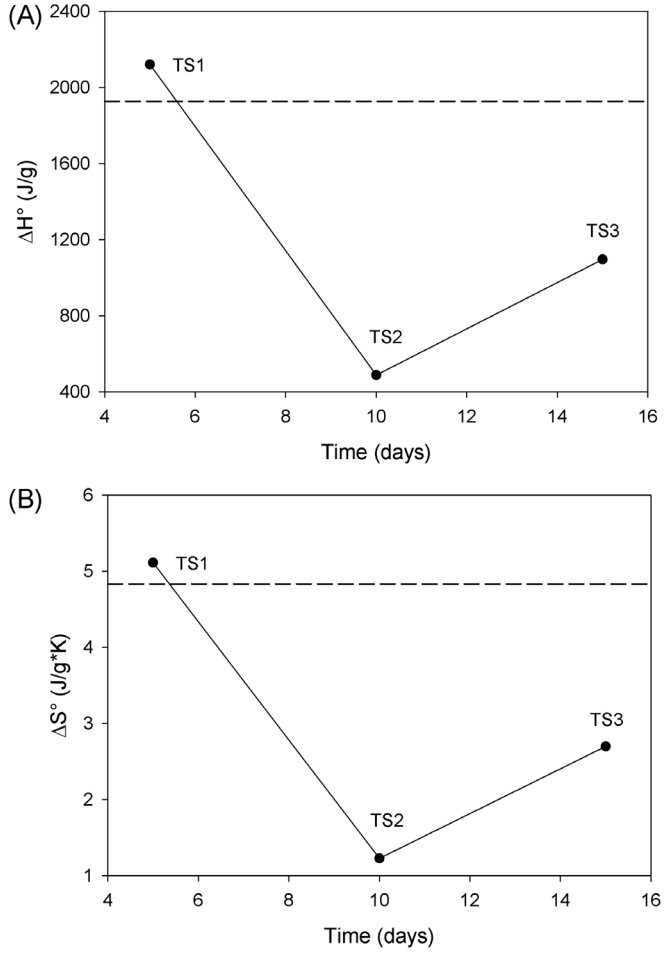

Figure 2. Correlation of enthalpy (A) and entropy (B) with time. The correlation coefficient between enthalpy and time was -0.621 (p=0.573) and between entropy and time was -0.615 (p=0.578). In both cases, no correlation was noted between any pairs of the parameters shown in the figures as p was >0.05. The dashed line in each plot represents the corresponding value of the native starch (TS0)

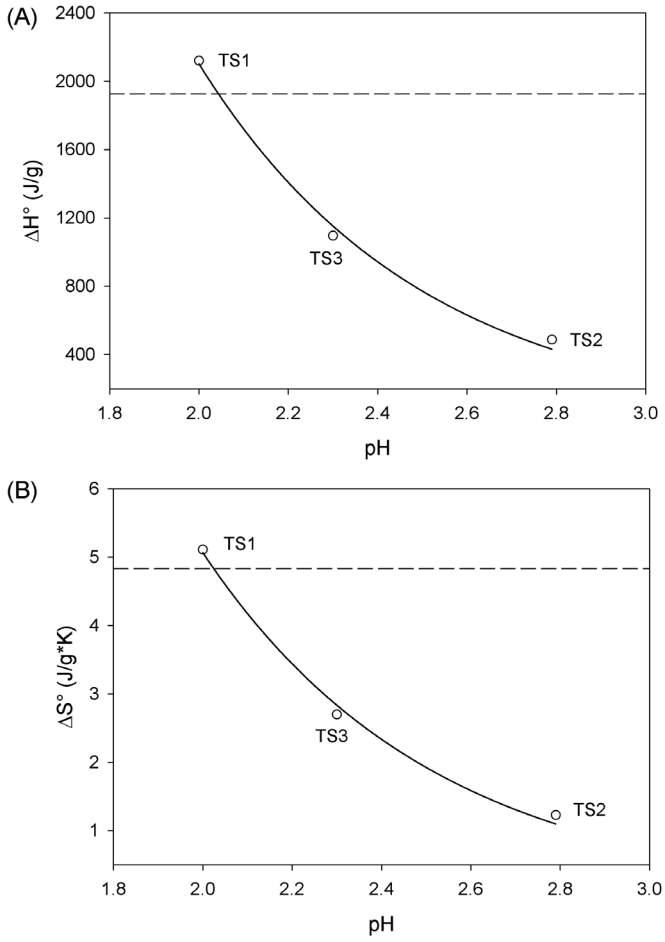

Figure 3. Correlation of pH with enthalpy (A) and entropy (B). Solid lines are the best fits of each case: Equation (3) in (A) and equation (4) in (B). The dashed line in each plot represents the value of the native starch (TS0)

was not statistically significant (t: 0.254, df: 2, p=0.823), strongly suggesting that enthalpy and entropy have a similar pH dependency. This numerical similarity is responsible for the high degree of correlation between enthalpy and entropy (Figure 1).

In conclusion, cross-linking of starch with citric acid at various pH values shows an enthalpy-entropy compensation. This compensation may be attributed to the similar quantitative relationship of pH with enthalpy and entropy. Finally, we would like to correct an error in the original paper that the unit of enthalpy of gelatinization is J/g and not J/g*K.

ACKNOWLEDGMENTS

Jonghoon KANG is grateful to James Nienow of the Department of Biology at Valdosta State University for insightful discussions.

Conflict of interest: No conflict of interest was declared by the authors. The authors are solely responsible for the content and writing of this paper.

REFERENCES

1. Olayemi B, Isimi CY, Ekere K, Johnson Isaac A, Okoh JE, Emeje M. Green Preparation of Citric Acid Crosslinked Starch for Improvement of Physicochemical Properties of *Cyperus* Starch. Turk J Pharm Sci. 2021;18:34-43.
2. González-Rivera J, Spepi A, Ferrari C, Duce C, Longo I, Falconieri D, Piras A, Tinè MR. Novel configurations for a citrus waste based biorefinery: from solventless to simultaneous ultrasound and microwave assisted extraction. Green Chem. 2016;18 6482-6492.
3. Shiotsubo T, Takahashi K. Differential thermal analysis of potato starch gelatinization. Agric Biol Chem. 1984;48:9-17.
4. Chang R. Physical Chemistry for the Chemical and Biological Sciences. Sausalito; University Science Books; 2000:142-144.
5. Cowan ML, Kang J. Enthalpy-Entropy Compensation in the Melting of Human Hair. Int J Trichology. 2019;11:141-142.

Turk J Pharm Sci 2021;18(4):388-397
DOI: 10.4274/tjps.galenos.2020.33341

ORIGINAL ARTICLE

Preparation of *Sterculia foetida*-pullulan-Based Semi-interpenetrating Polymer Network Gastroretentive Microspheres of Amoxicillin Trihydrate and Optimization by Response Surface Methodology

Sterculia foetida-pullulan Esaslı Yarı İç İçe Geçmeli Polimer Ağı Gastroretentif Amoksisilin Trihidrat Mikrosferlerinin Hazırlanması ve Yanıt Yüzey Metodolojisi ile Optimizasyonu

Jayshri HADKE, Shagufta KHAN*

Institute of Pharmaceutical Education and Research, Department of Pharmaceutics, Wardha, India

ABSTRACT

Objectives: In this study, a novel *Sterculia foetida* and pullulan-based semi-interpenetrating polymer network gastroretentive microsphere formulation was prepared using the emulsion crosslinking method and optimized by central composite design.

Materials and Methods: The effects of the amounts of glutaraldehyde, *S. foetida*, and pullulan on the percent drug entrapment efficiency (EE), percent mucoadhesion at 12 h, and percent *in vitro* drug release at 12 h were optimized. The microspheres were characterized using scanning electron microscopy, fourier transform infrared spectroscopy, and differential scanning calorimetry.

Results: The formulation containing 4% v/v glutaraldehyde, 8.28% w/v pullulan, and 2.14% w/v *S. foetida* had 88.75±1.18% EE, 80.43±1.2% drug release at 12 h, and 81.73±1.50% mucoadhesion at 12 h, which was considered optimum and was used in an *in vivo* radiographic study.

Conclusion: Semi-interpenetrating polymer network microspheres loaded with amoxicillin trihydrate were successfully prepared using *S. foetida* and pullulan. The prolonged retention of microspheres in the stomach with sustained drug release could effectively act against *Helicobacter pylori* reservoirs in the stomach and improve the therapeutic effect of amoxicillin trihydrate against *H. pylori*.

Key words: *Sterculia foetida*, pullulan, semi-interpenetrating polymeric network, central composite design, *in vivo* radiographic study

ÖZ

Amaç: Bu araştırmada, yeni bir *Sterculia foetida* ve pullulan bazlı yarı iç polimer polimer ağ gastroretentif mikrosfer formülasyonu, emülsiyon çapraz bağlama yöntemiyle hazırlanmış ve merkezi kompozit tasarım ile optimize edilmiştir.

Gereç ve Yöntemler: Glutaraldehit, *S. foetida* ve pullulan miktarlarının ilaç tutma etkinliği yüzdesi (DEE), 12 saatte yüzde mukoadezyon ve 12 saatte *in vitro* ilaç salım yüzdesi üzerindeki etkileri optimize edilmiştir. Mikro küreler ayrıca taramalı elektron mikroskobu, fourier dönüşümlü kızılötesi spektroskopisi ve diferansiyel tarama kalorimetrisi ile de tanımlanmıştır.

Bulgular: %4 h/h gluteraldehit, %8,28 a/h pullulan ve %2,14 a/h *S. foetida* içeren formülasyon, %88,75±1,18 EE sahip olarak bulunmuştur. On iki saat içinde %80,43±1,2 ilaç salımı ve 12 saat içinde %81,73±1,50 mukoza yapışması vermiştir ki bu optimum olarak kabul edilmiş ve *in vivo* radyografik çalışma için kullanılmıştır.

Sonuç: Çalışmadan amoksisilin trihidrat yüklü yüklü iç içe geçen polimer ağ mikrosferlerinin *S. foetida* ve pullulan zamkı kullanılarak başarıyla hazırlandığı sonucuna varılmıştır. Mide içerisinde sürekli ilaç salımı ile mikrokürelerin uzun süre tutulması, midedeki *Helicobacter pylori* rezervuarına etkili bir şekilde davranabilir ve amoksisilin trihidratın *H. pylori*'ye karşı terapötik etkinliğini artırabilir.

Anahtar kelimeler: *Sterculia foetida*, pullulan, yarı iç içe geçen polimerik ağ, merkezi kompozit tasarım, *in vivo* radyografik inceleme

***Correspondence:** shaguftakhan17@rediffmail.com, **Phone:** +07152-240284, **ORCID-ID:** orcid.org/0000-0002-2827-7939

Received: 17.11.2019, **Accepted:** 14.01.2020

INTRODUCTION

Several disease conditions necessitate the development of controlled and targeted drug delivery systems. Pharmaceutical technology is continuously expanding to provide sustainable, continuous, and therapy-optimal drug levels in the circulation. Drugs whose absorption site is the upper gastrointestinal tract or those that have stability issues can benefit when formulated as mucoadhesive microspheres.[1] Mucoadhesive microspheres can adhere in a specific absorptive part of the gastrointestinal region, thereby improving the drug absorption rate and enhancing bioavailability. Additionally, the microsphere size allows them to remain entrapped in the stomach mucosal lining for an extended duration.

Due to their gastroretention, mucoadhesive microspheres may build up a high drug concentration in the stomach mucosa, which may help eradicate peptic ulcers caused by *Helicobacter pylori* infection.[2] Warren and Marshall indicated that *H. pylori* infection predominantly affects the gastrointestinal tract, causing stomach inflammation, duodenal ulcers, gastric ulcers, and gastric carcinoma. It is reported that *H. pylori* is responsible for 90-100% of duodenal ulcers and 60-90% of gastric ulcers in patients. A literature survey showed that *H. pylori* infection increases the likelihood of developing peptic ulcers, and 10-15% of individuals with *H. pylori* infection have high chances of developing peptic ulcers in their lifetime.[3]

Amoxicillin trihydrate is a semisynthetic antibiotic widely considered effective in the treatment of peptic ulcers caused by *H. pylori*. It is a major component of standard therapy and is used in combination with other antibiotics and antacids. Clinically, it is effective, but drug-related problems and increased antibiotic resistance have decreased the success rate of eradicating *H. pylori* with conventional therapies. Amoxicillin, an acid-soluble drug, dissolves immediately in the stomach and is rapidly absorbed; therefore, it is difficult to retain it in the stomach for long durations unless some rate-controlling means are employed to counter *H. pylori*. Once *H. pylori* is colonized in an acidic stomach environment, it penetrates the stomach's deeper mucus membrane, which is a bacterium niche, owing to its good flagellar motility. Furthermore, *H. pylori* can attach to lipids and carbohydrates present in the membrane, helping it adhere to the epithelial cells. Several studies and reviews recommended that local drug delivery works more effectively than systemically administered antibiotics to eradicate *H. pylori*. Therefore, for enhanced therapeutic efficacy, the formulation should release the drug near the stomach lining. Mucoadhesive microspheres can adhere to the gastric mucosa and release the drug constantly for longer periods to the infected cells. Therefore, they can be proven to be very effective against *H. pylori*.[4,5]

Natural hydrophilic polymers possess structural flexibility; thus, they can be applied in the preparation of oral controlled-release formulations that provide the required drug release profile.[6] *Sterculia foetida* is a medicinally important polysaccharide obtained in the form of exudates from *Sterculia urens*, a small-to-medium-sized bushy tree that belongs to the Sterculiaceae family. It fixes itself with water molecules, although not in a completely soluble form. It can swell, increasing its total volume in relation to dry mass, which is 60 times more than the original volume. It possesses a rhamnogalacturonan-type partially acetylated ramified structure, and its molecular weight is $16x10^3$ kDa. Chemically, it is composed of 55-60% unbiased monosaccharide units (galactose and rhamnose), 8% acetyl groups, and 37-0% acid residues (galacturonic and glucuronic acids). The core part of its structure is α-D-galacturonic acid and L-rhamnose units.[7] *S. foetida* has several potential commercial applications, primarily in the food and pharmaceutical industries. It is edible, odorless, and flavorless; thus, it is used as a food additive. As a result of its bioadhesive, non-toxic, non-immunogenic, non-mutagenic, and non-carcinogenic properties,[8,9] it is considered promising for the development of drug-loaded microspheres. Moreover, *S. foetida* exhibits swelling properties and can modify drug release from the polymeric matrix.[10] In a previous study, *S. foetida* was blended with pectin to produce a sustained-release carrier having floating ability and increasing gastric residence.[11]

Currently, for the pharmaceutical industry, *S. foetida* is a promising plant polysaccharide. It exhibits acid stability due to acetyl groups in its structure; it also possesses good swelling capacity and good mucoadhesive and biodegradable properties. Various studies have reported the use of *S. foetida* in the treatment of ulcers, irritable bowel syndrome, persistent colonic diseases, and improving glucose metabolism without adverse effects on mineral balance. Furthermore, many researchers have formulated interpenetrating polymer network (IPN) microspheres using polysaccharides and have reported their use for sustained drug delivery.[12]

Recently, increasing attention has been given to polysaccharides obtained from microorganisms and yeast. Pullulan is a neutral homopolysaccharide of glucose composed of repeating maltotriose residues connected by α-1.6 glycosidic bonds and some interspersed maltotetraose units produced by *Aureobasidium pullulans*. Its additional advantages include its biocompatibility, non-toxicity, non-immunogenicity, and non-carcinogenicity. Pullulan is also used as a binder, thickener, lubricant, and gelling agent. Because of its unique linkage pattern, it can capture biomolecules and has exceptional oxygen barrier properties, which increase the stability of these molecules with increased shelf-life. Pullulan is highly soluble in water; thus, it can be used as a drug carrier; however, it involves uncontrolled hydration and drug release-related issues, restricting its applications. The hydrophilicity of pullulan can be reduced by crosslinking it with an anionic polymer such as *S. foetida*. In addition, pullulan can be easily crosslinked using glutaraldehyde, and adding *S. foetida* increases its mechanical strength.[13]

The number of naturally occurring polysaccharides through the formation of IPNs improves mechanical strength and provides the desired release characteristics of the entrapped drug. Several IPNs have been reported thus far and include interactions between *Delonix regia* gum and sodium alginate,[14]

calcium pectinate and tamarind seed gum,[15] carrageenan-alginate,[16] locust bean gum and alginate,[17] guar gum and chitosan,[18] and carboxymethyl xanthan and alginate.[19] However, no attempt has been made to formulate semi-IPN microspheres composed of pullulan with *S. foetida*. Therefore, in this study, *S. foetida*-pullulan-based semi-IPN microspheres were formulated for stomach-specific delivery of amoxicillin trihydrate that can provide good mechanical strength, prevent uncontrolled water uptake, and remain in the stomach to provide drug release over long periods for activity against *H. pylori.* It is proposed that *S. foetida* has antiulcer properties, which could act synergistically against *H. pylori* with amoxicillin trihydrate.

MATERIALS AND METHODS

Experimental part

Materials

Amoxicillin trihydrate was gifted by Ranbaxy Laboratories (Goregaon East, Mumbai, India). Pullulan, having a molecular weight of 200,000 Da, was procured from Kumar Organic Products Limited (Bangalore, India). *S. foetida* was gifted by Research Lab Fine Chem Industries (Mumbai, India); light liquid paraffin (LLP) was supplied by Hi-Media Laboratories Private Limited (Mumbai, India). Pioneer In-Organics (Delhi, India) supplied Span 80. Glutaraldehyde (25%, v/v) was procured from Merck Limited (Mumbai, India). Dichloromethane was obtained from Loba Chem. Private Limited (Mumbai, India). All chemicals used were of analytical grade.

Preparation of S. foetida–pullulan semi-IPN microspheres

The water-in-oil emulsification-crosslinking method was used to prepare *S. foetida*-pullulan-based semi-IPN microspheres containing amoxicillin trihydrate (ASP-MPs).[20] *S. foetida* and pullulan were hydrated in distilled water. First, the two polymeric solutions were homogenized together to obtain a uniform solution. The drug was incorporated into this polymeric solution, and the solution was uniformly mixed using a magnetic stirrer until a uniform drug-polymer mixture was obtained. Next, the drug-containing polymeric mixture with 1% w/v Span 80 was added gradually to LLP with constant stirring at 2.000 rpm for 10 min. After the formation of a a milky white emulsion, glutaraldehyde containing 0.5 mL of 1 N HCl was added gradually, and the resulting emulsion was stirred continuously for 2 h to obtain solid microspheres. The microspheres were then filtered and washed with dichloromethane to remove excess LLP and washed several times with water to remove unreacted glutaraldehyde. The resulting microspheres were then allowed to dry under vacuum at 40°C, and finally, they were stored in desiccators until further use.

Experimental design for optimizing the ASP-MP formulation

ASP-MPs were prepared and optimized using three factors and a three-level randomized central composite design to determine the effect of formulation variables on the prepared microspheres. The three independent variables, i.e., the volume of crosslinker glutaraldehyde (A), amount of pullulan (B), and amount of *S. foetida* (C), were varied at three levels (Table 1). The statistical trial design was generated and evaluated using Design-Expert version 12.0.3.0 software (Stat-Ease Inc., USA). Percent drug entrapment efficiency (DEE), cumulative percent drug release for 12 h, and percent mucoadhesion were selected as dependent variables. Design matrices showing the effect of the formulation variables on the studied response variables are shown in Table 2, and response surface plots are shown in Figure 1a-c. Optimization was performed by modeling the effect of independent variables on the responses using a quadratic mathematical model, as shown in equation

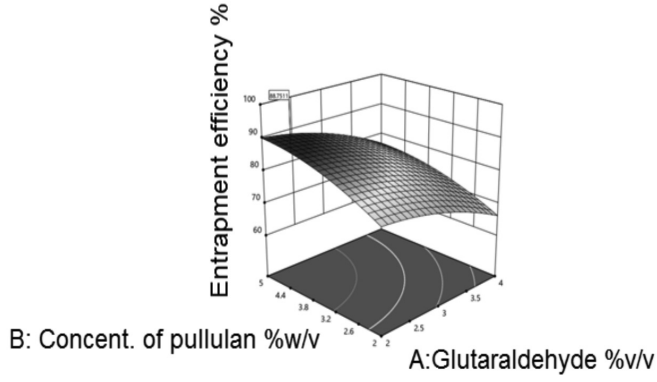

Figure 1a. 3D response surface plot graph showing the effect of pullulan and glutaraldehyde amount on percent DEE

DEE: Drug entrapment efficiency

Table 1. Coded levels of process variables used in the experiments

Independent variable	Level				
	1.68179	-1	0	+1	-1.68179
A- Glutraldehyde (% v/v)	9.3634	4	6	8	2.6364
B- Pullulan (% w/v)	12.0452	4	7	10	1.9546
C- *Sterculia foetida* (% v/v)	4.6818	2	3	4	1.3182
Dependent variables					
Y1	Entrapment efficiency in %	Maximize			
Y2	Drug release in 12 h in %	Maximize			
Y3	Mucoadhesion in %	Maximize			

1, and constraints on responses were maximum EE, maximum drug content, and maximum mucoadhesion.[21,22]

$$Y_o = b_o + b_1A + b_2B + b_3C + b_{12}AB + b_{13}AC + b_{23}BC + b_{11}A_2 + b_{22}B_2 + b_{33}C_2$$

equation (1)

where Y is the response; b_0 is the intercept; and A, B, and C are the independent formulation variables.

Characterization of ASP-MPs

Fourier-transform infrared spectroscopy (FTIR)

FTIR spectra of *S. foetida* gum, pullulan, amoxicillin trihydrate, and a physical mixture of *S. foetida* and pullulan with amoxicillin

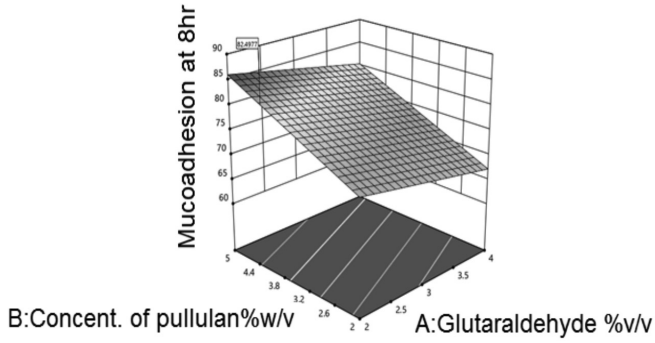

Figure 1b. 3D response surface plot graph showing the effect of pullulan and glutaraldehyde amount on percent mucoadhesion

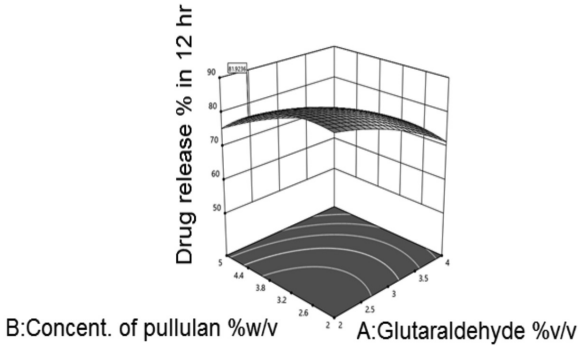

Figure 1c. 3D response surface plot graph showing the effect of pullulan and glutaraldehyde amount on percent drug release

Table 2. Design matrix and measured responses

Actual value of the independent variables						Responses		
Formulations	**Glutraldehyde % V/V (A)**	**Pullula % W/V (B)**	***Sterculia foetida* % W/V (C)**	**% EE**	**Drug content**	**% drug release at 12 hr**	**Mucoadhesion at 12 hr**	**Particle size**
APS-1	4	10	4	88.12±1.16	33.50±2.25	70.23±2.59	87.35±1.32	117.48±1.05
APS-2	4	10	2	84.53±1.18	30.52±2.82	78.56±1.79	83.32±1.87	111.75±0.76
APS-3	6	7	3	82.10±2.08	29.54±2.11	82.24±1.88	78.54±1.93	84.53±1.21
APS-4	8	10	2	72.15±1.70	25.36±1.17	68.86±1.98	80.54±2.28	94.73±1.28
APS-5	4	4	4	79.26±1.06	28.23±1.85	80.47±2.15	75.81±1.98	77.34±0.93
APS-6	4	4	2	73.60±1.67	26.13±1.83	89.41±1.99	68.51±1.77	69.94±1.14
APS-7	8	10	4	76.42±1.66	27.82±2.04	59.68±2.81	82.48±2.72	92.46±1.12
APS-8	9.36	7	3	63.49±1.69	20.43±1.78	64.63±1.23	69.24±2.53	60.70±0.82
APS-9	6	7	3	82.10±2.08	29.54±2.11	82.24±1.88	78.54±1.93	84.53±1.21
APS-10	6	7	3	82.10±2.08	29.54±2.11	82.24±1.88	78.54±1.93	84.53±1.21
APS-11	6	7	3	82.10±2.08	29.54±2.11	82.24±1.88	78.54±1.93	84.53±1.21
APS-12	6	7	4.6818	86.32±1.49	31.93±1.95	62.93±2.18	83.33±2.02	105.67±1.45
APS-13	6	1.9542	3	62.38±1.57	18.74±2.25	75.31±2.15	62.29±1.37	64.15±1.26
APS-14	6	7	1.3182	69.85±1.96	21.45±2.27	80.10±1.73	65.48±2.01	65.99±1.17
APS-15	2.62	7	3	87.69±2.65	32.56±2.21	84.59±2.46	79.63±1.76	96.76±0.72
APS-16	6	7	3	82.10±2.08	29.54±2.11	82.24±1.88	78.54±1.93	84.53±1.21
APS-17	6	7	3	82.10±2.08	29.54±2.11	82.24±1.88	78.54±1.93	84.53±1.21
APS-18	8	4	4	71.23±2.55	23.26±2.11	66.34±2.40	70.26±2.09	65.70±1.36
APS-19	8	4	2	60.37±1.85	16.64±2.06	72.90±2.26	60.78±2.13	57.99±1.53
APS-20	6	12.0453	3	88.24±2.46	34.80±2.20	60.32±2.09	81.16±1.42	121.90±1.38

Volume of aqueous phase was 100 mL, EE: Entrapment efficiency

trihydrate and ASP-MPs were obtained between 4.000 and 400 cm^{-1} using KBr pellets (FTIR-84005, Shimadzu Asia Pacific Pvt. Ltd. Singapore) (Figure 2).

Differential scanning calorimetry (DSC)

The thermal and crystalline properties of *S. foetida* gum, pullulan, and a physical mixture of *S. foetida* and pullulan with amoxicillin trihydrate and ASP-MPs were examined using DSC (Mettler Toledo AG, Analytical, Switzerland) at a heating rate of 10°C/min from 0°C to 400°C with continuous nitrogen purge at a rate of 50 mL/min (Figure 3).

X-ray diffraction (XRD)

XRD (Bruker model D8 advance theta/2theta) was conducted to study the crystalline properties of amoxicillin trihydrate upon entrapment in the microspheres. The radiation source was CuKα, at k¼1.5406 Å. The samples were spread over a low background sample holder (amorphous silica) and set in a goniometer. Scanning was performed at a scan speed of 5˚/min with increments at 0.02 and 2Θ from 0˚ to 80˚. The current and voltages were 40 mV and 35 mA, respectively (Figure 4).

Determination of particle size and surface morphology

The required quantity of microspheres was distributed in an insoluble solvent, and the suspension was diluted as needed. One drop of the suspension was placed on a glass slide and examined under a microscope; a digital picture was also taken (DMWBf model, Motic, China). The sample was placed on a piece of adhesive carbon tape set on a brass stub for scanning electron microscopy (SEM). The sample was then gold-coated using a sputtering unit (model: JFC1600, USA) for 10 s at 10 mA. Finally, the gold-coated sample was placed in an SEM chamber (Jeol, JSM 6390LA), and secondary electron images were recorded (Figure 5).

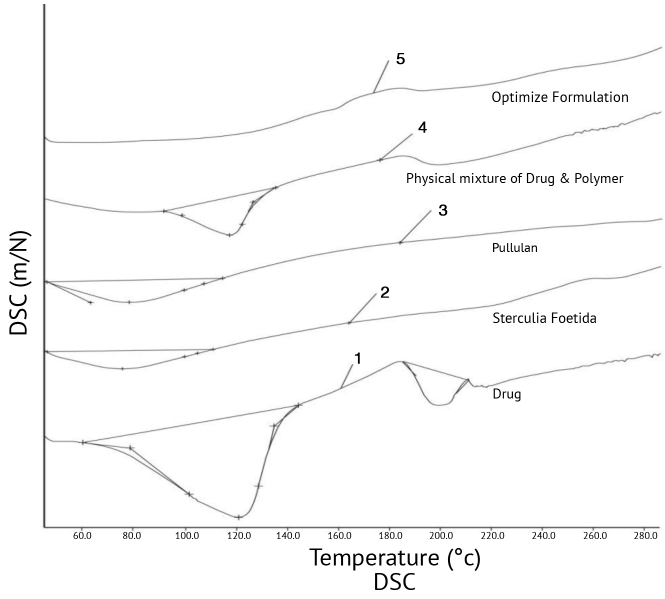

Figure 3. DSC thermogram of 1) pure drug, 2) *Sterculia foetida*, 3) pullulan, 4) physical mixture of drug and polymers, and 5) optimized formulation

DSC: Differential scanning calorimetry

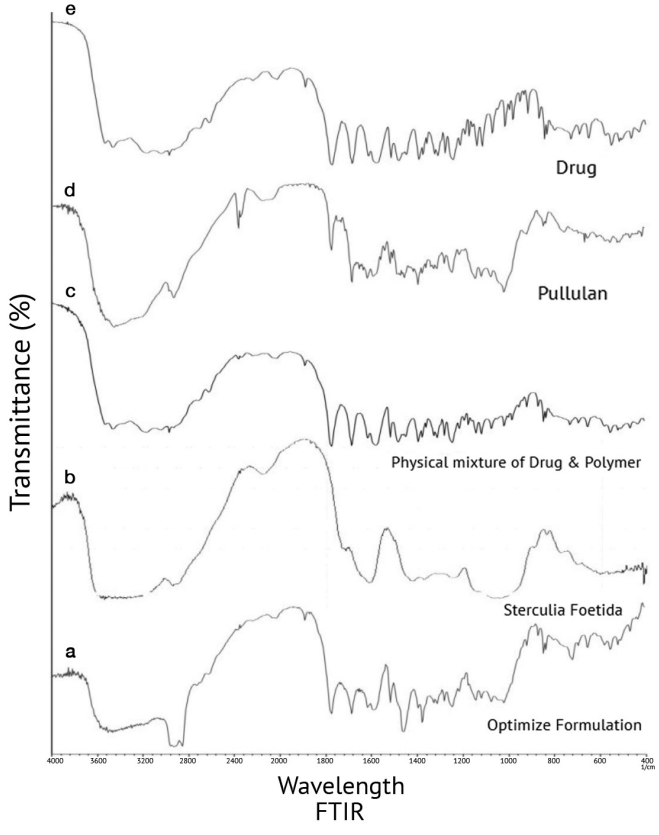

Figure 2. FTIR spectra of a) pure drug, b) pullulan, c) physical mixture of drug and polymers, d) *Sterculia foetida*, and e) optimized formulation

FTIR: Fourier-transform infrared spectroscopy

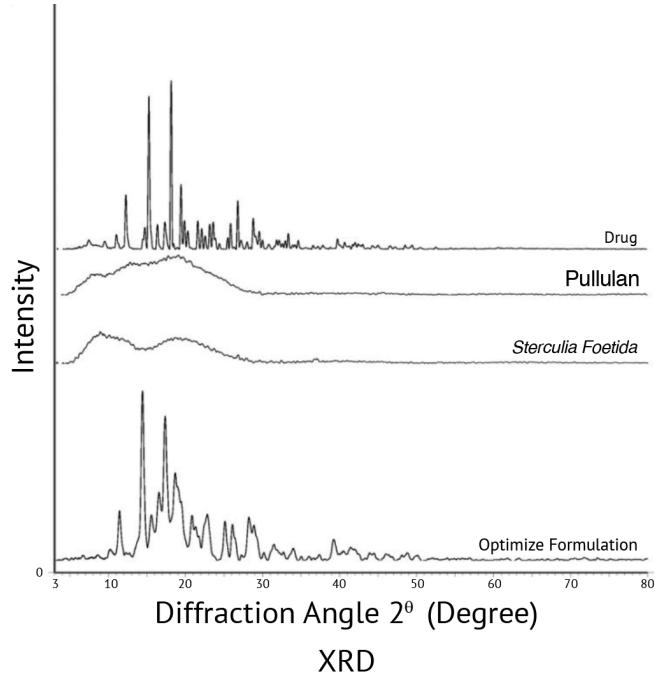

Figure 4. XRD pattern of a) pure drug, b) pullulan, c) *Sterculia foetida*, and d) optimized formulation

XRD: X-ray diffraction

Determination of percent drug loading and percent DEE

Fifty milligrams of microspheres were finely powdered and soaked in 50 mL of simulated gastrointestinal fluid [(SGF), pH 1.2] for 24 h. The resulting suspension was filtered, suitably diluted, and analyzed at 229 nm. Percent drug loading and DEE were then determined according to the following relationship:[23]

$$\% \text{ Drug loading} = \frac{\text{Amount of drug in microspheres}}{\text{Amount of microspheres}} \times 100$$

equation (2)

$$\text{DEE } (\%) = \frac{\text{Actual drug content in microspheres}}{\text{Theoretical drug content in microspheres}} \times 100$$

equation (3)

Evaluatin of mucoadhesive properties in vitro

Goat intestinal mucosa was used to study the mucoadhesive properties of semi-IPN microspheres. First, a dispersion of semi-IPN microspheres was sprayed on goat mucosa mounted on a glass slide. The glass slide was previously incubated in desiccators (90% relative humidity) for 20 min and then placed in the cell. Finally, the cell was attached to the outer assembly at an angle of 45˚. Next, SGF (pH 1.2) was circulated through the cell over the microspheres at a rate of 1 mL/min using a peristaltic pump. The washings were collected after fixed time intervals, and centrifuged and separated microspheres were dried at 40°C.

The weight of the washed microspheres was measured, and mucoadhesion (%) was calculated as follows:[23]

Percentage mucoadhesion=Qa-Ql × 100/Qa equation (4)

where Qa=weight of microspheres applied initially and Ql=weight of microspheres leached out.

In vitro drug release study

A type I USP dissolution apparatus (Electrolab, Mehsana, Gujrat, India) was used to measure the drug release in SGF (pH 1.2, 900 mL) at 37°C±0.5°C with a rotational speed of 100 rpm. Microspheres containing 500 mg of drug were placed in SGF. Every hour, 1 mL of the sample was suitably diluted and analyzed at 229 nm (Shimadzu/UV-1700, Japan). The aliquots withdrawn were replaced with drug-free buffer. Dissolution testing was performed for 12 h (Figure 6). Kinetic models such as the zero-order,[24] first-order,[25] Higuchi,[26] and Peppas[27] were used to explore the kinetics and mechanics of drug release.

In vivo radiographic study

To determine the location and extent of gastrointestinal transit, ASP-MPs were administered orally to rats and monitored using a radiological method. The Institutional Animal Ethics Committee approved the study (protocol no: 535/02/a/CPCSEA/S/Jan.2002). Six healthy albino Wistar rats (either sex, 400-500 g) were kept in individual cages in a sanitized room maintained at 27°C±0.5°C

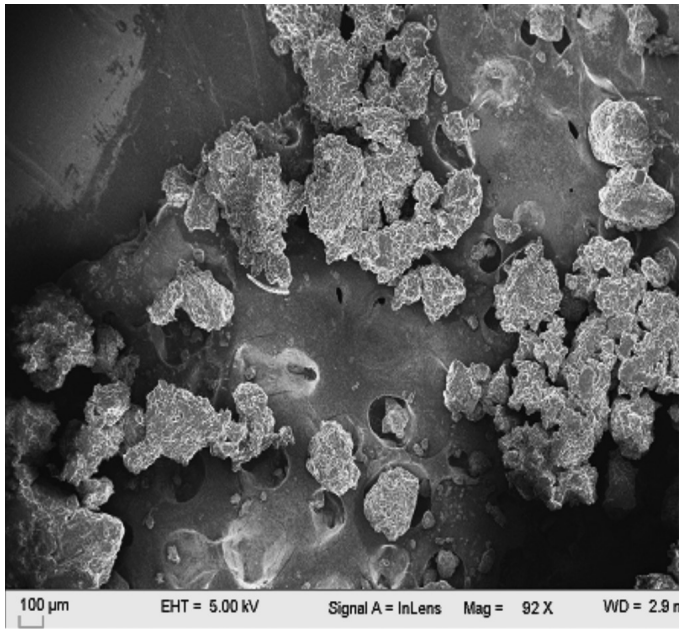

Figure 5. Scanning electron micrograph of optimized *Sterculia foetida*-pullulan microspheres loaded with amoxicillin trihydrate showing a rough surface

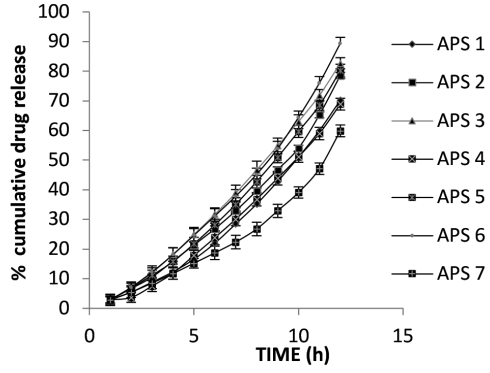

In vitro release profile of batches APS1-APS7

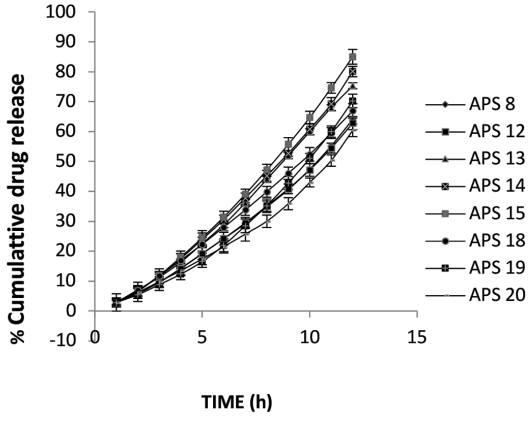

In vitro release profile of batches APS8-APS20

Figure 6. *In vitro* drug release profile of *Sterculia foetida*-pullulan microspheres loaded with amoxicillin trihydrate in simulated gastric fluid (pH 1.2) (mean ± SD; n=3)

SD: Standard deviation

at a 12 h light/dark cycle. Food was abstained for 12 h prior to the study, whereas water was allowed *ad libitum*. Radiopaque ASP-MPs were prepared by adding 50 mg of barium sulfate to the polymeric solution (the composition was the same as that of the optimized formulation) following the procedure used in the formulation of ASP-MPs. ASP-MPs were administered orally through the gastric tube along with 2 mL of water. The animals were subjected to fasting throughout the study (up to 12 h) with 1 mL of water allowed every hour. ASP-MPs were monitored in the gastric region of the rats at a predetermined time interval of 10 h using X-ray imaging (Siregraph-B, Siemens, Germany) (Figure 7).[28]

Statistical analysis

Statistical optimization of the formulations was conducted using Design-Expert® version 12.0.3.0 (Stat-Ease Inc.). Each measurement was performed in triplicate (n=3) and represented as mean ± standard deviation. Student's t-test was performed to compare the two groups.[29,30]

Stability testing

Stability testing of the optimized formulation was performed according to the ICH guidelines for 6 months.[31] The formulation was packed in laminated aluminum foil and placed in a stability chamber at 40°C±2°C and 75±5% relative humidity. The samples were examined at the end of 1, 3, and 6 months to check for significant differences in their mucoadhesion property, EE, and drug content. Differences were regarded as significant at $p<0.05$.

RESULTS AND DISCUSSION

Formulation of microspheres

In this study, ASP-MPs containing amoxicillin trihydrate were prepared using glutaraldehyde as a crosslinking agent.

a) 0 h **b) 10 h**

Figure 7. X-ray image of microspheres in the gastric region of rats

Pullulan is a highly water-soluble polymer; therefore, when it is used alone, it exhibits uncontrolled hydration, leading to instant release of high amounts of the drug. Therefore, to control hydration, *S. foetida* was coupled on a pullulan backbone with the help of glutaraldehyde. Water-soluble glutaraldehyde was selected as the crosslinking agent because of its ability to facilitate the formation of linkages from hydroxyl groups. The -CHO groups of glutaraldehyde (covalent crosslinker) react with the -OH groups of *S. foetida*, forming an acetal linkage that creates a three-dimensional IPN structure (Figure 2). The obtained microspheres were water-insoluble and had a three-dimensional network with amoxicillin entrapped in them. In an investigation conducted due to toxicity concerns of glutaraldehyde as a crosslinker, flavonoid-like rutin was used to crosslink gelatin microspheres, and a comparison was performed with glutaraldehyde. However, the crosslinking efficiency of rutin was low, and the glutaraldehyde-crosslinked microspheres were as safe as rutin-crosslinked microspheres.[32] The microspheres were washed several times with water to remove unreacted glutaraldehyde.

Influence of formulation composition on percent DEE (Y1)

The percent DEE increased from 60.37±1.85% to 88.24±2.46% as the concentration of polymers increased. From the response surface curve, it was determined that the encapsulation efficiency of the drug increased with an increase in the polymer concentration. The polynomial equation correlating percent DEE with independent variables is as follows.

$$EF(Y_1)= +82.11-6.30*A+5.88*B+3.81*C-0.3525*AB+0.7350*AC-1.08*BC-2.36*A^2-2.46*B^2-1.48*C^2 \quad \text{equation (5)}$$

where A is the volume of glutaraldehyde and B and C are the amounts of pullulan and *S. foetida*, respectively. The randomized central composite design showed a good fit. A high f value of 28.94 and a p value of <0.0500 indicated that the model was significant.

The influence of independent formulation variables on EE is depicted using response surface plots is shown in Figure 1a. The EE increased, possibly due to the high viscosity of the polymer blend, consequently reducing drug seepage during microsphere preparation. Further, the high polymer concentration may have caused increased entrapment of the drug inside the *S. foetida*-pullulan network. However, the encapsulation efficiency decreased with an increase in the glutaraldehyde concentration; this decrease might be due to an increase in the crosslinking density of the polymer matrix. This caused the formation of a rigid structure with a consequent reduction in free volume within the polymer matrix for drug entrapment.[33,34]

Influence of formulation composition on in vitro mucoadhesion

The percent mucoadhesion in SGF of all batches was between 60.78±1.62% and 87.35±1.83%. As the polymer concentration increased, mucoadhesion increased. The polynomial equation

correlating percent mucoadhesion with the independent variables is shown below:

Percent mucoadhesion= +76.072.81*A+6.59*B+3.86*C

equation (6)

The model f value of 35.43 and p value of <0.05 indicated that the model was significant. The predicted R^2 of 0.7856 was in agreement with the adjusted R^2 of 0.8446 as the difference between them was <0.2. The influence of independent formulation variables on mucoadhesion (%) is depicted using response surface plots in Figure 1b. An increase in mucoadhesion with polymer concentration may have occurred due to the availability of more OH groups for hydrogen bond formation with the mucus membrane.[29] Mucoadhesion decreases with an increase in glutaraldehyde levels. The decrease in mucoadhesion may be because of the formation of a strongly crosslinked polymeric matrix, causing decreased swelling and weaker interactions with the mucosal surface. The mucoadhesive properties of *S. foetida* are attributable to its capacity to form a mucoadhesive bond with mucin and interpenetration of the polymer chain in the interfacial area.[2,33,34]

Influence of formulation composition on percent drug release

All the formulations showed sustained release of amoxicillin over 12 h in SGF (pH 1.2). The cumulative drug release from semi-IPN microspheres after 12 h was between 60.32±2.09% and 89.41±1.99% (Table 2, Figure 6). The drug release rate decreased with an increase in polymer concentration. The correlation between drug release at 12 h and different independent variables is explained by the following polynomial equation:

Drug release= +82.15-6.18*A-4.17*B-4.53*C+1.30*AB+0.1912*AC-0.2513*BC-2.148A^2-4.54*B^2-3.23*C^2

equation (7)

The impact of formulation variables on percent drug release is depicted using surface response plots in Figure 1c. Increased *S. foetida* content in the blend membrane reduced the rate of drug release. The hydrophobicity of the microsphere matrix increased with *S. foetida* content due to an increase in ester linkages and methyl groups. Additionally, the reduction in the rate of drug release could be caused by a decrease in the molecular volume of *S. foetida* in the polymer matrix due to its decreased swelling and hydration capacity. Similarly, the drug release pattern was highly dependent on glutaraldehyde levels.[33] When the glutaraldehyde volume was increased from 2 mL to 4 mL, percent drug release was decreased from 89.41±1.99% to 60.32±2.09% in 12 h. This behavior may be a result of fewer free spaces in the glutaraldehyde-treated IPN matrices for unhindered drug diffusion through the polymer network.[34] The drug release followed Hixson-Crowell kinetics as it showed maximum R^2 (0.9964). The drug release mechanism followed super case-II (n=1.33 of Korsmeyer-Peppas), i.e., diffusion and chain relaxation. There could be a dominant role of chain relaxation at later time points due to waning of crosslinks over time.

Optimization by desirability function

Optimization was perfomed based on the desirability function. Microspheres were prepared under the model-predicted optimal condition with glutaraldehyde 4% v/v, pullulan 8.28% w/v, and *S. foetida* 2.14% w/v. Optimization was performed by placing constraints on the dependent variables. The response variables of the formulated microspheres under optimized conditions were nearly equal (low percentage bias) to the predicted values, ensuring reliability of the model (Table 3).

Influence of formulation composition on particle size

The microspheres had sizes of 57.99±1.53-121.90±1.38 µm. The variation in particle size due to formulation variables indicates that microsphere size was dependent on the glutaraldehyde amount and polymer concentration. When the amount of glutaraldehyde increased, the particle size decreased. This may be the result of the increased crosslink density, which caused shrinking of the internal phase to a greater extent, creating a low void space. Alternatively, when the polymer ratio was increased at a given quantity of glutaraldehyde, the particle size also increased. This could be because of increased drug entrapment in the voids present in the polymeric network. Additionally, when the drug concentration was increased, it needed more space in the polymeric networks and voids, consequently increasing the size.

Characterization of ASP-MPs

FTIR

Figure 2 depicts the FTIR spectrum of amoxicillin trihydrate, showing peaks at 1616.24 cm^{-1} for aromatic C=C stretching and 1685.67 cm^{-1} and 1577.66 cm^{-1} for C=O stretching and N-H deformation of amide, respectively. The peak at 1774.39 cm^{-1} was due to β-lactam C=O stretching, and the peaks at 2968.24 and 3039.60 cm^{-1} corresponded to C-H stretching for CH_3 and aromatic C-H stretching, respectively. All the prominent peaks of amoxicillin trihydrate were retained in the spectrum of a physical mixture of *S. foetida* and pullulan, indicating no interaction of the drug with the polymer. The FTIR spectrum of ASP-MP formulation revealed a broad absorption band from 3527.56^{-1} to 3105 cm^{-1} due to the OH group of *S. foetida* and CHO group of glutaraldehyde, which proves the formation of glutaraldehyde-

Table 3. Optimization by desirability function

Optimized formulation	Optimized level	Responses	Predictive value	Experimental value	% bias
Glutaraldehyde	4% v/v	Entrapment efficiency (%)	88.751	86.92	-2.06
Pullulan	8.28% w/v	Drug release in 12 h (%)	81.924	80.43	-1.81
Sterculia foetida	2.14% w/v	Mucoadhsion (%)	82.498	81.73	-0.92

crosslinked semi-IPN microspheres. Furthermore, bands from 3475^{-1} to 3620 cm^{-1} due to O-H stretching in the FTIR spectrum of *S. foetida* had shifted to the lower wavenumber from 3423^{-1} to 3519 cm^{-1} in the FTIR spectrum of APS-MPs. This shift can be attributed to hydrogen bond formation between *S. foetida* and amoxicillin in the microspheres. A similar finding was reported by Üstündağ Okur et al.[35]

DSC

Thermograms of amoxicillin, pullulan, *S. foetida* gum, physical mixture of *S. foetida*-pullulan with amoxicillin trihydrate, and ASP-MPs are shown in Figure 3. The pure drug exhibited a characteristic broad peak starting from 60°C to 140°C due to trihydrate dehydration and a broad endothermic peak starting from 185°C to 210°C with a peak at 199°C due to melting. DSC of pullulan revealed an endothermic peak from 0°C to 110°C, whereas *S. foetida* showed an endothermic peak from 0°C to 110°C due to dehydration. The endothermic peak of amoxicillin trihydrate due to the loss of water molecule is revealed in the DSC of the physical mixture, showing a lack of incompatibility. In contrast, the endothermic melting peak was diminished due to the masking of the drug in the polymers. The absence of a characteristic endothermic peak of amoxicillin in the ASP-MP thermogram might have accurred because of the entrapment of the drug in the microspheres, making it undetectable.

XRD

Sharp peaks with high intensity from 2ɵ 10˚-30˚ in the amoxicillin trihydrate XRD pattern indicated crystalline properties. The characteristic peaks present in the drug from 2ɵ 15˚-30˚ had broadened in microspheres, indicating a loss of crystallinity upon entrapment in microspheres (Figure 4).

SEM

SEM was performed to visualize the morphology of the ASP-MPs. The formed microspheres were slightly irregular and aggregated, with a rough surface (Figure 5). The rough surface might be due to the shrinkage of crosslinked *Sterculia* gum during drying of the IPN microspheres.

In vivo radiographic studies

X-ray images revealed the presence of microspheres in the stomach at 6 h after administration. The ASP-MPs were retained for an extended period of time due to mucoadhesion to the stomach mucosal lining (Figure 7).

CONCLUSION

Semi-IPN microspheres loaded with amoxicillin trihydrate were successfully prepared using *S. foetida* and pullulan by the emulsion crosslinking method using glutaraldehyde as the crosslinker. Microspheres prepared under optimized conditions (2.14% w/v *S. foetida*, 8.28% w/v pullulan, and 4% v/v glutaraldehyde) showed predicted values of EE, drug release, and mucoadhesion, with low percentage bias. Additionally, X-ray images revealed the presence of microspheres for 10 h. Thus, the prolonged retention of microspheres in the stomach with sustained drug release could effectively act against the *H. pylori* reservoir in the stomach and improve the therapeutic effectiveness of amoxicillin trihydrate against *H. pylori.*

Conflict of interest: No conflict of interest was declared by the authors. The authors are solely responsible for the content and writing of this paper.

REFERENCES

1. Benita S. Microencapsulation: methods and industrial applications. New York: Marcel Dekker Inc.;1996.
2. Patil S, Talele GS. Gastroretentive mucoadhesive tablet of lafutidine for controlled release and enhanced bioavailability. Drug Deliv. 2015;22:312-319.
3. Arora S, Bisen G, Budhiraja RD. Mucoadhesive and muco-penetrating delivery for eradication of *Helicobacter pyroli*. Asian J Pharm. 2012;6:18-30.
4. Patel J, Patel MM. Stomach specific anti-*helicobacter pylori* therapy: preparation and evaluation of amoxicillin-loaded chitosan mucoadhesive microspheres. Curr Drug Deliv. 2007;4:41-50.
5. Liu Z, Lua W, Qian L, Zhang X, Zeng P, Pan J. *In vitro* and *in vivo* studies on mucoadhesive microspheres of amoxicillin. J Control Release. 2005:102:135-144.
6. Rajinikanth PS, karunagaran LN, Balasubramaniam J, Mishra B. Formulation and evaluation of Clarithromycin microspheres for eradication of *Helicobacter pylori*. Chem Pharm Bull. 2008;56:1658-1664.
7. Gabriel A, Janeth MV, Ana claudia LC, Alberto J. Karaya gum: general topics and applications, macromolecules. MMAIJ. 2013;9:111-116.
8. Phillips GO, Williams PA, Handbook of hydrocolloids. In: Phillips GO, Williams Pai, eds. (2nd ed). Cambridge, England: Woodhead Publishing Limited; 2009.
9. Anderson DMW, Wang WP. The tree exudate gums permitted in foodstuffs as emulsifiers, stabilisers and thickeners. Chem Ind For Prod. 1994;14:73-83.
10. Singh B, Sharma N. Design of sterculia gum based double potential antidiarrheal drug delivery system. Colloids Surf B Biointerfaces. 2011;82:325-332.
11. Bera H, Boddupalli S, Nayak A. Mucoadhesive-floating zinc-pectinate-sterculia gum interpenetrating polymer network beads encapsulating ziprasidone HCl, Carbohydr Polym. 2015;131:108-118.
12. Prajapati VD, Jani GK, Khanda SM. Pullulan: an exopolysaccharide and its various applications. Carbohydr Polym. 2013;5:95:540-549.
13. Yua L, Deana K, Li L. Polymer blends and composites from renewable resources. Prog Polym Sci. 2006;31:576-602.
14. Dias RJ, Ghorpade VS, Havaldar VD, Mali KK, Hindurao N. Development and optimization of interpenetrating network beads of Delonix regia gum and sodium alginate using response surface methodology. J Appl Pharm Sci. 2015;5:56-64.
15. Nakay AK, Hasnain MS, Pal D. Gelled microspheres/Beads of sterculia gum and tamarind gum for sustained drug release. Polymer Gels. 2018:361-415.
16. Mohamadnia Z, Zohuriaan Mehr MJ, Kabiri K. pH-Sensitive IPN hydrogel beads of carrageenan-Alginate for controlled drug delivery. J Bioact Compat Polym. 2007;22:342-356.

17. Prajapati VD, Jani GK, Moradiya NG, Randeria NP, Maheriya PM, Nagar BJ. Locust bean gum in the development of sustained release mucoadhesive macromolecules of aceclofenac. Carbohydr Polym. 2014;113:138-148.

18. Mallikarjuna Reddy K, Ramesh Babu V, Sairam M, Subha MCS, Mallikarjuna NN, Kulkarni PV, Aminabhavi TM. Development of chitosan-guar gum semiinterpenetrating polymer network microspheres for controlled release of cefadroxil. Des Monomers Polym. 2006;9:491-501.

19. Ray S, Banerjee S, Maitis S, Laha B, Barik S, Sa B, Bhattacharyya UK. Novel interpenetrating network microspheres of xanthan gum-poly (vinyl alcohol) for the delivery of diclofenac sodium to the intestine-*in vitro* and *in vivo* evaluation in Drug Deliv. 2010;17:508-519.

20. Kulkarni RV, Mutalik S, Mangond BS, Nayak UY. Novel interpenetrated polymer network microbeads of natural polysaccharides for modified release of water soluble drug: *in-vitro* and *in-vivo* evaluation. J Pharm Pharmacol. 2012;64:530-540.

21. Nayak AK, Pal D, Santra K. Development of calcium pectinate-tamarind seed polysaccharide mucoadhesive beads containing metformin HCl. Carbohydr Polym. 2014;101:220-230.

22. Hooda A, Nanda A, Jain M, Kumar V, Rathee P. Optimization and evaluation of gastroretentive ranitidine HCl microspheres by using design expert software. Int J Biol Macromol. 2012;51:691-700.

23. Venkateswaramurthy N, Sambathkumar R, Perumal P. Design development and evaluation of amoxicillin trihydrate mucoadhesive microspheres for *Helicobactor pylori* eradication therapy. Int J Appl Pharm. 2010:2:23-25.

24. Costa P, Sousa LJM, Modelling and comparison of dissolution profiles. Eur J Pharm Sci. 2001;13:123-133.

25. Costa FO, Sousa JJ, Pais AA, Fornosinho SJ. Comparison of dissolution profile of ibuprofen pellets. J Control Release. 2003:89:199-212.

26. Higuchi T. Mechanism of sustained action medication theoretical analysis of rate of release of solid drugs dispersed in solid matrices. J Pharm Sci. 1963;52:1145-1149.

27. Peppas NA. Analysis of fickian and non-fickian drug release from polymers. Pharm Acta Helv. 1985;60:110-111.

28. Jain A, Pandey V, Ganeshpurkar A, Dubey N, Bansal D. Formulation and characterization of floating microballoons of Nizatidine for effective treatment of gastric ulcers in murine model. Drug Deliv. 2015;22:306-311.

29. Montgomery DC. Design and Analysis of Experiments. (50th ed). New York: Wiley; 2001.

30. Montgomery DC. Introduction to Statistical Quality Control. (40th ed). New Delhi: Wiley India (P) Ltd; 2008.

31. Srivastava AK, Wadhwa S, Ridhurkar D, Mishra B. Oral sustained delivery of atenolol from floating matrix tablets-formulation and *in vitro* evaluation. Drug Dev Ind Pharm. 2005;31:367-374.

32. Fabiana G, Thalita MC, Camila AO, Daniela DP, Michele GI, Joana M, Catarina R, Vladi OC, Telma MK, Maria VR, André R. Gelatin-based microspheres crosslinked with glutaraldehyde and rutin oriented to cosmetics. Brazil J Pharm Sci. 2016;52:603-612.

33. Raizaday A, Yadav HK, Kumar SH, Kasina S, Navya M, Tashi C. Development of pH sensitive microparticles of Karaya gum: by response surface methodology. Carbohydr Polym. 2015;134:353-363.

34. Guruguntla N, Palla KB, Yeggada M, Areti P, Chintha M. Interpenetrating polymer network hydrogel membranes of Karaya gum and sodium alginate for controlled release of Flutamide Drug, J Appl Pharm Sc. 2016;6:011-019.

35. Üstündağ Okur N, Hökenek N, Okur ME, Ayla Ş, Yoltaş A, Siafaka PI, Cevher E. An alternative approach to wound healing field; new composite films from natural polymers for mupirocin dermal delivery. Saudi Pharm J. 2019;27:738-752.

Turk J Pharm Sci 2021;18(4):398-404
DOI: 10.4274/tjps.galenos.2020.95776

ORIGINAL ARTICLE

Effects of Pregabalin, Nimodipine, and Their Combination in the Inhibition of Status Epilepticus and the Prevention of Death in Mice

Epilepsi Durumunun İnhibisyonuna ve Ölümün Önlenmesine Pregabalin, Nimodipin ve Bunların Kombinasyonunun Farelerdeki Etkileri

Itefaq QURESHI[1], Azra RIAZ[1], Rafeeq KHAN[2]*, Moona BAIG[1], Muhammad Ali RAJPUT[1]

[1]University of Karachi, Department of Pharmacology, Karachi, Pakistan
[2]Ziauddin University, Faculty of Pharmacy, Karachi, Pakistan

ABSTRACT

Objectives: The current study aims to evaluate the combined antiepileptic effects of pregabalin (PGB) and nimodipine (NMD) in an acute seizure model of epilepsy in mice.

Materials and Methods: This study assessed the combined antiepileptic effects of PGB with NMD on death protection in mice. Pentylenetetrazole was used to induce seizures. Both drugs were used singly and in combination to judge anticonvulsant effects on an acute seizure model of epilepsy in mice. Diazepam (DZ) and valproate (VPT) were used as standard antiepileptic drugs.

Results: The death protection in mice by both these drugs was observed in percentage and deliberated as marked change when the outcome of the tested drug was equal to ED_{50} of PGB and measured highly marked when the result was more than ED_{50} for PGB. Treatment with pregabalin and nimodipine combination revealed substantial mortality protection at 30+2.5 mg/kg dose and highly marked at doses from 35+5 mg/kg to 55+15 mg/kg, these effects were superior to individual effects of PGB, showing synergism, however lesser then classic drugs valproate and diazepam.

Conclusion: NMD showed synergistic anticonvulsant effect with PGB. However, clinical studies are required to establish the effectiveness of this combination in humans.

Key words: Pregabalin, nimodipine, valproate, diazepam, pentylenetetrazole

ÖZ

Amaç: Bu çalışma, farelerde akut epilepsi nöbet modelinde pregabalin (PGB) ve nimodipinin (NMD) kombine antiepileptik etkilerini değerlendirmeyi amaçlamaktadır.

Gereç ve Yöntemler: Bu çalışma, farelerde ölümü önlemek için PGB ve NMD ile kombine antiepileptik etkilerini değerlendirmiştir. Bu çalışma, farelerde ölümü önlemek için PGB'nin NMD ile kombine antiepileptik etkilerini değerlendirmiştir. Pentilentetrazol nöbetleri indüklemek için kullanılmıştır. Farelerde epilepsinin akut nöbet modeli üzerindeki antikonvülsan etkileri değerlendirmek için her iki ilaç tek başına ve kombinasyon halinde kullanılmıştır. Standart antiepileptik ilaç olarak diazepam (DZ) ve valproat (VPT) kullanılmıştır.

Bulgular: Farelerde bu ilaçların her ikisi tarafından ölüm koruması yüzde olarak gözlemlendi ve test edilen ilacın sonucu PGB'nin ED_{50}'sine eşit olduğunda belirgin değişiklik olarak düşünüldü ve sonuç PGB için ED_{50}'den fazla olduğunda oldukça belirgin olarak ölçüldü. Pregabalin ve nimodipin kombinasyonu ile tedavi, 30+2,5 mg/kg dozda önemli mortalite koruması gösterdi ve 35+5 mg/kg ila 55+15 mg/kg dozlarda oldukça belirgindi, bu etkiler PGB'nin bireysel etkilerinden üstündü, ancak sinerjizm gösteriyordu. Klasik ilaçlar valproat ve diazepamdan daha az bulunmuştur.

Sonuç: NMD, PGB ile sinerjistik antikonvülsan etki göstermiştir. Bununla birlikte, bu kombinasyonun insanlarda etkinliğini belirlemek için klinik çalışmalara ihtiyaç vardır.

Anahtar kelimeler: Pregabalin, nimodipin, valproat, diazepam, pentilentetrazol

***Correspondence:** rkhan1959@gmail.com, **Phone:** +92103218258742, **ORCID-ID:** orcid.org/0000-0002-8051-759X

Received: 01.05.2020, **Accepted:** 25.05.2020

INTRODUCTION

Status epilepticus is a severe condition of shared epilepsies.[1] It is a life-threatening neural health crisis,[2] which may lead to loss of life in many instances if not cured suitably: Lorazepam and diazepam (DZ) are the major drugs of choice for a short period to control status epilepticus.[3] However, lorazepam has been superior to DZ.[4] Valproate (VPT), phenobarbitone, and phenytoin are endorsed for the extended period of treatment of status epilepticus.[5] The selection of first-line drugs is limited to the management of status epilepticus, and the drugs suggested have serious side effects and drug-drug interactions.[6,7] Nimodipine (NMD) is a voltage-gated calcium channel inhibitor permitted by Food and Drug Administration (FDA) for hypertension since it inhibits the L-type calcium channels in blood vessels.[8]

NMD inhibits and modifies voltage-gated calcium channels in the central nervous system (CNS).[9] Low and high voltage-gated calcium channels have a crucial role in neuronal functions in major parts of the CNS, embracing excitability.[10,11] Hence, it seems appropriate for the calcium-channel blockers (CCBs) to be employed to treat epilepsy.[12,13] NMD in several animal studies showed increasing antiepileptic effects over other anti-convulsion drugs, e.g., carbamazepine, VPT, and lamotrigine, in the management of acute seizures.[14,15] Pregabalin (PGB) is well tolerated, efficient and FDA permitted its use in patients with epilepsy.[16,17] Its antiepileptic action relates to binding alpha-2-delta voltage-gated calcium channels, including many other pharmacodynamic anti-seizure actions in the CNS.[18] The current study aims to evaluate the combined antiepileptic effects of PGB and NMD in an acute seizure model of epilepsy in mice.

MATERIALS AND METHODS

Animals

Consent was obtained from the Board of Advanced Studies and Research (BASR) 10 (P) 04 dated June 19, 2015, to conduct the current study at the Department of Pharmacology, University of Karachi. The mice used in the study were managed as per the guidelines of the National Institute of Health.[19] The ethical approval for the use of animals was granted by the departmental research committee after the letter issued by the BASR dated September 30, 2015 (approval no: BASR/02521). The experiments were performed on male albino mice whose weight ranged from 20 to 25 g. The animals were kept in a controlled environment with regular provisions of food and water. The temperature was sustained at 21°C±2°C with 12-hour light/dark cycles. The animals were exposed to the location for 2-3 days before the experiments could be performed. The tests were done from 9:00 am to 12:30 pm.

Drug treatment

Acute attacks were induced by pentylenetetrazole (PTZ). Meanwhile, PGB and NMD were used as test drugs. DZ and VPT were employed to equate the antiepileptic effects of the test drugs. Normal saline was used for animals in the control group. The HEJ Research Center, University of Karachi, provided PTZ. DZ and VPT injections were acquired from a local market by Roche Pakistan Ltd. and Abbot Laboratories, Pakistan Ltd, Karachi, respectively. PGB capsules of Getz Pharma Pvt. Limited, Karachi were also obtained from the local market. Novartis Pharma, Pakistan Ltd, Karachi, provided the NMD injections.

PGB, NMD, and PTZ were liquefied in sterile, normal saline. Aluminum foil was used to cover the PTZ solution to avoid disintegration. The solutions were made regularly and used within an hour of their inception. PGB capsule contents were dissolved in sterile water and administer subcutaneously, while other drugs were given by the intraperitoneal route.

Procedure

Convulsions in all mice were induced via PTZ at a dose of 90 mg/kg through subcutaneous administration.[20] PGB and NMD were given separately and in combination as six different doses. All drugs, including the test substance and the standard drugs DZ and VPT, were administered 40 minutes earlier than PTZ, administered intraperitoneally. The mice were kept alone following PTZ administration and observed. The prevention of death was recorded in percentage.

The outcomes of mice that remained without seizures up to cut-off time were stated as 0. The number of mice survived (mortality protection) and died were recorded as a percentage. The anticonvulsant effect, seizure form, and mortality protection achieved by the combination regimen (PGB + NMD + PTZ) in six doses of the test drugs were equated with PTZ, individual effects of PGB + PTZ and NMD + PTZ. and with reference drugs (DZ + PTZ and VPT + PTZ).

A period of 60 minutes was the cut-off time for seizure defense after PTZ administration with or without the test drugs.[21-25] The antiepileptic effects of PGB and NMD were assessed by observing seizure prevention as a percentage.

All animals used in this study were distributed into three parts, i.e., A, B, and C, each part had ten groups, and each group included 12 mice. Group I in each part functioned as control and was given sterile, normal saline; group II mice were given PTZ, and animals in groups III to VIII were given different doses of the test drugs. Mice in groups IX and X were given DZ and VPT. DZ was given at a dose of 7.5 mg/kg and VPT 100 mg/kg, forty minutes before giving PTZ. Six groups of part-A were given PGB doses ranging from 30 to 55 mg/kg, with a difference of 5 mg/kg in each group. Animals of part-B were given NMD at doses of 2.5, 5, 7.5, 10, 12.5, and 15 mg/kg. Animals in part-C were given six different combinations of PGB + NMD, i.e., 30+2.5, 35+5, 40+7.5, 45+10, 50+12.5, and 55+15 mg/kg, forty minutes before giving PTZ.

Statistical analysis

No standard statistical procedure was performed in the current study. The results were expressed in percentages and produced a noticeable outcome when the tested drugs were equal to effective dose 50 (ED_{50}) of PGB and a highly substantial result when the outcome was more than ED50 for PGB.

RESULTS

Table 1 summarizes the results of all animals groups in the three sections however Figure 1 shows the results of animals only in section-A. PGB as a single agent in its six doses from 30 to 55 mg/kg protected mortality from 42% to 67%. Both the reference drugs VPT and DZ provided 100% mortality protection. The antiepileptic effects of PGB, when matched to the reference drugs VPT and DZ, were comparatively inferior in preventing all epileptic attacks.

Table 1 summarizes the results of all animals groups in the three sections however Figure 2 shows the results of animals only in section-B. NMD as a single agent in its first three doses, i.e., 2.5, 5, and 7.5 mg/kg, exhibited 100% mortality. However, at a dose of 10 mg/kg, the mortality protection was 8%, whereas at doses of 12.5 mg/kg and 15 mg/kg, the mortality protection was 17%. VPT and DZ prevented death in 100% of animals. The antiepileptic effect of NMD, when matched to standard drugs VPT and DZ, was highly inferior in all seizure forms.

Table 1. Antiepileptic outcome of pregabalin, nimodipine, and their combination in an acute model of epilepsy

Groups	Doses mg/kg	Mortality protection
Normal control	10 mL/kg	100
PTZ	90	00
PGB	30	42
PGB	35	42
PGB	40	50*
PGB	45	58**
PGB	50	67**
PGB	55	67**
NMD	2.5	00
NMD	5.0	00
NMD	7.5	00
NMD	10	8
NMD	12.5	17
NMD	15	17
PGB:NMD	30:2.5	50*
PGB:NMD	35:5	58**
PGB:NMD	40:7.5	58**
PGB:NMD	45:10	67**
PGB:NMD	50:12.5	83**
PGB:NMD	55:15	83**
VPT	100	100
DZ	7.5	100

*Marked as compared to 40 mg/kg PGB (ED_{50}), **Highly substantial as compared to 40 mg/kg PGB (ED_{50}), n=12, PTZ: Pentylenetetrazole, PGB: Pregabalin, NMD: Nimodipine, VPT: Valproate, DZ: Diazepam, ED_{50}: Effective dose 50

Table 1 summarizes the outcomes of all animals groups in the three sections. In contrast, Figure 3 shows the results of animals in section-C. The animals treated in combination dose of 30+2.5 mg/kg PGB and NMD prevented death in 50%, which was substantial compared with PGB 40 mg/kg. In contrast, animals treated with combination doses of 35+5 and 40+7.5 mg/kg PGB and NMD, respectively, showed a 58% mortality protection. The animals given the combination of PGB and NMD at doses of 45+10 mg/kg revealed a 67% mortality protection. However, the maximum mortality protection of 83% was observed by the combination doses of 50+12.5 mg/kg and 55+15 mg/kg of doses of PGB and NMD, respectively.

Table 2 and Figure 4 show the difference in the mortality protection among PGB, NMD, the combination of PGB + NMD,

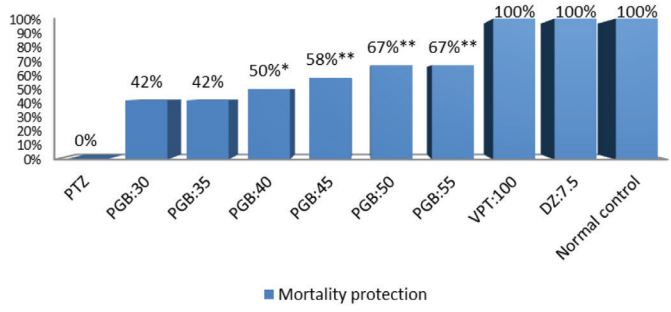

Figure 1. Comparative effects of pregabalin, valproate, and diazepam on mortality protection in an acute model of epilepsy

*Shows marked change and **shows highly substantial change in terms of percentage, PTZ: Pentylenetetrazole, PGB: Pregabalin, VPT: Valproate, DZ: Diazepam

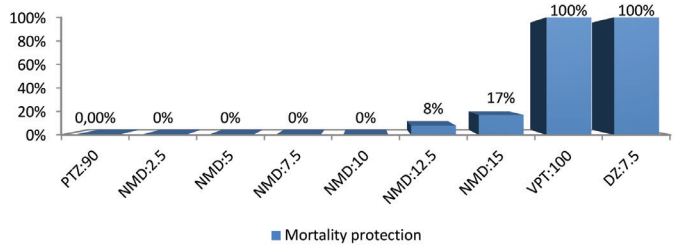

Figure 2. Comparative effects of nimodipine, valproate, and diazepam on the mortality protection in an acute model of epilepsy

PTZ: Pentylenetetrazole, NMD: Nimodipine, VPT: Valproate, DZ: Diazepam

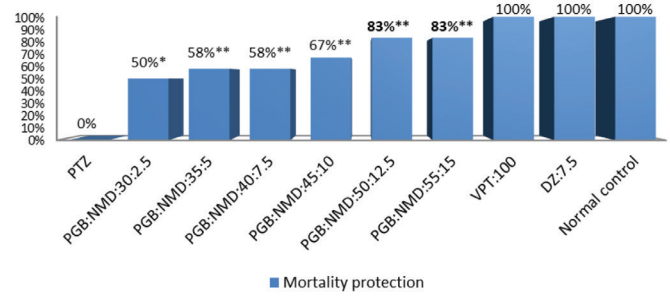

Figure 3. Comparative effects of pregabalin, nimodipine, valproate, and diazepam on the mortality protection in an acute model of epilepsy

*Marked as compared to 40 mg/kg PGB (ED_{50}), **Highly substantial as compared to 40 mg/kg PGB (ED_{50}), PTZ: Pentylenetetrazole, NMD: Nimodipine, VPT: Valproate, DZ: Diazepam, ED_{50}: Effective dose 50

and VPT. The difference in the mortality protection among NMD in the first three doses and VPT was -100. In contrast, NMD demonstrated a 92% less mortality protection compared to VPT at 10 mg/kg and 83% less mortality protection at 12.5 and 15 mg/kg. PGB demonstrated a 58% less mortality protection at 30 and 35 mg/kg doses reduced to 50% at the dose of 40 mg/kg. While at the dose of 45 mg/kg, a 42% less mortality protection was noted. However, at 50 and 55 mg/kg doses, PGB demonstrated 33% less mortality protection than VPT. The combination of PGB and NMD showed better results in reducing mortality. The difference in mortality protection at doses of 30+2.5 mg/kg and 35+5 mg/kg compared with VPT was only 50%, which improved to 42% at the combination dose of 40+7.5 mg/kg. The difference in the mortality protection improved to 33% at doses of 45+10 mg/kg and was reduced to 17% at the combination doses of 50+12.5 mg/kg and 55+15 mg/kg compared with VPT.

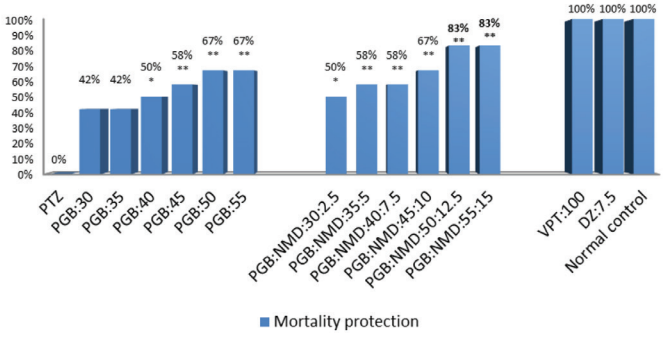

Figure 4. Comparative effects of pregabalin, nimodipine, valproate, and diazepam on the mortality protection in an acute model of epilepsy

*Marked as compared with 40 mg/kg PGB (ED_{50}), **Highly substantial compared with 40 mg/kg PGB (ED_{50}), PTZ: Pentylenetetrazole, PGB: Pregabalin, NMD: Nimodipine, VPT: Valproate, DZ: Diazepam, ED_{50}: Effective dose 50

Table 3 shows the comparisons of the prevention of death for PGB and combinations of PGB and NMD. The PGB and NMD combination at the dose of 30+2.5 mg/kg demonstrated an 8% higher prevention of death, whereas the combination dose of 35+5 mg/kg showed a 16% higher prevention of death. However, the combination doses of 40+7.5 and 45+10 for PGB and NMD demonstrated only 8% and 9% prevention of death, respectively. The rate of prevention of death was again consistently higher. It was up to 16% higher with the doses combination of 50+12 mg/kg and 55+15 mg/kg of PGB and NMD compared with PGB alone.

DISCUSSION

Although the discovery of new antiepileptic drugs (AEDs) have widened the selection of drugs to treat epilepsies on a long-term basis, none of the newer AEDs are permitted to treat status epilepticus. Also, the likelihood and usefulness of these new AEDs remain limited, and no AED has been found to retain its best properties.[26] Exploration of drug combinations that may have the potential to terminate and prevent status epilepticus is the main object of our study. Thus, newer AEDs with better effectiveness and unique mechanisms are now needed to deliver active combinations to treat epilepsy.[27] Animal models may only be employed to forecast drugs combinations that are effective in the clinical setting.[24]

AEDs may have inhibitory or additive effects. However, drugs possessing additive effects appear to be of medical importance.[21,28] Therefore, the present investigation evaluated PGB in combination with NMD for synergistic antiepileptic effects in an acute seizure model of epilepsy in mice. It was assumed that a combination of AEDs might potentiate their anticonvulsant effects. This hypothesis was supported by the additive actions of tiagabine and gabapentin. The outcomes

Table 2. Nimodipine, pregabalin, and PGB + NMD in comparison to valproate in the mortality protection in an acute model of epilepsy

NMD v/s VPT dose mg/kg	Difference in mortality protection	PGB v/s VPT	Difference in mortality protection	PGB:NMD v/s VPT dose mg/kg	Difference in mortality protection
NMD v/s VPT 2.5 100	-100	PGB v/s VPT 30:100	58	PGB:NMD v/s VPT 30:2.5/100	50
NMD v/s VPT 5 100	-100	PGB v/s VPT 35:100	58	PGB:NMD v/s VPT 35:5/100	42
NMD v/s VPT 7.5 100	-100	PGB v/s VPT 40:100	50	PGB:NMD v/s VPT 40:7.5/100	42
NMD v/s VPT 10 100	92	PGB v/s VPT 45:100	42	PGB:NMD v/s VPT 45:10/100	33
NMD v/s VPT 12.5 100	83	PGB v/s VPT 50:100	33	PGB:NMD v/s VPT 50:12.5/100	17
NMD v/s VPT 15 100	83	PGB v/s VPT 55:100	33	PGB:NMD v/s VPT 55:15/100	17

Difference in the mortality protection (%), PGB: Pregabalin, NMD: Nimodipine, VPT: Valproate

Table 3. Comparison of the mortality protection pregabalin and PGB + NMD in an acute model of epilepsy

Treatment groups	Mortality protection	Treatment groups with doses	Mortality protection	Difference in the mortality protection
PGB:30	42	PGB:NMD 30:2.5	50*	8
PGB:35	42	PGB:NMD 35:5	58**	16
PGB:40	50	PGB:NMD 40 :7.5	58**	8
PGB:45	58	PGB:NMD 45:10	67**	9
PGB:50	67	PGB:NMD 50:12.5	83**	16
PGB:55	67	PGB:NMD 55:15	83**	16

*Marked compared with 40 mg/kg PGB (ED_{50}), **Highly substantial compared with 40 mg/kg PGB (ED_{50}), n=12, doses (mg/kg), PGB: Pregabalin, NMD: Nimodipine, ED_{50}: Effective dose 50

of the present investigation demonstrated that the activation of the neurotransmitters might have produced an additive effect.[29] In another investigation, the anticonvulsant effects of oxcarbazepine and gabapentin were found to be a mixture of both drugs at the fixed ratios to exert the additive effects against electroconvulsions.[30]

PGB and NMD showed a 50% prevention of death when given a combination dose of 30+2.5 mg/kg. However, when PGB and NMD were given separately at doses of 30 mg/kg and 2.5 mg/kg, the prevention of death was 42% and 0%, respectively. Hence, there was an 8% increase in the prevention of death compared with PGB and a 50% increase compared with NMD alone (Table 1). Similarly, PGB and NMD showed a 58% prevention of death at the combination dose of 35+5 mg/kg. However, when these drugs were given separately at doses of 35 mg/kg and 5 mg/kg, the prevention of death was 42% and 0%, respectively. Therefore, a 16% increase in the prevention of death compared with PGB and a 58% increase in the response compared with NMD in PTZ-induced acute seizures (Table 1).

PGB and NMD showed a 67% prevention of death with the combination dose of 45+10 mg/kg. However, when PGB and NMD were given separately at doses of 45 mg/kg and 10 mg/kg, the prevention of death was 58% and 8%, respectively. Hence, there was a 9% increase in the prevention of death compared with PGB and a 59% increase in the prevention of death compared with NMD (Table 1). The animal groups received combination doses of 50+12.5 mg/kg and 55+15 mg/kg PGB. NMD exhibited maximum anticonvulsant effects with an 83% prevention of death. This was 17% and 67% more than the individual response to PGB and NMD, respectively. Hence, synergistic effects have been observed at all the combination doses of PGB and NMD. Thus, the combination regimen decreased the ED_{50} of the PGB from 40 mg/kg to 30 mg/kg. The decrease in ED_{50} was 10 mg/kg, which was a 25% decrease in the ED_{50} of the PGB in the treatment of acute seizures in mice (Table 1). This shows that adding the CCB NMD with PGB exerted remarkable synergistic anti-seizure effects by increasing the mortality protection but not abolishing the seizures completely.

The pharmacokinetic and pharmacodynamic profiles of PGB reveal it to be a well-tolerated drug.[17,31,32] The FDA has recognized it for the treatment of epilepsy.[33,34] PGB in several investigations has validated its value for the treatment of partial and generalized seizures. PGB has also shown its effectiveness in refractory epilepsy, and combination treatment may have a broader range to manage many forms of convulsions.[16] In this study, we anticipated that the antiepileptic actions of PGB could be amplified or altered when administered in combination with NMD. Calcium channel antagonists retain anticonvulsant effects in experimental models and enhance the guarding activity of some AEDs.[35] NMD is a dihydropyridine calcium channel antagonist that blocks N-and P/Q-type calcium channels, with greater affinity for both channels.[36,37] Numerous investigations have shown important augmented anticonvulsant actions of amlodipine and NMD on topiramate, VPT, phenobarbitone, and other AEDs.[15,30,38] Thus, there are convincing reasons illustrating that this investigation provides an essential medical perspective.

PGB as monotherapy in acute studies showed marginal to moderate effects on the prevention of death. The effects were inferior compared with the efficacy of VPT and DZ at all test doses. No doses of PGB as monotherapy in acute studies demonstrated a 100% prevention of death against PTZ. Moreover, the prevention of death with PGB monotherapy in the present study was dose-dependent. PGB demonstrated minimum prevention of death of 42% at 30 and 35 mg/kg, which was 58% less than both reference drugs. The prevention of death was enhanced to 50% at 40 mg/kg, 50% less than VPT and DZ. The maximum prevention of death of 67% by PGB was observed at the doses of 50 and 55 mg/kg in acute seizures but was 33% less than both reference drugs. The efficacy of PGB in acute seizures was 42% to 67% compared with the efficacy of VPT (Table 1, Figure 4).

Low-voltage-gated calcium channels have a wide distribution throughout the CNS and contribute to major processes like neuronal excitability and synaptic transmission.[39] Among the dihydropyridines, NMD blocks both the L- and T-type calcium channels.[40] The present study results suggest that the CCB NMD had some involvement in reducing seizures and the death rate, probably by inhibiting T-type low-voltage calcium channels. Therefore, the combination of PGB and NMD revealed greater antiepileptic activity compared with their individual effects at the same doses.

CONCLUSION

The antiepileptic combination used in the current study demonstrated marked seizure protection overall. However, PGB and NMD at the combination dose of 50+12.5 mg/kg showed maximum prevention of death, which was 83%. Therefore, it may be concluded that the CCB NMD exhibited anticonvulsant effects by potentiating the antiepileptic effects of PGB in the combination. The primary clinical importance of combination therapies would be a reduction in PGB doses with several times increase in efficacy.

The present study results provide clear evidence that the combination of PGB and NMD provides a better option to treat status epilepticus and typical and atypical epilepsies. The combination of PGB and NMD may have substantial potential to treat diverse types of epilepsies comprising resistant epilepsies due to channel-modifying effects. The major advantage of combination therapy would be the low doses of PGB with better anti-seizure effects. The essential point of this study is the use of combination regimens of PGB/NMD for the short- and long-term control of status epilepticus. However, this may require further animal and clinical studies.

Conflict of interest: No conflict of interest was declared by the authors. The authors are solely responsible for the content and writing of this paper.

REFERENCES

1. Hauser WA. Status epilepticus: frequency, etiology, and neurological sequelae. Adv Neurol. 1983;34:3-14.
2. Aminoff MJ, Simon RP. Status epilepticus: causes, clinical features and consequences in 98 patients. Am J Med. 1980;69:657-666.
3. Delgado-Escueta AV, Bajorek JG. Status epilepticus: mechanisms of brain damage and rational management. Epilepsia. 1982;23:S29-S41.
4. Alldredge BK, Gelb AM, Isaacs SM, Corry MD, Allen F, Ulrich S, Gottwald MD, O'Neil N, John M. Neuhaus JM, Segal MR and Lowenstein DH. A Comparison of Lorazepam, Diazepam, and Placebo for the Treatment of Out-of-Hospital Status Epilepticus. N Engl J Med. 2001;345:631-637.
5. Brophy GM, Bell R, Claassen J, Alldredge B, Bleck TP, Glauser T, Treiman DM. Guidelines for the evaluation and management of status epilepticus. Neurocrit Care. 2012;17:3-23.
6. Holopainen IE. Seizures in the developing brain: cellular and molecular mechanisms of neuronal damage, neurogenesis and cellular reorganization. Neurochem Int. 2008;52:935-947.
7. Shin HW, Davis R. Review of levetiracetam as a first line treatment in status epilepticus in the adult patients – what do we know so far? Front Neurol. 2013;4:111.
8. Triggle DJ. Calcium channel antagonists: clinical uses--past, present and future. Biochem Pharmacol. 2007;74:1-9.
9. Zapater P, Javaloy J, Román JF, Vidal MT, Horga JF. Anticonvulsant effects of nimodipine and two novel dihydropyridines (PCA 50922 and PCA 50941) against seizures elicited by pentylenetetrazole and electroconvulsive shock in mice. Brain Res. 1998;796:311-314.
10. Khosravani H, Zamponi GW. Voltage-gated calcium channels and idiopathic generalized epilepsies. Physiol Rev. 2006;86:941-966.
11. Iftinca MC, Zamponi GW. Regulation of neuronal T-type calcium channels. Trends Pharmacol Sci. 2009;30:32-40.
12. Knake S, Hamer HM, Rosenow F. Status epilepticus: A critical review. Epilepsy Behav. 2009;15:10-14.
13. Zamponi GW, Lory P, Perez-Reyes E. Role of voltage-gated calcium channels in epilepsy. Pflugers Arch. 2010;460:395-403.
14. Luszczki JJ, Trojnar MK, Trojnar MP, Kimber-Trojnar Z, Szostakiewicz B, Zadrozniak A, Borowicz KK, Czuczwar SJ. Effects of three calcium channel antagonists (amlodipine, diltiazem and verapamil) on the protective action of lamotrigine in the mouse maximal electroshock-induced seizure model. Pharmacol Rep. 2007;59:672-682.
15. Kamiński RM, Mazurek M, Turski WA, Kleinrok Z, Czuczwar SJ. Amlodipine enhances the activity of antiepileptic drugs against pentylenetetrazole-induced seizures. Pharmacol Biochem Behav. 2001;68:661-668.
16. Ryvlin P, Perucca E, Rheims S. Pregabalin for the management of partial epilepsy. Neuropsychiatr Dis Treat. 2008;4:1211-1224.
17. Toth C. Pregabalin: latest safety evidence and clinical implications for the management of neuropathic pain. Ther Adv Drug Saf. 2014;5:38-56.
18. Beydoun A, Uthman BM, Kugler AR, Greiner MJ, Knapp LE, Garofalo EA. Pregabalin 1008-009 study group. Safety and efficacy of two pregabalin regimens for add-on treatment of partial epilepsy. Neurology. 2005;64:475-480.
19. Council NR. Guide for the Care and Use of Laboratory Animals. 8th ed. The National Academic Press: Washington, DC;2011:6-47.
20. Mandhane SN, Aavula K, Rajamannar T. Timed pentylenetetrazol infusion test: a comparative analysis with s.c.PTZ and MES models of anticonvulsant screening in mice. Seizure. 2007;16:636-644.
21. Stafstrom CE. Mechanisms of action of antiepileptic drugs: the search for synergy. Curr Opin Neurol. 2010;23:157-163.
22. Rubio C, Rubio-Osornio M, Retana-Márquez S, Verónica Custodio ML, Paz C. *In vivo* experimental models of epilepsy. Cent Nerv Syst Agents Med Chem. 2010;10:298-309.
23. Loscher W. Critical review of current animal models of seizures and epilepsy used in the discovery and development of new antiepileptic drugs. Seizure. 2011;20:359-368.
24. Kandratavicius L, Balista PA, Lopes-Aguiar C, Ruggiero RN, Umeoka EH, Garcia-Cairasco N, Bueno-Junior LS, Leite JP. Animal models of epilepsy: use and limitations. Neuropsychiatr Dis Treat. 2014;10:1693-1705.
25. Grone BP and Baraban SC. Animal models in epilepsy research: legacies and new directions. Nat Neurosci. 2015;18:339-343.
26. Franco V, French JA, Perucca E. Challenges in the clinical development of new antiepileptic drugs. Pharmacol Res. 2016;103:95-104.

27. Moshe SL, Perucca E, Ryvlin P, Tomson T. Epilepsy: new advances. Lancet. 2015;385:884-898.

28. Czuczwar SJ, Borowicz KK. Polytherapy in epilepsy: the experimental evidence. Epilepsy Res. 2002;52:15-23.

29. Luszczki JJ, Czuczwar SJ. Isobolographic profile of interactions between tiagabine and gabapentin: A preclinical study. Naunyn-Schmiedeberg's Arch Pharmacol. 2004;369:434-446.

30. Luszczki JJ. Interactions of tiagabine with ethosuximide in the mouse pentylenetetrazole-induced seizure model: an isobolographic analysis for non-parallel dose-response relationship curves. Naunyn-Schmiedeberg's Arch Pharmacol. 2008;378:483-492.

31. Shneker BF, McAuley JW. Pregabalin: A new neuromodulator with broad therapeutic indications. Ann Pharmacother. 2005;39:2029-2037.

32. Sills GJ. The mechanisms of action of gabapentin and pregabalin. Curr Opin Pharmacol. 2006;6:108-113.

33. Arroyo S, Anhut H, Kugler AR, Lee CM, Knapp LE, Garofalo EA, Messmer S. Pregabalin add-on treatment: a randomized, double-blind, placebo-controlled and dose-response study in adults with partial seizures. Epilepsia. 2004;45:20-27.

34. Frampton JE, Foster RH. Pregabalin: in the treatment of postherpetic neuralgia. Drugs. 2005;65:111-118; discussion 119-120.

35. Bian F, Li Z, Offord J, Davis MD, McCormick J, Taylor CP, Walker LC. Calcium channel alpha 2-delta type 1 subunit is the major binding protein for pregabalin in neocortex, hippocampus, amygdala, and spinal cord: an *ex vivo* auto-radiographic study in alpha 2-delta type 1 genetically modified mice. Brain Res. 2006;1075:68-80.

36. Asconape JJ. Some common issues in the use of antiepileptic drugs. Semin Neurol. 2002;22:27-39.

37. Kulak W, Sobaniec W, Wojtal K, Czuczwar S. Calcium modulation in epilepsy. Pol J Pharmacol. 2004;56:29-41.

38. Khanna N, Bhalla S, Verma V and Sharma KK. Modulatory effects of nifedipine and nimodipine in experimental convulsions. Indian J Pharmacol. 2000;32:347-352.

39. Rajakulendran S, Hanna MG. The Role of Calcium Channels in Epilepsy. Cold Spring Harb Perspect Med. 2016;6:a022723.

40. Kopecky BJ, Liang R, Bao J. T-type Calcium Channel Blockers as Neuroprotective Agents. Pflugers Arch. 2014;466:757-765.

Turk J Pharm Sci 2021;18(4):405-409
DOI: 10.4274/tjps.galenos.2020.50024

ORIGINAL ARTICLE

Effects of Bee Propolis on FBG, HbA1c, and Insulin Resistance in Healthy Volunteers

Sağlıklı Gönüllülerde Arı Propolisinin FBG, HbA1c ve İnsülin Direnci Üzerine Etkileri

Fawaz A ALASSAF[1], Mahmood H M JASIM[2]*, Mohanad ALFAHAD[3], Mohannad E QAZZAZ[4], Mohammed N ABED[2], Imad A-J THANOON[5]

[1]Mosul University College of Pharmacy, Department of Pharmacology and Toxicology, Mosul, Iraq
[2]Mosul University College of Pharmacy, Department of Pharmaceutical Chemistry, Mosul, Iraq
[3]Mosul University College of Pharmacy, Department of Pharmaceutics, Mosul, Iraq
[4]Mosul University College of Pharmacy, Department of Pharmacognosy and Medicinal Plants, Mosul, Iraq
[5]Mosul University College of Medicine, Department of Pharmacology, Mosul, Iraq

ABSTRACT

Objectives: Bee propolis is a natural substance that is used in traditional medicine due to its versatile pharmacological actions. This study evaluates whether short term use of bee propolis supplementation could have an impact on glycemic control in healthy individuals.

Materials and Methods: A single daily dose of 1000 mg of bee propolis was administered orally to a total of 34 healthy individuals for 60 days. Body weight, body mass index (BMI), fasting blood glucose (FBG), glycosylated hemoglobin (HbA1c), and insulin resistance were measured in all participants before and after the use of bee propolis.

Results: The results of this study showed that bee propolis was associated with a significant increase in body weight and BMI of healthy volunteers. Bee propolis supplementation decreased FBG and HbA1c, but did not affect insulin resistance.

Conclusion: Based on these results, bee propolis supplementation has a potential effect on glycemic control in healthy individuals and this should be considered when using this supplement in medical conditions.

Key words: Bee propolis, insulin resistance, healthy volunteers, fasting blood glucose, natural products

ÖZ

Amaç: Arı propolisi, çok yönlü farmakolojik etkileri nedeniyle geleneksel tıpta kullanılan doğal bir maddedir. Bu çalışma, kısa süreli arı propolis takviyesi kullanımının sağlıklı bireylerde glisemik kontrol üzerinde bir etkisi olup olmadığını değerlendirmektedir.

Gereç ve Yöntemler: Toplam 34 sağlıklı bireye 60 gün boyunca günde tek doz 1000 mg arı propolisi oral yoldan verilmiştir. Arı propolisinin kullanımı öncesi ve sonrasında tüm katılımcılarda vücut ağırlığı, vücut kitle indeksi (VKİ), açlık kan şekeri (AKŞ), glikozile hemoglobin (HbA1c) ve insülin direnci ölçülmüştür.

Bulgular: Bu çalışmanın sonuçları, arı propolisinin sağlıklı gönüllülerin vücut ağırlığında ve VKİ'sinde belirgin bir artış ile ilişkili olduğunu göstermiştir. Arı propolisi takviyesi AKŞ ve HbA1c'yi azaltmış, ancak insülin direncini etkilememiştir.

Sonuç: Bu sonuçlara dayanarak, arı propolis takviyesinin sağlıklı bireylerde glisemik kontrol üzerinde potansiyel bir etkisi olduğu söylenebilir ve bu takviye tıbbi durumlarda kullanılırken bu dikkate alınmalıdır.

Anahtar kelimeler: Arı propolisi, insülin direnci, sağlıklı gönüllüler, açlık kan şekeri, doğal ürünler

***Correspondence:** mh.jasim@uomosul.edu.iq, **Phone:** +009647704503960, **ORCID-ID:** orcid.org/0000-0002-8198-8246

Received: 16.07.2020, **Accepted:** 08.09.2020

INTRODUCTION

Natural products are promising candidates for the development of new medications. Bee propolis is one such product. It is a resinous substance that is synthesized by bees from bees' wax and saliva combined with exudates from plants. Bees make use of their synthesized propolis for the building and maintenance of their hives.[1] Anciently, bee propolis has been used in traditional medicine for healing purposes, such as wound and ulcer healing.[2] The constituents of raw propolis are resins (50%), waxes (30%), essential oils (10%), pollen (5%), and various other organic compounds (5%). Chemically, bee propolis is composed of more than 300 natural ingredients, including coumarins, phenolic compounds and esters, flavonoids, steroids, aldehydes, amino acids sesquiterpenes, and stilbene terpenes.[3,4]

Bee propolis has become a healthy supplement, with several studies demonstrating an association of bee propolis consumption with remarkable biological and pharmacological effects. Bee propolis has demonstrated antimicrobial,[5] antiinflammatory,[6] antioxidant,[7] antiviral,[8] anticancer,[9] immunoregulatory actions,[10] and protective effects on the liver, pancreas, heart, and brain.[11,12] It has been documented that the main constituents of propolis responsible for its therapeutic effects include flavonoids, phenols, and aromatic compounds.[13] Flavonoids and phenolic compounds in bee propolis exhibit a potent antioxidant activity against oxygen radicals and protect biological membranes from lipid peroxidation.[14] Oxidative stress is involved, among others, in β-cell dysfunction, insulin resistance, and impaired glucose tolerance, and it poses a higher risk for the development of type 2 diabetes.[15,16] In this context, bee propolis can be considered for glycemic control because of its high antioxidant properties. More recently, studies have demonstrated that bee propolis results in a significant decrease in the blood glucose levels, serum glycosylated hemoglobin (HbA1c) levels, and serum insulin levels, with improvement of insulin resistance in patients with type 2 diabetes.[17,18]

The acclaimed beneficial effect of bee propolis in diabetes was the main motivation for conducting this study to ascertain the safety of this dietary supplement in non-diabetic individuals. Bee propolis is used by many healthy, or at least, non-diabetic people as a dietary supplement. Since it has shown some beneficial effects in people with diabetes, this study aimed to investigate the effects of bee propolis, if any, on fasting blood glucose (FBG), HbA1c, and insulin sensitivity in healthy subjects.

MATERIALS AND METHODS

Study design and methodology

This study was conducted in compliance with the research ethics standards of the institutional and national ethical committees. This study is also ethically compliant with the 1975 Helsinki declaration and its following revisions. Approval for conducting the study was obtained from the scientific and ethical committees at the College of Pharmacy, University of Mosul and Nineveh Health Directorate, respectively. The Scientific and Ethical Research Committee within Nineveh Health Directorate approved the study, with its session numbered 180 on January 02, 2019.

The study was conducted on apparently healthy volunteers of both genders who were aged between 25 and 40 years and had a body mass index (BMI) that ranged from 18.5 $kg.m^{-2}$ to 25 $kg.m^{-2}$ (Table 1). Subjects with BMI <18.5 kg/m^2 and >25 kg/m^2, those with FBG >120 $mg.dL^{-1}$, and those with chronic diseases or on dietary supplements were excluded from the study. Subjects were selected randomly from different levels of employees at the College of Pharmacy, University of Mosul. Volunteers were recruited for the study from January to April 2019. A convenient sample of 40 subjects was initially taken; however, 6 people were excluded from the study due to the lack of compliance. All participants involved in this study were well-informed of the approved study protocol and were asked to sign an informed consent form before taking part in the study. The participants received 60 capsules of 1000 mg of bee propolis (Woods Supplements, United Kingdom), which they were instructed to take for 2 months as a single daily dose. Before and after treatment with bee propolis, 5 mL venous blood samples were collected from each individual following a minimum of 8 hours fasting period between 9 am and 11 am. HbA1c test was performed using DCA Vantage Analyzer (Siemens®) and completed within 2 hours of blood collection.[19] For other tests, blood samples were centrifuged for 10 minutes at room temperature and serums were collected and stored at -20°C until the day of assay. FBG was measured using the hexokinase method with an automated analyzer (Cobas c111, Roche) following the manufacturer's instructions.[20,21] Serum insulin was measured using electro-chemiluminescence technology for immunoassay analysis (Cobas e 411 Roche).[22] FBG and serum insulin readings were used to calculate homeostasis model assessment-insulin resistance (HOMA-IR) according to the following equation:

$$\text{HOMA-IR} = \text{Fasting glucose (mg/dL)} \times \text{fasting insulin } (\mu U\ mL^{-1})/405.$$[23]

Statistical analysis

Data obtained from this study were normally distributed as all sample sets passed the D'Agostino & Pearson normality test. All results were presented as mean ± standard deviation. Student's paired t-test for single data comparison was performed using

Table 1. General characteristics of healthy volunteers

Parameters	Values
Age, (mean) years	36.88
Male, n	23
Female, n	11
Weight, (mean) kg	73.4
BMI, (mean) kg/m^2	24.2
Smoker, n	7

BMI: Body mass index

GraphPad Prism 8.0 software. Differences between means were considered significant at $p<0.05$.

RESULTS

Thirty-four healthy individuals aged 25-45 years were chosen according to the inclusion criteria of the current study. The mean age of participants was 36.88 years. Females represented 32.4% of the participants, whereas males represented 67.6% (Table 1). The effect of bee propolis on body weight and BMI after 60 days is shown in Figure 1. At the end of the study, the mean weight and mean BMI increased significantly from 73.4±7.2 to 74.8±7.5 kg and from 24.2±1.2 to 24.7±1.5 kg m^{-2} ($p<0.01$), respectively.

FBG, HbA1c, and serum insulin levels were measured at the onset of the study and on day 60 after the administration of bee propolis, as shown in Figure 2. There was significant reduction in the mean FBG level from 101.9±9.1 to 92.69±13 mg dL^{-1} ($p<0.01$) and in the mean HbA1c level from 5.1±0.3 to 4.8±0.4 ($p<0.01$) after consuming bee propolis for 60 days. Insulin levels (which reduced from 7.3±1.7 to 7.2±2, p=0.1) and HOMA-IR (which reduced from 1.7±06 to 1.66±0.6, p=0.1) were not significantly affected by the administration of bee propolis.

DISCUSSION

Globally, people consume dietary supplements to boost their health. The past 20 years have seen a widespread use of dietary supplements as these products provide several health benefits. Bee propolis is one of these natural dietary supplements that has several health-promoting effects, thereby making it gain high popularity recently. However, more studies are required to substantiate the contribution of bee propolis to human health.

In this study, it was observed that the daily administration of 1000 mg of bee propolis for 60 days resulted in an increase in body weight and BMI, with a reduction in FBG and HbA1c levels in healthy volunteers. This study did not find any significant change in human insulin level levels. Similarly, no significant effect of bee propolis on insulin resistance was observed.

This study has not validated the previous research on the effect of bee propolis on weight and BMI. Zakerkish et al.[17] and Samadi et al.[18] did not report any significant changes in body weight following the administration of bee propolis for 3 months in their clinical studies. Moreover, other studies demonstrated a weight loss in animals as a result of the laxative effect and prevention of intestinal fat absorption by bee propolis.[24,25] In the present study, the administration of bee propolis for 2 months was associated with a significant increase in body weight and BMI of the participants. One suggested mechanism is probably the propolis-stimulated hepatic glycolysis and glucose uptake by peripheral tissues via the increase of insulin-sensitive glucose transporter, which also has a beneficial effect on glycemic control.[26-28] In this study, it was observed that appetite was enhanced among the volunteers and this could be another possible mechanism for an increase in body weight and BMI.

The present study also demonstrated a favorable effect of bee propolis on FBG and HbA1c levels in healthy subjects; however, none of the subjects experienced hypoglycemic symptoms. This

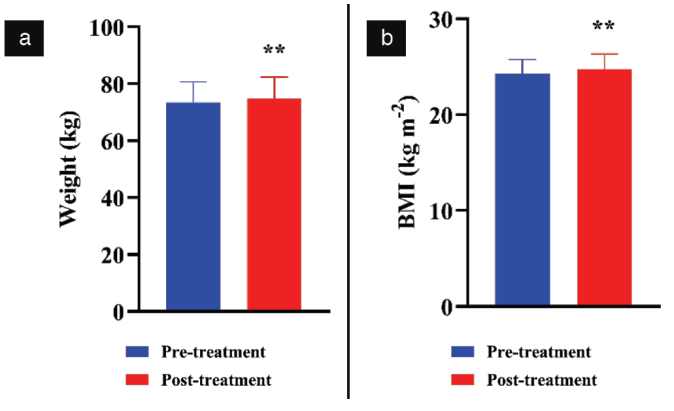

Figure 1. Effect of bee propolis treatment on body weight (a) and BMI (b). Bee propolis was administered orally as 1 gram per day for 60 days. The measurements were done before (pre-treatment) and after the bee propolis treatment (post-treatment). Data were presented as mean ± standard deviation

**P<0.01 indicates a difference with statistical significance (Student's paired t-test) between pre- and post-treatments, BMI: Body mass index

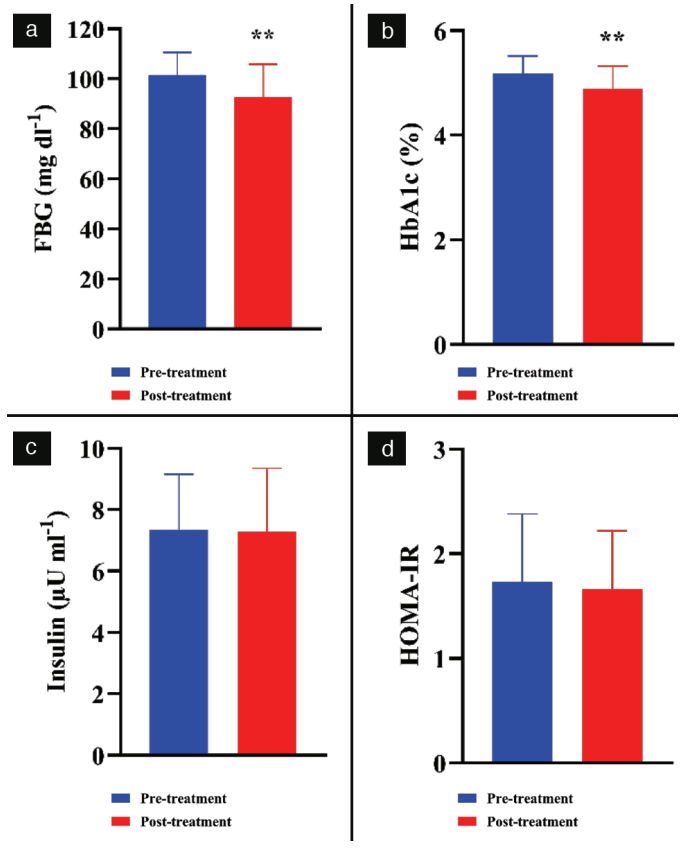

Figure 2. Effect of bee propolis treatment on FBG (a), HBA1c (b), serum insulin (c), and HOMA-IR (d). Bee propolis was administered orally as 1 gram per day for 60 days. Measurements were done before (pre-treatment) and after the bee propolis treatment (post-treatment). Data were presented as mean ± standard deviation

**P<0.01 indicates a difference with statistical significance (Student's paired t-test) between pre- and post-treatments, FBG: Fasting blood glucose, HBA1c: Glycosylated hemoglobin, HOMA-IR: Homeostasis model assessment-insulin resistance

is consistent with some studies that showed a reduction in FBG and HbA1c levels in type 2 diabetic patients.[17,18,29,30] As a possible mechanism, a decrease in intestinal glucose absorption due to reduction in carbohydrate digestion, which is attributed to the inhibition of intestinal α-glucosidase and sucrase by aqueous ethanolic propolis extract, was proposed.[26,31] Moreover, propolis extracts stimulate the β-cells of the islets of Langerhans, causing an enhancement of insulin secretion.[32]

Insulin is a pancreas-secreted hormone that is responsible for glucose utilization by body cells, consequently resulting in a decrease in blood glucose levels.[33] In this research, bee propolis was found to lower blood glucose levels. To ascertain whether this outcome was associated with the production of insulin, insulin levels and insulin resistance were determined and the results indicated that propolis had no effect on these parameters in healthy subjects. However, some studies demonstrated that prescribed propolis supplementation can significantly decrease the level of serum insulin and insulin resistance indices in patients with type 2 diabetes mellitus.[17,34-36] Zakerkish et al.[17] demonstrated that insulin levels and insulin resistance in patients with type 2 diabetes receiving propolis supplementations for 3 months were lower than those in healthy controls.

Furthermore, the present study did not show any gender-related difference in the results (data not shown) and this is in agreement with Jasprica et al.[37] who found that the levels of glucose, iron binding proteins, and uric acid, in addition to lipid profile parameters, were not different between men and women. However, in their study, there was a significant gender-based variation in the oxidative status and this was attributed to estrogen, which is known to exhibit a potent antioxidant effect in women.[37]

Study limitations

The sample size and the short time of data collection are the main limitations of this study, which suggest the need for future studies with extended period of propolis administration (more than 2 months) and larger sample size. However, based on our results, we recommend that the BMI and waist circumference of individuals receiving bee propolis should be monitored regularly. The bee propolis used in this study was supplied as a concentrate of whole propolis product prepared in the form of capsules and not as an extract of a single or few active compounds. Our rationale for this choice of formulation was that propolis effect may be obtained as a result of the synergistic action of its numerous components rather than one active compound. Nevertheless, future studies are still needed to identify the exact quantitative composition of the active compounds, and knowledge of the concentrations of the active components might further help to explain the obtained results.

CONCLUSION

This study revealed that a daily intake of 1000 mg of bee propolis supplements for 2 months is associated with an increase in body weight and BMI as well as a decrease in FBG and HbA1c levels in healthy individuals. Moreover, the possible long-term effects of increased weight or BMI could provoke insulin resistance, despite the fact that propolis enhanced glucose tolerance by increasing glucose uptake. Increased weight gain may be a result of this increased glucose uptake, and therefore, a vicious circle of events may be propagated, especially with enhanced appetite.

ACKNOWLEDGEMENTS

The authors are grateful to Dr. Ahmed Mohammed Ibrahim and Ms Merbad Momtaz at the University of Mosul, College of Pharmacy for their assistance in collecting blood samples from the volunteers. The contribution of the University of Mosul and the College of Pharmacy to the successful completion of this work is deeply appreciated by the authors.

Conflict of interest: No conflict of interest was declared by the authors. The authors are solely responsible for the content and writing of this paper.

REFERENCES

1. Búfalo MC, Candeias JM, Sforcin JM. *In vitro* cytotoxic effect of Brazilian green propolis on human laryngeal epidermoid carcinoma (HEp-2) cells. Evid Based Complement Alternat Med. 2009;6:483-487.
2. Ghisalberti EL. Propolis: A review. Bee World. 1979;60:59-84.
3. Burdock GA. Review of the biological properties and toxicity of bee propolis (propolis). Food Chem Toxicol. 1998;36:347-363.
4. Pietta PG, Gardana C, Pietta AM. Analytical methods for quality control of propolis. Fitoterapia. 2002;73(Suppl 1):S7-S20.
5. Verma MK, Pandey RK, Khanna R, Agarwal J. The antimicrobial effectiveness of 25% propolis extract in root canal irrigation of primary teeth. J Indian Soc Pedod Prev Dent. 2014;32:120-124.
6. Bueno-Silva B, Rosalen PL, Alencar SM, Mayer MPA. Anti-inflammatory mechanisms of neovestitol from Brazilian red propolis in LPS-activated macrophages. J Funct Foods. 2017;36:440-447.
7. Zhang J, Shen X, Wang K, Cao X, Zhang C, Zheng H, Hu F. Antioxidant activities and molecular mechanisms of the ethanol extracts of Baccharis propolis and Eucalyptus propolis in RAW64.7 cells. Pharm Biol. 2016;54:2220-2235.
8. Sartori G, Pesarico AP, Pinton S, Dobrachinski F, Roman SS, Pauletto F, Rodrigues LC Jr, Prigol M. Protective effect of brown Brazilian propolis against acute vaginal lesions caused by herpes simplex virus type 2 in mice: involvement of antioxidant and anti-inflammatory mechanisms. Cell Biochem Funct. 2012;30:1-10.
9. Demir S, Aliyazicioglu Y, Turan I, Misir S, Mentese A, Yaman SO, Akbulut K, Kilinc K, Deger O. Antiproliferative and proapoptotic activity of Turkish propolis on human lung cancer cell line. Nutr Cancer. 2016;68:165-172.
10. Orsatti CL, Missima F, Pagliarone AC, Bachiega TF, Búfalo MC, Araújo JP Jr, Sforcin JM. Propolis immunomodulatory action *in vivo* on Toll-like receptors 2 and 4 expression and on pro-inflammatory cytokines production in mice. Phytother Res. 2010;24:1141-1146.
11. Tolba MF, Azab SS, Khalifa AE, Abdel-Rahman SZ, Abdel-Naim AB. Caffeic acid phenethyl ester, a promising component of propolis with a plethora of biological activities: a review on its anti-inflammatory, neuroprotective, hepatoprotective, and cardioprotective effects. IUBMB Life. 2013;65:699-709.

12. Babatunde IR, Abdulbasit A, Oladayo MI, Olasile OI, Olamide FR, Gbolahan BW. Hepatoprotective and pancreatoprotective properties of the ethanolic extract of nigerian propolis. J Intercult Ethnopharmacol. 2015;4:102-108.

13. Toreti VC, Sato HH, Pastore GM, Park YK. Recent progress of propolis for its biological and chemical compositions and its botanical origin. Evid Based Complement Alternat Med. 2013;2013:697390.

14. Kolankaya D, Selmanoğlu G, Sorkun K, Salih B. Protective effects of Turkish propolis on alcohol-induced serum lipid changes and liver injury in male rats. Food Chem. 2002;78:213-217.

15. Szulińska M, Stępień M, Kręgielska-Narożna M, Suliburska J, Skrypnik D, Bąk-Sosnowska M, Kujawska-Łuczak M, Grzymisławska M, Bogdański P. Effects of green tea supplementation on inflammation markers, antioxidant status and blood pressure in NaCl-induced hypertensive rat model. Food Nutr Res. 2017;61:1295525.

16. Sun L, Dutta RK, Xie P, Kanwar YS. Myo-Inositol Oxygenase Overexpression Accentuates Generation of Reactive Oxygen Species and Exacerbates Cellular Injury following High Glucose Ambience: a new mechanism relevant to the pathogenesis of diabetic nephropathy. J Biol Chem. 2016;291:5688-5707.

17. Zakerkish M, Jenabi M, Zaeemzadeh N, Hemmati AA, Neisi N. the effect of iranian propolis on glucose metabolism, lipid profile, insulin resistance, renal function and inflammatory biomarkers in patients with type 2 diabetes mellitus: a randomized double-blind clinical trial. Sci Rep. 2019;9:7289.

18. Samadi N, Mozaffari-Khosravi H, Rahmanian M, Askarishahi M. Effects of bee propolis supplementation on glycemic control, lipid profile and insulin resistance indices in patients with type 2 diabetes: a randomized, double-blind clinical trial. J Integr Med. 2017;15:124-134.

19. Zercher A, Schulman S, Boone J. Quantitative measurement of hemoglobin A1c on the DCA Vantage Point-of-Care Analyzer as a diagnostic test for diabetes: An internal validation study. Clin Chem Lab Med. 2014:1-8.

20. Vanlin A. Applicable To Detail. Gundersen. 2018:2-5. Available from: https://www.gundersenhealth.org/app/files/public/6478/Lab-Policies-Glucose---Cobas-c-111-Lab-1587.pdf

21. Bowling JL, Katayev A. An evaluation of the Roche cobas c 111. Lab Med. 2010;41:398-402.

22. TechPubs. Ins - Insulin (ECLIA), #12017547122. 2010;(Ldl). Available from: https://healthabc.nia.nih.gov/sites/default/files/insulin on roche.pdf

23. Borai A, Livingstone C, Kaddam I, Ferns G. Selection of the appropriate method for the assessment of insulin resistance. BMC Med Res Methodol. 2011;11:158.

24. Koya-Miyata S, Arai N, Mizote A, Taniguchi Y, Ushio S, Iwaki K, Fukuda S. Propolis prevents diet-induced hyperlipidemia and mitigates weight gain in diet-induced obesity in mice. Biol Pharm Bull. 2009;32:2022-2028.

25. Sakai T, Ohhata M, Fujii M, Oda S, Kusaka Y, Matsumoto M, Nakamoto A, Taki T, Nakamoto M, Shuto E. Brazilian green propolis promotes weight loss and reduces fat accumulation in C57BL/6 mice fed a high-fat diet. Biol Pharm Bull. 2017;40:391-395.

26. Matsui T, Ebuchi S, Fujise T, Abesundara KJ, Doi S, Yamada H, Matsumoto K. Strong antihyperglycemic effects of water-soluble fraction of Brazilian propolis and its bioactive constituent, 3,4,5-tri-O-caffeoylquinic acid. Biol Pharm Bull. 2004;27:1797-1803.

27. Sameni HR, Ramhormozi P, Bandegi AR, Taherian AA, Mirmohammadkhani M, Safari M. Effects of ethanol extract of propolis on histopathological changes and anti-oxidant defense of kidney in a rat model for type 1 diabetes mellitus. J Diabetes Investig. 2016;7:506-513.

28. Al-Hariri M, Eldin TG, Abu-Hozaifa B, Elnour A. Glycemic control and anti-osteopathic effect of propolis in diabetic rats. Diabetes Metab Syndr Obes. 2011;4:377-384.

29. Li Y, Chen M, Xuan H, Hu F. Effects of encapsulated propolis on blood glycemic control, lipid metabolism, and insulin resistance in type 2 diabetes mellitus rats. Evid Based Complement Alternat Med. 2012;2012:981896.

30. Oladayo MI. Nigerian propolis improves blood glucose, glycated hemoglobin A1c, very low-density lipoprotein, and high-density lipoprotein levels in rat models of diabetes. J Intercult Ethnopharmacol. 2016;5:233-238.

31. Zhang H, Wang G, Beta T, Dong J. Inhibitory properties of aqueous ethanol extracts of propolis on alpha-glucosidase. Evid Based Complement Alternat Med. 2015;2015:587383.

32. Rivera-Yañez N, Rodriguez-Canales M, Nieto-Yañez O, Jimenez-Estrada M, Ibarra-Barajas M, Canales-Martinez MM, Rodriguez-Monroy MA. Hypoglycaemic and antioxidant effects of propolis of chihuahua in a model of experimental diabetes. Evid Based Complement Alternat Med. 2018;2018:4360356.

33. Joshi SR, Parikh RM, Das AK. Insulin--history, biochemistry, physiology and pharmacology. J Assoc Physicians India. 2007;55(Suppl):19-25.

34. Sforcin JM, Bankova V. Propolis: is there a potential for the development of new drugs? J Ethnopharmacol. 2011;133:253-260.

35. Kitamura H, Naoe Y, Kimura S, Miyamoto T, Okamoto S, Toda C, Shimamoto Y, Iwanaga T, Miyoshi I. Beneficial effects of Brazilian propolis on type 2 diabetes in ob/ob mice: possible involvement of immune cells in mesenteric adipose tissue. Adipocyte. 2013;2:227-236.

36. Aoi W, Hosogi S, Niisato N, Yokoyama N, Hayata H, Miyazaki H, Kusuzaki K, Fukuda T, Fukui M, Nakamura N, Marunaka Y. Improvement of insulin resistance, blood pressure and interstitial pH in early developmental stage of insulin resistance in OLETF rats by intake of propolis extracts. Biochem Biophys Res Commun. 2013;432:650-653.

37. Jasprica I, Mornar A, Debeljak Z, Smolcić-Bubalo A, Medić-Sarić M, Mayer L, Romić Z, Bućan K, Balog T, Sobocanec S, Sverko V. *In vivo* study of propolis supplementation effects on antioxidative status and red blood cells. J Ethnopharmacol. 2007;110:548-554.

Turk J Pharm Sci 2021;18(4):410-419
DOI: 10.4274/tjps.galenos.2020.70962

ORIGINAL ARTICLE

Development and Validation of a Stability-Indicating RP-HPLC Method for the Simultaneous Estimation of Bictegravir, Emtricitabine, and Tenofovir Alafenamide Fumarate

Biktegravir, Emtrisitabin ve Tenofovir Alafenamid Fumaratın Eşzamanlı Kestirimi için Stabilite Göstergeli RP-HPLC Yönteminin Geliştirilmesi ve Validasyonu

Tanuja ATTALURI[1]*, Ganapaty SERU[1], Satya Narayana Murthy VARANASI[2]

[1]Department of Pharmaceutical Analysis and Quality Assurance, Gitam Institute of Pharmacy, GITAM (Deemed to be University), Rushikonda, Visakhapatnam, India
[2]Dr. Reddy's Laboratories, Hyderabad, India

ABSTRACT

Objectives: The focal intent of the current research work is to develop and validate a novel and reliable stability-indicating reverse-phase high performance liquid chromatographic method for the simultaneous estimation of a few anti-retrovirals, i.e., bictegravir, emtricitabine, and tenofovir alafenamide fumarate (AF).

Materials and Methods: The novel method employs inertsil octyldecylsilyl C_{18} (4.6×250 mm, 5 mm) using 0.2% triethylamine buffer and methanol in a ratio of 40:60% (v/v) as the mobile phase to attain optimal elution. The detection wavelength was 260 nm with a 1.2 mL/min flow rate and a 20 µL injection volume.

Results: The linearity ranges for bictegravir, emtricitabine and tenofovir AF were 25-125 µg/mL, 100-500 µg/mL, and 12.5-62.5 µg/mL, respectively. The retention times for bictegravir, emtricitabine, and tenofovir AF were found to be 5.998 min, 2.805 min, and 4.537, min respectively. The percent recoveries of bictegravir, emtricitabine, and tenofovir AF were within the range of 98-102% w/w.

Conclusion: The novel method was successfully validated as per International Conference on Harmonization guidelines. In forced degradation studies, emtricitabine was found to be sensitive to thermal conditions; bictegravir and tenofovir AF, to oxidative conditions. The developed method is economical and reliable for routine analysis concerning all validated parameters.

Key words: Bictegravir, emtricitabine, tenofovir AF, RP-HPLC, validation, forced degradation studies

ÖZ

Amaç: Mevcut araştırma çalışmasının odak amacı, birkaç anti-retroviralin [biktegravir, emtrisitabin ve tenofovir alafenamid fumarat (AF)] eş zamanlı tahmini için yeni ve güvenilir bir stabilite gösteren ters fazlı yüksek performanslı sıvı kromatografik yöntemi geliştirmek ve doğrulamaktır.

Gereç ve Yöntemler: Yeni yöntem, optimal elüsyona ulaşmak için mobil faz olarak %0,2 trietilamin tamponu ve %40:60 (h/h) oranında metanol kullanan inertsil octyldesilsilil C_{18}'i (4,6×250 mm, 5 mm) kullanmaktadır. Deteksiyon dalga boyu 260 nm, akış hızı 1,2 mL/dk ve enjeksiyon hacmi 20 µL idi.

Bulgular: Biktegravir, emtrisitabin ve tenofovir AF'nin doğrusallık ranjı sırasıyla 25-125 µg/mL, 100-500 µg/mL ve 12.5-62.5 µg/mL idi. Biktegravir, emtrisitabin ve tenofovir AF'nin retansiyon zamanları sırasıyla 5,998 dk, 2,805 dk ve 4,537 idi. Biktegravir, emtrisitabin ve tenofovir AF'nin yüzde gerikazanımları %98-102 a/a aralığında idi.

Sonuç: Yeni yöntem, Uluslararası Uyumlaştırma Konferansı yönergelerine göre başarıyla doğrulanmıştır. Zorla bozunma çalışmalarında, emtrisitabin termal koşullara biktegravir ve tenofovir AF ise, oksidatif koşullara duyarlı olduğu bulunmuştur. Geliştirilen yöntem, tüm valide edilmiş parametrelerle ilgili rutin analizler için ekonomik ve güvenilirdir.

Anahtar kelimeler: Biktegravir, emtrisitabin, tenofovir AF, RP-HPLC, validasyon, zorla bozunma çalışmaları

***Correspondence:** attaluriswathi@gmail.com, **Phone:** 9014299789, **ORCID-ID:** orcid.org/0000-0001-7627-2625

Received: 26.04.2020, **Accepted:** 08.09.2020

INTRODUCTION

Human immunodeficiency virus (HIV) is a fatal viral infection that targets and alters the immune system, increasing the risk and impact of other infections and diseases. If left untreated, the infection might progress to an advanced disease stage called acquired immunodeficiency syndrome (AIDS). With the use of multiple specialized anti-retroviral medications that are commercially available, the state of HIV/AIDS infection can be controlled, de-escalated, and treated. Among numerous anti-retroviral formulations and combinations available, bictegravir is an oral tablet that contains three anti-retroviral drugs [bictegravir + emtricitabine + tenofovir alafenamide fumarate (AF)] under the brand name "BIKTARVY". Bictegravir belongs to the class of HIV-1 integrase strand transfer inhibitors (INSTIs); emtricitabine and tenofovir alafenamide, to the class of HIV-1 nucleoside analog reverse transcriptase inhibitors. Hence "BIKTARVY" can be considered as the sole regimen for HIV-1 (type 1) infected patients.[1-3] The INSTIs comprise two nucleoside reverse transcriptase inhibitors and recommended components during the initial stages of anti-retroviral therapy. Bictegravir is an effective INSTI with a high *in vitro* barrier that shows strong resistance toward the clinically relevant drug-drug interactions and possesses specific activity against HIV-1 and HIV-2. Bictegravir is metabolized by cytochrome P450 3A4 and a uridine diphosphate glucuronosyl transferase 1A1. It binds to the active site of HIV integrase and prevents HIV replication. Compared with other INSTIs, bictegravir possesses a high barrier to in vitro resistance and a lower potential to drug interactions among other readily available anti-retrovirals.[4,5] Emtricitabine and tenofovir AF act on DNA synthesis via HIV reverse transcriptase, resulting in viral DNA chain termination and preventing the replication of HIV.[6,7] The US Food and Drug Administration has approved "bictegravir" as a fixed-dose regimen (once daily) to treat HIV-1 infection.[8,9] The chemical structures of the three active pharmaceutical ingredients are shown in Figure 1-3. The dosage regimen is as follows:

Bictegravir (50 mg) + emtricitabine (20 mg) + tenofovir AF (25 mg).

According to the "Department of Health and Human Services",[10,11] the current combination regimen is intended to treat HIV-1 patients. Biktarvy can be administered with or without food and is not recommended with other anti-retrovirals.[12] A literature survey was performed, and very few stability-indicating reverse-phase high performance liquid chromatographic (HPLC) isocratic elution methods to estimate the drugs of interest are reported.

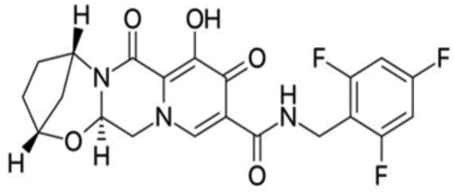

Figure 1. Bictegravir

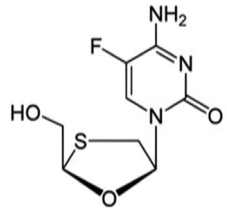

Figure 2. Emtricitabine

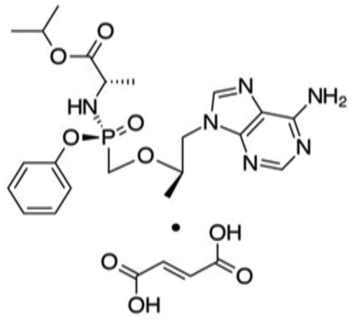

Figure 3. Tenofovir alafenamide fumarate

However, the available methods for determination of bictegravir, emtricitabine, and tenofovir AF in pharmaceutical formulations are scanty and vary in establishing multiple experimental variables during the validation of the method; the current method developed was found to be more sensitive and reliable. The details are outlined in Table 1.

Therefore, in the present work we developed a novel, reliable, and efficient method for the quantification of the drugs of interest. The stability of the drug indicates its shelf-life and bio-availability, which affect the chemical, pharmacological, and toxicological characteristics of the drug moieties; hence, stability studies were performed according to the International Conference on Harmonization (ICH) guidelines, and the results are reported.

MATERIALS AND METHODS

Experiment

Collection of drugs

Bictegravir of purity 99%w/w, emtricitabine of purity 99% w/w, and tenofovir AF of purity 99% w/w were procured from Hetero Labs, Hyderabad.

Chemicals and reagents

HPLC grade methanol (Rankem), Milli-Q grade water for HPLC (Merck), and HPLC grade triethylamine (Fine Chem Industries Research Laboratory) were used.

Apparatus

The HPLC WATERS system (2695 separation module 7 auto sampler) used in this method was equipped with a photodiode array (PDA) detector. Empower chromatography software (EMPOWER-2) was used for liquid chromatogram peak integration. Empower-2 software was used in data acquisition and processing.

Table 1. Comparison with similar existing methods

Kokkirala and Suryakala[13]	Sneha and Valli Kumari[14]	Sattar and Achanta[15]	Meenaksh and Shyam Sunder[16]	Current method	Remarks
Buffer and acetonitrile in a ratio of 50:50	Buffer and acetonitrile in a ratio of 55:45 v/v	Mobile phase ratio was (30:70 v/v) ortho-phosphoric acid buffer (adjust the pH 2.5 with NaOH solution): methanol	Buffer phosphoric dihydrogen phosphate as mobile phase A and methanol and water (70:30) as mobile phase B of the gradient program	0.2% triethylamine buffer and methanol in the ratio of 40:60 %v/v	Less expensive solvents were employed to obtain substantial results
C_{18} column (150 mm×4.6 mm, 5 µm)	Zodiac C_{18} 150×4.6 mm, 5 µm	Inspire C_{18} column (150×4.6 mm) 5.0 µm	Inertsil 30V C_{18} Column (250×4.6 mm, 5 µm)	Octyldecylsilyl C_{18} (4.6×250 mm, 5 µm)	Good peak shape and resolution acquired
272 nm	272 nm	272 nm	265 nm	260 nm	Detection of eluted peaks acquired at a shorter wavelength

a- The inertsil octadecylsilica (ODS) C_{18} (4.6×250 mm, 5 µm) column was found to be ideal for analyzing the selected drugs.

b- A rheodyne injector (20 µL loop) was used to inject the samples.

c- A ultraviolet (UV)-visible spectrophotometer (LABINDIA UV 300^{0+}) with UV Win software was used to establish the analytical wavelength.

d- Other instruments included an afcoset ER-200A electronic weighing balance, micropipettes, pipettes, burettes, micro-pore filtration assembly, ultra-sonic water bath for sonication of the mobile phase, and pH meter (Adwa-AD 1020).

Optimized chromatographic conditions

Once several trials had been conducted for optimization, the appropriate conditions were selected for the study, the details of which are as follows:

Instrument: HPLC (waters) with auto sampler

Detector: PDA detector

Temperature: Ambient

Column: ODS C_{18} (4.6×250 mm, 5 µm)

Mobile phase: 0.2% triethyl amine (TEA), buffer: Methanol (40:60 v/v)

Flow rate: 1.2 mL/min

Run time: 15 min

Wavelength: 260 nanometers (nm)

Preparation of 0.2% TEA buffer solution

TEA (2 mL) was measured accurately by pipetting into 1000 mL HPLC grade water and dissolved. The pH was adjusted to 3.5 with dilute formic acid.

Preparation of the mobile phase

Four hundred milliliters (40%) of the above-prepared buffer and 600 mL (60%) of methanol were measured accurately and mixed well.

Standard and sample preparation (emtricitabine, tenofovir AF, and bictegravir)

Standard preparation

Emtricitabine (100 mg), tenofovir AF (12.5 mg), and bictegravir (25 mg) working standards were weighed into a volumetric flask and added to 100 mL of diluent to makeup the volume. From the prepared stock solution, 3 mL was diluted to 10 mL. The resulting solution contained each of 300 ppm of emtricitabine, 37.5 ppm, of tenofovir AF, and 75 ppm of bictegravir.

Sample preparation

Ten tablets [prepared in-house by weighing the quantities as stated in the marketed formulation of emtricitabine (200 mg), tenofovir AF (25 mg), and bictegravir (50 mg)] were weighed accurately, and quantities equal to emtricitabine (100 mg), tenofovir AF (12.5 mg), and bictegravir (25 mg) samples were diluted to 100 mL. Three milliliters of each stock solution was diluted to 10 mL containing 300 ppm of emtricitabine, 37.5 ppm, of tenofovir AF, and 75 ppm of bictegravir.

Procedure

The % assay was estimated from the obtained peak areas of standard and sample using the formula:

$$\%\,Assay = \frac{AT}{AS} \times \frac{WS}{DS} \times \frac{DT}{WT} \times \frac{Average\ weight}{Label\ Claim} \times \frac{P}{100} \times 100$$

Where;

AT: Average area counts of test (sample) preparation.

AS: Average area counts of standard preparation.

WS: Weight of working standard taken in mg.

DS: Dilution of working standard in mL.

DT: Dilution of test (sample) in mL.

WT: Weight of test (sample) taken in mg.

P: Percentage purity of working standard.

Method validation

The analytical method validation for the developed method was implemented to ensure that the method meet the intended requirements as stated in the respective guidelines.[17] The results obtained for the method validation can be considered to determine the reliability and consistency of the developed method. The proposed method was validated according to the ICH guidelines with respect to the following parameters.[18-21]

Calibration curves were obtained at concentrations of 25-125 µg/mL for bictegravir, 100-500 µg/mL for Emtricitabine, and 12.5-62.5 µg/mL for tenofovir AF.

Linearity

Linearity can be illustrated by examining different concentrations of active pharmaceutical ingredients. The linearity of a method can be evaluated from the calibration plots of bictegravir, emtricitabine, and tenofovir AF constructed from peak response vs. concentration, which approaches a straight line.

Emtricitabine (100 mg), tenofovir AF (12.5 mg), and bictegravir (25 mg) were diluted to 100 mL. From this stock solution, 1-5 mL was pipetted into five different 10 mL volumetric flasks, and a series of aliquots was prepared and analyzed.

Accuracy

Accuracy was illustrated from the % recovery of standard containing known concentrations of active pharmaceutical ingredients.

Emtricitabine (100 mg), tenofovir AF (12.5 mg), and bictegravir (25 mg) working standards were diluted to 100 mL.

Three milliliters of the resulting stock solution was diluted to 10 mL. This solution thus contained emtricitabine (300 ppm), tenofovir AF (37.5 ppm), and bictegravir (75 ppm). The standard solutions for accuracy determination, 50%, 100%, and 150%, were prepared and injected, and the recovery values for emtricitabine, tenofovir AF, and bictegravir were calculated.

Precision

Precision was evaluated on the basis of the closeness between the obtained results.

Emtricitabine (100 mg), tenofovir AF (12.5 mg), and bictegravir (25 mg) working standards were diluted to 100 mL. Three milliliters of this stock solution was diluted to 10 mL.

Specificity

Specificity can be illustrated by ensuring that the peaks are free from interference.

It is determined by injecting a blank and a standard into the chromatographic system and corroborating that no interference exists.

Detection limit (DL) and quantification limit (QL)

DL and QL values deal with the method's sensitivity. DL is the analyte's lowest detectable concentration, while QL is the lowest quantifiable concentration.

DL

Emtricitabine (100 mg), tenofovir AF (12.5 mg), and bictegravir (25 mg) working standards were weighed and diluted separately to 100 mL. From this stock solution, 3 mL was diluted to 10 mL. From the above, 1 mL of each of the above stock solutions (emtricitabine, tenofovir AF, and bictegravir) was dispensed into different 10 mL volumetric flasks and diluted with diluent. Emtricitabine stock solution (0.35 mL), tenofovir AF (1 mL), and bictegravir stock (1 mL) solutions were further diluted to 10 mL.

QL

Emtricitabine (100 mg), tenofovir AF (12.5 mg), and bictegravir (25 mg) working standards were diluted to 100 mL. From the stock solution, 3 mL was diluted to 10 mL. Further, emtricitabine (1 mL), tenofovir AF stock (1 mL) solutions, and bictegravir stock solution (3 mL) were diluted to 10 mL. Further pipette emtricitabine stock (1.1 mL) solution, tenofovir AF (4.1 mL) and bictegravir stock solution (3.9 mL) were diluted to 10 mL.

Robustness

Robustness can be illustrated by evaluating the impact of deliberate changes on the proposed method.

Degradation studies

The guideline of the "ICH" entitled "Stability testing of new drug substances and products" states that stress testing is performed to evaluate the instinct stability attributes of the active pharmaceutical substance. Stress degradation studies on emtricitabine, tenofovir AF, and Bbictegravir[22-27] were performed in the current work.

Preparation of stock

Emtricitabine (100 mg), tenofovir AF (12.5 mg), and bictegravir (25 mg) working standards were weighed and diluted to 100 mL. The resulting stock solution was used for stability testing. All the stress conditions were applied, and the percent degradation was studied for the selected drugs bictegravir, emtricitabine, and tenofovir AF. The stress conditions include acidic, alkali, thermal, oxidative, and photolytic conditions to study the nature of drugs and their stability against the above-mentioned conditions.

Statistical analysis

The data were processed through the "EMPOWER-2". The results were calculated as mean ± standard deviation (SD) for accuracy, and the relative SD (RSD) was calculated for precision. The coefficient of regression was also calculated for the linearity parameter.

RESULTS AND DISCUSSION

Optimization of the method

For the selection of a suitable mobile phase for simultaneous estimation of the selected drugs, various solvents such as water, ACN, TEA, and methanol varying in polarity were used in different combinations of concentrations to obtain high peak resolutions within a shorter runtime. Among all the different

mobile phase combinations employed, the mobile phase comprising 0.2% TEA buffer and methanol in the ratio of 40:60 v/v exhibited well-defined peaks.

Different flow rates from 0.5 to 1.2 mL/min have been studied to achieve a good peak resolution. Among all the flow rates employed, 1.2 mL/min was selected as optimal for the study.

The column temperature was set at 25, 30, and 35°C for optimization, according to its effect on peak resolutions and RT of the drug samples.

During the method optimization, the selected combinations of three drugs were analyzed using different columns, the column [ODS C_{18} (4.6×250 mm, 5 μm)] that exhibited good peak shape and resolution was selected for current study. The details are specified in Table 2.

Also, based on the UV-absorption spectra of the three drugs scanned over the range of 200-400 nm, the wavelength of 260 nm was selected as the ideal wavelength for the study.

System suitability

According to the optimized experimental conditions, the retention times obtained for bictegravir, emtricitabine, and tenofovir AF are 5.998 min, 2.805 min, and 4.537 min. The optimized chromatogram with tailing factor (<2), theoretical plates (>2000), resolution (>2), capacitance factor (>1) is shown in (Figure 4). Hence, the proposed method proved "selective" to determine the drugs (bictegravir, emtricitabine, and tenofovir AF). The system suitability results of the standard injections are tabulated in Table 3.

Assay of marketed formulation

The assay results obtained for the three drugs (bictegravir, emtricitabine, and tenofovir AF) are detailed in Table 4. No interference of the excipients was noticed in the current method; hence, the method is "specific". The typical chromatogram for assay of the commercial formulation (in-house preparation) is shown in Figure 5.

Linearity

To construct the calibration curve, different concentration ranges of bictegravir (25-125 μg/mL), emtricitabine (100-500 μg/mL), and tenofovir AF (12.5-62.5 μg/mL) were considered. The correlation coefficient (r^2) values obtained were found satisfactory. The results obtained are summarized in Table 5. The calibration plots of three drugs are as shown in (Figure 6-8).

Table 2. Comparison of optimum conditions

S. no.	Column used	Specification	Remarks
1	Hypersil	5.0×250 mm, 10 μm	Deformed peak shape was observed
2	Lichrosorb	4.6×250 mm, 5 μm	Low resolution observed
3	Inertsil ODS C_{18}	4.6×250 mm, 5 μm	Peak shape is sharp and free from Tailing with high resolution

ODS: Octyldecylsilyl

Accuracy

Accuracy was determined at 50%, 100%, and 150% of the test concentrations by calculating the individual recovery and mean recovery values of emtricitabine, tenofovir AF, and bictegravir. The recoveries ranged from 99.26% to 100.30% for bictegravir, 99.06% to 100.79% for emtricitabine, and 99.66% to 100.06% for tenofovir AF. The recovery values obtained were found to meet the acceptance criteria (not less than 98.0% and not more than 102.0%). The RSD values obtained were <2 with respect to three drugs. The accuracy results are outlined in Table 6.

Precision

The precision for the developed method is estimated as follows:

- System precision
- Intermediate precision
- Method precision

System precision

The % RSD of six standard injection areas were found to be less than 2% (acceptance criteria: Not more than 2%), hence the method is "precise". The results for emtricitabine, tenofovir AF, and bictegravir are summarized in Table 7.

Intermediate precision/ruggedness

No significant effect was observed in the recoveries, the peak area responses of all the three drugs, thus indicating that the proposed and developed method is rugged.

The results are summarized for emtricitabine, tenofovir AF, and bictegravir in Table 8.

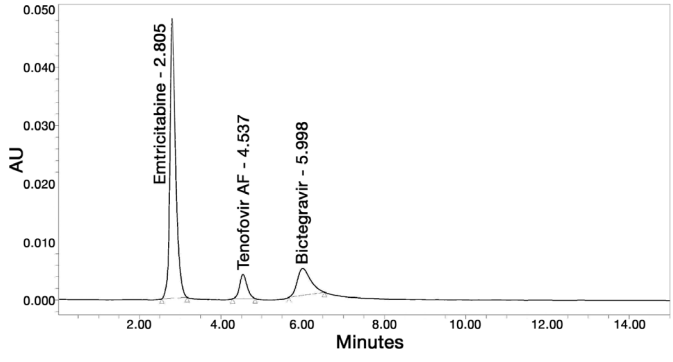

Figure 4. Optimized chromatogram showing the simultaneous elution of bictegravir, emtricitabine and tenofovir alafenamide fumarate

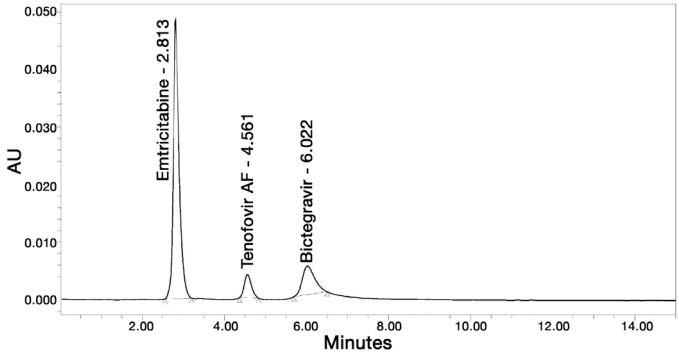

Figure 5. Assay chromatogram for marketed formulation of bictegravir, emtricitabine and tenofovir alafenamide fumarate

Table 3. System suitability results

S. no.	Parameter	Acceptance criteria	Bictegravir	Emtricitabine	Tenofovir alafenamide fumarate
1	Tailing factor	Not more than 2.0	1.33	1.30	1.13
2	Theoretical plates	Not less than 2000	2214.41	2185.90	2973.76
3	Resolution for the Tenofovir AF and bictegravir	Not less than 2	3.14	-	6.05
4	Capacitance factor	Not less than 1.0	4.36	1.54	3.09
5	Selectivity	Not more than 2.0	0.5	-	0.7

AF: Alafenamide

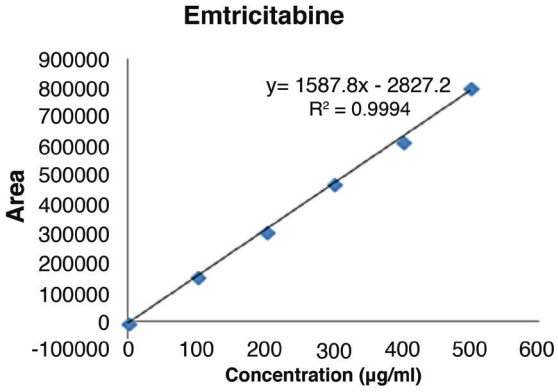

Figure 6. Linearity graph of emtricitabine

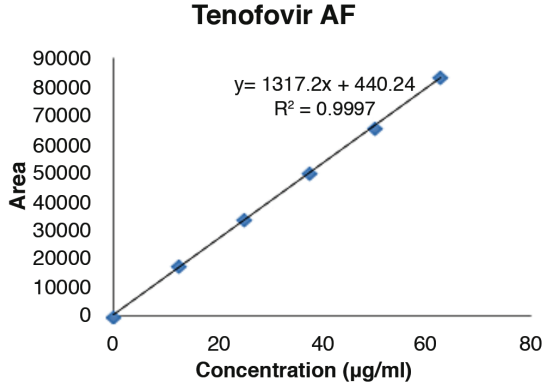

Figure 7. Linearity graph of tenofovir AF
AF: Alafenamide

Table 4. Assay results for % recoveries of marketed formulation

S. no.	Parameter	% Recovery of bictegravir	% Recovery of emtricitabine	% Recovery of tenofovir AF
1	Assay (specification: NLT 98.0 and NMT 102.0% w/w) (n=3)	99.97%	100.48%	99.82%

n: Number of determinations, NLT: Not less than, NMT: Not more than, AF: Alafenamide

Table 5. Results of linearity

S. no.	Parameters	Bictegravir	Emtricitabine	Tenofovir AF
1	Linearity range (µg/mL)	25-125	100-500	12.5-62.5
2	Correlation coefficient (r^2)	0.999	0.999	0.999
3	Slope	1287.3	1587.8	1317.2
4	Intercept	1224.6	2827.2	440.24

AF: Alafenamide

Table 6. Results of accuracy

S. no.	% Concentration (at specification level) (n=3)	% Recovery of bictegravir	% Recovery of emtricitabine	% Recovery of tenofovir AF
1	50%	99.26	100.44	100.06
2	100%	100.30	100.79	99.66
3	150%	100.01	99.06	99.75

n: Number of determinations, AF: Alafenamide

Method precision

To evaluate the method precision, the % assay was calculated from six individual samples solutions analyzed on same day. The % RSD obtained with respect to the results of the method precision met the acceptance criteria (not more than 2%), and the details of peak areas and % RSD values are summarized in Table 9.

Robustness

Robustness is defined as how the method can resist (less impact) small and deliberate changes in analytical procedure parameters such as the flow rate (±10%) and the organic phase composition (±10%). Minor changes did not affect the peak area responses of the method significantly; hence, the proposed method is robust.

The flow rate (1.08 mL/min and 1.32 mL/min) and organic phase composition (lesser to more organic) were altered, and there was no significant variation in the results obtained when deliberate changes were made to the developed method. The results obtained for the parameter robustness are summarized in Table 10-15.

DL and QL

DL and QL values were estimated using the formulas:

DL=3.3×(σ/S)

QL=10×(σ/S)

where;

σ=standard deviation;

S=slope.

The DL values for bictegravir, emtricitabine, and tenofovir AF obtained were 2.7, 1.05, and 1.35 µg/mL, with signal to noise ratio of 3:1, and the QL values for bictegravir, emtricitabine, and tenofovir AF obtained were 8.78, 3.30, and 4.61 µg/mL, with a signal to noise ratio of 10:1, which indicates that the "sensitivity" of the method is adequate. The results are summarized in Table 16.

Hydrolytic degradation under acidic conditions

To 3.0 mL of the stock solution, 3 mL of 1N HCl was added, diluted to 10 mL, and incubated at 60°C for 6 hours. The resulting solution was neutralized with 1N NaOH and adjusted to the mark with the diluent. There was no remarkable acid degradation with respect to the subject drugs, and the chromatogram is shown in Figure 9.

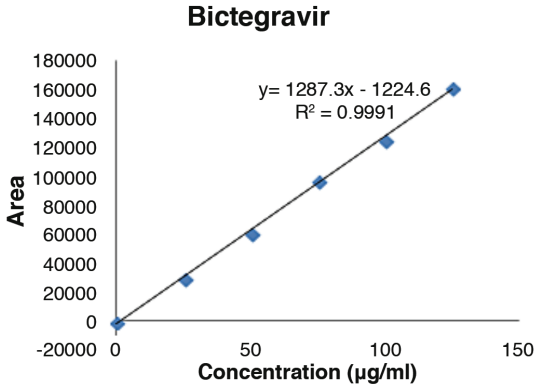

Figure 8. Linearity graph of bictegravir

Table 7. Results of system precision

Injection	Peak areas		
	Emtricitabine	Tenofovir AF	Bictegravir
Injection-1	4,74.652	50.304	97.274
Injection-2	4,70.806	50.532	96.658
Injection-3	4,79.900	50.680	97.574
Injection-4	4,73.621	50.727	97.021
Injection-5	4,75.167	50.255	98.232
Injection-6	4,76,538	50.235	97,987
Average	4,75,114.0	50,455.5	97,457.7
Standard deviation	3,031.1	219.9	592.8
% RSD (n=6)	0.6	0.4	0.6

n: Number of determinations, RSD: Relative standard deviation, AF: Alafenamide

Hydrolytic degradation under alkaline conditions

To 3.0 mL of the stock solution, 1N NaOH (3 mL) was added, diluted to 10 mL, and incubated at 60°C for 6 hours. Later, the solution was neutralized with 1N HCl. There was no significant degradation with respect to the three drugs, and the chromatogram obtained for alkali degradation is shown in Figure 10.

Thermal-induced degradation

The subject samples were placed separately in Petri dishes and remained in an oven at 110°C for a period of 24 hours. There was a minimal effect of thermal degradation

Table 8. Results of intermediate precision/ruggedness

Injection	Peak areas		
	Emtricitabine	Tenofovir AF	Bictegravir
Injection-1	4,77.752	49.821	97.234
Injection-2	4,74.159	50.388	96.991
Injection-3	4,69.272	50.289	95.433
Injection-4	4,69,317	50.176	96.414
Injection-5	4,77.171	50.337	97.491
Injection-6	4,73.102	50.073	97.166
Average	4,73,462.2	50.180.7	96,788.2
Standard deviation	3,674.6	209.8	755.4
% RSD (n=6)	0.8	0.4	0.8

n: Number of determinations, RSD: Relative standard deviation, AF: Alafenamide

Table 9. Results for method precision

Parameter	Sample weight (mg)	Peak areas		
		Emtricitabine	Tenofovir AF	Bictegravir
Method precision-1	174.2	4,75.652	50.166	97.455
Method precision-2	174.5	4,76.888	50.425	97.563
Method precision-3	174.1	4,75.988	50.253	97.234
Method precision-4	174.3	4,75.377	50.497	97.331
Method precision-5	174.2	4,76.765	50.556	97.548
Method precision-6	174.3	4,76.653	50.335	97.397
Average	-	4,76,220.5	50,372.0	97,421.3
Standard deviation	-	635.3	148.5	127.4
% RSD (n=6)	-	0.1	0.3	0.1

n: Number of determinations, RSD: Relative standard deviation, AF: Alafenamide

with respect to the drug emtricitabine and no significant effect with respect to bictegravir and tenofovir AF. The chromatogram obtained for thermal degradation is shown in (Figure 11).

Oxidative degradation

To the above stock solution, 3 mL of 3% (w/v) hydrogen peroxide (1 mL) was added in a 10 mL, and the flask was retained at ambient temperature for 12 minutes. There was a minimal effect of thermal degradation on bictegravir and tenofovir AF and no significant effect noticed with respect to emtricitabine. The chromatogram obtained for the oxidative degradation is shown in (Figure 12).

Photo degradation

The sample solution was exposed to external sunlight. No significant degradation was noticed with respect to the subject drugs, and the chromatogram obtained for the photolytic degradation is shown in (Figure 13).

A stability study was conducted for the drugs emtricitabine, tenofovir AF, and bictegravir under the respective stress conditions. The peak areas obtained, the % assay calculated,

Table 10. System suitability results for emtricitabine at a flow rate variation of ±10%

S. no.	Flow rate (mL/min)	System suitability results	
		USP tailing (T_f)	USP plate count (N)
1	1.08	1.37	2371.09
2	1.2	1.30	2185.90
3	1.32	1.31	2231.87

T_f: Tailing factor

Table 11. System suitability results for tenofovir AF at a flow rate variation of ±10%

S. no.	Flow rate (mL/min)	System suitability results		
		USP resolution (R)	USP tailing (T_f)	USP plate count (N)
1	1.08	6.32	1.25	3223.82
2	1.2	6.05	1.13	2973.76
3	1.32	6.07	1.06	2863.39

AF: Alafenamide, T_f: Tailing factor

Table 12. System suitability results for bictegravir at a flow rate variation of ±10%

S. no.	Flow rate (mL/min)	System suitability results		
		USP resolution (R)	USP tailing (T_f)	USP plate count (N)
1	1.08	3.28	1.31	2143.54
2	1.2	3.14	1.33	2214.41
3	1.32	3.20	1.40	2183.37

T_f: Tailing factor

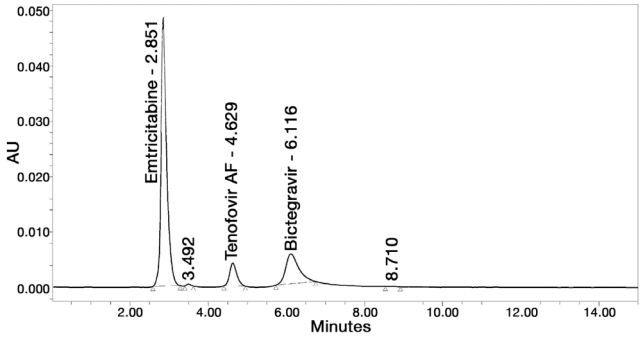

Figure 9. Acidic degradation chromatogram of bictegravir, emtricitabine and tenofovir alafenamide fumarate

AF: Alafenamide

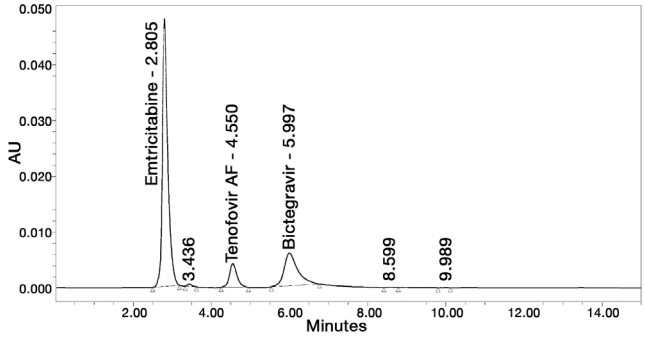

Figure 10. Alkali degradation chromatogram of bictegravir, emtricitabine and tenofovir alafenamide fumarate

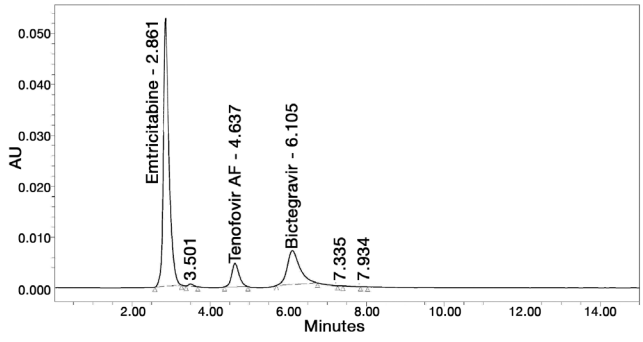

Figure 11. Thermal degradation chromatogram of bictegravir, emtricitabine and tenofovir alafenamide fumarate

AF: Alafenamide

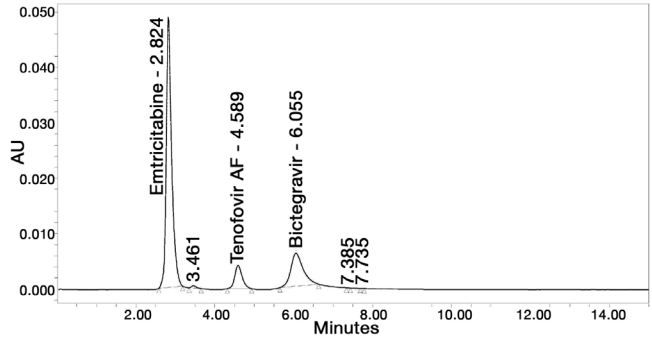

Figure 12. Oxidative degradation chromatogram of bictegravir, emtricitabine and tenofovir alafenamide fumarate

AF: Alafenamide

Table 13. System suitability results for emtricitabine at variation of the organic phase ±10%

S. no.	Organic phase ratio	System suitability results	
		USP tailing (T_f)	USP plate count (N)
1	Less organic	1.38	2254.66
2	Actual	1.30	2185.90
3	More organic	1.32	2263.23

T_f: Tailing factor

Table 14. System suitability results for tenofovir AF at variation of the organic phase ±10%

S. no.	Organic phase ratio	System suitability results		
		USP resolution (R)	USP tailing (T_f)	USP plate count (N)
1	Less organic	9.22	1.05	3228.79
2	Actual	6.05	1.13	2973.76
3	More organic	4.09	1.26	2672.79

T_f: Tailing factor, AF: Alafenamide

Table 15. System suitability results for bictegravir at variation of the organic phase ±10%

S. no.	Organic phase ratio	System suitability results		
		USP resolution	USP tailing	USP plate count
1	Less organic	4.65	1.10	2113.59
2	Actual	3.14	1.33	2214.41
3	More organic	2.16	1.49	2195.87

Table 16. Results of detection limit and quantification limit

S. no.	Sample	DL (µg/mL)	QL (µg/mL)	DL S/N ratio	QL S/N ratio
1	Bictegravir	2.7	8.78	3.02	10
2	Emtricitabine	1.05	3.30	3	9.98
3	Tenofovir AF	1.35	4.61	2.96	10.02

DL: Detection limit, QL: Quantification limit, S: Selectivity

Table 17. Results of % degradation by stability testing

	Emtricitabine			Tenofovir AF			Bictegravir		
	Area	% assay	% degradation	Area	% assay	% degradation	Area	% assay	% degradation
Standard	4,71,374.3	100	-	50,381.7	100	-	97,131.3	100	-
Acid	4,62.673	98.15	1.85	49.565	98.38	1.62	95.766	98.59	1.41
Base	4,59.782	97.54	2.46	48.566	96.40	3.60	94.866	97.67	2.33
Peroxide	4,52.736	96.05	3.95	47.687	94.65	5.35	93.145	95.90	4.10
Thermal	4,47.733	94.98	5.02	48.446	96.16	3.84	94.577	97.37	2.63
Photo	4,53.888	96.29	3.71	48.675	96.61	3.39	93.766	96.54	3.46

AF: Alafenamide

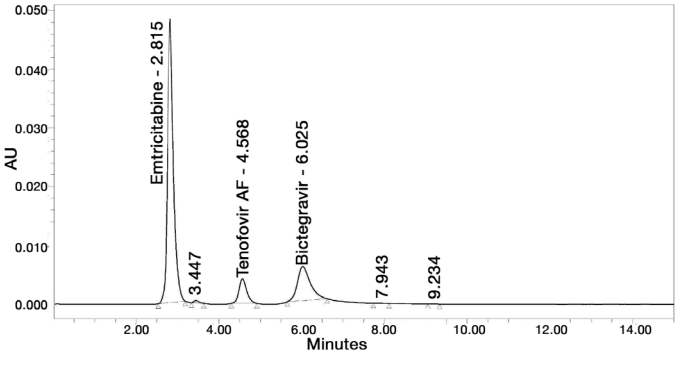

Figure 13. Photolytic degradation chromatogram of bictegravir, emtricitabine & tenofovir alafenamide fumarate

AF: Alafenamide

and the % degradation observed are summarized and detailed in Table 17. From the above data, it is evident that the drug "emtricitabine" is sensitive to thermal conditions, "tenofovir AF" and "bictegravir" are sensitive to oxidative conditions.

CONCLUSION

The newly developed method affirms good resolution between the three drugs bictegravir, emtricitabine, and tenofovir AF. The current method, method validation, and stability studies were found to be in line with the ICH guidelines and with official methods. The method requires no core extraction techniques; moreover, economical solvents are employed for the analysis, and good resolution is attained. No interference from any pharmaceutical dosage form or any remarkable impurities of degraded substance(s) was observed. Since the subject drugs of interest were analyzed by employing less expensive solvents and obtaining high resolution and shorter retention times with respect to the current method, the new proposed method is recommended for routine quality control analysis to provide simple, reliable, economical, and reproducible quantitative analysis for simultaneous estimation of the selected anti-retroviral fixed-dose regimen (bictegravir, emtricitabine, and tenofovir AF).

ACKNOWLEDGMENTS

Authors extend intense gratitude to M/S Pharma Train Labs, Hyderabad for providing the required research facilities and to Hetero Labs, Hyderabad for providing gift samples of bictegravir, emtricitabine and tenofovir AF.

Conflict of interest: No conflict of interest was declared by the authors. The authors are solely responsible for the content and writing of this paper.

REFERENCES

1. Atkinson MJ, Petrozzino JJ. An evidence-based review of treatment-related determinants of patients' nonadherence to HIV medications. AIDS Patient Care STDs. 2009;23:903-914.
2. Hester EK. HIV medications: an update and review of metabolic complications. Nutr Clin Pract. 2012;27:51-64.
3. Margolis AM, Heverling H, Pham PA, Stolbach A. A review of the toxicity of HIV medications. J Med Toxicol. 2014;10:26-39.
4. Tsiang M, Jones GS, Goldsmith J, Mulato A, Hansen D, Kan E, Tsai L, Bam RA, Stepan G, Stray KM, Niedziela-Majka A. Antiviral activity of bictegravir (GS-9883), a novel potent HIV-1 integrase strand transfer inhibitor with an improved resistance profile. Antimicrobial Agents Chemother. 2016;60:7086-7097.
5. Hassounah SA, Alikhani A, Oliveira M, Bharaj S, Ibanescu RI, Osman N, Xu HT, Brenner BG, Mesplède T, Wainberg MA. Antiviral activity of bictegravir and cabotegravir against integrase inhibitor-resistant SIVmac239 and HIV-1. Antimicrobial Agents Chemother. 2017;61:e01695-17. doi: 10.1128/AAC.01695-17.
6. Neogi U, Singh K, Aralaguppe SG, Rogers LC, T NJENDA D, Sarafianos SG, Hejdeman B, Sönnerborg A. Ex vivo antiretroviral potency of newer integrase strand transfer inhibitors cabotegravir and bictegravir in HIV-1 non-B subtypes. AIDS (London, England). 2018;32:469.
7. Pharmaceutical Benefits Scheme. Summary of Changes (March 2019). Canberra: Department of Health, 2019. Last Accessed Date: 16.04.2019. Available from: https://www.pbs.gov.au/info/publication/schedule/archive
8. Pharmaceutical Benefits Scheme. PBS Schedule: Bictegravir + emtricitabine + tenofovir alafenamide. Canberra: Department of Health, 2019. Last Accessed Date: 16.04.2019. Available from: https://www.pbs.gov.au/medicine/item/11649D
9. Pharmaceutical Benefits Scheme. Public Summary Documents: Bictegravir + emtricitabine + tenofovir alafenamide fixed dose combination (March 2018). Canberra: Department of Health, 2018. Last Accessed Date: 20.02.2019.Available from: https://www.pbs.gov.au/pbs/industry/listing/elements/pbac-meetings/psd/2018-03/bictegravir-emtricitabine--psd-march-2018
10. Gilead Sciences Pty Ltd. Bictegravir + emtricitabine + tenofovir alafenamide (Biktarvy) product information. Melbourne: Gilead Sciences, 2018. Last Accessed Date: 20.02.2019. Available from: https://www.tga.gov.au/sites/default/files/auspar-bictegravir-emtricitabine-tenofovir-alafenamide-190801-pi.pdf
11. Stellbrink HJ, Lazzarin A, Woolley I, Llibre JM. The potential role of bictegravir/emtricitabine/tenofovir alafenamide (BIC/FTC/TAF) single-tablet regimen in the expanding spectrum of fixed-dose combination therapy for HIV. HIV medicine. 2020 Mar;21:3-16.
12. Jules Levin, Kirsten White, Tomas Cihlar and Michael D. Miller, Potent Activity of Bictegravir (BIC; GS-9883), a Novel Unboosted HIV-1 Integrase Strand Transfer Inhibitor (INSTI), Against Patient Isolates with INSTI-Resistance ASM/ICAAC 2016 June 16-20 Boston, MA.
13. Kokkirala TK, Suryakala D. RP-HPLC method development and validation for the estimation of Emtricitabine, Bictegravir and Tenofovir alafenamide in bulk and pharmaceutical dosage form. J Taibah Univ Sci. 2019;13:1137-1146.
14. Sneha M, Valli Kumari RV Stability indicating RP-HPLC method for simultaneous estimation of emtricitabine, bictegravir and tenofovir alafenamide in bulk and formulation. Int J Pharm Anal Res. 2019;8:281-292.
15. Sattar MA, Achanta S. Analytical method development and validation for the determination of emtricitabine and tenofovir disoproxil fumarate using reverse phase hplc method in bulk and tablet dosage form. J Pharm Sci Res. 2018;10:1207-1212.
16. Meenaksh R, Shyam Sunder R. Method development and validation by RP-HPLC for simultaneous estimation of emtricitabine, bictegravir, tenofovir alafenamide in fixed dosag. Indo Am J Pharm Sci. 2018;5:7123-7131.
17. Dighe NS, Shinde GS, Magar SD, Deodhe AV. Development and validation of RP-HPLC method for simultaneous estimation of emtricitabine and tenofovir disoproxil fumarate in bulk and tablet dosage form. J Drug Deliv Ther. 2019;9:693-698.
18. Kalamkar CS, Bhawar SB. Development and validation of RP-HPLC method for the simultaneous estimation of tenofovir alafenamide fumarate and emtricitabine in bulk and tablet dosage form. J Drug Deliv Ther. 2019;9:243-247.
19. Liao C, Marchand C, Burke Jr TR, Pommier Y, Nicklaus MC. Authentic HIV-1 integrase inhibitors. Future Med Chem. 2010;2:1107-1122.
20. Carr GP, Wahlich JC. A practical approach to method validation in pharmaceutical analysis. J Pharm Biomed Anal. 1990;8:613-618.
21. Asian Rockville MD. The United States Pharmacopeia: USP 24: the National Formulary: NF 19: by authority of the United States Pharmacopoeial Convention, Inc., meeting at Washington, D.C., March 9-12, 1995 ; prepared by the Committee of Revision and published by the Board of Trustees. Washington: United States Pharmacopoeia Convention Inc; 2000.
22. ICH. "International Conference on Harmonization of Technical Requirements for Registration of Pharmaceuticals for Human Use. Validation of Analytical Procedures: Text and Methodology". 2005.
23. Procedures, Analytical. "Method Validation. US Food and Drug Administration." Center for Drugs and Biologics, Department of Health and Human Services 2000.
24. Blessy MR, Patel RD, Prajapati PN, Agrawal YK. Development of forced degradation and stability indicating studies of drugs—a review. J Pharm Anal. 2014;4:159-165.
25. Venkataraman S, Manasa M. Forced degradation studies: Regulatory guidance, characterization of drugs, and their degradation products-a review. Drug Invention Today. 2018;10:137-146.
26. Aggarwal NN, Bhat KI, Jacob JT. Stability indicating assay method development and validation for tenofovir alafenamide fumarate by RP-HPLC. Pharm Anal Acta. 2018;9:601.
27. Vetapalem R, Yejella RP, Atmakuri LR. Development and validation of a stability indicating RP-HPLC method for simultaneous estimation of teneligliptin and metformin. Turk J Pharm Sci. 2020;17:141-147.

Turk J Pharm Sci 2021;18(4):420-429
DOI: 10.4274/tjps.galenos.2020.69008

ORIGINAL ARTICLE

Effects of Oleuropein on Epirubicin and Cyclophosphamide Combination Treatment in Rats

Oleuropeinin Sıçanlarda Epirubisin ve Siklofosfamid Kombinasyon Tedavisi Üzerine Etkileri

Metin Deniz KARAKOÇ[1]*, Selim SEKKİN[2]

[1]Aydın Adnan Menderes University Health Sciences Institute, Department of Pharmacology and Toxicology, Aydın, Turkey
[2]Aydın Adnan Menderes University Faculty of Veterinary Medicine, Department of Pharmacology and Toxicology, Aydın, Turkey

ABSTRACT

Objectives: Oleuropein is the main bioactive polyphenolic compound in olive leaves, olive, and olive oil. Its anticancer, antioxidant, and antiinflammatory effects have been proven through several *in vitro* and *in vivo* studies. This study aimed to explore the effects of oleuropein on cyclophosphamide- and epirubicin-induced toxicity in female rats.

Materials and Methods: Seven groups containing eight rats in each group were formed. Four cycles of 16 mg/kg/week of cyclophosphamide and 2.5 mg/kg/week of epirubicin were administered to the rats through intraperitoneal injection. Oleuropein (150 mg/kg/week) was simultaneously applied via oral gavage. The effects of oleuropein were examined with hemogram tests in whole blood samples and biochemical analysis in serum samples. Interleukin-6 (IL-6) and tumor necrosis factor-α (TNF-α) in the serum samples were analyzed through enzyme-linked immunosorbent assay. Subsequently, a comet assay was performed using lymphocyte DNA. The levels of oxidant [i.e., malondialdehyde (MDA)] and antioxidants [i.e., catalase (CAT), glutathione (GSH), and superoxide dismutase (SOD)] were measured in the heart, kidney, and liver tissues.

Results: Oleuropein could reduce DNA damage and serum TNF-α and IL-6 levels. It also ameliorated some hemogram and biochemical parameters that deteriorated due to antineoplastic drugs. It increased the amounts of antioxidants (GSH, SOD, and CAT) and reduced the level of MDA in the heart, kidney, and liver tissues.

Conclusion: Oleuropein might be a beneficial agent against toxicity caused by the combination treatment of cyclophosphamide and epirubicin. Further studies should be performed to demonstrate the protective effects of oleuropein against antineoplastic induced-toxicity precisely.

Key words: Oleuropein, epirubicin, cyclophosphamide, toxicity, oxidative stress

ÖZ

Amaç: Oleuropein zeytin yaprağı, zeytin meyvesi ve zeytinyağında bulunan başlıca biyoaktif polifenolik bileşiktir. Antikanser, antioksidan ve antienflamatuvar etkileri birçok *in vitro* ve *in vivo* çalışmayla doğrulanmıştır. Bu çalışma, oleuropeinin siklofosfamid ve epirubisin kaynaklı toksisite üzerindeki etkilerini dişi sıçanlarda araştırmayı amaçlanmıştır.

Gereç ve Yöntemler: Her grupta sekiz sıçan içeren yedi grup oluşturulmuştur. Sıçanlara intraperitoneal enjeksiyon yoluyla dört döngü 16 mg/kg/hafta siklofosfamid ve 2,5 mg/kg/hafta epirubisin uygulanmıştır. Oleuropein (150 mg/kg/hafta) eş zamanlı olarak oral gavaj yoluyla verilmiştir. Oleuropeinin etkileri tam kan örneklerinde hemogram testleri ve serum örneklerinde biyokimyasal analizlerle incelenmiştir. Serum numunelerindeki interlökin-6 (IL-6) ve tümör nekroz faktörü-α (TNF-α), enzime bağlı immünosorbent yöntemi ile analiz edilmiştir.

Ardından, lenfosit DNA'sı kullanılarak Comet yöntemi gerçekleştirilmiştir. Son olarak, kalp, böbrek ve karaciğer dokularında oksidan [malondialdehit (MDA)] ve antioksidan [katalaz (CAT), süperoksit dismutaz (SOD) ve glutatyon (GSH)] parametreler ölçülmüştür.

Bulgular: Oleuropeinin, DNA hasarını ve TNF-α ile IL-6 gibi proenflamatuvar sitokinlerin serum düzeylerini azaltabildiği belirlenmiştir. Ayrıca, oleuropeinin antineoplastik ilaçlara bağlı olarak bozulan bazı hemogram ve biyokimyasal parametrelerini düzelttiği tespit edilmiştir. Ayrıca, oleuropeinin kalp, böbrek ve karaciğer dokularında antioksidan parametrelerde (GSH, SOD ve CAT) artışa neden olduğu ve MDA miktarını azalttığı belirlenmiştir.

Sonuç: Oleuropein, siklofosfamid ve epirubisinin kombinasyon tedavisinin neden olduğu toksisiteye karşı faydalı bir ajan olabilir. Oleuropeinin antineoplastik kaynaklı toksisiteye karşı koruyucu etkilerini tam olarak göstermek için daha ileri çalışmalar yapılmalıdır.

Anahtar kelimeler: Oleuropein, epirubisin, siklofosfamid, toksisite, oksidatif stres

***Correspondence:** mdkarakoc@gmail.com, **Phone:** +90 258 263 93 11, **ORCID-ID:** orcid.org/0000-0003-3188-8738

Received: 25.06.2020, **Accepted:** 24.09.2020

INTRODUCTION

Breast tumors are the most frequently diagnosed cancer type and the leading cause of cancer-related deaths among women worldwide.[1] Oxidative stress induced by chronic inflammation is an important determinant in the progression of cellular changes, which help enhance in the production of reactive oxygen species (ROS) and the proliferation of cells. Inflammation caused by cytokines, such as interleukin-6 (IL-6) and tumor necrosis factor-alpha (TNF-α), has been linked to the increased production of ROS and breast tumor formation.[2,3]

Chemotherapy is a frequently used method to treat breast cancer. Although some antineoplastic drugs can be used as a single agent for chemotherapy, two or three antineoplastic agents are generally administered together as a combination therapy regimen to enhance their effectiveness.[4] For instance, cyclophosphamide is a frequently used alkylating agent in the treatment of various types of cancers.[5] Epirubicin is an anthracycline used in the treatment of various tumor types. It inhibits DNA, RNA, and protein synthesis through the intercalation of DNA, the hindering of topoisomerase II activity, and the production of reactive oxygen radicals. Epirubicin and cyclophosphamide can be used as single agents in breast cancer chemotherapy. Moreover, the combination treatment of epirubicin and cyclophosphamide is one of the frequently used chemotherapy regimens in the early and metastatic stages of breast tumor development.[6,7] Nonetheless, these agents are associated with an increased risk of hepatotoxicity, nephrotoxicity, cardiotoxicity, and hematologic toxicity in patients with breast cancer.[8-10] These toxic effects may reduce the quality of life of patients and affect the success of their treatment. As such, novel remedies should be investigated to reduce the toxic effects on patients with breast cancer under the combination chemotherapy of epirubicin and cyclophosphamide; through such treatments, morbidity can be minimized, and patients' quality of life can be improved.

Some plant-derived polyphenols have pharmacological effects, such as antiinflammatory, antioxidant, and antitumor properties. Therefore, studies have focused on the use of natural dietary antioxidants to alleviate the toxic effects of antineoplastic drugs.[11] Oleuropein (3,4-dihydroxyphenylelenolic acid) is a non-toxic secoiridoid glycoside and the major polyphenolic compound in olive tree (*Olea europaea* L.) and olive oil. It is responsible for the bitter taste of the leaves and fruits of olive tree. Oleuropein and its bioactive derivatives, such as hydroxytyrosol, have antioxidant, cardioprotective, anticancer, antiinflammatory, neuroprotective, and hepatoprotective effects by modulating several mechanisms.[12,13] In a novel study, oleuropein does not lead to a decrease in the efficacy of anthracycline-based chemotherapy in breast tumor-induced female BALB/c mice. On the contrary, oleuropein elicits a synergistic antitumoral effect with antineoplastic agents.[14] Therefore, our study aimed to explore the effects of oleuropein on epirubicin- and cyclophosphamide-induced toxicity in rats.

MATERIALS AND METHODS

The effects of oleuropein on cyclophosphamide- and epirubicin-induced toxicity in rats were examined using different methods. Whole blood samples were examined through hemogram tests, and serum samples were subjected to biochemical analysis. IL-6 and TNF-α in the serum samples were analyzed through enzyme-linked immunosorbent assay (ELISA). Subsequently, a comet assay was performed by using lymphocyte DNA. The levels of oxidant [i.e., malondialdehyde (MDA)] and antioxidants [i.e., catalase (CAT), glutathione (GSH), and superoxide dismutase (SOD)] were measured in the heart, kidney, and liver tissues.

Chemicals

The following commercially available chemicals were used in this study: Oleuropein (high-performance liquid chromatography grade ≥98%; Santa Cruz Biotechnology®, Santa Cruz Biotechnology Inc., California, USA); epirubicin (Pirucin®, Saba Ilaç AŞ, Istanbul, Turkey); cyclophosphamide (Endoxan®, Baxter Oncology GmbH, Frankfurt, Germany); ketamine (Ketalar®, Pfizer Inc., Istanbul, Turkey); and xylazine (Rompun®, Bayer LLC, Istanbul, Turkey). All the other chemicals used in this study were obtained from Sigma-Aldrich Inc. (Missouri, USA).

Animals

Fifty-six healthy 3-month-old female Sprague-Dawley rats weighing 220 g±20 g were obtained from the Aydın Adnan Menderes University Experimental Animals Research and Application Center (Aydın, Turkey). They were kept inside polycarbonate cages in an air-conditioned room (23°C±2°C) and relative humidity of 50-55% with 12 h/12 h light/dark cycle. Standard rat food and water were provided ad libitum. The rats were held in the room and acclimatized to the laboratory environment for a week before the drug administration phase. This study was approved by the Local Ethics Committee for Experiments on Animals of Aydın Adnan Menderes University (Ethics Committee permission no: 64583101/2017/117) and performed in accordance with the ethical rules of the Helsinki Declaration.

Experimental design

The rats were separated into seven equal groups (n=8 in each group): Group I (control), 1 mL of saline administered once a week for four cycles; group II (epirubicin, "E"), 2.5 mg/kg/week epirubicin administered for four cycles; group III (cyclophosphamide "C"), 16 mg/kg/week cyclophosphamide administered for four cycles; group IV (epirubicin + cyclophosphamide, "EC"), 2.5 mg/kg/week epirubicin + 16 mg/kg/week cyclophosphamide administered for four cycles; group V (epirubicin + oleuropein, "EO"), 2.5 mg/kg/week epirubicin + 150 mg/kg/week oleuropein administered for four cycles; group VI (cyclophosphamide + oleuropein, "CO"), 16 mg/kg/week cyclophosphamide + 150 mg/kg/week oleuropein administered for four cycles; and group VII (epirubicin + cyclophosphamide + oleuropein, "ECO"), 2.5 mg/kg/week epirubicin + 16 mg/kg/week cyclophosphamide + 150 mg/kg/week oleuropein administered for four cycles.

Epirubicin and cyclophosphamide were administered via intraperitoneal (i.p.) injection, and oleuropein was administered through oral gavage (p.o.). Epirubicin, cyclophosphamide, and oleuropein were freshly prepared in saline and administered at the same time of the day in every cycle. The doses of epirubicin and cyclophosphamide administered to the rats in the study were determined by converting the human doses, which were stated in the United States National Comprehensive Cancer Network Guidelines (available at https://www.nccn.org). Dose conversions between humans and rats were calculated as described in the United States Food and Drug Administration Guidelines (available at https://www.fda.gov). The dose of oleuropein used in the study was determined from previous studies.[15-19]

The rats were treated for 4 weeks and anesthetized with 50 mg/kg ketamine (i.p) and 5 mg/kg xylazine (i.p.) 1 week after the last treatment. Blood samples were taken by cardiac puncture for comet assay, ELISA, hemogram tests, and biochemical analysis. Then, the rats were sacrificed, and the heart, liver, and kidneys were taken for the analysis of oxidant/antioxidant parameters. The organs were removed immediately and kept frozen (-80°C) until they were analyzed.

Hemogram tests

Blood samples were taken into tubes containing ethylene diamine tetra acetic acid. The samples were analyzed within the first hour after they were received from the rats. Routine hematological parameters such as leukocyte (WBC), lymphocyte (LYM), monocyte (MONO), granulocyte (GRA), lymphocyte %, monocyte % (MONO %), granulocyte % (GRA %), hemoglobin (HGB), erythrocyte (RBC), hematocrit (HCT), mean cell volume, mean cell hemoglobin concentration (MCHc), MCH, erythrocyte distribution width concentration (RDWc), platelet (PLT), platelet count/the values of other cells % ratio (PCT), platelet distribution width (PDWc), and platelet/cell number ratio (MPV) were analyzed using an automated Diatron® Abacus Junior Vet (Diatron Medical Instruments Plc, Hungary) hematology analyzer.

Biochemical analysis

Plasma was separated through centrifugation from the whole blood and used to determine biochemical parameters in rat serum: Urea, uric acid, creatinine, aspartate aminotransferase (AST), creatinine kinase (CK), alanine aminotransferase (ALT), gamma glutamyl transferase (GGT), CK-myocardial band (CK-MB) isoenzyme 3, direct biluribin, and total bilirubin. Analysis was initially performed within the first hour after the blood samples were taken from the rats by using a Roche® Cobas c501 autoanalyzer (Roche Diagnostics, Switzerland) and Roche® commercial kits.

Serum IL-6 and TNF-α levels were determined using a commercially available Thermo Fisher® (Thermo Fisher Scientific Co., USA) ELISA kits in accordance with the manufacturer's instructions.

Comet assay

The comet assay protocol was implemented as described in Singh et al.[20] In brief, lymphocytes were placed to low-melting agarose (0.7% in phosphate-buffered saline) and placed in a lysis solution (2.5 M NaCl, 100 mM Na2EDTA, 10 mM Tris-HCl, pH 10, containing freshly added before use 1% Triton X-100 and 10% dimethyl sulfoxide) for 1 h at 4°C. Then, the samples were placed on slides.

The slides were placed on a horizontal Cleaver® gel electrophoresis tank connected to a Cleaver® Scientific CS 300 power supply (Cleaver Scientific Ltd., UK) and a Julabo® FL300 recirculating cooler (Julabo GmbH, Germany). The tank was filled with alkaline solution (1 mM Na_2EDTA and 300 mM NaOH, pH 13) until the liquid level covered the samples. Then, the lid of the tank was closed and waited for 30 min at 4°C. Electrophoresis was continued at 4°C in the dark for 30 min at 25 V and 300 mA, and the samples were rinsed with 400 mM Tris buffer with pH 7.5 for 7 min to neutralize surplus alkali. The neutralized slides were kept in ethanol for 5 min and then dried at room temperature. The slides were stained with 70 µL (10 µg/mL) 4',6-diamidino-2-phenylindole dihydrochloride (DAPI) before microscopic examination.

Comets were analyzed after the specimens were stained at 400x magnification by using a Leica® fluorescence microscope (Leica Microsystems GmbH, Germany) equipped with a 50 W mercury lamp. Then, 100 cells were randomly counted for each slide. The extension of each comet was examined through Comet Assay® IV (Perceptive Instruments Ltd., UK) computerized image analysis. The damage ratio of each sample was expressed as "tail moment" and "% tail intensity," as described in Collins et al.[21]

Measurement of oxidant/antioxidant parameters

In this procedure, 0.5 g of tissue samples was taken from each organ (kidneys, heart, and liver) for homogenization. Tissues were homogenized at 2.000 rpm for 1 min by using a Teflon-glass stirrer (IKA Overhead Stirrer; IKA-Werke GmbH & Co., KG, Germany) in a 10-fold volume of ice-cold 10% of 150 mM phosphate buffer (pH 7.4). The homogenate was centrifuged (Hettich Zentrifugen, Mikro 200 R, Germany) at 12.000 rpm for 10 min at 4°C. The supernatants, referred to as homogenate, were stored at -80°C (Glacier Ultralow Temperature Freezer, Japan) until CAT, SOD, GSH, and MDA levels were examined. All oxidant/antioxidant levels were analyzed through spectrophotometric measurements by using a Shimadzu® ultraviolet-1601 (Shimadzu Scientific Instruments, Japan) spectrophotometer. Protein concentrations were measured in accordance with the Biuret method by using a spectrophotometer and commercially available kits (Archem Diagnostic Ind., Ltd., Turkey). The results were expressed in milligrams per milliliter of protein.

MDA levels were determined as described previously by Ohkawa et al.[22] The MDA concentration (nmol/mg of tissue protein) was calculated on the basis of absorbance: Absorbance coefficient (ε)=1.56×10^5/M/cm. CAT activity (k/mg tissue protein) was evaluated as described by Aebi.[23] SOD activity (U/mg of tissue protein) was determined as described by Sun et al.[24] GSH levels (mg/g tissue protein) were spectrophotometrically determined at 412 nm by using the method described by Tietze.[25]

Statistical analysis

Data were statistically analyzed using SPSS 22.0. All the parameters were examined for the homogeneity of variance with Levene's test and normal distribution with the Shapiro-Wilk test. The intra-group repeated measurements of rat weights were evaluated with the Friedman test. Because of the Shapiro-Wilk test results did not match normal distribution, data were compared between groups by using Kruskal-Wallis ANOVA. Post-hoc binary comparisons were performed using the Bonferroni-corrected Mann-Whitney U test. Differences were considered statistically significant if $p<0.05$. All data were expressed as mean ± standard deviation.

RESULTS

Body weight changes

In this study, the weight of the rats in the combination therapy (EC) group significantly decreased, whereas the weight of the rats in all the other groups significantly increased ($p<0.05$). Although the initial body weights did not vary among the groups, the weights of the control group significantly differed from those of the E, C, EC, and CO groups at the end of the study ($p<0.05$). The results of the body weight measurements of the rats from the day of the determination of the groups (day 0) until the day the study was terminated (day 35) are presented in Table 1.

Hemogram tests

MONO, GRA, MONO %, GRA %, RDWc, PCT, MPV, and PDWc did not significant vary ($p>0.05$), but these data were not shown to simplify the results in the table. The results of the hemogram tests and their statistical differences between the experimental groups are given in Table 2.

Most of the parameters generally deteriorated in all the groups administered with the antineoplastic drugs alone in the single and combination therapies. These results significantly differed from those observed in the control group ($p<0.05$). WBC, LYM, RBC, HGB, HCT, and PLT, which are related to neutropenia and bone marrow suppression, significantly varied between the groups treated with antineoplastic drugs alone (E, C, and EC) and the groups treated with oleuropein + antineoplastic drug (EO, CO, and ECO; $p<0.05$). However, the hemogram test results of the groups treated with oleuropein + antineoplastic drug were generally closer to those of the healthy control group than to the groups treated with antineoplastic drugs alone.

Biochemical analysis

The biochemical parameters and their significant differences between the experimental groups are given in Table 3. Urea, GGT, direct bilirubin, and CK parameters did not significantly differ among the groups ($p>0.05$). Therefore, these data were not shown to simplify the results in the table.

AST and ALT, which are important biochemical indicators of liver damage, significantly differed ($p<0.05$) between the groups treated with antineoplastic drugs alone (E, C, and EC) and the groups treated with oleuropein + antineoplastic drugs (EO, CO, and ECO). Oleuropein ameliorated these parameters and decreased them to levels similar to those of the healthy control group ($p>0.05$). These biochemical parameters indicated that oleuropein helped alleviate liver damage. Although oleuropein was beneficial to some parameters, which are related to heart and kidney damages, no considerable effects were observed in most of the other parameters.

The administered antineoplastic agents as single or in combination significantly increased the serum IL-6 and TNF-α levels compared with those in the control group ($p<0.05$). These levels decreased and were similar to those of the healthy control group in all oleuropein-treated groups ($p>0.05$). The results of the ELISA tests are presented in Figure 1.

Comet assay

The tail moment and % tail intensity results of the comet assay are presented in Figure 2. The degree of DNA damage was considerably higher in the experimental groups than in

Table 1. Body weight measurement results

Groups (n=8)	Day 0	Day 7*	Day 14	Day 21	Day 28	Day 35**	p***	X^2
Control	210.0±0.007	216.1±0.012	224.5±0.011$^{a, b}$	232.1±0.013$^{a, b, c, d}$	240.0±0.014$^{a, b, c, d, e}$	247.7±0.018$^{a, b, c, d}$	p<0.001	39.014
E	209.2±0.009	212.6±0.008	214.8±0.007	218.8±0.006^{a}	223.5±0.006^{a}	222.3±0.013^{a}	p<0.001	35.180
C	218.5±0.013	221.1±0.014	223.6±0.011^{c}	225.2±0.009	228.3±0.006^{b}	228.0±0.014^{b}	p<0.05	18.157
EC	216.5±0.003	221.3±0.008	217.1±0.007^{d}	212.6±0.006$^{b, e}$	206.2±0.005^{cf}	200.2±0.005^{ce}	p<0.001	36.025
EO	207.3±0.003	209.7±0.006	214.2±0.007^{a}	217.3±0.008^{c}	228.0±0.010^{d}	235.0±0.012	p<0.001	37.929
CO	209.1±0.008	212.8±0.007	214.3±0.010$^{b, c}$	219.2±0.010^{d}	225.1±0.010^{e}	232.8±0.010^{d}	p<0.001	36.577
ECO	215.5±0.009	218.7±0.009	227.8±0.009^{d}	232.0±0.010^{e}	236.5±0.009^{f}	241.2±0.011^{e}	p<0.001	38.000
p****	p>0.05	p>0.05	p<0.05	p<0.05	p<0.05	p<0.05	-	-
X^2	11.266	10.616	15.524	22.423	31.647	30.044		

*Day of the first drug administration, **Day of sacrification, ***Intra-group Friedman test results, ****Kruskal-Wallis analysis of body weight changes between groups. $^{a, b, c, d, e}$The same superscript letters in the columns indicate significant differences with one another. Differences were considered statistically significant if $p<0.05$. Weight is expressed in grams. E: Epirubicin, C: Cyclophosphamide, EC: Epirubicin + cyclophosphamide, EO: Epirubicin + oleuropein, CO: Cyclophosphamide + oleuropein, ECO: Epirubicin + cyclophosphamide + oleuropein. The results are given as mean ± standard deviation

Table 2. Hemogram results of the experimental groups

	Groups (n=8)							p
Parameters	Control	E	C	EC	EO	CO	ECO	X^2
WBC	6.02±0.39 $^{a, b, c, d}$	3.45±0.29$^{a, e}$	3.41±1.48$^{b, c}$	3.10±0.48$^{c, e}$	4.65±0.51$^{d, e}$	5.73±0.98^{c}	5.70±0.29^{e}	p<0.001 40.491
LYM	3.53±0.41$^{a, b, c}$	1.98±0.88$^{a, d}$	1.83±0.50$^{b, e}$	1.71±0.41$^{c, f}$	3.54±0.37^{d}	3.42±0.18^{e}	3.37±0.63^{f}	p<0.001 34.950
LY %	73.86±17.43$^{a, b, c, d, e}$	56.38±17.14^{a}	47.04±17.54^{b}	44.70±15.09^{c}	70.24±15.11	58.91±22.67^{d}	59.49±17.13^{e}	p<0.05 17.538
RBC	6.94±0.34$^{a, b, c, d}$	5.76±0.79$^{a, e}$	5.91±0.36$^{b, f}$	5.58±1.13$^{c, g}$	6.70±0.25^{e}	6.77±0.47^{f}	6.57±0.31$^{d, g}$	p<0.001 31.528
HGB	11.70±0.49$^{a, b, c, d}$	9.66±1.34$^{a, e}$	10.73±0.88$^{b, f}$	9.41±0.99$^{c, g}$	11.25±0.30$^{d, e}$	11.77±0.44^{f}	11.64±0.50^{g}	p<0.001 35.829
HCT	40.85±2.74$^{a, b, c, d}$	33.99±4.32$^{a, e}$	36.80±3.37$^{b, f}$	33.07±5.44$^{c, g}$	39.40±1.30^{e}	43.15±3.72^{f}	36.80±7.16$^{d, g}$	p<0.001 33.134
MCV	58.00±0.75$^{a, b, c}$	59.13±1.13	65.13±5.82^{a}	59.88±4.48	58.75±1.22	64.00±5.40^{b}	61.25±4.20^{c}	p<0.05 17.034
MCH	17.03 ± 0.42^{a}	21.99±14.56	23.73±15.11^{a}	17.26±1.24	16.61±0.51	17.65±1.07	17.24±1.21	p<0.05 13.259
MCHc	29.28±0.69$^{a, b, c, d, e}$	28.36±0.56^{a}	28.08±0.84^{b}	28.83±0.72	28.24±0.48^{c}	27.71±1.09^{d}	28.23±0.96^{e}	p<0.05 14.908
PLT	705.48±214$^{a, b, c, d}$	509.37±174$^{a, e}$	483.63±122$^{b, f}$	674.50±163^{g}	860.63±117$^{c, e}$	675.25±131^{f}	1006.38±110$^{d, g}$	p<0.001 33.510
MPV	9.43±3.60$^{a, b, c, d}$	9.16±5.78$^{a, e}$	8.81±2.57$^{b, f}$	9.80±7.55^{g}	9.76±5.30$^{c, e}$	9.08±5.59^{f}	9.08±8.21$^{d, g}$	p>0.05 2.371

WBC, LYM, and PLT are expressed in 10^9/L; RBC is expressed in 10^{12}/L; other parameters are presented in percentage (%).$^{a, b, c, d, e, f, g}$The same superscript letters in the lines indicate significant differences with one another. Differences were considered statistically significant if p<0.05. E: Epirubicin, C: Cyclophosphamide, EC: Epirubicin + cyclophosphamide, EO: Epirubicin + oleuropein, CO: Cyclophosphamide + oleuropein, ECO: Epirubicin + cyclophosphamide + oleuropein. The results are given as mean ± standard deviation. WBC: Leukocyte, LYM: Lymphocyte, LY %: Lymphocyte %, RBC: Erythrocyte, HGB: Hemoglobin, HCT: Hematocri, MCV: Mean cell volume, MCH: Mean cell hemoglobin, MCHc: Mean cell hemoglobin, PLT: Platelet, MPV: Mean platelet volume

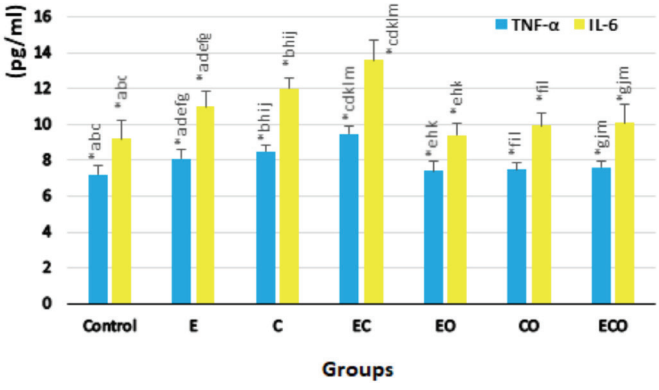

Figure 1. Serum TNF-α and IL-6 levels of the experimental groups; results were expressed as mean ± standard deviation. *Whiskers on the boxes indicates standard deviation. The same superscript letters on the boxes indicates significant statistical difference with each other. Differences were considered statistically significant if p<0.05. E: Epirubicin, C: Cyclophosphamide, EC: Epirubicin + cyclophosphamide, EO: Epirubicin + oleuropein, CO: Cyclophosphamide + oleuropein, ECO: Epirubicin + cyclophosphamide + oleuropein, TNF-α: Tumor necrosis factor-α, IL-6: Interleukin-6.

the control group. However, the considerable DNA damage caused by EC significantly decreased in the ECO (p<0.001). The fluorescent microscope images of some DNA samples are shown in Figure 3.

Oxidant/antioxidant levels

The levels of MDA and GSH and the measurement of SOD and CAT activities in the liver, heart, and kidneys of the experimental groups are given in Table 4. The SOD activity was considerably higher in the ECO group than in the EC group (p<0.05). Moreover, the SOD activity in the heart did not significantly vary between the control and ECO groups (p>0.05).

Oleuropein showed protective effects on the heart tissues by increasing GSH levels and decreasing MDA levels. The increased MDA levels were due to the decrease in the antineoplastic drugs (p<0.05) in the oleuropein-treated groups, but these levels decreased to levels similar to those of the control group (p>0.05). Although the GSH levels in the groups treated with antineoplastic drugs alone (E, C, and EC) decreased, these levels increased remarkably (p<0.05) in the oleuropein-treated groups (EO, CO, and ECO) and reached levels similar to those of the control group (p>0.05).

Table 3. Biochemical parameters of the experimental groups

	Groups (n=8)							p
Parameter	Control	E	C	EC	EO	CO	ECO	X^2
Creatinine	0.46±0.03[a]	0.41±0.05[b]	0.49±0.07	0.51±0.07	0.51±0.05[b]	0.48±0.04	0.58±0.11[a]	p<0.05 17.707
Uric acid	1.31±0.34[a, b, c, d, e, f]	1.93±0.57[a]	2.32±0.46[b]	2.51±0.71[c]	2.05±0.22[d]	2.08±0.77[e]	2.55±0.65[f]	p<0.05 20.705
AST	169.63±29.97[a, b, c, d]	211.87±43.00[a, e]	219.25±35.09[b, f]	210.88±30.38[c, g]	141.00±22.86[e]	135.88±25.39[d, f]	152.38±29.57[g]	p<0.001 32.313
ALT	54.25±5.65[a, b, c, d]	63.25±4.06[a, e]	62.38±7.13[b, f]	64.63±4.98[c, g]	48.25±4.98[d, e]	52.13±5.80[f]	52.88±7.04[g]	p<0.001 32.844
Total bilirubin	0.03±0.01[a, b]	0.03±0.01	0.06±0.01[a]	0.03±0.01	0.02±0.01	0.04±0.01[b]	0.03±0.01	p<0.05 19.559
CK-MB	1207.30±142.56[a, b, c, d, e]	1287.50±240.28	746.75±216.14[a]	819.25±147.39[b]	893.88±149.67[c]	987.13±308.33[d]	792.88±170.75[e]	p<0.001 27.203

Creatine kinase myocardial band (CK-MB), total bilirubin, alanine transaminase (ALT), and aspartate transaminase (AST) are expressed in units per liter. Uric acid and creatinine are expressed in milligrams per deciliter. [a, b, c, d, e, f, g]The same superscript letters in the lines indicate significant differences with one another. Differences were considered statistically significant if p<0.05. E: Epirubicin, C: Cyclophosphamide, EC: Epirubicin + cyclophosphamide, EO: Epirubicin + oleuropein, CO: Cyclophosphamide + oleuropein, ECO: Epirubicin + cyclophosphamide + oleuropein. The results are given as mean ± standard deviation

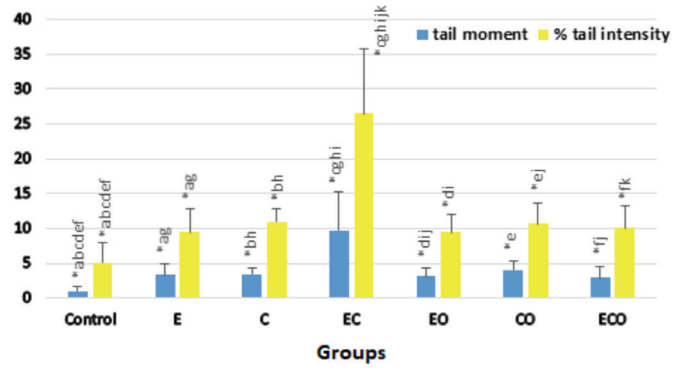

Figure 2. Tail moment and % tail intensity results of the comet assay; results were expressed as mean ± standard deviation. *Whiskers on the boxes indicates standard deviation. The same superscript letters on the boxes indicates significant statistical difference with each other. Differences were considered statistically significant if p<0.05. E: Epirubicin, C: Cyclophosphamide, EC: Epirubicin + cyclophosphamide, EO: Epirubicin + oleuropein, CO: Cyclophosphamide + oleuropein, ECO: Epirubicin + cyclophosphamide + oleuropein.

The SOD and CAT activities in the kidneys of the rats treated with the antineoplastic drugs alone (E, C, and EC) significantly decreased compared with those of the rats in the control group (p<0.05). The administration of oleuropein led to an amelioration of SOD and CAT activities in the kidneys, thereby reaching levels similar to those of the healthy control group.

The MDA levels in the kidneys were lower in the ECO group than in the EC group (p<0.05). However, the differences between the healthy control group and the ECO group were not significant (p>0.05). This result indicated that oleuropein could significantly lower the elevated MDA level, which is a marker of oxidative damage. Therefore, it showed cell-protective effects on the kidneys.

The results of the GSH, SOD, and CAT analysis in the liver tissues were generally compatible with one another. In most of the oleuropein-treated groups, the antioxidant parameters were similar (p>0.05) to those of the healthy control group and significantly higher (p<0.05) than those of the groups treated with antineoplastic drugs alone. Oleuropein increased the antioxidant capacity in the liver tissues to levels similar to those

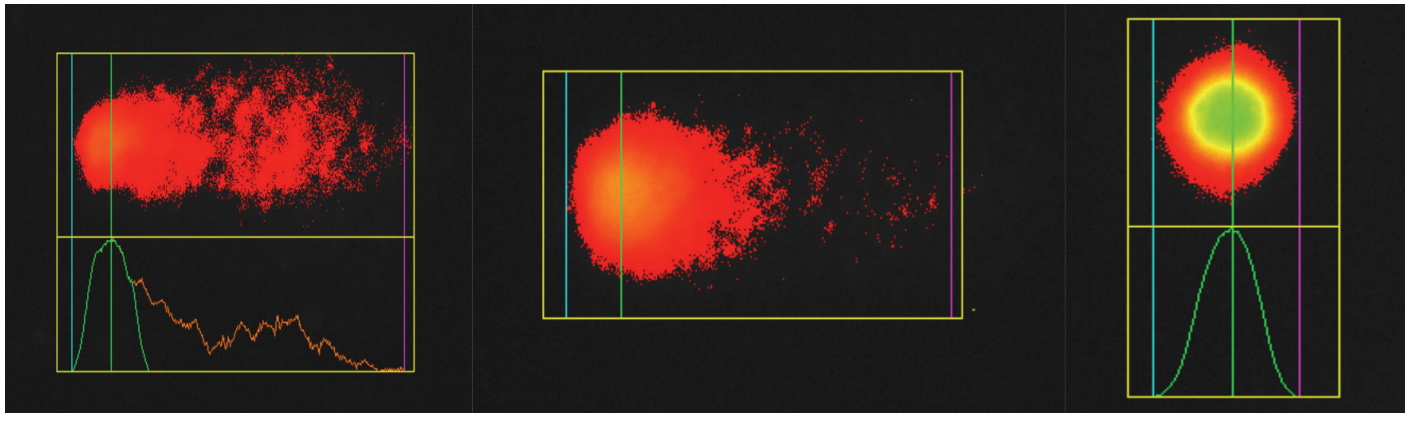

Figure 3. Fluorescence microscopy images of highly damaged (left), moderately damaged (middle), and intact (right) DNA samples in comet analysis

Table 4. Measurement results of MDA and GSH levels and CAT and SOD activities in the heart, kidney, and liver tissues of the experimental groups

	Groups (n=8)							p	X^2
Parameters*	Control	E	C	EC	EO	CO	ECO		
Heart									
SOD	7.04±0.63[a, b, c, d, e]	6.39±0.14[a]	5.36±2.17[b]	3.40±2.17[c, f]	6.44±0.32[d]	6.16±0.35[e]	6.74±0.16[f]	p<0.001	28.420
CAT	3.88±1.23[a, b, c, d, e, f]	1.86±0.71[a]	1.75±0.53[b]	1.68±0.53[c]	2.28±0.65[d]	1.69±0.45[e]	1.74±0.38[f]	p<0.001	21.767
GSH	13.70±2.53[a, b, c]	9.58±2.53[a, d]	9.88±2.54[b, e]	9.43±2.54[c, f]	14.37±3.59[d]	13.70±3.02[e]	13.47±1.35[f]	p<0.001	23.871
MDA	70.08±6.08[a, b, c]	93.65±4.78[a, d]	90.88±13.43[b, e]	99.98±13.43[c, f]	75.99±7.18[d]	76.93±16.47[e]	77.92±5.52[f]	p<0.001	32.860
Kidneys									
SOD	7.40±0.22[a, b, c, d]	6.69±0.27[a, e]	6.31±1.20[b, f]	5.96±1.20[c, g]	7.24±0.39[e]	7.10±0.28[d, f]	7.16±0.21[g]	p<0.001	36.481
CAT	3.74±1.93[a, b]	2.82±0.88[c]	3.65±1.01[d]	2.49±1.01[e]	6.80±1.88[a, c]	6.29±1.34[b, d]	4.95±2.20[e]	p<0.001	30.219
GSH	20.43±2.53[a, b, c, d, e, f]	13.77±2.35[a, g]	11.90±3.02[b, h]	8.98±3.02[c, i]	17.07±2.88[d, g]	16.62±3.00[e, h]	16.39±2.61[f, i]	p<0.001	33.858
MDA	49.11±2.93[a, b, c, d, e]	61.10±5.77[a]	70.87±9.04[b, f]	74.62±9.04[c, g]	54.38±5.83[d]	60.34±8.00[e, f]	52.30±2.86[g]	p<0.001	32.409
Liver									
SOD	7.04±0.15[a, b, c, d, e]	6.39±0.33[e]	5.36±0.20[b, f]	6.54±0.02[c, g]	7.49±0.02[e]	7.27±0.13[d, f]	7.37±0.15[g]	p<0.001	41.283
CAT	3.88±7.22[a]	1.86±5.55[b]	1.75±5.65	6.18±5.65[c]	7.90±3.49[b]	21.34±16.96[a]	15.07±7.74[c]	p<0.05	20.521
GSH	13.70±3.81[a, b, c, d]	9.58±2.35[a, e]	9.88±2.30[b, f]	11.90±2.30[c, g]	21.78±3.38[e]	19.76±3.59[d, f]	19.98±2.02[g]	p<0.001	33.699
MDA	70.08±2.08[a, b, c, d, e, f]	93.65±7.80[a, g]	90.88±12.04[b, h]	88.25±12.05[c, i]	72.01±2.63[d, g]	77.54±5.86[e, h]	78.39±8.01[f, i]	p<0.001	31.320

*MDA is expressed in nanomole per milligram of protein; GSH is expressed in milligrams per gram of protein; CAT is expressed in k per milligram of protein; SOD is expressed in units per milligram of protein. [a, b, c, d, e, f, g, h, i]The same superscript letters in the lines indicate significant differences with one another. Differences were considered significant if p<0.05. SOD: Superoxide dismutase, CAT: Catalase, GSH: Reduced glutathione, MDA: Malondialdehyde; E: Epirubicin, C: Cyclophosphamide, EC: Epirubicin + cyclophosphamide, EO: Epirubicin + oleuropein, CO: Cyclophosphamide + oleuropein, ECO: Epirubicin + cyclophosphamide + oleuropein. The results are given as mean ± standard deviation

of the control group. By contrast, it decreased oxidative stress and degradation products. Unlike the SOD, GSH, and CAT levels in the cardiac and renal tissues, their levels in the liver were even higher in the oleuropein-treated groups than in the healthy control group.

DISCUSSION

In this study, the efficacy of oleuropein against the toxic effects of the combination therapy of epirubicin and cyclophosphamide, which are frequently used to treat breast tumors, was investigated using healthy female rats. This study was the first to demonstrate the effects of oleuropein against toxicity induced by a combination chemotherapy based on anthracycline and alkylating agents. Many parameters were investigated and important data were obtained in this study, but this study had limitations because it did not involve a histopathological examination of the tissues and an investigation of other serum cytokine levels, such as IL-8 and IL-1β, which are involved in inflammation.

Weight loss, vomiting, appetite loss, anorexia, and neutropenia are the important side effects of the combination therapy of epirubicin and cyclophosphamide.[26] In our study, the initial and final body weights of the rats in the EC group significantly differed (p<0.05). Similar weight gain results were detected in the ECO group compared with those in the healthy control group (p>0.05). These results suggested that oleuropein might be a useful agent to prevent the weight loss of the rats in this combination chemotherapy group. However, a previous study showed that rats in oleuropein-treated groups that receive a fat-rich diet gain less weight than those in other groups (p<0.05).[27] Another study has demonstrated that rats administered with oleuropein + bisphenol A (BPA) have less weight gains than those treated with BPA alone (p<0.05).[28] Based on the outcomes of these studies, our conclusion was that oleuropein treatment likely had a regulatory role in various mechanisms by which an ideal weight could be maintained rather than inducing weight loss or weight gain.

A limited number of studies on the effects of oleuropein or other olive products (leaves, fruits, olive oil, and olive mill waste water extracts) have examined the hemogram parameters. In one study, oleuropein administered to rats with cisplatin-induced toxicity ameliorates the hemogram parameters that reach levels similar to those of the healthy control group.[29] These consistent results indicated that oleuropein might have beneficial ameliorating effects on most of the hemogram parameters, which deteriorated because of epirubicin and cyclophosphamide toxicity.

The comet assay showed that oleuropein might be a beneficial agent that could reduce the oxidative DNA damage caused by antineoplastics. In literature search, no data were found in the effects of oleuropein in terms of a comet assay for epirubicin and cyclophosphamide toxicity. As such, studies

have compared oleuropein-rich olive plant (leaf, fruit, and olive mill waste water extracts) and olive oil extracts between mouse and human peripheral mononuclear blood cells. These compounds significantly reduce oxidative damage levels and show DNA protective activities.[30-34] In this regard, our results were consistent with previous findings.

The biochemical parameter results indicated that oleuropein could reduce the elevated AST and ALT levels, which are associated with liver damage. However, no significant differences were observed in most parameters. In a previous study, oleuropein administration considerably decreased the elevated levels of AST, ALT, urea, and creatinine in rats with BPA-induced toxicity.[35] In another study, oleuropein significantly decreased the increased ALT and AST levels in a hepatic fibrosis mouse model and may be a pharmacologically useful agent in hepatic fibrosis.[36]

The increased risk of myocardial infarction is an important side effect of anthracycline-derived drugs.[26] CK-MB is an important biochemical marker in monitoring the risk of myocardial infarction.[37] In our study, conflicting results were obtained on the effects of oleuropein in the CK-MB parameter. These results might be related to the dose of oleuropein administered.[16] Therefore, the pharmacological effects on this parameter might be observed through the administration of higher doses.

Proinflammatory cytokines, such as TNF-α and IL-6, are involved in the formation and progression of breast tumors.[2,38] Most antineoplastic agents used in the treatment of breast tumors cause an increase in tissue and serum IL-6 and TNF-α levels.[39-41] In another study, the effects of different doses of oleuropein (5, 10, and 20 mg/kg) are investigated against cisplatin-induced toxicity in mice. Cyclooxygenase-2, nuclear factor kappa B, and TNF-α levels in the kidneys decreased compared with the administered dose of oleuropein, which may help reduce cisplatin-induced toxicity in the kidneys.[40] In another study on human synovial sarcoma cells (SW982), IL-6 and TNF-α levels increase as a result of the induction of IL-1β-mediated inflammation and significantly decrease after oleuropein administration compared with those in the control group.[42] Several studies have investigated the effect of oleuropein against the toxicity induced by different agents in terms of serum and tissue cytokine levels in rats. They have shown that oleuropein can significantly reduce IL-6 and TNF-α levels in serum and tissues and elicit protective effects on organs. In other studies, oleuropein can decrease the elevated IL-6 and TNF-α levels induced by various compounds in direct proportion with doses.[39,43-45] In this regard, previous findings were consistent with our results. Animal experiments have also revealed that oleuropein can decrease IL-6 and TNF-α levels in a wide dose range (10-2000 mg/kg/day). The selected dose in our study (150 mg/kg/week) also decreased the levels of these cytokines compared with that in the healthy control group. Similar results were obtained even at different doses in these studies. This situation might be related to the purity of oleuropein used in previous studies.

Oxidative stress plays a crucial role in the pathogenesis of the hepatotoxic, nephrotoxic, and cardiotoxic effects of epirubicin and cyclophosphamide.[7,10] The protective effects of oleuropein have been attributed to several mechanisms, such as the reduction of nitrosative and oxidative stress and antiinflammatory and antioxidant activities.[12,13,39] In our study, the reduced GSH, CAT, SOD, and MDA levels in the kidney, hepatic, and cardiac tissues were determined as indicators of oxidative stress and organ damage. Reduced GSH plays a major role in cellular defense against toxicity and ROS scavenging. SOD converts highly reactive superoxide anions to H_2O_2. Subsequently, CAT is the enzyme responsible for the conversion of H_2O_2 formed in cellular processes into molecular oxygen and water. Moreover, MDA is a lipid peroxidation product and indicator of oxidative damage caused by ROS generation.[46-48]

Our study showed that oleuropein could decrease the MDA level and increase the GSH level and SOD and CAT activities in the liver, heart, and kidneys of the rats compared with those of the rats treated with antineoplastic drugs alone. However, studies have yet to reveal the effects of oleuropein on endogenous oxidant/antioxidant parameters in the combination chemotherapy of epirubicin and cyclophosphamide. Therefore, our findings were compared with the results of studies on the effects of oleuropein against toxicity induced by cyclophosphamide, doxorubicin, and other chemical agents in rats. In these studies, oleuropein was administered in a wide dose range of between 5 and 2000 mg/kg/day. These studies reported that oleuropein decreased the amount of MDA and increased the amount of antioxidant markers (GSH, SOD, and CAT) in many organs, including the liver, heart, and kidneys, at a dose of ≥10 mg/kg/day.[15-19,33,35,39] Our findings were parallel to previous results. Furthermore, studies have explored different doses and demonstrated that total antioxidant capacity also increases as the administration doses of oleuropein increase.[16,18,39,48]

CONCLUSION

Oleuropein is a promising compound with antiinflammatory and antioxidant effects against chemical toxicity. Its anti-tumoral properties and synergistic effects with some antineoplastics increase the importance of oleuropein, especially in patients with cancer. This study showed that oleuropein could reduce the levels of DNA damage and serum proinflammatory cytokines, such as TNF-α and IL-6. It ameliorated some of the deteriorated hemogram (WBC, LYM, and HGB) and biochemical parameters (AST, ALT, and total bilirubin) because of antineoplastic drugs. Oleuropein could also increase the amounts of antioxidant parameters (SOD, CAT, and GSH) in the tissues and caused a decrease in the levels of MDA, which is a cellular degradation product. These results suggested that oleuropein might have protective effects against the toxicity induced by the combination chemotherapy of epirubicin and cyclophosphamide. Further studies should be performed to demonstrate the protective effects of oleuropein against antineoplastic induced-toxicity precisely.

Conflict of interest: No conflict of interest was declared by the authors. The authors are solely responsible for the content and writing of this paper.

REFERENCES

1. Bray F, Ferlay J, Soerjomataram I, Siegel RL, Torre LA, Jemal A. Global cancer statistics 2018: GLOBOCAN estimates of incidence and mortality worldwide for 36 cancers in 185 countries. CA Cancer J Clin. 2018;68:394-424.
2. Alokail MS, Al-Daghri NM, Mohammed AK, Vanhoutte P, Alenad A. Increased TNF α, IL-6 and ErbB2 mRNA expression in peripheral blood leukocytes from breast cancer patients. Med Oncol. 2014;31:38.
3. Esquivel-Velázquez M, Ostoa-Saloma P, Palacios-Arreola MI, Nava-Castro KE, Castro JI, Morales-Montor J. The role of cytokines in breast cancer development and progression. J Interferon Cytokine Res. 2015;35:1-16.
4. Jiang L, Jing C, Kong X, Li X, Ma T, Huo Q, Chen J, Wang X, Yang Q. Comparison of adjuvant ED and EC-D regimens in operable breast invasive ductal carcinoma. Oncol Lett. 2016;12:1448-1454.
5. Rehman MU, Tahir M, Ali F, Qamar W, Lateef A, Khan R, Quaiyoom A, Oday-O-Hamiza, Sultana S. Cyclophosphamide-induced nephrotoxicity, genotoxicity, and damage in kidney genomic DNA of Swiss albino mice: the protective effect of Ellagic acid. Mol Cell Biochem. 2012;365;119-127.
6. Mirzaei HR, Nasrollahi F, Mohammadi Yeganeh L, Jafari Naeini S, Bikdeli P, Hajian P. Dose-dense epirubicin and cyclophosphamide followed by weekly paclitaxel in node-positive breast cancer. Chemother Res Pract. 2014;2014:259312.
7. Li H, Hu B, Guo Z, Jiang X, Su X, Zhang X. Correlation of UGT2B7 polymorphism with cardiotoxicity in breast cancer patients undergoing epirubicin/cyclophosphamide-docetaxel adjuvant chemotherapy. Yonsei Med J. 2019;60:30-37.
8. Domercant J, Polin N, Jahangir E, Cardio-oncology: a focused review of anthracycline-, human epidermal growth factor receptor 2 inhibitor-, and radiation-induced cardiotoxicity and management. Ochsner J. 2016;16:250-256.
9. Ejlertsen B, Tuxen MK, E. H. Jakobsen EH, Jensen MB, Knoop AS, Højris I, Ewertz M, Balslev E, Danø H, Vestlev PM, Kenholm J, Nielsen DL, Bechmann T, Andersson M, Cold S, Nielsen HM, Maae E, Carlsen D, Mouridsen HT. adjuvant cyclophosphamide and docetaxel with or without epirubicin for early TOP2A-normal breast cancer: DBCG 07-READ, an open-label, phase III, randomized trial. J Clin Oncol. 2017;35:2639-2646.
10. Kurauchi K, Nishikawa T, Miyahara E, Okamoto Y, Kawano Y. Role of metabolites of cyclophosphamide in cardiotoxicity. BMC Res Notes. 2017;10:406.
11. León-González AJ, Auger C, Schini-Kerth VB. Pro-oxidant activity of polyphenols and its implication on cancer chemoprevention and chemotherapy. Biochem Pharmacol. 2015;98:371-380.
12. Shamshoum H, Vlavcheski F, Tsiani E. Anticancer effects of oleuropein. Biofactors. 2017;43:517-528.
13. Ahmad Farooqi A, Fayyaz S, Silva AS, Sureda A, Nabavi SF, Mocan A, Nabavi SM, Bishayee A. Oleuropein and cancer chemoprevention: the link is hot. Molecules. 2017;22:705.
14. Elamin MH, Elmahi AB, Daghestani MH, Al-Olayan EM, Al-Ajmi RA, Alkhuriji AF, Hamed SS, Elkhadragy MF. Synergistic anti-breast-cancer effects of combined treatment with oleuropein and doxorubicin *in vivo*. Altern Ther Health Med. 2019;25;17-24.
15. Alirezaei M, Dezfoulian O, Neamati S, Rashidipour M, Tanideh N, Kheradmand A. Oleuropein prevents ethanol-induced gastric ulcers via elevation of antioxidant enzyme activities in rats. J Physiol Biochem. 2012;68:583-592.
16. Janahmadi Z, Nekooeian AA, Moaref AR, Emamghoreishi M. Oleuropein offers cardioprotection in rats with acute myocardial infarction. Cardiovasc Toxicol. 2015;15:61-68.
17. Alirezaei M, Rezaei M, Hajighahramani S, Sookhtehzari A, Kiani K. Oleuropein attenuates cognitive dysfunction and oxidative stress induced by some anesthetic drugs in the hippocampal area of rats. J Physiol Sci. 2017;67;131-139.
18. Janahmadi Z, Nekooeian AA, Moaref AR, Emamghoreishi M. Oleuropein attenuates the progression of heart failure in rats by antioxidant and antiinflammatory effects. Naunyn Schmiedebergs Arch Pharmacol. 2017;390;245-252.
19. Sherif IO. The effect of natural antioxidants in cyclophosphamide-induced hepatotoxicity: role of Nrf2/HO-1 pathway. Int Immunopharmacol. 2018;61;29-36.
20. Singh NP, McCoy MT, Tice RR, Schneider EL. A simple technique for quantitation of low levels of DNA damage in individual cells. Exp Cell Res. 1988;175:184-191.
21. Collins AR, Ma AG, Duthie SJ. The kinetics of repair of oxidative DNA damage (strand breaks and oxidised pyrimidines) in human cells. Mutat Res. 1995;336:69-77.
22. Ohkawa H, Ohishi N, Yagi K. Assay for lipid peroxides in animal tissues by thiobarbituric acid reaction. Anal Biochem. 1979;95:351-358.
23. Aebi H. Catalase *in vitro*. Methods Enzymol. 1984;105:121-126.
24. Sun Y, Oberley LW, Li Y. A simple method for clinical assay of superoxide dismutase. Clin Chem. 1988;34:497-500.
25. Tietze F. Enzymic method for quantitative determination of nanogram amounts of total and oxidized glutathione: applications to mammalian blood and other tissues. Anal Biochem.1969;27:502-522.
26. Ejlertsen B. Adjuvant chemotherapy in early breast cancer. Dan Med J. 2016;63:B5222.
27. Hadrich F, Mahmoudi A, Bouallagui Z, Feki I, Isoda H, Feve B, Sayadi S. Evaluation of hypocholesterolemic effect of oleuropein in cholesterol-fed rats. Chem Biol Interact. 2016;252:54-60.
28. Mahmoudi A, Hadrich F, Feki I, Ghorbel H, Bouallagui Z, Marrekchi R, Fourati H, Sayadi S. Oleuropein and hydroxytyrosol rich extracts from olive leaves attenuate liver injury and lipid metabolism disturbance in bisphenol A-treated rats. Food Funct. 2018;9:3220-3234.
29. Geyikoğlu F, Çolak S, Türkez H, Bakır M, Koç K, Hosseinigouzdagani MK, Çerığ S, Sönmez M. Oleuropein ameliorates cisplatin-induced hematological damages via restraining oxidative stress and DNA injury. Indian J Hematol Blood Transfus. 2017;33:348-354.
30. Fuccelli R, Sepporta MV, Rosignoli P, Morozzi G, Servili M, Fabiani R. Preventive activity of olive oil phenolic compounds on alkene epoxides induced oxidative DNA damage on human peripheral blood mononuclear cells. Nutr Cancer. 2014;66:1322-1330.
31. Kalaiselvan I, Dicson SM, Kasi PD. Olive oil and its phenolic constituent tyrosol attenuates dioxin-induced toxicity in peripheral blood mononuclear cells via an antioxidant-dependent mechanism. Nat Prod Res. 2015;29:2129-2132.
32. Topalović DŽ, Živković L, Čabarkapa A, Djelić N, Bajić V, Dekanski D, Spremo-Potparević B. Dry olive leaf extract counteracts L-thyroxine-

induced genotoxicity in human peripheral blood leukocytes *in vitro*. Oxid Med Cell Longev. 2015;2015:762192.

33. Rosignoli P, Fuccelli R, Sepporta MV, Fabiani R. *In vitro* chemo-preventive activities of hydroxytyrosol: the main phenolic compound present in extra-virgin olive oil. Food Funct. 2016;7:301-307.
34. Fuccelli R, Fabiani R, Rosignoli P. Hydroxytyrosol exerts anti-inflammatory and anti-oxidant activities in a mouse model of systemic inflammation. Molecules. 2018;23:3212.
35. Mahmoudi A, Ghorbel H, Bouallegui Z, Marrekchi R, Isoda H, Sayadi S. Oleuropein and hydroxytyrosol protect from bisphenol A effects in livers and kidneys of lactating mother rats and their pups'. Exp Toxicol Pathol. 2015;67:413-425.
36. Kim SW, Hur W, Li TZ, Lee YK, Choi JE, Hong SW, Lyoo KS, You CR, Jung ES, Jung CK, Park T, Um SJ, and Yoon SK. Oleuropein prevents the progression of steatohepatitis to hepatic fibrosis induced by a high-fat diet in mice. Exp Mol Med. 2014;46:e92.
37. Fan J, Ma J, Xia N, Sun L, Li B, Liu H. Clinical value of combined detection of CK-MB, MYO, cTnI and Plasma NT-proBNP in diagnosis of acute myocardial infarction. Clin Lab. 2017;63:427-433.
38. Katanov C, Lerrer S, Liubomirski Y, Leider-Trejo L, Meshel T, Bar J, Feniger-Barish R, Kamer I, Soria-Artzi G, Kahani H, Banerjee D, Ben-Baruch A, Regulation of the inflammatory profile of stromal cells in human breast cancer: prominent roles for TNF-α and the NF-κB pathway. Stem Cell Res Ther. 2015;6:87.
39. Andreadou I, Mikros E, Ioannidis K, Sigala F, Naka K, Kostidis S, Farmakis D, Tenta R, Kavantzas N, Bibli SI, Gikas E, Skaltsounis L, Kremastinos DT, Iliodromitis EK. Oleuropein prevents doxorubicin-induced cardiomyopathy interfering with signaling molecules and cardiomyocyte metabolism. J Mol Cell Cardiol. 2014;69:4-16.
40. Potočnjak I, Škoda M, Pernjak-Pugel E, Peršić P, Domitrović R. Oral administration of oleuropein attenuates cisplatin-induced acute renal injury in mice through inhibition of ERK signaling. Mol Nutr Food Res. 2016;60:530-541.
41. Fan C, Georgiou KR, Morris HA, McKinnon RA, Keefe DMK, Howe PR, Xian CJ. Combination breast cancer chemotherapy with doxorubicin and cyclophosphamide damages bone and bone marrow in a female rat model. Breast Cancer Res Treat. 2017;165:41-51.
42. Castejón ML, Rosillo MÁ, Montoya T, González-Benjumea A, Fernández-Bolaños JG, Alarcón-de-la-Lastra C. Oleuropein down-regulated IL-1β-induced inflammation and oxidative stress in human synovial fibroblast cell line SW982, Food Funct. 2017;8:1890-1898.
43. Ryu SJ, Choi HS, Yoon KY, Lee OH, Kim KJ, Lee BY. Oleuropein suppresses LPS-induced inflammatory responses in RAW 264.7 cell and zebrafish. J Agric Food Chem. 2015;63:2098-2105.
44. Sun W, Wang X, Hou C, Yang L, Li H, Guo J, Huo C, Wang M, Miao Y, Liu J, Kang Y. Oleuropein improves mitochondrial function to attenuate oxidative stress by activating the Nrf2 pathway in the hypothalamic paraventricular nucleus of spontaneously hypertensive rats. Neuropharmacology. 2017;113:556-566.
45. Koc K, Cerig S, Ozek NS, Aysin F, Yildirim S, Cakmak O, Hosseinigouzdagani M, Geyikoglu F. The efficacy of oleuropein against non-steroidal anti-inflammatory drug induced toxicity in rat kidney. Environ Toxicol. 2019;34:67-72.
46. Dunning S, Ur Rehman A, Tiebosch MH, Hannivoort RA, Haijer FW, Woudenberg J, van den Heuvel FA, Buist-Homan M, Faber KN, Moshage H. Glutathione and antioxidant enzymes serve complementary roles in protecting activated hepatic stellate cells against hydrogen peroxide-induced cell death. Biochim Biophys Acta. 2013;1832:2027-2034.
47. Lemire J, Alhasawi A, Appanna VP, Tharmalingam S, Appanna VD. Metabolic defence against oxidative stress: the road less travelled so far. J Appl Microbiol. 2017;123:798-809.
48. Khalili A, Nekooeian AA, Khosravi MB. Oleuropein improves glucose tolerance and lipid profile in rats with simultaneous renovascular hypertension and type 2 diabetes. J Asian Nat Prod Res. 2017;19:1011-1021.

Turk J Pharm Sci 2021;18(4):430-437
DOI: 10.4274/tjps.galenos.2020.44538

ORIGINAL ARTICLE

Phytochemical Study and Antioxidant Activities of the Water-Soluble Aerial Parts and Isolated Compounds of *Thymus munbyanus* subsp. *ciliatus* (Desf.) Greuter & Burdet

Thymus munbyanus subsp. *ciliatus* (Desf.) Greuter & Burdet Bitkisinin Suda Çözünen Topraküstü Kısımları ve İzole Edilen Bileşenleri Üzerine Fitokimyasal Çalışmalar ve Antioksidan Aktiviteleri

Massika CHAOUCHE[1], İbrahim DEMİRTAŞ[2]*, Serkan KOLDAŞ[3], Ali Rıza TÜFEKÇİ[3], Fatih GÜL[2], Tevfik ÖZEN[4], Nouioua WAFA[5], Ahcène BOUREGHDA[1], Neslihan BORA[4]

[1]Mentouri Constantine Valorization of Natural Resources University, Department of Chemistry, Bioactive Molecules and Biological Analysis Unit, Constantine, Algeria
[2]Iğdır University Faculty of Arts and Sciences, Department of Biochemistry, Iğdır, Turkey
[3]Çankırı Karatekin University Faculty of Science, Department of Chemistry, Çankırı, Turkey
[4]Ondokuz Mayıs University Faculty of Arts and Sciences, Department of Chemistry, Samsun, Turkey
[5]Ferhat Abbas Setif University Faculty of Natural Life and Sciences, Laboratory of Phytotherapy Applied to Chronic Diseases, El Bez, Algeria

ABSTRACT

Objectives: The present study aimed to determine the phenolic compounds present in the water-soluble extracts of *Thymus munbyanus* subsp. *ciliatus* using high pressure liquid chromatography-time-of-flight mass spectrometry (MS). These phenolic compounds were further isolated and characterized for their antioxidant activities.

Materials and Methods: The aerial parts of *T. munbyanus* subsp. *ciliatus* were air dried, powdered, and extracted using water:methanol three times. The concentrated hydromethanolic extract was further dissolved in H_2O, filtered, and successively extracted using ethyl acetate, chloroform, and *n*-butanol. *T. munbyanus* extracts were further purified using column chromatography, and the purified extracts were subjected to *in vitro* antioxidant assays.

Results: Two previously undescribed compounds, namely methyl 2,3,5,6-tetrahydroxybenzoate and 4-hydroxy-5-methoxy-2-oxo-2H-pyran-3-carboxylic acid, and 14 known compounds, including 3 flavonoids; namely 3',5,5',7-tetrahydroxyflavanone, luteolin, and isorhamnetin-3-O-β-glucoside; a sterol glucoside named daucosterol; and 10 phenolic compounds, namely salicylic acid, ferulic acid, pluchoic acid, ethyl caffeate, methyl caffeate, protocatechuic acid, rosmarinic acid, p-coumaric acid, tyrosol, and protocatechuic aldehyde, were isolated from ethyl acetate and *n*-butanol extracts. The isolated compounds were characterized using 1D-2D $^{-1}H^{-13}C$ nuclear magnetic resonance and MS methods.

Conclusion: The compounds isolated from ethyl acetate and *n*-butanol extracts exhibited excellent antioxidant and 2,2-diphenyl-1-picrylhydrazyl scavenging activities. All these results highlighted the antioxidant potential of the isolated phenolic compounds and extracts, which could be further utilized for different pharmacological applications.

Key words: *Thymus munbyanus* subsp. *ciliatus*, phenolics, isolated compounds, antioxidant activity

***Correspondence:** ibdemirtas@gmail.com, **Phone:** +90 530 546 50 36, **ORCID-ID:** orcid.org/0000-0001-8946-647X
Received: 25.01.2020, **Accepted:** 11.10.2020

ÖZ

Amaç: Bu çalışmanın amacı, yüksek basınçlı sıvı kromatografisi-uçuş zamanlı-kütle spektrometresi (MS) kullanılarak *Thymus munbyanus* subsp. *ciliatus*'un suda çözünür ekstraktından fenolik bileşiklerin belirlenmesi, bileşiklerin izolasyonu, karakterizasyonu ve antioksidan aktivitelerinin belirlenmesidir.

Gereç ve Yöntemler: *Thymus munbyanus* subsp. *ciliatus* bitkisi küçük parçalar halinde kesilmiş ve üç kez metanol/su ile ekstre edilmiştir. Konsantre hidrometanolik ekstrakt saf su içerisinde tekrar çözünmüş; daha sonra süzülmüş ve art arda kloroform, etil asetat ve *n*-bütanol ile ekstre edilmiştir. *T. munbyanus* ekstreleri, kolon kromatografisi kullanılarak daha da saflaştırılmış ve saflaştırılmış ekstrelerde *in vitro* antioksidan deneyler yapılmıştır.

Bulgular: Önceden tanımlanmamış iki bileşik olan metil 2,3,5,6-tetrahidroksibenzoat ve 4-hidroksi-5-metoksi-2-okso-2H-piran-3-karboksilik asit ve 3 flavonoid dahil 14 bilinen bileşik; yani 3',5,5',7-tetrahidroksiflavanon, luteolin ve isorhamnetin-3-0-p-glukozit; daucosterol adlı bir sterol glikozit; ve etil asetat ve *n*-bütanol ekstraktlarından salisilik asit, ferulik asit, plukoik asit, etil kafeat, metil kafeat, protokateşik asit, rosmarinik asit, p-kumarik asit, tirosol ve protokateşik aldehit olmak üzere 10 fenolik bileşik izole edilmiştir. İzole edilen bileşikler, 1D-2D-1H-13C nükleer manyetik rezonans ve MS yöntemleri kullanılarak karakterize edilmiştir.

Sonuç: Etil asetat ve *n*-bütanol ekstraktlarından izole edilen bileşikler, mükemmel antioksidan ve 2,2-difenil-1-pikrilhidrazil süpürme aktiviteleri sergilemiştir. Tüm bu sonuçlar, farklı farmakolojik uygulamalar için daha fazla kullanılabilecek izole fenolik bileşiklerin ve ekstraktların antioksidan potansiyelini vurgulamıştır.

Anahtar kelimeler: *Thymus munbyanus* subsp. *ciliatus*, fenolikler, izole bileşikler, antioksidan aktivite

INTRODUCTION

Lamiaceae family of plants comprises of a variety of medicinal and aromatic plants. Among these, the members of *Thymus* genus are known to exhibit numerous biological activities, including antiviral, antifungal, and antioxidant activities.[1-3] *Thymus* genus mainly comprises of approximately 400 species of aromatic perennial plants and subshrubs, which grow mostly in Southern Europe, the Mediterranean region, North Africa, and Asia.[4] Among these, 15 species, including *Thymus munbyanus* subsp. *ciliatus* (Desf.) Greuter & Burdet, are known to be distributed in Algeria. This subspecies is also known as *Thymus ciliatus* (Desf.) Benth., and it is addressed as "Zaatar" in Arabic. Several previous studies have reported the volatile chemical composition (essential oil) and antioxidant activities of *T. munbyanus* extracts; however, no information regarding the phytochemical nature of *T. munbyanus* extracts is available.[5-11]

In this study, the secondary metabolites present in the aerial parts of *T. munbyanus* subsp. *ciliatus* were analyzed, isolated, and assessed for their *in vitro* antioxidant activities. To the best of our knowledge, this was the first study to identify and characterize compounds isolated from this plant.

MATERIALS AND METHODS

Chemicals and plant material

Most of the chemicals and reagents used in this study were purchased from Sigma (St. Louis, MO, USA). Some chemicals of analytical grade quality were procured from other commercial companies Roche (Darmstadt, Germany), Panreac Quimica (Spain) and MERCK (Germany). The aerial parts of *T. munbyanus* subsp. *ciliatus* were collected from Babor near Setif City, Algeria in May 2013. This plant was identified by Dr. W. Nouioua based on the information regarding Algerian flora.[12] A voucher specimen was deposited in the laboratory herbarium unit of the University of Constantine 1, VARENBIOMOL Research Unit (TC/123/05-13). The plant materials were stored at -20°C in a freezer until used for extraction.

Extraction and isolation of compounds

Air-dried parts (9.5 kg) of *T. munbyanus* subsp. *ciliatus* were powdered using a blender and extracted three times with MeOH/water (80/20, v/v). The hydromethanolic extracts were concentrated, dissolved in H_2O (1000 mL), and filtered. Further, the water-soluble part was extracted three times sequentially with chloroform, ethyl acetate, and *n*-butanol. Following extraction, chloroform (17.7 g), ethyl acetate (33 g), and *n*-butanol (59.2 g) extracts were collected.

Then, 32 g of ethyl acetate extract was fractionated using column chromatography, with a Sephadex LH-20 column. For elution, an isocratic system of $CHCl_3$/MeOH/hexane (7/2/1) was used and 26 fractions were collected. The precipitate from fraction 9 (155 mg) showed one spot contaminated with chlorophyll, which was washed with diethyl ether and acetone to give compound 5 (15 mg) and fraction 10 (2.5 g). The fractions were again fractionated using column chromatography, with a Sephadex LH-20 column, and elution was performed with an isocratic system of hexane/MeOH/$CHCl_3$ (1/2/7). This was subsequently followed by fractionation using a preparative column comprising silica gel, wherein elution with toluene/ethyl acetate/formic acid (10/6/1) yielded compounds 6 (3.1 mg), 11 (2.4 mg), 7 (5.5 mg), and 14 (2.7 mg). Moreover, fraction 11 (145 mg) and fraction 12 (124.18 mg) were purified on preparative plates of silica gel, and elution with toluene/ethyl acetate/formic acid (10/4/1) yielded compound 9 (1.7 mg) and compound 8 (7.3 mg), respectively. Further, fraction 14 (345 mg) was purified using a preparative column comprising silica gel, and elution with the same solvent mixture, at same ratio, resulted in the isolation of compounds 15 (5.5 mg), 12 (1.7 mg), and 1 (20 mg). Besides this, fraction 15 (3.12 g) was separated via column chromatography using a Sephadex LH-20 column, wherein samples were eluted isocratically with chloroform/methanol (7/3). This was followed by subsequent fractionation using a preparative silica gel, and elution with toluene/ethyl acetate/formic acid (10/2/1) yielded compounds 2 (3.2 mg), 3 (1.3 mg), 10 (3.4 mg), and 16 (9.1 mg).

The butanoic extract (10 g) was further subjected to fractionation on a polyamide column (SC6) with a gradient of toluene-

MeOH, which further increased solvent polarity and yielded 21 fractions. Further, fraction 5 (0.37 g) was subjected to column chromatography on a Sephadex LH-20 column using isocratic $CHCl_3$/MeOH (6/4), which yielded 10 subfractions. Subfraction 7 (61.2 mg) was purified using thin-layer chromatography with EtOAc/MeOH/H_2O (18/1/1) to yield compound 13 (11 mg). Additionally, fraction 6 (76.3 mg) was separated using column chromatography, with Sephadex LH-20 as a stationary phase and methanol as a solvent phase, which resulted in the isolation of compound 4 (17 mg).

High-pressure liquid chromatography coupled with time-of-flight mass spectrometry (HPLC-TOF/MS) analysis

Phenolic contents present in organic solvent extracts, i.e., chloroform, ethyl acetate, and *n*-butanol extracts, were analyzed using HPLC-TOF/MS. HPLC analysis was performed using an Agilent 1260 Infinity Binary System (Agilent Technologies, Santa Clara, CA, USA) coupled with a 6210 TOF LC/MS detector on a ZORBAX SB-C18 (4.6x100 mm, 3.5 µm) column. Ultrapure water with 0.1% formic acid was used in mobile phase A, whereas mobile phase B contained 100% acetonitrile. The chromatographic separation was performed as per the following gradient: 0-1 min 10% B, 1-20 min 50% B, 20-23 min 80% B, and 23-30 min 10% B, with a flow rate of 0.6 mL. The column temperature was set at 35°C, and the injection volume was 10 µL. Retention times and m/z values were recorded for the phenolic compounds and in terms ofcompared with those of standard components. The crude extracts were dissolved in methanol at 25°C to obtain a concentration of 200 ppm and filtered using 0.45 µm PTFE filters.[13]

In vitro antioxidant assays

Total antioxidant capacity

To evaluate the antioxidant activities of the extracts and isolated compounds, ammonium phosphomolybdenum assay was performed, as previously described by Prieto et al.[14] To prepare reaction solutions, sample solutions were prepared at different concentrations, 25, 50, and 100 µg/mL (0.3 mL each), mixed with 3 mL of reagent solution (ammonium molybdate-sodium phosphate-sulfuric acid), and vortexed to obtain homogeneous solutions. Further, the closed tubes containing the reaction solutions were incubated in a hot water bath for 90 min. Following this, the mixtures were cooled in an ice bath, and the absorbance of each solution was measured at 695 nm using a ultraviolet-visible spectrophotometer (UV-Vis) (Thermo Scientific Evaluation Array UV-Vis Spectrophotometer). For blank, 0.3 mL of solvent was used.

Free radical scavenging capacity

The scavenging activity of the samples was evaluated according to the method previously reported by Blois.[15] In the present study, 1.5 mL of different concentrations of extracts and isolated compounds were mixed with 2,2-diphenyl-1-picrylhydrazyl ($DPPH^{\cdot}$) solution (0.5 mL) in a test tube to get a homogeneous solution. Each mixture was incubated at 25°C for 30 min in a dark environment. The absorbance of resulting solutions was measured at 517 nm using a UV-Vis spectrophotometer (Thermo Scientific Evaluation Array UV-Vis spectrophotometer). The scavenging activity was calculated as per the following formula:

% activity = $[(A_{1\,(517\ nm)} - A_{2\,(517\ nm)}) / A_{1\,(517\ nm)}] \times 100$; where A_1 denotes control absorbance and A_2 denotes absorbance of the sample.

Statistical analysis

The antioxidant activity of the samples was evaluated in triplicates, and the results were presented as an average of the three experiments. Data were analyzed using SPSS 20.0 software, and $p<0.05$ was considered to be statistically significant.

RESULTS AND DISCUSSION

Characterization of isolated compounds

The present study aimed to detect, isolate, and characterize the phenolic compounds present in the aerial extracts of *T. munbyanus* subsp. *ciliatus*. Two previously undescribed compounds, namely methyl 2,3,5,6-tetrahydroxybenzoate (1) and 4-hydroxy-5- methoxy-2-oxo-2H-pyran-3-carboxylic acid (16), and 14 known compounds, including 3 flavonoids; 3',5,5',7-tetrahydroxyflavanone (2), luteolin (3), and isorhamnetin-3-O-β-glucoside (4); a sterol glucoside named daucosterol (5); and 11 phenolic compounds, namely salicylic acid (6), pluchoic acid (7), methyl caffeate (8), ethyl caffeate (9), protocatechuic acid (10), ferulic acid (11), *p*-coumaric acid (12), rosmarinic acid (13), tyrosol (14), and protocatechuic aldehyde (15), were isolated from *n*-butanol and ethyl acetate extracts of *T. munbyanus* subsp. *ciliatus*. The structures of all compounds isolated from *T. munbyanus* are shown in Figure 1.

Compound (1) was obtained as colorless amorphous powder. The molecular formula of compound 1 was determined to be $C_8H_8O_6$ using EI-MS with negative ion m/z 198.08 $(M-H)^-$, which indicated that the molecule had five degrees of unsaturation. The ^{1}H- nuclear magnetic resonance (NMR) spectrum in acetone-d6 exhibited just two singlets: first at δ_H 7.33 (s, 1H, H-4), which indicated the presence of penta substituted benzene ring, and second at δ_H 3.88 (s, 3H), corresponding to the presence of methoxy groups.

Further, ^{13}C NMR, HSQC, and DEPT spectra exhibited six carbon signals, including one methoxy group at δ_c 55.73 (C-8), one methine at δ_c 107.23 (C-4), and four quaternary carbons. The four quaternary carbons included three aromatic carbons at δ_c 120.59 (C-1), 147.39 (C-2/C-6), and 140.39 (C-3/C-5) and one carbon at δ_c 166.55 (C-7), which was characterized as a carbonyl carbon of an ester group.

A long-range C-H correlation was observed for C-4 aromatic proton in the HMBC spectrum ($^2J_{CH}$ and $^3J_{CH}$ correlations) with C-3/C-5 and C-2/C-6. The structure was further confirmed by the HMBC spectrum. Thus, compound 1 was identified as methyl 2,3,5,6-tetrahydroxybenzoate.

Compounds 2-15 have been previously isolated and characterized, and data for these compounds are given in Supplementary Information.

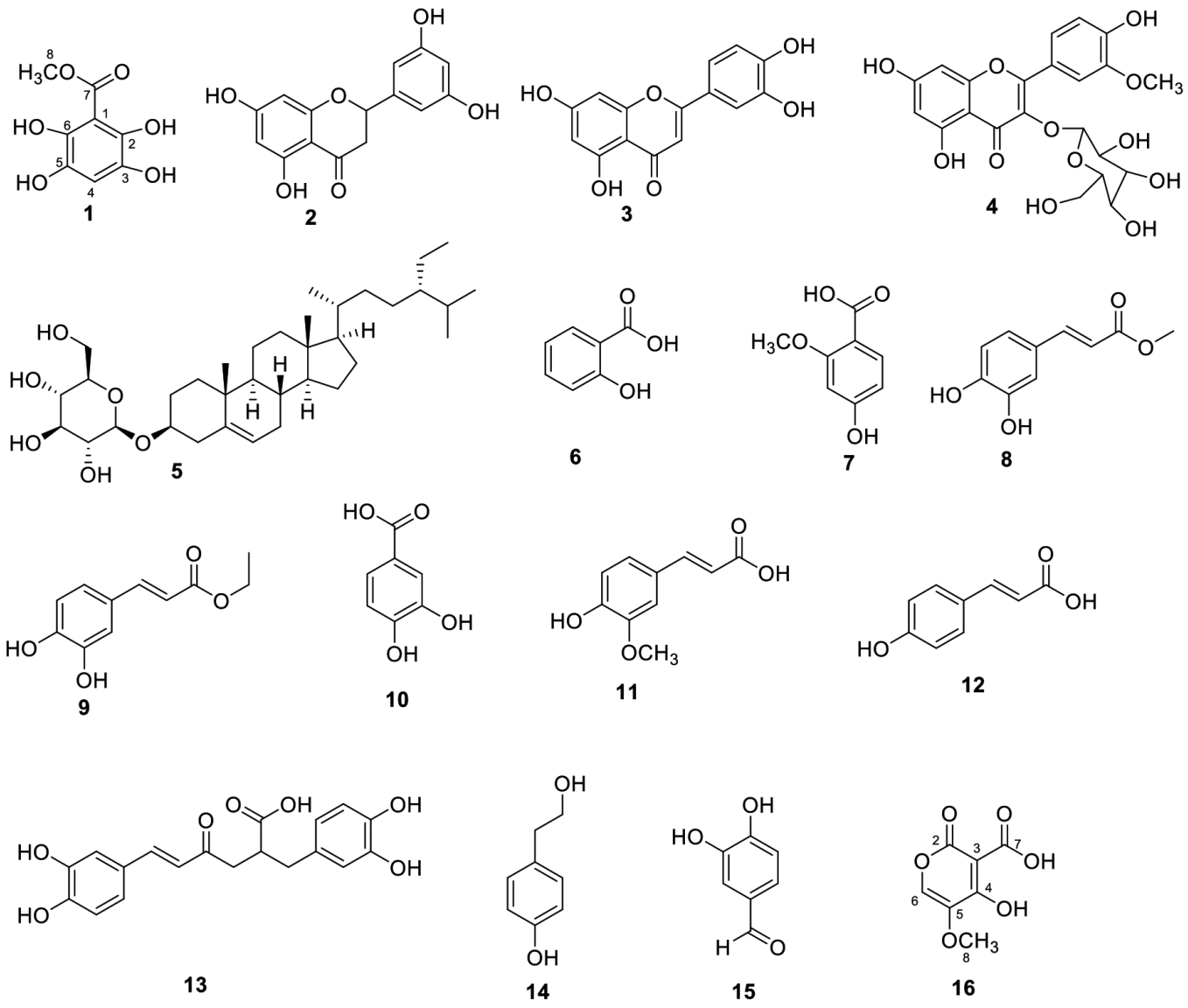

Figure 1. Structures of compounds isolated from *Thymus munbyanus* subsp. *ciliatus* as methyl 2,3,5,6-tetrahydroxybenzoate (1), 3',5,5',7-tetrahydroxyflavanone (2), luteolin (3), isorhamnetin-3-O-β-glucoside (4), daucosterol (5), salicylic acid (6), pluchoic acid (7), methyl caffeate (8), ethyl caffeate (9), protocatechuic acid (10), ferulic acid (11), *p*-coumaric acid (12), rosmarinic acid (13), tyrosol (14), protocatechuic aldehyde (15) and 4-hydroxy-5-methoxy-2-oxo-2H-pyran-3-carboxylic acid (16)

Compound 16 was obtained as a yellowish-brown solid. The molecular formula for this compound was found to be $C_7H_6O_6$, which suggested the presence of five degrees of unsaturation. The ^{13}C NMR and DEPT spectra further confirmed the presence of seven carbon atoms that included one methoxy group at δ_c 55.31; four vinyl carbons with one methine at δ_c 106.57 (C-6); quaternary carbon atoms at δ_c 128.11 (C-3), 137.54 (C-5), and 146.91 (C-4); and the carbonyl region with two peaks at δ_c 173.81 and 168.83, which were indicative of the presence of a carbonyl carbon of the carboxylic acid and carbonyl carbon of the α-pyrone ring, respectively. The ^1H NMR and HSQC spectra further confirmed the hypothesis. In particular, it displayed one singlet of one proton at δ_H 7.33 that was assigned to H-6. Besides this, three proton singlets were reported at δ_H 3.87 for OCH_3. The HMBC measurements showed long-range correlations between the protons at δ_H 7.33 and two quaternary carbons at δ_c 137.54 (C-5) and δ_c 146.91 (C-4). The HMBC experiments also showed connectivity between the methoxy protons at δ_H 3.87 and the quaternary carbon at δ_c 146.91 (C-4). These findings indicated that the carboxylic acid was connected to C-3, whereas a methoxy functional group was connected to C-5. Therefore, compound 16 was assigned the structure of 4-hydroxy-5-methoxy-2-oxo-2H-pyran-3-carboxylic acid.

Quantification of the polar constituents of T. munbyanus subsp. ciliatus extracts

The extracts of *T. munbyanus* were analyzed using HPLC-TOF/MS. The compounds isolated from the extracts were identified in terms of their retention times and m/z values, and these values were compared with those of standard samples. Altogether,

the results of spectral analysis revealed the presence of 29 compounds, including 11 phenolic acids and 18 flavonoids and phenolics (Table 1). Interestingly, the concentration of these compounds was found to be very less in the chloroform extract. The highest concentrations of scutellarin, baicalin, and fumaric acid were reported in the butanoic extract; however, these compounds were present in very low amounts in the ethyl acetate extract. Whereas, quercetin-3-β-D-glucoside, caffeic, and 4-hydroxybenzoic acid were found to be the major consitutents of the ethyl acetate extract.

Thus, these results highlight that the analyzed extracts of *T. munbyanus* subsp. *ciliatus*, i.e., ethyl acetate and butanoic extracts, comprised of complex mixtures of plant secondary metabolites. These active ingredients, particularly flavonoids and phenolic acids, are previously known to exhibit antioxidant properties.[16,17]

Total antioxidant capacity

The antioxidant activities of the isolated and extracted samples were measured and expressed as absorbance values. This assay involved the reduction of $Mo^{+6} \rightarrow Mo^{+5}$, and the antioxidant activity was confirmed if a green phosphate/Mo^{5+} complex was formed, which showed maximum absorption at 695 nm at acidic pH.[14] This assay has been widely used to evaluate the total antioxidant capacity of various extracts and isolates. The results for total antioxidant activity of the isolates and extracts obtained from *T. munbyanus* subsp. *ciliatus* are shown in Figure 2. Here, higher absorbance of the antioxidant denoted the presence of antioxidant property. It was observed that ethyl acetate extract and compound 8 exhibited similar antioxidant activities at concentrations of 25, 50, and 100 µg/mL as compared to butylated hydroxyanisole (BHA) and butylated hydroxytoluene (BHT), $p<0.05$. Phenolic compounds have long been explored as a therapeutic option to prevent cancer, owing to its effective antioxidant potency.[18] It has also been reported that compounds having antioxidant activity play an important role in the inhibition of lipid peroxidation.[19] These results highlighted that the isolated compounds and different solvent extracts, obtained from *T. munbyanus*, acted as promising natural sources of nontoxic and natural antioxidants.

Free radical scavenging activity

DPPH˙ free radical scavenging assay is generally applied to determine the antioxidant levels of extracts in a relatively short period of time. In particular, the ability of compounds to deliver hydrogen is assessed. The utility of this assay has been established and compared with that of other experiments.[20] It has been shown that natural chemicals reduce DPPH˙ due to their ability to donate hydrogen atom.[21] When an antioxidant and DPPH˙ (a synthetic radical) are mixed, the antioxidant gives an electron to $DPPH_2$ and the purple color is converted into yellow color.

Interestingly, the free radical scavenging activitiy of natural contents was found to increase in a dose-dependent manner, $p<0.05$. In particular, compounds 2, 7, 8, 10, and 15 displayed a higher scavenging activity at high doses than BHA and BHT (Figure 3). This might be attributed to two different -OH substitutions that favor DPPH˙ scavenging activity.[22] The stabilization of radicals by two subsequent -OH substitutions of phenolic groups for compounds 3, 8, and 15 are shown in Figure 4. In particular, compounds 3, 8, and 15 showed their ability to remove radicals, which is attributed to their resonance stability and presence of hydroxyl groups. It can act as a radical inhibitor and stop the radical reaction. Plant

Table 1. Phenolic compounds isoalted from *Thymus munbyanus* subsp. *ciliatus* extracts, as determined using high-pressure liquid chromatography coupled with time-of-flight mass spectrometry

Phenolic compounds, mg of phenolic compound/kg	$CHCl_3$ extract	Ethyl acetate extract	*n*-butanol extract
Fumaric acid	nd	0.44	9.07
Gentisic acid	0.14	3.82	0.72
Chlorogenic acid	0.09	0.73	2.14
4-hydroxybenzoic acid	1.04	21.03	0.91
Protocatechuic acid	nd	0.78	1.06
Caffeic acid	0.11	24.96	0.50
Vanillic acid	0.26	1.62	0.39
Syringic acid	0.99	3.55	1.25
Rutin	nd	0.11	1.00
4-hydroxybenzaldehyde	0.02	tr	tr
Polydatine	tr	0.90	tr
Scutellarin	0.39	0.64	40.29
Quercetin-3-β-D-glucoside	tr	17.14	5.52
Naringin	1.09	1.50	2.12
Diosmin	0.65	2.45	2.35
Taxifolin	tr	0.12	tr
Neohesperidin	tr	0.06	tr
Baicalin	tr	tr	15.58
p-coumaric acid	tr	0.13	tr
Morin	0.23	2.36	0.70
Salicylic acid	tr	0.33	tr
Quercetin	tr	1.48	tr
Cinnamic acid	0.32	0.30	0.51
Apigenin	0.05	4.05	tr
Naringenin	tr	0.29	tr
Kaempferol	tr	1.13	tr
Diosmetin	tr	4.37	nd
Eupatorin	0.32	tr	tr
Wogonin	0.90	tr	Nd

tr: Trace; nd: Not detected

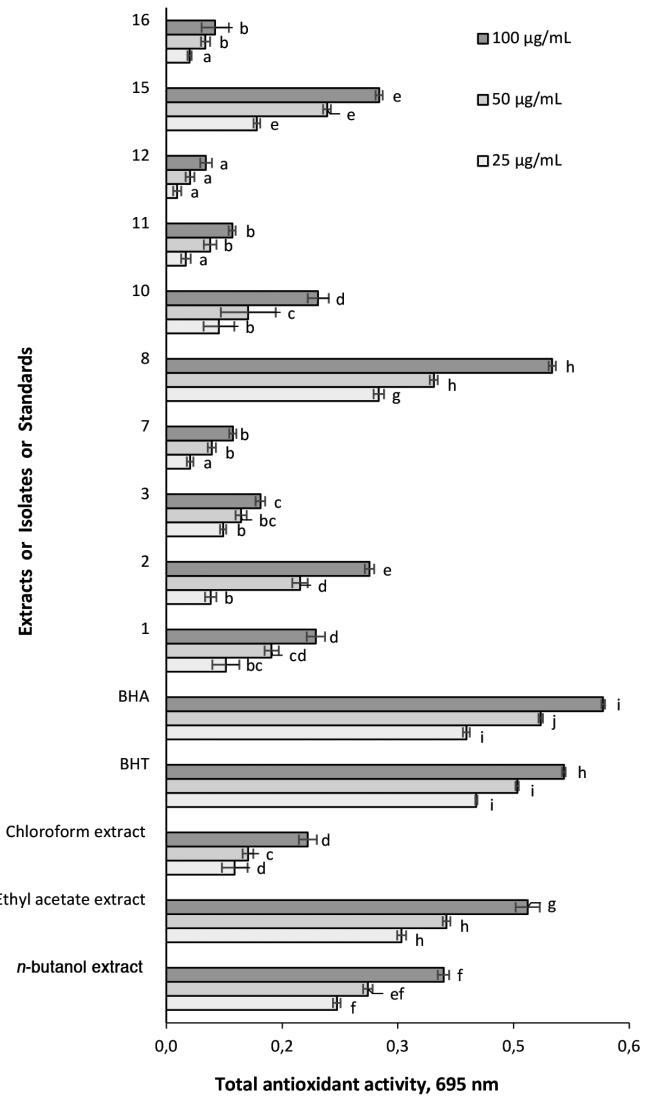

Figure 2. Total antioxidant activity of isolated and extracted samples
BHA: Butylated hydroxyanisole, BHT: Butylated hydroxytoluene

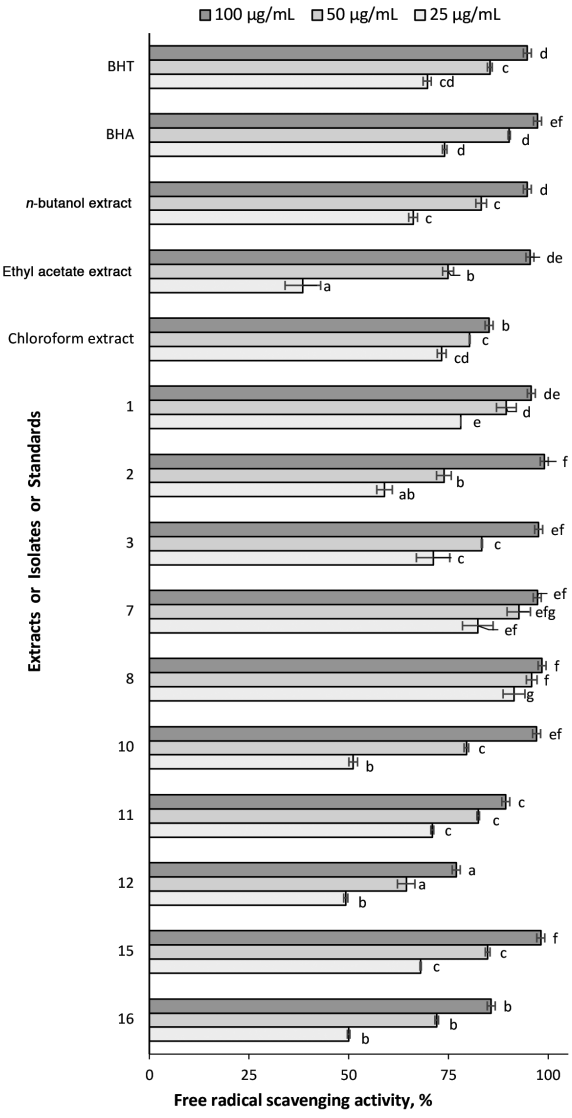

Figure 3. Free radical (DPPH˙) scavenging activities of isolates and extracts
BHA: Butylated hydroxyanisole, BHT: Butylated hydroxytoluene

phenolics generally include superoxide radicals, lipid alkoxyl radicals, lipid peroxyl radicals, and nitric oxide radical, which are known to exhibit cleansing, metal chelating, antiallergic, estrogenic, and antiviral effects.[23] In general, polymeric polyphenols are known to be more effective antioxidants than monomeric phenolics.[24] The presence of -OH group in the ortho or para position of phenol increases the antioxidant activity of a compound.

CONCLUSION

This is the first study to report the isolation and characterization of phenolic compounds from *T. munbyanus* subsp. *ciliatus* species grown in Algeria. In particular, the study reported the isolation of two new compounds, named methyl 2,3,5,6-tetrahydroxybenzoate and 4-hydroxy-5-methoxy-2-oxo-2H-pyran-3-carboxylic acid, and 14 previously known compounds that belonged to different chemical classes, namely flavonoids, sterol, and phenolic derivatives. The ethyl acetate extract exhibited excellent free radical scavenging activity *in vitro*, which correlated well with the presence of polyphenol derivatives in compounds 3, 8, and 15.

Thus, all these findings provide scientific basis for the use of *T. munbyanus* subsp. *ciliatus* derivatives as functional ingredients in Algerian traditional medicine.

ACKNOWLEDGMENTS

This work was supported by a grant from State Planning Organization of Turkey (DPT:2010K120720).

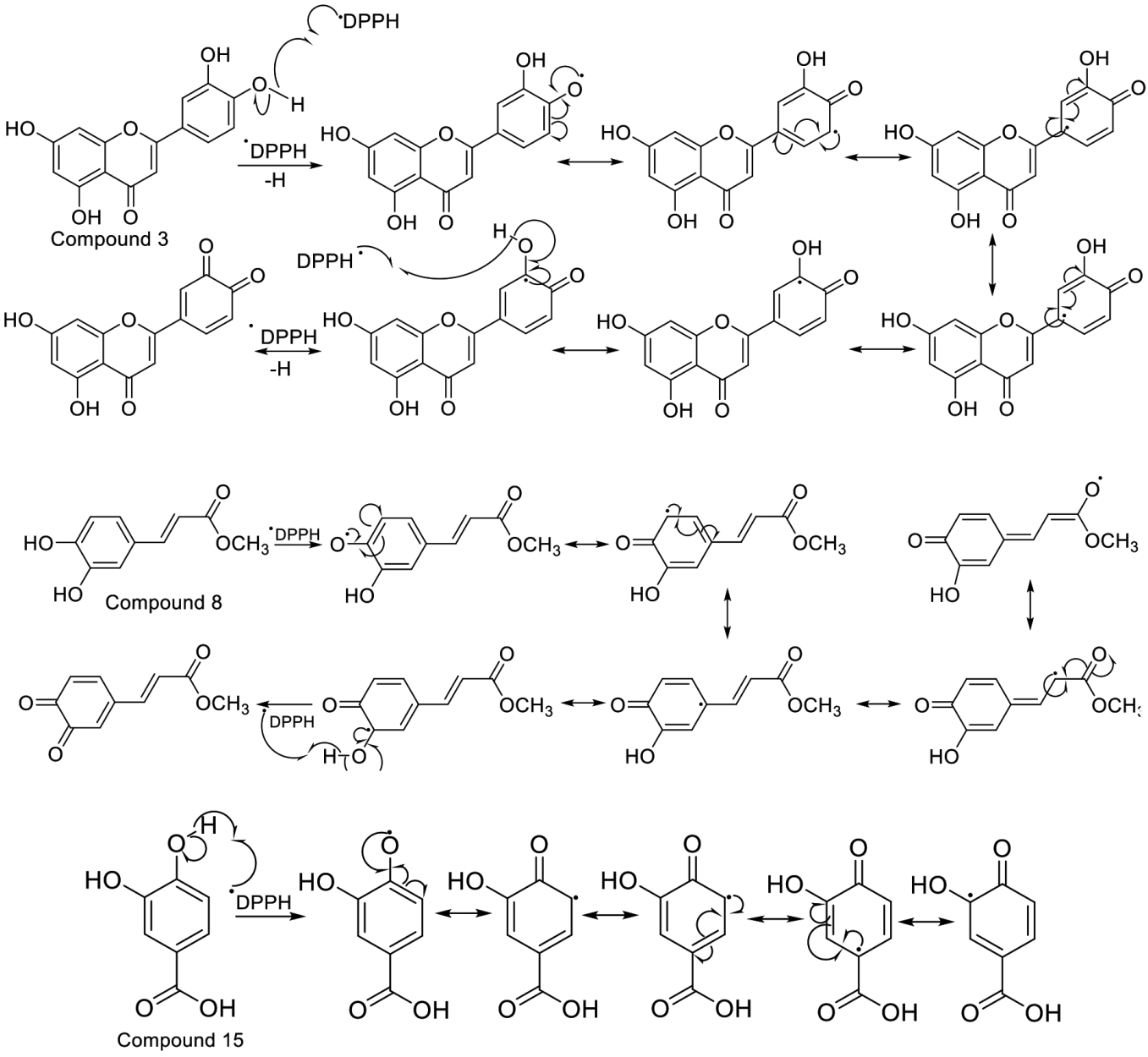

Figure 4. Free radical (DPPH˙) scavenging reaction for compounds 3, 8, and 15

Conflict of interest: No conflict of interest was declared by the authors. The authors are solely responsible for the content and writing of this paper.

REFERENCES

1. Baharfar R, Azimi R, Mohseni M. Antioxidant and antibacterial activity of flavonoid-, polyphenol- and anthocyanin-rich extracts from Thymus kotschyanus boiss & hohen aerial parts. J Food Sci Technol. 2015;52:6777-6783.
2. Olennikov D, Chirikova NK. Phenolic Compounds from Siberian Species Thymus baicalensis and T. sibiricus. Chem Nat Compd. 2018;572-576.
3. Maksimović Z, Stojanović D, Šoštarić I, Dajić Z, Ristić M. Composition and radical-scavenging activity of *Thymus glabrescens* Willd. (Lamiaceae) essential oil. J Sci Food Agric. 2008;88:2036-2041.
4. Salhi A, Bouyanzer A, El Mounsi I, Bendaha H, Hamdani I, El Ouariachi EM, Chetounani A, Chahboun N, Hammouti B, Desjobert JM, Costa J. Chemical composition, antioxidant and anticorrosive activities of Thymus Algeriensis. J Mater Environ Sci. 2016;7:3949-3960.
5. Kabouche A, Ghannadi A, Kabouche Z. Thymus ciliatus--the highest thymol containing essential oil of the genus. Nat Prod Commun. 2009;4:1251-1252.

6. Jamali CA, El Bouzidi L, Bekkouche K, Lahcen H, Markouk M, Wohlmuth H, Leach D, Abbad A. Chemical composition and antioxidant and anticandidal activities of essential oils from different wild Moroccan Thymus species. Chem Biodivers. 2012;9:1188-1197.
7. Ghorab H, Kabouche A, Semra Z, Ghannadi A, Sajjadi SE, Touzani R, Kabouche Z. Biological activities and compositions of the essential oil of Thymus ciliatus from Algeria. Der Pharm Lett. 2013;5:28-32.
8. Ghorab H, Kabouche A, Kabouche Z. Comparative compositions of essential oils of Thymus growing in various soils and climates of North Africa. Sahara. 2014;355:13.
9. Heni S, Bennadja S, Abdelghani D. Chemical composition and antibacterial activity of the essential oil of *Thymus ciliatus* growing wild in North Eastern Algeria. J Appl Pharm Sci. 2015;5:56-66.
10. Touhami A, Chefrour A, Boukhari A, Ismail F. Comparative study of chemical compositions and antimicrobial effect of different genius of Thymus harvested during two period of development. JAPS. 2016;6:051-056.
11. Sofiane G, Nouioua W, Khaled A, Amar O. Antioxidant and antimicrobial activities of flavonoids extracted from Thymus ciliatus (Desf.) Benth. Der Pharmacia Lettre. 2015;7:358-363.
12. Quézel P, Santa S. Nouvelle flore de l'Algérie et des régions désertiques méridionales. 1963.
13. Abay G, Altun M, Koldaş S, Tüfekçi AR, Demirtas I. Determination of Antiproliferative Activities of Volatile Contents and HPLC Profiles of Dicranum scoparium (Dicranaceae, Bryophyta). Comb Chem High Throughput Screen. 2015;18:453-463.
14. Prieto P, Pineda M, Aguilar M. Spectrophotometric quantitation of antioxidant capacity through the formation of a phosphomolybdenum complex: specific application to the determination of vitamin E. Anal Biochem. 1999;269:337-341.
15. Blois MS. Antioxidant determinations by the use of a stable free radical. Nature. 1958;181:1199-1200.
16. Bors W, Heller W, Michel C, Saran M. Flavonoids as antioxidants: determination of radical-scavenging efficiencies. Methods Enzymol. 1990;186:343-355.
17. Laughton MJ, Evans PJ, Moroney MA, Hoult JR, Halliwell B. Inhibition of mammalian 5-lipoxygenase and cyclo-oxygenase by flavonoids and phenolic dietary additives. Relationship to antioxidant activity and to iron ion-reducing ability. Biochem Pharmacol. 1991;42:1673-1681.
18. Ozen T, Yildirim K, Toka M. The impacts of *Elaeagnus umbellata* Thunb. leaf and fruit aqueous extracts on mice hepatic, extrahepatic antioxidant and drug metabolizing enzymes related structures. Braz J Pharm Sci. 2017;53.
19. Demirtas I, Erenler R, Elmastas M, Goktasoglu A. Studies on the antioxidant potential of flavones of Allium vineale isolated from its water-soluble fraction. Food Chem. 2013;136:34-40.
20. Polterait O. Antioxidants and Free-Radical Scavengers of Natural Origin. Current Organic Chemistry. 1997;1:415-440.
21. Habashy NH, Serie MMA, Attia WE, Abdelgaleil SAM. Chemical characterization, antioxidant and anti-inflammatory properties of Greek *Thymus vulgaris* extracts and their possible synergism with Egyptian *Chlorella vulgaris*. 2018;40:317-328.
22. Xie J, Schaich KM. Re-evaluation of the 2,2-diphenyl-1-picrylhydrazyl free radical (DPPH) assay for antioxidant activity. J Agric Food Chem. 2014;62:4251-4260.
23. Halliwell B. The chemistry of free radicals. Toxicol Ind Health. 1993;9:1-21.
24. de Beer D, Joubert E, Gelderblom WCA, Manley M. Phenolic Compounds: A Review of Their Possible Role as *In Vivo* Antioxidants of Wine. S Afr J Enol Vitic. 2017;23:48-61.

Turk J Pharm Sci 2021;18(4):438-444
DOI: 10.4274/tjps.galenos.2020.58897

ORIGINAL ARTICLE

Analytical Method Development and Validation for Simultaneous Determination of Simvastatin and Mupirocin Using Reverse-Phase High-pressure Liquid Chromatographic Method

Ters Faz Yüksek Basınçlı Sıvı Kromatografik Yöntem Kullanılarak Simvastatin ve Mupirosin Eşzamanlı Belirlenmesi için Analitik Yöntem Geliştirme ve Validasyon

Rupali KALE[1]*, Pratiksha SHETE[2], Dattatray DOIFODE[1], Sohan CHITLANGE[2]

[1]Dr. D.Y. Patil Institute of Pharmaceutical Sciences and Research, Department of Pharmaceutics, Pimpri-Chinchwad, India
[2]Dr. D.Y. Patil Institute of Pharmaceutical Sciences and Research, Department of Quality Assurance, Pimpri-Chinchwad, India

ABSTRACT

Objectives: This study was aimed to develop and validate the use of reverse-phase high pressure liquid chromatographic method for the estimation of simvastatin (SIM) and mupirocin (MUP) simultaneously.

Materials and Methods: The chromatographic method developed is optimized for flow rate with the column, solvent, and buffer used and mobile phase ratio, molarity, and pH. The validation of the optimized method and the forced degradation studies of both drugs (under acidic, alkaline, oxidation, heat, light, and neutral conditions) were conducted following the The International Council for Harmonisation of Technical Requirements for Pharmaceuticals for Human Use guidelines.

Results: Kromasil C18 column (250 mm × 4.6 mm, 5 µm) with ultraviolet detection at 224 nm and acetonitrile/phosphate buffer (30 mM, 70:30 v/v, pH 3.5; adjustment done using orthophosphoric acid) as mobile phase at a flow rate of 1.1 mL/min were observed to provide a good resolution for MUP and SIM at retention times of 2.32±0.008 and 13.55±0.254 min, respectively, with high accuracy (percent recovery was 99.69±0.82 for MUP and 101.10±0.02 for SIM) and linearity in the range of 5-30 µg/mL (r^2: 0.9969 for MUP and r^2: 0.9959 for SIM). The diagnostic limit and the lower limit of determination were 0.771±0.234 and 2.338±0.246 µg/mL for MUP and 0.595±0.282 and 1.803±0.334 µg/mL for SIM, respectively. The validated method was used to understand the degradation behavior of both drugs after the forced degradation studies.

Conclusion: The analytical method developed is determined to be specific, sensitive, precise, and accurate for the estimation of MUP and SIM simultaneously in the combined dosage form.

Key words: Simvastatin, mupirocin, validation, stability

ÖZ

Amaç: Bu çalışmanın amacı, simvastatin (SIM) ve mupirosin (MUP) tahmininde eş zamanlı olarak ters fazlı yüksek performanslı sıvı kromatografik yöntemin kullanımını geliştirmek ve doğrulamaktır.

Gereç ve Yöntemler: Geliştirilen kromatografik yöntem kolon, çözücü ve tampon kullanılan akış hızı, mobil faz oranı, molarite ve pH için optimize edilmiştir. Optimize edilmiş yöntemin doğrulanması ve her iki uyuşturucunun (asidik, alkali, oksidatif, termal, ışık ve nötr koşullar için) zorunlu bozunma çalışmaları İnsan Kullanımına Yönelik Farmasötikler için Teknik Gereksinimlerin Uyumlaştırılması Uluslararası Konseyi yönergelerine göre gerçekleştirilmiştir.

Bulgular: Ultraviyole saptaması 224 nm'deki C18 kolon (kromasil; 250 mm × 4,6 mm, 5 µm) ve mobil fazda 1,1 mL/dk akış hızında ortofosforik asit ile ayarlanmış pH 3,5 asetonitril: fosfat tamponunun (30 mM) (70:30 v/v) MUP ve SIM çözünürlüğünü sırasıyla 2,32±0,008 dk ve 13,55±0,254 dk

*Correspondence: rupalikale07@gmail.com, Phone: +9376927834, ORCID-ID: orcid.org/0000-0001-9777-5133
Received: 14.05.2020, Accepted: 16.10.2020

tutma sürelerinde yüksek doğrusallık (% geri kazanım, MUP için 99,69±0,82 ve SIM için 101,10±0,02) ve 5-30 µg/mL aralığında doğrusallık ile (MUP için r^2: 0,9969 ve SIM için r^2: 0,9959) sağladığı bulunmuştur. Tespit limiti ve kantitasyon limiti sırasıyla MUP için 0,771±0,234 ve 2,338±0,246 µg/mL, SIM için 0,595±0,282 ve 1,803±0,334 µg/mL olarak bulunmuştur. Valide yöntem, zorunlu bozunma çalışmalarından sonra her iki ilacın bozunma davranışını anlamak için kullanılmıştır.

Sonuç: Geliştirilen analitik yöntemin, kombine dozaj formunda MUP ve SIM'nin aynı anda tahmini için spesifik, hassas, kesin ve doğru olduğu belirlenmiştir.

Anahtar kelimeler: Simvastatin, mupirosin, validasyon, stabilite

INTRODUCTION

Mupirocin (MUP), chemically known as (αE,2S,3R,4R,5S)-5-[(2S,3S,4S,5S)-2,3-epoxy-5-hydroxy-4-methylhexyl] tetrahydro-3,4-dihydroxy-β-methyl-2H-pyran-2-crotonic acid, ester with 9-hydroxynonanoic acid, calcium salt (2:1), dihydrate, is the most commonly used topical antibiotics.[1,2] MUP is known to be active against *Staphylococcus aureus* and *Staphylococcus epidermidis*, which are aerobic Gram-positive cocci, and methicillin-resistant *S. aureus*, which is Gram-negative cocci.[3] Topical ointment of 2% MUP is used as an antimicrobial agent for prophylaxis use in burns, operative wounds, and ulcers, as well as for the treatment of skin infections.[4,5] Simvastatin (SIM), chemically known as (1S,3R,7S,8S,8aR)-8-[2-[(2R,4R)-4-hydroxy-6-oxotetrahydro-2H-pyran-2-yl]ethyl]-3,7-dimethyl-1,2,3,7,8,8a-hexahydronaphthalen-1-yl 2,2-dimethylbutanoate, is traditionally used in the treatment of various types of hypercholesterolemia, which decrease cholesterol by inhibiting the rate-limiting step in the synthesis of cholesterol.[6] Other than this traditional application, the wound-healing activity of SIM has been recently explored as it improves vascular endothelial growth factor production, thereby stimulating angiogenesis, reducing oxidative stress, improving microvascular function, and enhancing endothelial function, which ultimately improves the wound-healing activity.[7] These properties make SIM a drug of choice to be used in combination with antimicrobial agents.[8]

Various analytical methods for the analysis of individual drugs, as well as in combination with other drugs, have been reported, including ultraviolet (UV) spectrophotometry and high-performance liquid chromatography (HPLC). Abu-Nameh et al.[9] proposed a simple HPLC method for the rapid analysis of SIM in commercial tablet formulation using a C18 Hypersil column and mobile phase composed of acetonitrile (ACN), phosphate buffer, and methanol with the ratio of 5:3:1 v/v/v and UV detection at 230 nm. Bana et al.[10] reported the development of the UV spectroscopy and HPLC methods for the simultaneous estimation of halobetasol propionate and MUP. Effat and Masoud[11] proposed the development and validation of the derivative spectrophotometric method for the analysis of SIM and ezetimibe by simultaneous estimation. Meanwhile, Dixit et al.[12] proposed the development of the reverse-phase (RP)-HPLC method for the stability-indicating studies of the same drug combination. Patel et al.[13] developed the RP-HPLC method for the simultaneous determination of aspirin in combination with SIM using the analytical quality by design approach.

Literature search for prior articles on methods for the simultaneous analysis of SIM and MUP indicated no information reported for the simultaneous analysis of these two drugs by HPLC. The present study focused on the development of a simple, precise, and accurate RP-HPLC method for the simultaneous analysis of SIM and MUP in the combined dosage form.[14]

MATERIALS AND METHODS

Materials

Pure SIM and MUP were procured as gift samples from SAVA Healthcare Ltd. with their assay values. HPLC-grade solvents and chemicals purchased from Merck were used in this study.

Instrument

The instrument used in the proposed HPLC method was Agilent 1120 Compact LC System connected to a UV detector for analysis purposes. All of the data were acquired and processed using the EZChrom Elite Compact software. An analytical balance (Shimadzu) with 1 mg sensitivity was used to weigh the samples.

Development and optimization of the method for chromatographic conditions

Method development and optimization for chromatographic conditions were conducted by varying the molarity (i.e., 25 and 30 mM), pH (i.e., 3.0, 3.5, and 4.0), and volume of ACN (i.e., 55, 65, and 75 mL) of the mobile phase and flow rate (1.0, 1.1, and 1.2 mL/min).

Mobile phase

The mobile phase was prepared by mixing ACN and phosphate buffer, and its pH was adjusted using orthophosphoric acid. The mobile phase was filtered through 0.45 µm membrane filter paper after 15 min of sonication at room temperature before using it for analysis.

Standard stock solution

The standard stock solution of SIM and MUP was prepared individually. Accurately weighed 10 mg of SIM was dissolved in 10 mL of the mobile phase in a volumetric flask (1.000 µg/mL). A 1 mL aliquot from this solution was diluted with 10 mL of the mobile phase to obtain the final concentration of 100 µg/mL SIM. The same procedure was repeated for MUP to obtain a solution of 100 µg/mL MUP.

Sample solution

The combined dosage form, which is in the form of a topical spray, is composed of 1.0% w/v each of SIM and MUP.[14] Accurately measured quantity of 1.0 mL of the formulation consisting of SIM (10 mg) and MUP (10 mg) was transferred to a 100.0 mL volumetric flask, followed by the addition of 30

mL mobile phase, ultrasonication of this solution for 20 min at room temperature, and volume make up to the mark with the mobile phase to obtain a concentration of 100 µg/mL for SIM and 100 µg/mL MUP.

Optimization of chromatographic conditions

Various preliminary trials were conducted during method development to understand the effect of certain parameters on their responses. For the mobile phase, the solvent was selected from ACN and methanol and the buffer was selected from ammonium acetate buffer and phosphate buffer based on the chromatographic responses received. The mobile phase was further optimized by varying the molarity of the buffer used and adjusting the pH from 3.0 to 4.5 using orthophosphoric acid.

Chromatographic method for analysis

After baseline stabilization (for approximately 30 min), using the optimized chromatographic conditions, a standard solution of 20 µg/mL was successively injected into the system to record the chromatogram of the satisfactory reproducibility of the peak areas. This procedure was repeated for the sample solution, and the peak areas of the standard and sample were acquired to determine the concentrations of SIM and MUP in the sample. This analysis was repeated six times.

Validation of the optimized method

The International Harmonization Conference (ICH) Q2 (R1) guidelines[15] were used to validate the developed analytical method. The validation parameters include system suitability test, specificity, accuracy, precision, linearity, robustness, limit of detection (LOD), limit of quantitation (LOQ), and stability.

System suitability test

The developed method was checked for system suitability using standard solutions (100 µg/mL) of SIM and MUP. Parameters of the resolution, tailing factor (T), capacity factor, and theoretical plates (*N*) were evaluated as results of system suitability with percent relative standard deviation (% RSD) of six replicate injections.

Specificity

Method specificity was evaluated by comparing the chromatograms of the placebo and sample solutions prepared using the formulation consisting of SIM and MUP to check the interference of excipients. The placebo formulation has nearly the same composition as that of the sample solution, except that SIM and MUP were used to prepare the sample solution.

Accuracy

To determine the accuracy of the method, three different concentration levels of 80%, 100%, and 120% for SIM and MUP were selected. These samples were analyzed in six replicates using the proposed method. The recovery studies for SIM were done by adding standard SIM at concentrations of 8, 12, and 24 µg/mL to the known concentration of the sample (10 µg/mL) to be analyzed through the standard addition method. The content of the recovered SIM was analyzed. A similar procedure was repeated for the recovery studies of MUP. The percent recovery for both drugs was calculated separately.

Precision

The proposed method was evaluated for precision by checking its performance with intraday and interday variations of 8, 12, and 24 µg/mL of SIM and MUP. For intraday precision, six replicates of each concentration of the standard and sample solutions were injected consecutively on the same day. For interday precision, the same standard and sample solutions were injected on three different days. The % RSD was calculated by determining the percent content of each sample injected.

Linearity and range

Six standard solutions of 5, 10, 15, 20, 25, and 30 µg/mL, with accuracy between 98% and 102% and precision of less than 2% RSD, were selected to assess linearity. These solutions were injected using the optimized method conditions, and the response acquired in terms of peak area was plotted against the respective concentrations. The linear relationship between peak area and concentration was evaluated by calculating the correlation coefficient, intercept, and slope.

LOD and LOQ

To calculate the LOD and LOQ of SIM and MUP, the lower concentrations of the standard solution were injected. The LOD and LOQ for both drugs were determined based on the 3.3 s/n and 10 s/n rule where s/n is the signal-to-noise ratio.

Robustness

The robustness of the proposed method is evaluated to check its potential to resist small but intentional variations in the optimized parameters. For the robustness studies of the proposed chromatographic conditions, the mobile phase was varied as follows: ACN/phosphate buffer ratio by ±2%, flow rate by ±0.1 mL/min, wavelength by ±1 nm, pH by ±0.2, and molarity of the buffer by ±2 mM.

Forced degradation studies

Standard samples of SIM and MUP were exposed to different stress conditions, such as acidic, alkaline, oxidative, thermal, photostability, and neutral conditions, for the forced degradation studies. In the case of acidic and alkaline degradation, samples were treated with 0.1 M HCl and 0.1 M NaOH at 40°C for 24 h. Oxidative degradation was done using 3% v/v H_2O_2 at 30°C for 24 h. Thermal degradation was conducted by exposing the powder sample to 60°C for 24 h in an oven. Photostability was checked by exposing the sample to UV light by placing the sample in a UV chamber for 24 h. For degradation under neutral conditions, the drugs were treated with water for 2 h at 80°C. After the stipulated time, all of the samples were cooled to room temperature and analyzed using the optimized chromatographic conditions to assess the stability of the drugs.

Stability

The stability of the stock and sample solutions for the short-term and long-term durations was checked by storing the solutions for 24 h and 3 days at room temperature, respectively.

Each solution was observed individually for the appearance of solution after storage and analyzed in six replicates by HPLC using the optimized conditions. The retention time, peak shape, and assay of active substances were compared with freshly prepared solutions statistically.

Statistical analysis

All of the samples were analyzed in six replicates, and the RSD values were computed for all of the samples. Ethics committee approval or patient informed consent is not required for the proposed method.

RESULTS AND DISCUSSION

The RP-HPLC method was selected for the development of the analytical method for the estimation of SIM and MUP simultaneously because of its simplicity and suitability. The analytical method was developed and optimized to determine suitable chromatographic conditions for obtaining sharp and well-resolved peaks of SIM and MUP with minimal tailing.

Column selection

The C8 and C18 columns were checked for their performance in the proposed method. The drugs eluted earlier in the C18 column exhibited a satisfactory peak shape compared with the C8 column. Therefore, the Kromasil C18 column (250 mm×4.6 mm, 5 µm) was selected for the proposed method of simultaneous estimation of SIM and MUP.

Mobile phase composition

Mobile phase selection was done based on the polarity, pKa, and solubility of SIM and MUP, as well as the available literature data. Phosphate buffer (pH 3.5) or ammonium acetate buffer was selected as the aqueous phase and methanol or ACN was selected as the organic phase for mobile phase composition. Because ammonium acetate buffer did not show any peak for SIM and methanol was observed to increase column pressure and peak tailing, both were eliminated from the study and the combination of phosphate buffer and ACN was optimized further. Variation in the ACN/phosphate buffer ratio led to substantial changes in the chromatographic responses. A decrease in the ACN/phosphate buffer ratio resulted in increased retention time, as well as peak split; hence, the ACN/phosphate buffer ratio of 70:30 (v/v) was selected for further optimization. Decreasing the molarity of the buffer from 30 mM to 10 mM resulted in a tailing factor of more than 2. The mobile phase pH of less than 3.0 resulted in peak split, and the mobile phase pH of more than 4.0 resulted in increased retention time. The flow rate was optimized based on the peak properties (i.e., peak shape and symmetry) and retention time.

By conducting trials of different compositions of the mobile phase, the optimized mobile phase composition for the simultaneous estimation of SIM and MUP was ACN/30 mM pH 3.5 phosphate buffer (70:30, v/v) with a flow rate of 1.1 mL/min These optimized parameters were selected based on several factors, namely, theoretical plate (should be more than 2.000), retention time of both drugs (RSD should be less than 2), and tailing factor of both drugs (should be less than 2).

Wavelength selection for detection

The detection wavelength for the proposed method was determined by analyzing the isobasic points of SIM and MUP. Standard solutions of both drugs were prepared using stock solution (20 µg/mL each), scanning was done in the UV range of 400-200 nm using a UV-visible spectrophotometer (Shimadzu 1800), and overlaid spectra were recorded (Figure 1). The isobasic point of the overlaid spectra where the two substances absorb light of that specific wavelength (224 nm) to the same extent at the same analytical concentration was selected as the wavelength for detection during the analysis of MUP and SIM in the combined dosage form.

Validation of the optimized method

System suitability test

System suitability test is often used as the control strategy, which is an essential component of the HPLC method. The system suitability test is normally conducted to verify if the developed method has adequate resolution and reproducibility for the analysis to be conducted. For the proposed method, system suitability results viz. resolution (29.66±1.20), capacity factor (1.15±0.01 for MUP and 11.31±0.01 for SIM), retention time (RSD values of 0.01 for MUP and 0.25 for SIM), theoretical plate (5.162±0.02 for MUP and 8.518±0.07 for SIM), and tailing factor (0.976±0.02 for SIM and 1.16±0.02 for MUP) were determined to be satisfactory.

Specificity

The results for the specificity of the proposed method are shown in Figure 2. The figure shows no interference in the retention time of SIM and MUP with a clear separation of peaks.

Accuracy

The accuracy of the proposed method was determined by conducting recovery experiments. The results for accuracy at different levels are listed in Table 1.

The percent recovery of SIM and MUP was determined to be close to 100%, and the RSD values are less than 2%, which

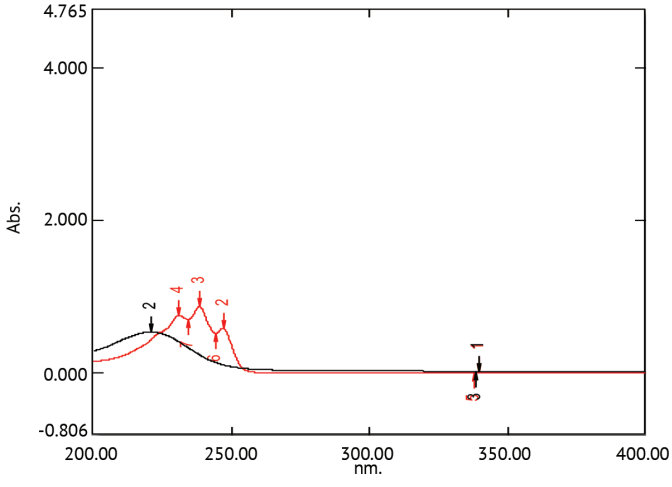

Figure 1. Overlaid spectra of MUP and SIM

MUP: Mupirocin, SIM: Simvastatin

fulfills the acceptance criteria for accuracy as indicated in the ICH guidelines. Hence, the method developed can be considered reliable for analytical application.

Precision

The results of intraday and interday precision using 8, 12, and 24 µg/mL concentrations of both SIM and MUP are listed in Table 2.

Linearity and range

The developed method was assessed for linearity at the concentration range of 5-30 µg/mL. Calibration curve analysis indicated good correlation coefficients (r^2: 0.9969 for MUP and r^2: 0.9959 for SIM) for SIM and MUP in the given concentration range for both drugs. The regression equation for SIM was expressed as y: 431.45x+228.54 and the regression equation for MUP was expressed as y: 449.25x-101.93, where y denotes the peak area and x denotes the concentration.

LOD and LOQ

The LOD and LOQ of the proposed method were determined to be 0.595±0.282 and 1.803±0.334 for SIM and 0.771±0.234 and 2.338±0.246 µg/mL for MUP, respectively.

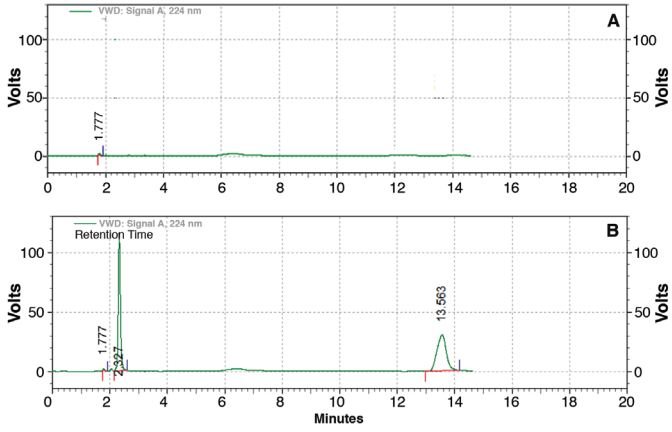

Figure 2. (A) Chromatogram of the placebo solution. (B) Chromatogram of the formulation showing simultaneous estimation of MUP at 2.33 min and SIM at 13.56 min of retention time

MUP: Mupirocin, SIM: Simvastatin

Table 1. Percent recovery studies at three levels

Active ingredients	Analyte concentration (µg/mL)	Mean recovery (%) ± SE	RSD (%)
SIM	8.00	101.10±0.01	0.02
MUP		99.67±0.02	0.04
SIM	12.00	101.08±0.16	0.39
MUP		99.69±0.35	0.82
SIM	24.00	100.29±0.01	0.90
MUP		99.41±0.01	0.81

SE: Standard error, RSD: Relative standard deviation, MUP: Mupirocin, SIM: Simvastatin

Robustness

The results of the robustness of the developed method evaluated by changing the flow rate, mobile phase ratio, wavelength, pH, and molarity of the buffer with the respective % RSD values are listed in Table 3. The calculated assay (%) values were in the acceptable range of 95.00% to 105.00% with % RSD lower than 2, which indicated no significant effect on the results of

Table 2. Intraday and interday precision results of the proposed method

Actual concentration (µg/mL)	Measured mean concentration (µg/mL) ± SE	RSD (%)	Measured mean concentration (µg/mL) ± SE	RSD (%)
	SIM		MUP	
Intraday				
8.00	7.98±0.42	1.02	8.12±0.47	1.15
12.00	11.87±0.62	1.51	12.12±0.52	1.27
24.00	23.46±0.04	0.19	23.27±0.04	0.20
Interday				
8.00	8.10±0.49	1.21	7.61±0.11	0.06
12.00	11.97±0.40	0.97	12.02±0.39	0.95
24.00	23.76±0.05	0.28	23.48±0.03	0.74

%RSD values lower than 2% indicate acceptable precision of the developed method. SE: Standard error, RSD: Relative standard deviation, MUP: Mupirocin, SIM: Simvastatin

Table 3. Robustness results of the proposed method

Factor	Variation	SIM		MUP	
		Mean amount (%)	RSD (%)	Mean amount (%)	RSD (%)
Flow rate (mL/min)	1.0	98.86	1.28	98.54	1.25
	1.1	98.60	1.03	98.32	0.98
	1.2	98.31	1.43	98.13	1.63
ACN/ phosphate buffer (70:30, v/v)	68:32	98.38	1.54	98.12	1.39
	70:30	98.73	0.98	99.10	1.34
	72:28	98.67	1.27	98.78	1.28
Wavelength (nm)	223	97.59	1.50	97.30	1.23
	224	98.60	0.97	99.21	1.32
	225	98.01	1.38	98.45	1.30
pH	3.30	97.67	0.58	97.84	1.01
	3.50	97.50	0.76	97.19	0.51
	3.70	97.67	0.94	97.67	0.79
Molarity of the buffer (mM)	28.00	97.39	0.82	97.67	0.78
	30.00	97.70	0.78	97.70	1.18
	32.00	97.51	0.77	97.38	1.13

RSD: Relative standard deviation, MUP: Mupirocin, SIM: Simvastatin

the analysis. These results showed that the developed method is robust to minor variations in system parameters.

Forced degradation studies

The analytical results after forced degradation of the samples are listed in Table 4, followed by the respective figures of the peaks after degradation. SIM was observed to degrade completely in alkaline conditions, followed by oxidative conditions (10.64%), thermal conditions (9.89%), and acidic conditions (4.85%). Degradation in neutral conditions and photodegradation was observed to be less than 1%. Dixit et al.[12] reported similar results for the degradation behavior of SIM. In the case of MUP, maximum degradation was observed in acidic, oxidative, and neutral conditions (approximately 7%), followed by thermal conditions (6.6%). Degradation in alkaline conditions and photodegradation was observed to be less than 2%. The capability of the proposed method to reveal the degradation peaks after forced degradation studies indicates the potential of the method as a stability-indicating analytical method. The degradation peaks did not show any interference in the retention times of the respective drugs, indicating the specificity of the analytical method developed (Figure 3-8).

Stability

The short-term stability (24 h) and long-term stability (3 days) of the stock and sample solutions did not show any precipitation or any other change in the appearance of the solution. The stock and sample solutions also did not show any significant difference in chromatographic responses, such as peak shape and retention time. The percent deviation between assay of freshly prepared and stored stock solutions was determined to be 1.12% for SIM and 0.91% for MUP in the case of short-term stability and 1.02% for SIM and 1.24% for MUP in the case of long-term stability. By contrast, the percent deviation between assay of freshly prepared and stored sample solutions was determined to be 1.21% for SIM and 0.45% for MUP in the case of short-term stability and 0.07% for SIM and 1.45% for MUP

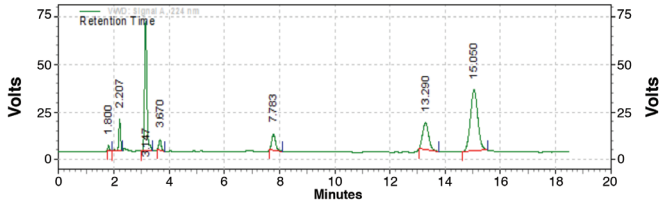

Figure 3. Degradation patterns of MUP and SIM under acidic conditions
MUP: Mupirocin, SIM: Simvastatin

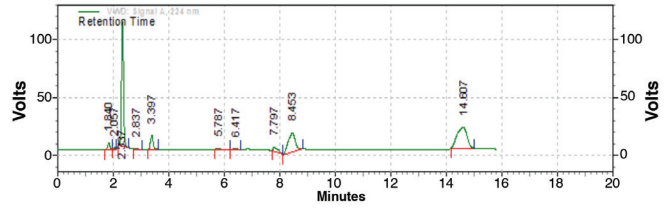

Figure 4. Degradation patterns of MUP and SIM under alkali conditions
MUP: Mupirocin, SIM: Simvastatin

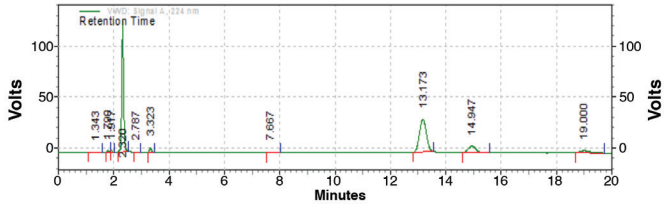

Figure 5. Degradation patterns of MUP and SIM under oxidative conditions
MUP: Mupirocin, SIM: Simvastatin

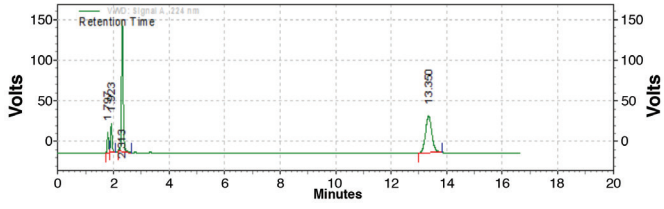

Figure 6. Degradation patterns of MUP and SIM under neutral conditions
MUP: Mupirocin, SIM: Simvastatin

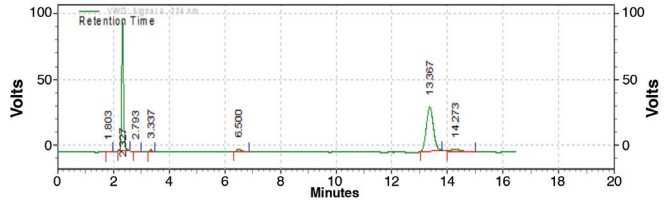

Figure 7. Degradation patterns of MUP and SIM under thermal conditions
MUP: Mupirocin, SIM: Simvastatin

Table 4. Results of the forced degradation studies of the proposed method

Stress conditions	Amount of recovered SIM		Amount of degraded SIM		Amount of recovered MUP		Amount of degraded MUP	
	Mean (%)	RSD (%)	Mean (%)	RSD (%)	Mean (%)	RSD (%)	Mean (%)	RSD (%)
Acidic	95.14	1.51	4.85	0.08	92.79	1.82	7.21	0.18
Alkali	-	-	100.00	1.02	99.91	1.71	0.09	0.03
Oxidative	89.32	1.21	10.64	0.15	92.65	0.91	7.35	0.30
Neutral	99.14	1.32	0.85	0.01	92.65	1.35	7.35	0.26
Thermal	90.81	1.77	9.89	0.07	93.40	1.43	6.60	0.07
Photodegradation	99.01	1.24	0.99	0.02	98.57	1.59	1.43	0.09

RSD: Relative standard deviation, MUP: Mupirocin, SIM: Simvastatin

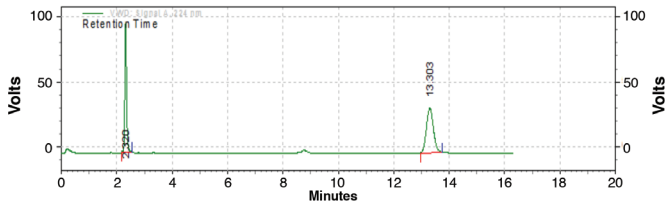

Figure 8. Degradation patterns of MUP and SIM after photodegradation
MUP: Mupirocin, SIM: Simvastatin

in the case of long-term stability. These results indicate the stability of the stock and sample solutions for 3 days at room temperature.

Analysis of the developed formulation

The developed HPLC method was applied to the quantification of SIM and MUP in the developed formulation. The percent content of each drug was determined to be 97.80±0.31 for MUP and 97.80±0.45 for SIM. Hence, the developed method can be applied to the routine analysis of SIM and MUP in topical spray formulation, which has a combination of these two drugs.

CONCLUSION

A simple and convenient RP-HPLC method for the analysis of SIM and MUP in the combined dosage form was developed and validated. Kromasil C18 column (250 mm×4.6 mm, 5 µm) with UV detection at 224 nm and mobile phase composed of ACN/30 mM pH 3.5 phosphate buffer (70:30, v/v) at a flow rate of 1.1 mL/min were observed to provide a good resolution for MUP and SIM. The method was validated as per ICH guidelines, and the proposed method was determined to be specific, accurate, precise, and robust for the quantitation of SIM and MUP and can be applied to the routine analysis of the developed topical spray formulation, which has a combination of both drugs.

ACKNOWLEDGMENTS

The authors would like to thank SAVA Healthcare Ltd. for supplying the samples of MUP and SIM.

Conflict of interest: No conflict of interest was declared by the authors. The authors are solely responsible for the content and writing of this paper.

REFERENCES

1. Sujata S. Recent advances in topical wound care. Indian J Plast Surg. 2012;45:379-387.
2. Thornton SC, Taylor SC, Weinberg JM. Topical antimicrobial agents in dermatology. Clin Dermatol. 2003;21:70-77.
3. Dumville JC, Lipsky BA, Hoey C, Cruciani M, Fiscon M, Xia J. Topical antimicrobial agents for treating foot ulcers in people with diabetes. Cochrane Database Syst Rev. 2017;14;6.
4. Dai T, Huang YY, Sharma SK, Hashmi JT, Kurup DB, Hamblin MR. Topical antimicrobials for burn wound infections. Recent Pat Antiinfect Drug Discov. 2010;5:124-151.
5. Sarabahi S. Recent advances in topical wound care. Indian J Plast Surg. 2012;45:379-387.
6. Tripathi KD. Essentials of Medical Pharmacology, (6th ed). New Delhi: Jaypee Brothers Medical Publishers Ltd. 2008;636:776.
7. Bitto A, Minutoli L, Altavilla D, Polito F, Fiumara T, Marini H, Galeano M, Calò M, Lo Cascio P, Bonaiuto M, Migliorato A, Caputi AP, Squadrito F. Simvastatin enhances VEGF production and ameliorates impaired wound healing in experimental diabetes. Pharmacol Res. 2008;57:159-169.
8. Akira E. A historical perspective on the discovery of statins. Proc Jpn Acad Ser B Phys Biol Sci. 2010;86:484-493.
9. Abu-Nameh ESM, Shawabkeh RA, Ali A. High-performance liquid chromatographic determination of simvastatin in medical drugs. Am J Anal Chem. 2006;61:63-66.
10. Bana A, Sathe MA, Rajput SJ. Analytical Method Development and Validation for Simultaneous Estimation of Halobetasol Propionate and Mupirocin in the ratio 1:40 by U.V. Spectroscopy And RP- HPLC Method. Int J Pharm Sci Res. 2019;10:1392-1401.
11. Effat S, Masoud A. Development and validation of a derivative spectrophotometric method for simultaneous determination of simvastatin and ezetimibe. J Chem. 2010;7:S197-S202.
12. Dixit RP, Barhate CR, Padhye SG, Viswanathan CL, Nagarsenker MS. Stability indicating RP-HPLC method for simultaneous determination of simvastatin and ezetimibe from tablet dosage form. Indian J Pharm Sci. 2010;72:204-210.
13. Patel KG, Patel AT, Shah PA, Gandhi TR. Multivariate optimization for simultaneous determination of aspirin and simvastatin by reverse phase liquid chromatographic method using AQbD approach. Bull Fac Pharm Cairo Univ. 2017;55:293-301.
14. Kale R, Doifode D, Shete P. Film forming, antimicrobial and growth promoting wound healing spray formulation. Int J Pharm Invest. 2020;10:320-325.
15. ICH Q2 (R1). Validation of analytical procedures: Text and Methodology. International conference on harmonization of technical requirements for the registration of pharmaceutical for human use. Geneva, Switzerland: 2005. Available from: https://www.ema.europa.eu/en/documents/scientific-guideline/ich-q-2-r1-validation-analytical-procedures-text-methodology-step-5_en.pdf

Turk J Pharm Sci 2021;18(4):445-451
DOI: 10.4274/tjps.galenos.2020.88319

ORIGINAL ARTICLE

Validation of a Knowledge Test in Turkish Patients on Warfarin Therapy at an Ambulatory Anticoagulation Clinic

Ayaktan Antikoagülasyon Kliniğinde Varfarin Tedavisi Alan Türk Hastalarında Bir Bilgi Testinin Validasyonu

Meltem TÜRKER[1], Mesut SANCAR[1], Refik DEMİRTUNÇ[2], Nazlıcan UÇAR[1], Osman UZMAN[3], Pınar AY[4], Ömer KOZAN[5], Betul OKUYAN[1]*

[1]Marmara University Faculty of Pharmacy, Department of Clinical Pharmacy, Istanbul, Turkey
[2]University of Health Sciences Turkey, Haydarpasa Numune Training and Research Hospital, Clinic of Internal Medicine, Istanbul, Turkey
[3]Kars Sarıkamış State Hospital, Clinic of Cardiology, Kars, Turkey
[4]Marmara University Faculty of Medicine, Department of Public Health, Istanbul, Turkey
[5]Baskent University, Istanbul Hospital, Clinic of Cardiology, Istanbul, Turkey

ABSTRACT

Objectives: This study aimed to evaluate the validity and reliability of an oral anticoagulation knowledge (OAK) test in Turkish patients on warfarin therapy at an anticoagulant outpatient clinic.

Materials and Methods: This study was conducted at an ambulatory anticoagulation clinic and included patients older than 18 years who had been using warfarin for at least six months. Patients' demographic and clinical data were collected. Internal consistency was calculated using the Kuder-Richardson 20 (KR-20) coefficient, and the test-retest reliability of the Turkish version of the OAK test was assessed.

Results: Patients' mean age was 59.83±11.93 (26-90) years (n=240; 133 women). The mean score of the OAK test was 14.19±3.01. The test-retest reliability of the scale (n=30) was moderate for the total score ($p<0.001$). The KR-20 value, a measure of internal consistency, was 0.671. Patients of a younger age and higher educational level were more likely to have higher levels of anticoagulation knowledge than patients of an older age and lower education level ($p<0.05$ for both comparisons).

Conclusion: The Turkish version of the OAK test can be used to determine the patients' knowledge on oral anticoagulation.

Key words: Warfarin, anticoagulant, knowledge, pharmacist

ÖZ

Amaç: Bu çalışmada, bir antikoagülan polikliniğinde varfarin tedavisi alan Türk hastalarda oral antikoagülasyon bilgisi (OAK) testinin geçerlilik ve güvenilirliğinin değerlendirilmesi amaçlanmıştır.

Gereç ve Yöntemler: Bu çalışma ayaktan antikoagülasyon kliniğinde yürütülmüştür ve en az altı aydır varfarin kullanan 18 yaşından büyük hastaları kapsamaktadır. Hastaların demografik ve klinik verileri toplanmıştır. Kuder-Richardson 20 (KR-20) katsayısı kullanılarak iç tutarlılık hesaplanmış ve OAK testinin Türkçe versiyonunun test-tekrar test güvenilirliği değerlendirilmiştir.

Bulgular: İki yüz kırk hastanın (133 kadın) yaş ortalaması 59,83±11,93 (26-90) idi. Oral antikoagülasyon bilgi testinin ortalama skoru 14,19±3,01 olarak hesaplanmıştır. Ölçeğin test-tekrar test güvenirliği (n=30) toplam skor için orta düzeyde bulunmuştur ($p<0,001$). İç tutarlılık güvenirliği, hesaplanan KR-20 değeri (0,671) ile doğrulanmıştır. Daha genç ve yüksek eğitim düzeyindeki hastalar, daha ileri yaşta ve düşük eğitim düzeyindeki hastalarla karşılaştırıldığında daha yüksek antikoagülasyon bilgisine sahip olarak belirlenmiştir (her iki karşılaştırma için $p<0,05$).

Sonuç: Hastaların oral antikoagülasyon konusundaki bilgilerini belirlemek için OAK testinin Türkçe versiyonu kullanılabilir.

Anahtar kelimeler: Varfarin, antikoagülan, bilgi, eczacı

***Correspondence:** betulokuyan@yahoo.com, **Phone:** +90 216 777 52 00 **ORCID-ID:** orcid.org/0000-0002-4023-2565
Received: 03.09.2020, **Accepted:** 21.10.2020

INTRODUCTION

Warfarin is mostly used as an oral anticoagulant for the prophylaxis and management of primary and secondary thromboembolism.[1-3] Although, recently, new oral anticoagulants have been developed, warfarin remains the most commonly prescribed vitamin K antagonist in the clinical settings.[2-4] However, patients are subject to risks when on warfarin.[1,2] Bleeding is a common adverse event that occurs at an annual rate of 7-8% among patients on warfarin. Additionally, it was reported that the most common cause of drug-induced emergency department admissions was related to warfarin use.[5] Warfarin's narrow therapeutic range and wide dose-response variability should be considered when managing its use in treatment.[1] Patients treated with warfarin should be closely monitored to ensure their adherence to warfarin therapy and detect and prevent adverse events.[6] Serious problems may occur if patients adhered poorly to medications, especially those with a narrow therapeutic range, such as warfarin. Missed doses decrease the efficacy of the medication, and overdoses cause various adverse events.[7]

Wang et al.[8] showed a relationship between the level of medication adherence and level of medication knowledge among patients using warfarin. In the study conducted in Turkey, poor medication adherence of patients receiving anticoagulant therapy was associated with a poor time in therapeutic range (TTR), poor warfarin knowledge, and higher bleeding score.[9] Based on the findings of a multicenter study conducted in Turkey, poor knowledge of potential warfarin-food interactions was more common in older patients.[10]

To our best knowledge, there is no valid and reliable anticoagulation knowledge test in Turkish. Few validated anticoagulation knowledge tests exist for this purpose.[11-13] The oral anticoagulation knowledge (OAK) test used in our study was short compared with other questionnaires[11,12] and is commonly used as a reliable and valid tool in the United States,[14] Malaysia,[15] and Brazil[1] to identify and evaluate patients' knowledge of anticoagulation. This study aimed to evaluate the validity and reliability of a knowledge test in Turkish patients on warfarin therapy at an ambulatory anticoagulation clinic.

MATERIALS AND METHODS

Participants and setting

A previous research suggested that the number of test items should be multiplied by 10 to obtain the number of participants, so, for this methodological study, 200 patients were required for an adequate sample size.[16] On allowing for a 20% loss due to missing data or participants discontinuing the medication during the study, the necessary sample size was 240 patients.

This methodological study was conducted at the outpatient anticoagulation clinic of a university hospital located in Istanbul between 15 April 2017 and 15 October 2017. The clinic provided a service that adjusted the patients' warfarin dose according to their international normalized ratio (INR). Patients older than 18 years who had been using warfarin for at least the past six months and had at least four INR measures in their medical records were eligible for this study. Patients who could not read were excluded from the study.

The study was approved by the Ethical Committee of Marmara University, Institute of Health Sciences (03.04.2017-121). Informed consent was obtained from all participants.

Data collection

Patients' demographic and clinical data, including their age, gender, educational level, total number of medications used, indication for oral anticoagulant therapy, and previous INR measurements, were collected using individual interviews and patients' medical charts. Individual interviews were conducted by a single researcher (MT). At least four consecutive INR measurements taken at least a month and no more than two months apart were retrospectively recorded from patients' medical charts. Patients' TTR was calculated using the method developed by Rosendaal et al.[17]

Translation and cross-cultural adaptation of the OAK test

Permission to use the OAK test for this study was obtained from Zeolla et al.[14] This knowledge test includes a total of 20 questions about follow-up, drug-drug interactions, fundamental medication information, adverse effects, and nutritional problems. Higher test scores indicate a better level of oral anticoagulant knowledge.[14] Patients were classified into three groups according to their total score in the OAK test based on previous studies.[1,13,18] Patients with total OAK test scores of less than 10 (<50%) had low anticoagulation knowledge; patients with total OAK test scores between 10 and 15 (50-75%) had moderate anticoagulation knowledge; patients with total OAK test scores of more than 15 (>75%) had good anticoagulation knowledge.

The original English test was translated into Turkish independently by two native Turkish speakers, who were also fluent in English. Then, two researchers (MS and RD) reviewed the translations and reconciled them into one Turkish version. This Turkish version was back translated into English independently by two native English speakers, who were also fluent in Turkish. Differences between this draft English version and the original English version were evaluated by two researchers (MT and BO). After the translation process, the draft Turkish version was evaluated for grammar, conceptual equivalence, and cultural compatibility by a group of experts (two clinical pharmacists, an internal medicine specialist, a cardiologist, a nurse, and a Turkish literature lecturer). A pilot study was conducted on a group of patients (n=20) for cultural adaptation. It took approximately 10-12 minutes to complete the test. To assess the test-retest reliability, the knowledge test was completed by 30 patients from the study population within two weeks. To analyze the construct validity, demographic and clinical data in each group were evaluated.

Statistical analysis

Categorical data were presented as numbers and percentages. Continuous data were presented as mean ± standard deviation or median and interquartile range (IQR). The Kolmogorov-Smirnov test was used for the normality of distribution. The test-retest

reliability was assessed using Spearman's correlation test. To measure the internal consistency, a Kuder-Richardson 20 (KR-20) coefficient value was calculated for the OAK test. Continuous data between two or more groups were analyzed using the Mann-Whitney U test or Kruskal-Wallis test, respectively. Categorical data were analyzed using the chi-square test. In this study, p values <0.05 were statistically significant.

RESULTS

This study included 240 patients (133 women) who were on warfarin. Patients' demographic and clinical data are shown in Table 1. Participants' mean age was 59.83±11.93 (26-90) years. The mean score of OAK test was 14.19±3.01. The most frequent wrong responses were related to drug-drug and drug-food interactions. Less than half of the patients did not know the correct way to distinguish between different strengths of warfarin. The correct answer to this question varied from that in the original scale developed by Zeolla et al.[14], due to differences between the national health systems in each country. This was emphasized in the validation study of the Brazilian version of the OAK test.[1] The right answer in Turkish version was "size" rather than "color", and this was taken into consideration during scoring. The percentage of correct answers, corrected item-total correlation, and KR-20 coefficients, if each item was deleted, is shown in Table 2.

The KR-20 coefficient was 0.671. There was a strong correlation between the test-retest results of patients' total score in the OAK test at baseline and two weeks later (r=0.739; p<0.001; data not shown).

Patients of a younger age and higher educational level were more likely to have higher OAK test scores than those of an older age and lower educational level (p<0.05; Table 3). There was no significant difference in TTR scores or the number of medications used between patients with low, moderate, and high anticoagulant knowledge (p>0.05; Table 3). Evaluation of related factors (demographic and clinical characteristics of the patients) in groups according to patients' anticoagulant knowledge is shown in Table 3.

DISCUSSION

In this study, the validity and reliability of the Turkish version of the OAK test were evaluated. The Turkish version of the OAK test was valid and reliable. The KR-20 value in the study conducted in Brazil was 0.818.[1] In the United States, the KR-20 value was 0.76.[14] Although the value obtained in our study was acceptable, it was lower than the values obtained in the previously mentioned studies. The rate of the right responses in the present study was similar to that obtained by da Silva Praxedes et al.[1] The total number of correct responses in studies conducted in the United States,[14] Brazil,[1] India,[18] and Saudi Arabia[13] was also similar to our study.

According to a study conducted in India, 50% of patients using oral anticoagulants had OAK test of less than 10, 37% had scores between 10 and 15, and 13% had scores greater than 15.[18] According to a study conducted in Denmark, patients

Table 1. Demographic and clinical characteristics of the participants (n=240)

Characteristics	
Age, mean (SD) **Median (IQR)**	59.83 (11.93) 61.0 (52.0-68.8)
Age group, n (%)	
18-40	16 (6.7)
41-60	102 (42.5)
61-80	116 (48.3)
>80	6 (2.5)
Sex, n (%)	
Female	133 (55.4)
Male	107 (44.6)
Marital status, n (%)	
Married	199 (82.9)
Single	41 (17.1)
Education, years, mean (SD) **Median (IQR)**	6.6 (3.7) 5.0 (5.0-8.0)
Education group according to the years of education, n (%)	
<8 years	164 (68.3)
≥8 years	76 (31.7)
TTR, mean (SD) **Median (IQR)**	52.2 (30.4) 52.0 (28.0-77.0)
Group of TTR, n (%)	
TTR <50%	114 (47.5)
TTR 50-75%	64 (26.7)
TTR >75%	62 (25.8)
The number of medications used, mean (SD) **Median (IQR)**	3.68 (2.37) 3.0 (2.0-5.0)
Polypharmacy (defined as the concurrent use of 5 or more medications), n (%)	
Yes	174 (72.5)
No	66 (27.5)
Indication, n (%)	
Prosthetic heart valve	126 (46.5)
AF	62 (22.9)
Valvular heart disease	35 (12.9)
DVT/PTE	44 (16.3)
Acute MI/recurrent TIA	5 (1.5)
20 questions of oral anticoagulation knowledge test percentage mean ± SD **Median (IQR)**	14.2±3.0 12.0 (14.0-16.0)
Oral anticoagulation knowledge categories, n (%)	
<50% (low level of knowledge)	21 (8.8)
50-75% (moderate level of knowledge)	134 (55.8)
>75% (high level of knowledge)	85 (35.4)

SD: Standard deviation, TTR: Time in therapeutic range, AF: Atrial fibrillation, DVT: Deep vein thrombosis, PTE: Pulmonary thromboembolism, MI: Myocardial infarction, TIA: Transient ischemic attack

Table 2. Percentage of correct answers, corrected item-total correlation, and Kuder-Richardson coefficients if an item is deleted (n=240)

Questions	Correct answers	Percentage of correct answers (n)	Corrected item-total correlation	Kuder-Richardson coefficients if an item is deleted
1. Missing one dose of warfarin:	b. Can alter the drug's effectiveness	66.7 (160)	0.293	0.654
2. You can distinguish between different strengths of warfarin tablets by what?	c. Size	36.2 (87)	0.205	0.665
3. A patient on warfarin therapy should contact the physician or healthcare provider who monitors it when:	d. All of the above	85.0 (204)	0.189	0.665
4. Occasionally eating a large amount of leafy greens vegetables while taking warfarin can:	b. Reduce the effectiveness of the warfarin	41.7 (100)	0.295	0.654
5. Which of the following vitamins interacts with warfarin?	d. Vitamin K	40.8 (98)	0.438	0.635
6. When is it safe to take a medication that interacts with warfarin?	b. If your healthcare provide is aware of the interaction and checks your PT/INR ("Protime") regularly	60.8 (146)	0.214	0.664
7. PT/INR ("prothrombin time") test:	a. A blood test used to monitor your warfarin therapy	98.3 (236)	0.063	0.672
8. Warfarin may be used to:	a. Treat people that already have a blood clot	99.2 (238)	0.129	0.670
9. A patient with a PT/INR ("Protime") value below their "goal range":	b. Is at an increase the risk of having a clot	77.9 (187)	0.365	0.646
10. Taking a medication containing aspirin or other non-steroidal antiinflammatory medications such as ibuprofen while on warfarin will:	b. Increase your risk of bleeding from the warfarin	60.0 (144)	0.339	0.648
11. A person on warfarin should seek immediate medical attention:	b. If they notice blood in their stool when going to the bathroom	48.3 (116)	0.292	0.654
12. Skipping even one dose of your warfarin can:	c. Cause your PT/INR ("Protime") to be below the "goal range"	79.2 (190)	0.261	0.658
13. Drinking alcohol while taking warfarin:	b. May affect your PT/INR ("Protime")	82.1 (197)	0.367	0.647
14. Approximately how often should you have PT/INR ("prothrombin time") measured when you are stabilized with the correct warfarin dose (PT/INR is at target values)?	b. Once a month	94.2 (226)	0.251	0.662
15. It is important for a patient taking warfarin to monitor for signs of bleeding:	b. At all times	80.8 (194)	0.038	0.681
16. The best thing to do if you miss a dose of warfarin is to.....?	b. Take the next scheduled dose and tell your healthcare provider	81.2 (195)	0.169	0.668
17. When it comes to diet, people taking warfarin should:	c. Be consistent and eat a diet that includes all types of food	84.2 (202)	0.086	0.675
18. Each time you get your PT/INR ("Protime") checked, you should:	d. Let your doctor know if you missed any doses of warfarin	90.0 (216)	0.108	0.671
19. Which of the following over-the-counter products is most likely to interact with warfarin?	b. Herbal/dietary supplements	32.9 (79)	0.421	0.638
20. A patient with a PT/INR ("Protime") value above the "goal range":	c. Is at an increased risk of bleeding	79.6 (191)	0.313	0.652

PT: Prothrombin time, INR: International normalized ratio

Table 3. Factors (demographic and clinical characteristics of the patients) in groups divided according to patients' anticoagulation knowledge test score (n=240)

	The anticoagulation knowledge test score			p
	<50% (n=21)	50-75% (n=134)	>75% (n=85)	
Age, mean ± SD Median (IQR)	64.4±13.0 68.0 (53.5-72.5)	61.2±11.3 61.0 (53.8-69.2)	56.4±11.9 58.0 (48.0-64.0)	<0.01
Education, years, mean ± SD Median (IQR)	6.5±4.0 5.0 (5.0-9.5)	5.4±2.9 5.0 (5.0-5.0)	8.5±3.9 8.0 (5.0-11.0)	<0.001
TTR, mean ± SD Median (IQR)	49.5±27.0 45.0 (29.0-74.5)	51.4±30.8 50.5 (28.0-76.0)	54.0±30.8 59.0 (26.0-80.5)	NS
The number of medications used, mean ± SD Median (IQR)	3.6±2.4 3.0 (2.0-5.0)	3.7±2.4 3.0 (2.0-5.0)	3.7±2.3 3.0 (2.0-5.0)	NS
Gender				
Female, n (%)	5 (2.1)	81 (33.8)	47 (19.6)	<0.01
Male, n (%)	16 (6.7)	53 (22.1)	38 (15.8)	
Education group according to the years of education				
<8 years, n (%)	15 (6.2)	108 (45.0)	41 (17.1)	<0.01
≥8 years, n (%)	6 (2.5)	26 (10.8)	44 (18.3)	
Marital status				
Married, n (%)	19 (7.9)	107 (44.6)	73 (30.4)	NS
Single, n (%)	2 (0.8)	27 (11.2)	12 (5.0)	

SD: Standard deviation, TTR: Time in therapeutic range, NS: Non-significant

had a low knowledge of vitamin K antagonist.[19] In a study conducted in Toronto, more than half of the participants had insufficient knowledge of vitamin K antagonists.[20] Patients had higher knowledge levels in our study compared with these previous studies. In a study conducted in Brazil, similar to the one conducted in Turkey, 71% had insufficient knowledge.[1] In a study conducted in Malaysia, 11.2% had insufficient knowledge.[15] When the OAK test score in a study conducted in Singapore was evaluated, patients had a moderate knowledge level.[8] However, another study reported that more than half of the participants had a poor knowledge level.[13] Consistent with this study, other studies reported similar results, ranging from 61.2% to 70%.[21,22] These results highlight the need for intensive training and awareness programs to increase patients' knowledge of such serious issues.

In this study, women had better knowledge of oral anticoagulants than men. Similar results were obtained in a study conducted in Saudi Arabia.[13,21] In other studies, contrasting results were obtained.[20,22,23] Studies conducted in Toronto[20] and in North India[2] indicated that the total OAK test score was higher when participants had a higher educational level. These results were similar to our findings and those from other studies, which showed that OAK test scores were lower in older patients.[2,14,24,25]

In this study, no significant correlation was found between TTR and OAK test scores, which suggested that there was no correlation between good anticoagulant knowledge and good INR control. A similar result was obtained in studies conducted in Saudi Arabia.[13,23] Similar to our study, using the Rosendaal method, some international studies concluded that there was no significant relationship between patients' knowledge of oral anticoagulants and anticoagulation controls[15,26,27] In another study conducted in the United States, it was concluded that there was no significant correlation between patients' knowledge of warfarin and their INR control.[28] In a study conducted in China, a different result was obtained.[29] Shilbayeh et al.[13] stated that incompatible results could be attributed to differences in test items, languages, settings, INR control measures, and different sample sizes.

When examining the OAK tests developed so far, the scale we used in terms of both content and validity was like the scale developed by Briggs et al.[11] However, while the scale we used was valid only for vitamin K antagonists, the scale developed by Obamiro et al.[12] can be used for vitamin K antagonists and direct-acting oral anticoagulants. While the scale, which is developed by Obamiro et al.[12] includes multiple-choice and open-ended questions, the scale we used included only multiple-choice questions. Based on our best knowledge, no existing validated tests assess patients' knowledge of oral anticoagulants in our country.

In future studies, the potential impact of duration of warfarin therapy on patients' anticoagulant knowledge test result should be evaluated. Besides assessing the patients' anticoagulant knowledge level, the problems related with medication

administration (such as dose adjustment difficulty, which is, particularly, due to limited strengths of warfarin tablets in Turkey) might be also assessed. It is necessary to provide comprehensive patient education for patients' receiving warfarin therapy. Using the OAK test in a clinical setting could provide an opportunity for healthcare providers to identify and resolve patients' misunderstandings and/or correct any misinformation they may have encountered. This brief test could easily be conducted in outpatient clinics, as it only requires a short time to complete (10-12 minutes).

Study limitations

The generalizability of the results to different patient groups in Turkey may be limited in this study, because it was conducted in a single outpatient clinic in Turkey. Another limitation of the study was that the OAK test designed by Zeolla et al.[14] was to be self-administered by individuals with an educational level of at least the seventh grade. However, in most studies, including this study, which used the OAK test, individuals with an educational level lower than the seventh grade took the test.

CONCLUSION

The Turkish version of OAK test can be used to determine the patients' knowledge of oral anticoagulation. This test would be helpful for identifying patients who need education and counseling regarding warfarin therapy. Additionally, it can be used to assess changes in patients' knowledge after receiving education and/or counseling. The test can be used to identify and resolve patients' misunderstandings of anticoagulant therapy and/or correct misinformation to which they may have been exposed. Test items may remind patients and providers of key points to consider during warfarin therapy.

Conflict of interest: No conflict of interest was declared by the authors. The authors are solely responsible for the content and writing of this paper.

REFERENCES

1. da Silva Praxedes MF, de Abreu MHNG, Paiva SM, de Melo Mambrini JV, Marcolino MS, Martins MAP. Assessment of psychometric properties of the Brazilian version of the oral anticoagulation knowledge test. Health Qual Life Outcomes. 2016;14:96.
2. Joshua JK, Kakkar N. Lacunae in patient knowledge about oral anticoagulant treatment: results of a questionnaire survey. Indian J Hematol Blood Transfus. 2015;31:275-280.
3. Dumas S, Rouleau-Maillous E, Bouchama N, Lahcene H, Talajic M, Tardif JC, Gualin MJ, Provost S, Dubé MP, Perreault S. Pillbox use and INR stability in a prospective cohort of new warfarin users. J Manag Care Spec Pharm. 2016;22:676-684.
4. Gallagher J, Mc Carthy S, Woods N, Ryan F, O'Shea S, Byrne S. Economic evaluation of a randomized controlled trial of pharmacist-supervized patient self-testing of warfarin therapy. J Clin Pharm Ther. 2015;40:14-19.
5. de Terline MD, Hejblum G, Fernandez C, Cohen A, Antignac M. Discrepancies between patients' preferences and educational programs on oral anticoagulant therapy: a survey in community pharmacies and hospital consultations. PloS One. 2016;11:e0146927.
6. Barnes GD, Nallamothu BK, Sales AE, Froehlich JB. Reimagining anticoagulation clinics in the era of direct oral anticoagulants. Circ Cardiovasc Qual Outcomes. 2016;9:182-185.
7. Kimmel SE, Troxel AB, French B, Loewenstein G, Doshi JA, Hecht TE, Laskin M, Brensinger CM, Meussner C, Volpp K. A randomized trial of lottery-based incentives and reminders to improve warfarin adherence: the warfarin incentives (WIN2) trial. Pharmacoepidemiol Drug Saf. 2016;25:1219-1227.
8. Wang Y, Kong MC, Lee LH, Ng HJ, Ko Y. Knowledge, satisfaction, and concerns regarding warfarin therapy and their association with warfarin adherence and anticoagulation control. Thromb Res. 2014;133:550-554.
9. Baykız D, Akyuz A, Alpsoy S, Fidan C. The influence of warfarin adherence on time in therapeutic range among patients with mechanical heart valves. J Heart Valve Dis. 2018;27:55-64.
10. Çelik A, İzci S, Kobat MA, Ateş AH, Çakmak A, Çakıllı Y, Yılmaz MB, Zoghi M. The awareness, efficacy, safety, and time in therapeutic range of warfarin in the Turkish population: WARFARIN-TR. Anatol J Cardiol. 2016;16:595.
11. Briggs AL, Jackson TR, Bruce S, Shapiro NL. The development and performance validation of a tool to assess patient anticoagulation knowledge. Res Social Adm Pharm. 2005;1:40-59.
12. Obamiro KO, Chalmers L, Bereznicki LR. Development and validation of an oral anticoagulation knowledge tool (AKT). PloS One. 2016;11:e0158071.
13. Shilbayeh SAR, Almutairi WA, Alyahya SA, Alshammari NH, Shaheen E, Adam A. Validation of knowledge and adherence assessment tools among patients on warfarin therapy in a Saudi hospital anticoagulant clinic. Int J Clin Pharm. 2018;40:56-66.
14. Zeolla MM, Brodeur MR, Dominelli A, Haines ST, Allie ND. Development and validation of an instrument to determine patient knowledge: the oral anticoagulation knowledge test. Ann Pharmacother. 2006;40:633-638.
15. Matalqah L, Radaideh K, Sulaiman S, Hassali MA, Abdul Kader MAS. Relationship between patients' warfarin knowledge and anticoagulation control: results of a validated tool in Malaysia. J Pharm Biomed Sci. 2013;30:967-974.
16. Streiner DL, Norman GR, Cairney J, Health measurement scales: a practical guide to their development and use. 3rd ed. New York; Oxford University Press; 2003.
17. Rosendaal F, Cannegieter S, Van der Meer F, Briet E. A method to determine the optimal intensity of oral anticoagulant therapy. Thromb Haemost. 1993;70:236-239.
18. Alphonsa A, Sharma KK, Sharma G, Bhatia R. Knowledge regarding oral anticoagulation therapy among patients with stroke and those at high risk of thromboembolic events. J Stroke Cerebrovasc Dis. 2015;24:668-672.
19. Nybo M, Skov J. Patient knowledge of anticoagulant treatment does not correlate with treatment quality. Public Health. 2016;141:17-22.
20. Hu A, Chow CM, Dao D, Errett L, Keith M. Factors influencing patient knowledge of warfarin therapy after mechanical heart valve replacement. J Cardiovasc Nurs. 2006;21:169-175.
21. Al-Omair SF, Musallam NA, Al-Deghaither NY, Al-Sadoun NA, Bayoumy NM. Compliance with and awareness about long-term oral anticoagulant therapy among Saudi patients in a University Hospital Riyadh, Saudi Arabia. J Appl Hematol. 2016,7;10.

22. Elbur AI, Albarraq A, Maugrabi M, Alharthi S. Knowledge of, satisfaction with and adherence to oral anticoagulant drugs among patients in King Fasial Hospital: Taif, Kingdom Saudi Arabia. Int J Pharm Sci Res. 2015;31:274-280.

23. Mayet AY. Association between oral anticoagulation knowledge, anticoagulation control, and demographic characteristics of patients attending an anticoagulation clinic in Saudi Arabia: A cross-sectional prospective evaluation. Trop J Pharm Res. 2015;14:1285-1291.

24. Davis NJ, Billett HH, Cohen HW, Arnsten JH. Impact of adherence, knowledge, and quality of life on anticoagulation control. Ann Pharmacother. 2005;39:632-636.

25. Tang EOY, Lai CS, Lee KK, Wong RS, Cheng G, Chan TY. Relationship between patients' warfarin knowledge and anticoagulation control. Ann Pharmacother. 2003;7:34-39.

26. Khudair I, Hanssens Y. Evaluation of patients' knowledge on warfarin in outpatient anticoagluant clinics in a teaching hosiptal in Qatar. Saudi Med J. 2010;31:672-677.

27. Barcellona D, Contu P, Marongiu F. Patient education and oral anticoagulant therapy. Haematologica. 2002;87:1081-1086.

28. Ryals CA, Pierce KL, Baker JW. INR goal attainment and oral anticoagulation knowledge of patients enrolled in an anticoagulation clinic in a Veterans Affairs medical center. J Manag Care Pharm. 2011;17:133-142.

29. Li X, Sun S, Wang Q, Chen B, Zhao Z, Xu X. Assessment of patients' warfarin knowledge and anticoagulation control at a joint physician- and pharmacist-managed clinic in China. Patient Prefer Adherence. 2018;12:783.

Turk J Pharm Sci 2021;18(4):452-464
DOI: 10.4274/tjps.galenos.2020.08522

ORIGINAL ARTICLE

QbD-based Formulation Optimization and Characterization of Polymeric Nanoparticles of Cinacalcet Hydrochloride with Improved Biopharmaceutical Attributes

Geliştirilmiş Biyofarmasötik Özelliklere Sahip Sinakalset Hidroklorürün Polimerik Nanopartiküllerinin QbD Tabanlı Formülasyon Optimizasyonu ve Karakterizasyonu

Debashish GHOSE[1]*, Chinam Niranjan PATRA[1], Bera Varaha Venkata RAVI KUMAR[1], Suryakanta SWAIN[2], Bikash Ranjan JENA[3], Punam CHOUDHURY[1], Dipthi SHREE[1]

[1]Roland Institute of Pharmaceutical Sciences, Berhampur (Affiliated to Biju Patnaik University of Technology, Rourkela), Odisha, India
[2]Department of Pharmacy, School of Health Sciences, The Assam Kaziranga University, Jorhat, Assam, India
[3]School of Pharmacy and Life Sciences, Centurion University of Technology and Management (CUTM), Bhubaneswar, Odisha India

ABSTRACT

Objectives: The aim of the present work was to prepare QbD enabled optimization, and to improve the oral bioavailability of freeze–dried polymeric nanoparticles of cinacalcet hydrochloride manufactured by nanoprecipitation and ultrasonication methods using polymers PLGA, and poloxamer-188.

Materials and Methods: The initial screening and optimization were carried out for the formulations by employing Taguchi and Box-Behnken Designs. The FT-IR and DSC revealed no interactions and had no incompatibility among the selected drug and polymers. The nanoparticles were characterized for % drug release, particle size analysis, zeta potential, PDI, SEM, TEM, P-XRD, TGA, DTA, *in vitro*, and *in vivo* drug release study.

Results: *In vitro* drug release study showed sustained release of the drug from the optimized batch by diffusion mechanism. The optimized nanoparticle formulation was recognized by numerical and graphical methods using validation of the experimental model. The optimized batch was stable as per the ICH stability guidelines for 6 months with no considerable alternation noticed in particle size, entrapment efficiency, and *in vitro* drug release. The pharmacokinetic parameters of AUC and Cmax data for the optimized formulation increased 3- and 2.9-folds compared to the pure-drug suspension.

Conclusion: The prepared polymeric nanoparticles formulation is an alternative delivery system for enhanced therapeutic efficacy and bioavailability potential of a model drug to manage long-term normocalcemia in patients with preliminary hyperparathyroidism.

Key words: PLGA, polymeric nanoparticles, Taguchi, P-XRD, optimization, bioavailability potential

ÖZ

Amaç: Mevcut çalışmanın amacı, QbD özellikli optimizasyon hazırlamak ve polimerler PLGA ve poloksamer-188 kullanılarak nano-prepikipitasyon ve ultrasonikasyon yöntemleri ile üretilen cinacalcet hidroklorürün dondurularak kurutulmuş polimerik nanopartiküllerinin oral biyoyararlanımını geliştirmekti.

Gereç ve Yöntemler: Formülasyonlar için taguchi ve Box-Behnken Tasarımları kullanılarak ilk tarama ve optimizasyon gerçekleştirildi. FT-IR ve DSC hiçbir etkileşim ortaya koydu ve seçilen ilaç ve polimerler arasında uyumsuzluk yoktu. Nanopartiküller % ilaç salınımı, partikül boyutu analizi, zeta potansiyeli, PDI, SEM, TEM, P-XRD, TGA, DTA, *in vitro* ve *in vivo* ilaç salınım çalışması ile karakterize edildi.

Bulgular: *In vitro* ilaç salınım çalışması, ilacın difüzyon mekanizması ile optimize edilmiş partiden sürekli olarak salındı. Optimize edilmiş nanopartikül formülasyonu, deneysel modelin doğrulanması kullanılarak sayısal ve grafiksel yöntemlerle tanındı. Optimize edilmiş parti, parçacık boyutu, tuzak

*Correspondence: dave.ghose87@gmail.com, Phone: +91-9658961202/7008716377, ORCID-ID: orcid.org/0000-0001-9845-2758
Received: 19.08.2020, Accepted: 26.10.2020

verimliliği ve *in vitro* ilaç salınımında fark edilen önemli bir değişiklik olmadan 6 ay boyunca ICH stabilite yönergelerine göre kararlıydı. Optimize edilmiş formülasyon için AUC ve Cmax verilerinin farmakokinetik parametreleri, saf ilaç süspansiyonu ile karşılaştırıldığında 3 ve 2,9 kat arttı.

Sonuç: Hazırlanan polimerik nanopartiküller formülasyonu, ön hiperparatiroidisi olan hastalarda uzun süreli normokalsemiyi yönetmek için model bir ilacın gelişmiş terapötik etkinliği ve biyoyararlanım potansiyeli için alternatif bir doğum sistemidir.

Anahtar kelimeler: PLGA, polimerik nanopartiküller, Taguchi, P-XRD, optimizasyon, biyoyararlanım potansiyeli

INTRODUCTION

Nanodrug delivery systems in medicine have evolved as a dependable and reliable technological boon as site-specific drug targeting in nanodrug development in the previous two decades.[1,2] Polymeric-based nanoparticles are colloidal nature systems measuring around 10-100 nm. The experimental findings achieved are mostly within proximity of 100-500 nm. The polymeric-based nanoparticulate systems have been considered an area of extensive research in novel drug delivery systems because of their all-encompassing biocompatibility and ease of altering properties.[3]

Numerous scientists worldwide have discovered abundant approaches, such as nanoprecipitation, solvent evaporation, salting out, emulsification-diffusion, and supercritical fluid technology.[4] The polymeric nanoparticulate (PN) systems offer high applicability as an active delivery system. These PN versions comprehensively avail the drug near the intended site with augmented therapeutic activity and minimal adverse effects.[5] These biopolymeric systems offer pivotal effectiveness with diminished toxicity and a potentiated therapeutic index.[6,7]

The polymeric micelle systems offer supplementary properties for safe and effective drug targeting at the tissue site, consistent biocompatibility, and potentiated stability during effective drug release.[8-10] The current methodology of the drug cinacalcet hydrochloride (CIH) encompasses the investigations streamlined to enhance the adequate oral bioavailability by nanoprecipitation-sonication techniques.[11-15] These findings may lead to achieve enhanced stability, effective dissolution rate, and less toxicity.[16] Nowadays, a heavy focus of attention has evolved in applying such materials for drug delivery implementation. These polymeric micelles are usually biodegradable and biocompatible hydrophobic polymer blocks, such as PCL, PLA, PEG, etc.[17,18] From the varied range of biopolymers, poly-lactic-co-glycolic acid (PLGA) is considered an efficient and suitable class of copolymers that can be utilized for different Food and Drug Administration-approved therapeutic devices.[19-23]

CIH, a modern-day, first-line, well-known calcimimetic drug, is indicated for the safer management of tertiary hyperparathyroidism in people with chronic renal disorder, dialysis, and hypercalcemia in patients with parathyroid carcinoma.[24,25] The oral form of CIH is considered the frontline medication in the generation of agents (i.e., the calcimimetics), with an innovative mechanism of action with absolute bioavailability of 20-25% and a log p value of 6.8.[26,27]

The overall productiveness of the concept of QbD in optimizing the appropriate experimental design space is boosting vast acceptance in the development of pharmaceuticals.[28,29] Box-Behnken Design (BBD) optimization is a notable response surface method, which is predictable in determining the specific interactions of the parameters opted in optimization.[30-32]

Few research findings on freeze-dried PNs of CIH, prepared by the nanoprecipitation with the ultrasonication method, except for few commercially marketed tablets of the strength of 30, 60, and 90 mg, are available in the literature. An alternative system of drug delivery can be developed for an enhanced therapeutic efficacy and bioavailability potential of CIH.

MATERIALS AND METHODS

Materials

CIH was obtained as a gift sample from Cadila Healthcare Pvt. Ltd., Mumbai, India. PLGA was obtained as a gift sample from Dr. Reddy's lab, Hyderabad, India. Poloxamer-188 was received from Himedia, Mumbai, India. Mannitol was obtained from Himedia Chemicals Pvt. Ltd., Mumbai, India. Further, the necessary reagents, chemicals, and solvents used in this study were of analytical grade and utmost quality. The most authentic ARRIVE guidelines recommended that all animal studies or experiments be conducted in an alliance including Scientific Procedures Act, 1986 in the UK and insisted on allied, EU Directive 2010/63/EU guidelines for experiments on animals were authorized by the Animal Care Committee, RIPS, Berhampur, Institutional Animals Ethics (926/PO/Re/5/06/CPCSEA, approval no: 87).

Methods

Target product profile (TPP)

TPP was predefined for the PN drug delivery system formulation of CIH to improve the oral bioavailability of the drug. The imperative principles of quality TTP (QTPP), such as the strength, administration route of the formulations, and their related pharmacokinetics-based process determining variables and factors, packaging stability attributes, drug release, and pharmacokinetic profiles of the drug.[17,28]

Critical quality attributes (CQAs)

Among the entire TPPs, several crucial and promising QAs are designated as CQAs on the basis of the criticality of effect upon patients' benefit. From the prepared polymeric formulations, CQAs such as time of stirring, mean particle size distribution, and zeta potential (ZP) were selected as per the TPPs.[17,27]

Screening of formulation excipients

Intrinsic solubility analysis

Drug substance intrinsic solubility was estimated in various solvents, such as water, acetonitrile, phosphate buffer pH of

6.8 and 7.4, 0.1N HCl, methanol, ethanol, dimethyl sulfoxide (DMSO), acetone, PEG200, PEG 400, and n-octanol. The drug's adequate capacity was included in each solvent and set aside on a mechanical shaker (Rivotek, Rivieria Glass Pvt. Ltd., Mumbai, India) along with a water bath regulated at 37±0.5°C for 72 h. The vials were subsequently observed from distinct intervals for absolute solubilization of the drug substance, and afterward, the drug was further included if essential. All notable excipients were permitted to move into the centrifuged tubes (Spinwin MC02, TarsonsPvt Ltd.) Kolkata, India). The distinct quantity of the solubilized drug was detected and analyzed by ultraviolet-visible (UV-vis) spectroscopy (UV-vis spectrophotometer, Labindia Ltd., Mumbai, India) for isolation of the undissolved or immiscible drug at a wavelength-maximum of 279 nm (i.e., λ max of the drug) from the supernatant fraction.[20]

Development of analytical method by ultrafast liquid chromatography (UFLC)

A simple, rapid reverse phase RP-UFLC method was used for the quantification of CIH. Drug separation was performed on a 250×4.6 mm ID, ODS C_{18} column. The mixture of (50:50, %v/v) acetonitrile:phosphate buffer i.e., TBHS solution of 25 mL as a mobile phase and filtered through a 0.45 µm millipore filter at a flow rate of 0.5 mL/min. Chromatographic detection was performed at a λmax of 223 nm, and an analytical column was maintained at a constant temperature (25±1°C).[33]

Identification of QTPPs and CQAs in product development

The QTPPs and CQAs are the major QbD elements to achieve product development and objectives for CIH nanoparticles, and the QTPP elements were set up based on drug sustained release, ZP, poly dispersibility index, and particle size. The QTPPs and CQAs parameters are depicted in Table 1.

Preliminary screening of influential factors using Taguchi design

The fundamental screening was attempted by exercising a combination of the 7-factors 2-levels Taguchi design to establish the significant vital factor(s) affecting the CQAs. For the Taguchi design, a combination of eight formulations was suggested and prepared.

Preparation of PN formulation

The development of PNs was attempted by adopting nanoprecipitation, followed by the ultrasonication method. The required quantity of PLGA was dissolved in the organic phase (acetone) at 50°C and added to the acetone solution of drug CIH. The organic phase was included drop-wise into the additive (stabilizer) solution of poloxamer-188 (aqueous phase) with the glass syringe outfitted with a needle (gauge size, 26) at 3 mL/min and a stirring speed of 5000-15000 rpm at 25°C (sample homogenizer T18 DIGITAL IKA RV, Germany). The ultrasound state parameter was set to 3 s with an interval of 2 s at 40 W for 5 min. The residual amount of acetone was evaporated at 40°C beneath condensed pressure, using a Rotary evaporator (IKA RV 10 digital, Germany) for 2 min. The obtained nanosuspension was centrifuged (RC 4815F, Eltek India) at 9000 rpm for 30 min and lyophilized for 36 h at -54°C.

Systematic formulation optimization studies

The BBD response surface design with 3-factors and 3-levels of mixture components was taken into account for optimizing the PN formulations. Design expert ver. 12.1.1 software (Stat-Ease, Minneapolis, MN, USA) was used for generating the experimental trials, where the ratio of Drug:PLGA (mg) (X1), poloxamer-188 concentration % w/v (X2), and stirring speed (X3) was utilized as the independent variables or factors and with 3-levels (-1, 0, and 1) was built to estimate the significant effect of these assorted variables or responses, namely cumulative % drug release QT24% (Y1), particle size in nm (Y2), ZP in mV (Y3), and polydispersity index (Y4). A sum of 17 trial formulations was organized together with five consecutive cumulative replicates of the center point trial, and further CQAs were formulated for evaluation.

Lyophilization of optimized PNs

Extensive research has proven that the samples obtained by lyophilization exhibit a porous structure with increased redispersibility and long-term steadiness.[34] The lyophilized process was performed by using lyophilizer using ALPHA 1- 2 LO Plus CHRIST in order to produce the powdered freeze-dried state at a pressurized vacuum of 0.01 KPa for about 48 h at -50°C to obtain a drug loaded lyophilized PNs in case of run

Table 1. Quality target product profile and critical quality attributes for developing polymeric nanoparticles of cinacalcet hydrochloride

QTTPs	Target	CQAs	Pre-determined target	Justification
Dosage type	Extended-release dosage forms	Cumulative drug release at 24 h (QT24%)	75-85%	Sustained release of drug is the objective of the study and is important for better absorption
Dosage form	Polymeric nanoparticles	Zeta potential	≥±20 mV	Highly critical factor as per the stability perspective of the nano suspensions
Drug release and absorption	C_{max} and AUC higher compared to pure drug	Mean particle size (nm)	100-200 nm	Particle size in these ranges is highly critical and important for better absorption of drug
Dispersity	High dispersity	PDI	0-0.4	Uniformity in the particle distribution by size is essential for therapeutic activity and, hence, is highly critical

QTTPs: Quality target product profiles, CQAs: Critical quality attributes, C_{max}: Maximum plasma concentration, AUC: Area under curve, PDI: Polydispersity index

no: 16. The selected optimized formulation was further freeze-dried to the powder form by applying a suitable cryoprotectant (i.e., mannitol (2%) and then subjected to micrometric characterization.

Characterization of freeze-dried PNs

Fourier-transform infrared spectroscopy (FT-IR)

The FT-IR spectroscopy was performed effectively for estimating the possible physical interactions of drug CIH. FT-IR spectra of selected CIH and physical mixture (PM) with PLGA and poloxamer-188 were recorded on IR using KBr around the 4 cm^{-1} resolution. The compatibility studies of the drug-excipients were undertaken by computing the range of transmittance from 4000 to 400 cm^{-1}. Peak matching was done to identify and determine any significant interactions among the other additives with CIH.[35]

Differential scanning calorimetry (DSC)

DSC studies were done to assess the interaction between the drug and the polymer. All the required samples (10 mg) were subjected to heat in aluminum pans through effluent gas containing dry nitrogen. The DSC thermograms of pure drug of CIH, excipients, and their respective PMs with CIH were determined.[36]

Entrapment efficiency (EE)

The percentage EE of CIH in the formulated or prepared PNs was anticipated directly by collecting the CIH content in the PNs. Samples of 10 mL of CIH PNs were allowed to centrifuge at 9000 rpm for 30 min at -4°C using a cooling centrifuge. The unencapsulated free drug can be removed using centrifugation dialysis.[37] The supernatant free drug was calculated and validated, employing the UV-spectrophotometric method at wavelength 279 nm. The drug EE (DEE) or (DEE %) of nanoparticles was determined and calculated as indicated below by equation (1).

% Entrapment Efficiency=(Total amount of drug-Free Drug)/(Amount of total drug content)×100.....(Eq.1)

Particle size and ZP measurement

Particle size, polydispersity index, and ZP were effectively determined by Photon Correlation Spectroscopy using the Zeta-sizer Nano-ZS Make-Malvern instrument. ZP implies that its value can be associated with the steadiness of colloidal dispersions. A high ZP will present the immovability or steadiness intended for molecules and particles that are small enough.[38]

In vitro diffusion studies

In this *in vitro* drug release study, the dialysis bag diffusion technique was implemented for pure-drug CIH. Formulations (5 mL) were placed in the dialysis bag, hermetically sealed, and dropped into 150 mL of 0.1 N HCl under sink conditions for the first 2 h. Then it was transferred into phosphate buffer solution of pH 6.8 for 24 h. The whole system was kept at 37°C with continuous magnetic stirring at 200 rpm. A sample (2 mL) was used by pipetting it from the compartment of the receptor at prefixed time intervals and replaced by a fresh and accurate quantity of 0.1 N HCl and phosphate buffer of pH 6.8. Then, this 1 mL sample was taken, and 1 mL of ethyl acetate was added. The sample was vortexed in a cyclomixer, and 0.5 mL of this solution's supernatant layer was made in a test tube, kept for drying, and the mobile phase was added to this test tube and analyzed under RP-UFLC.[38-41] Using a non-Fickian diffusion mechanism, kinetic studies were analyzed, allied with a concentration gradient, diffusion mechanics, and the extent of swelling.[42,43]

Solid-state characterization

Powder X-ray diffraction (P-XRD)

P-XRD (Rigaku, Japan, Smart Lab 9 kW) was implemented for diffraction studies. P-XRD studies were performed on the samples by exposure to nickel-filtered CuKa radiation (40 kV, 30 mA) and allowed for the scan. Samples required for P-XRD related investigation were pure drug and optimized lyophilized PNs of CIH. The results were then recorded as peak height (intensity) versus time (h).

Scanning electron microscopy (SEM)

SEM studies the texture or exact appearance of nanoparticles. A high resolution SEM (Jeol, Japan, JSM-6390LV) at 30 kV was used. The formulation bearing to be tested sticks to the metallic stub, which is carbon-coated. SEM is useful for a detailed study of surface morphology. A high-energy electron helps to scan across the surface of a specimen, having an Au and Pt coating, which assists in improving contrast and the signal-to-noise ratio.[44] The pure drug and optimized lyophilized PNs of CIH were studied and appropriately examined for determining surface morphology.

Transmission electron microscopy (TEM)

The exterior appearance or outline of the PNs was determined by TEM (100s, JEOL Ltd, Japan) and the PNs of CIH, which was lyophilized and diluted with 2 mL of distilled water and consistently mixed by ultrasonication for 3 min. The samples were arranged by inserting a drop of PNs of CIH upon a coated copper grid and air-dried.[45]

Thermogravimetric analysis (TGA)

TGA studies were implemented to justify the moisture content associated with weight loss in isothermal or non-isothermal stability studies. TGA denotes a vital aspect to identify and measure the amount of moisture content in pharmaceutical preparations.[46] During the stages of preformulation investigations, it is considered as an accurate method for the distinctness of polymorphs from hydrates or identification of monohydrates from among other hydrates, which may not be possible by DSC alone.[34,47]

Differential thermal analysis (DTA)

It is well understood that thermal analytical techniques are highly requisite to study the polymorphisms and predict drug stability, solvation, degradation, drug compatibility with excipients, and impurity studies. Moreover, as compared to all, DTA is a well-established thermal method intended for an improvement to the melting point determination.[48]

In vivo pharmacokinetic study

A single dosage bioavailability technique was intended in animals under an unfed state. The estimation of the oral bioavailability for the optimized CIH formulation with respect to an aqueous suspension of CIH pure drug was determined in rabbits.[49] The male rabbits of a healthy breed were selected for the present investigation. Then 1 mL of blood was collected carefully from the ear vein of the animal as a blank sample. Then 6.3 mg of pure drug dissolved in 12.6 mL of distilled water was given to the animal orally, and 2.6 mL of formulation was given to another animal. The blood sample from the ear vein of both rabbits was drawn periodically of 2 h interval at a range of time points (0, 2, 4, 6, 12, 18, and 24 h). The collected samples of blood were subjected to a centrifuge for 20 min, at 5000 rpm, after 20 min. The supernatant layer of serum was carefully collected with the aid of a micropipette. The bioanalysis of the collected samples was done by using the analytical UFLC technique. A collection of pharmacokinetic criteria like half-life (t1/2), maximum plasma concentration (C_{max}), elimination rate constant (K), maximum time to attain peak plasma concentration (T_{max}), and area under the curve (AUC) were calculated. The Animal Care Committee permitted the pharmacokinetic study, RIPS, Berhampur, Institutional Animals Ethics (926/PO/Re/5/06/CPCSEA, approval no: 87). All the animal experimentation congregated in accordance with the guidelines of ARRIVE and performed in association with the UK Animals (Scientific Procedures) Act, 1986 and connected guidelines, EU Directive 2010/63/EU for animal experiments.

Accelerated stability study

The accelerated stability studies were performed as per the ICH guidelines of optimized nanoparticles filled with hard gelatin capsules dosages form was subjected to accelerated stability at temperature 40°C and RH of 75% (i.e., relative humidity) for a 6-month period applying stability chamber (TH-200G, Thermolab, Thane, India). The samples were removed carefully from stability at 0,1,2,3, and 6-month time intervals and subjected for evaluation of particle analysis, ZP, and drug release.

RESULTS

Excipients selection on the basis of solubility studies

CIH showed a mean saturation solubility in selected solvents of 3660 µg/mL, 3256 µg/mL, and 2.471 µg/mL in acetone, DMSO, and ethanol. Among different solvents, acetone showed the highest quantitative solubility and, hence, was selected. Most negligible solubilities were observed in methanol 0.000345 µg/mL.

Taguchi screening design for identifying critical factors

The preliminary screening (Taguchi OA design) was applied to filter out the most influential factors with several trials for each element; two levels opted for low and high (1 and 2). Table 2 shows the respective coded and actual values for the formulations based on the CQAs. The influence of multiple factors, like A-PLGA concentration, B-poloxamer-188 concentration, C-Stirring speed, D-Stirring time, E-Ultrasonication time, F-Temperature, and G-Stirring type were studied. The p values of the regression coefficients (R^2) were determined to evaluate the relevance of each factor on each response. The model factors A, B, and C are significant since the p value is less than the standard α value (0.05), and other factors having p values higher than 0.1000 indicate the model terms are not significant. Thus, from the factor screening study, the factors A-Drug:PLGA concentration, B-poloxamer-188 concentration, and C-Stirring speed were finally selected as influential factors for further optimization.

Experimental design, optimization, and analysis

By keeping the other factors constant at a low level, the concentrations of PLGA, poloxamer-188, and stirring speed were changed. On the basis of preliminary data from Pareto-chart analysis, three levels were selected (-1, 0, and 1) for each of the factors. Table 3 represents a total of 17 runs on applying a three-factor at three-level 3^3 BBD. The characterization studies of each formulation were done to investigate the effect of different factors, like A-Drug:PLGA concentration, B-poloxamer-188 concentration, and C-Stirring speed on individual CQAs.

Response surface analysis of 2D and 3D plot

Effect of the factor on CQA QT24%

Figure 1a, it portrays the 2D (contour) and 3D plots of the CQA QT24%. Thorough understanding, it is anticipated that at a low level (-1) of Drug:PLGA concentration and high level (1) level of poloxamer-188 concentration, the red region is prevalent, more than 75% of drug release in 24 hr. run no: 16 has a maximum percentage of drug release, i.e., 76.945 %. In contrast, run no: 14 has a minimum QT24% value, i.e., 29.411 %, due to the high level (1) of Drug:PLGA concentration. Increased polymer concentration increases the level of particle size distribution and aggregation, which retards the release behavior. The result suggests an optimum drug concentration: Polymer ratio is required for better dissolution of the drug. It can also be inferred that the concentration of stabilizer (poloxamer-188) has a noticeable impact on improved drug dissolution.

Effect of the factor on CQA PS

Figure 1b, portrays the 2D (contour) and 3D plot of the CQA PS. The particle size ranges from 147.898 nm for run 16 to 450.211 nm for run 8. It has been noted that at low level (-1) of factors A-Drug:PLGA concentration and high level (1) of B-poloxamer-188 concentration indicated by the blue zone, where the lower range of particle size is achieved.[50] It can be assumed that at the lower level of A-Drug:PLGA concentration efficiently assists in getting a reduction in the particle size, and this characteristic increases significantly concerning a higher level, depicted by the dark yellowish zone. An increase in the stirring rate also influences the particle size, i.e., size reduction.[51]

Effect of the factor on CQA ZP

Figure 1c, portrays the 2D (contour) and 3D plots of the CQA polydispersity index (PDI). Both A-Drug:PLGA concentration and

B-poloxamer-188 concentration seem to influence the CQA ZP. It ranges from -6.321 mV for run 12-22.7 mV for run 16 at a low level 0.5 of A-Drug:PLGA concentration and B-poloxamer-188 concentration at more than level 1 show higher value, which predicts to have a substantial impact on the CQA.[52]

Effect of the factor on CQA PDI

Figure 1d, portrays the contour plot and the 3D plot of the CQA PDI. Both A-DRUG: PLGA concentration and B-poloxamer-188 concentration seem to equally influence the PDI. It ranges from 0.12 to run 14 to 0.65 for run 8. The results showed that, PDI's value remains below 0.2 only when both A-Drug:PLGA concentration and B-poloxamer-188 concentration have a value above the level 0.5. Uniform-size distribution is a vital requirement for getting drug absorbed at GI membrane. The stabilizer system is responsible for maintaining uniform-size distribution.

Analysis of variance (ANOVA) of BBD design

The summary of ANOVA for different factors and their significance with respect to the quadratic model was determined. After conducting the design matrix, the resultant model F value for QT24%, PS, ZP, and PDI is calculated as 21.76, 11.80, 5.06, and 5.72, respectively. P values of the model for various CQAs was less than 0.05 (α=0.05), which justifies that the quadratic model is significant. The lack-of-fit p values for QT24%, PS, ZP, and PDI were calculated as 0.565, 0.157, 0.001, and 0.455. It is not significant, relative to pure error (i.e., p value $>$ α), which is desirable for a fit model. For the CQA QT24%, the model terms, such as A, B, and C^2 are significant. For the CQA PS, the model term B is substantial. A, AB, A^2 are significant model terms regarding of ZP. In PDI as CQA, the model terms such as B, AB, and B^2 are significant. P values less than 0.05 indicate the model terms are significant.

DISCUSSION

Summary of BBD quadratic model

The BBD quadratic model summary in the optimization process is applied to optimize the PNs of CIH. In CQA QT24%, the predicted R^2 of 0.7627 is acceptable, with the adjusted R^2 of 0.9211. The precision ratio of 17.021 estimates good signal-to-noise ratio. In PS's case, the predicted R^2 of 0.2844 is not close to the adjusted R^2 of 0.8586 because it may indicate a significant block effect, with the precision ratio of 12.012 indicating an adequate signal. For ZP, the predicted R^2 of -1.0737 implies that the overall mean may be a better predictor with the adjusted R^2

Table 2. Design matrix for factor screening as per Taguchi design along with the experimental results of various CQAs and factors with their respective low and high levels

Runs	A	B	C	D	E	F	G	QT24%	Particle size (nm)	ZP (mV)	PDI
1	2	1	2	1	2	1	2	47.983	252.4	-27.8	0.299
2	2	2	1	1	2	2	1	67.342	181.0	22.32	0.175
3	1	2	2	2	2	1	1	32.341	276.3	-22.3	0.356
4	2	2	1	2	1	1	2	72.903	191.5	18.231	0.127
5	1	1	1	2	2	2	2	47.785	266.7	-22.3	0.368
6	2	1	2	2	1	2	1	70.234	224.1	-17.312	0.221
7	1	1	1	1	1	1	1	59.234	266.7	-23.6	0.368
8	1	2	2	1	1	2	2	63.456	286.7	-29.1	0.653
Factors	**Codes**							**Low level (-1)**		**High level (+1)**	
PLGA concentration (mg)	A							20		60	
Poloxamer-188 concentration (gm%)	B							0.5%		1.5%	
Stirring speed (rpm)	C							5000		10000	
Stirring time (h)	D							1		2	
Ultrasonication time (min)	E							5		10	
Temperature °C	F							25		40	
Stirring type	G							Magnetic		Mechanical	

CQAs: Critical quality attributes, PLGA: Poly-lactic-co-glycolic acid, PDI: Polydispersity index, ZP: Zeta potential

of 0.6956. For PDI, the predicted R^2 of 0.0433 is not as close to the adjusted R^2 of 0.7264, with a precision ratio of 7.696, indicating an adequate signal.

Analysis for identification of overlay plot and design space

In the case of optimization, the preferable target was allotted for various responses regarding QT24%, PS, ZP, and PDI as per the target identified in finding various QTPPs and CQAs. Based on the required quality target product profiles (QTTP), limits for different CQAs were set and processed for optimization. Run 16 was the optimized PNs of CIH, where BBD achieved comprising 30 mg of CIH: 30 mg of PLGA, poloxamer-188 (1.5% w/v) concentration, and stirring speed of 10000 rpm. Evaluation of the proposed optimized formulation showed QT24% of 76.945%, PS of 147.898 nm, ZP of 22.7 mV, and PDI of 0.398. The optimized PNs of CIH exhibited to achieve the QTTP in an optimum composition.

Characterization of PNs

FT-IR

CIH-polymer interactions were assessed for CIH and physical PM with PLGA and poloxamer-188. The observations were recorded on IR using KBr with a resolution of 4 cm^{-1} over the region 4000-400 cm^{-1}, FT-IR analysis for pure CIH exhibited absorption spectral bands as shown in Figure 2, at 1517 cm^{-1} designated to methyl (-CH3), 1338 cm^{-1} assigned to (-CH2), 2909 cm^{-1} selected to amide (-NH), 796 cm^{-1} fixed to the trifluoromethyl (-CF3), and absorption bands at 805 cm^{-1} assigned to be designated to benzene ($-C_6H_6$). The corresponding peaks obtained for the PM from the spectral analysis showed no alterations. The outcome showed the compatibility between CIH and other excipients.

DSC

DSC curve of CIH exhibited an endothermic peak at a temperature of 181.9°C, the onset temperature of 178.3°C, and the end set temperature of 184.9°C, matching its melting point. The DSC thermograms of CIH and PMs of CIH with excipients were observed. The thermogram of CIH showed an intense endothermic sharp peak at fusion temperature of 181.90°C with onset temperature at 178.33°C, and latent heat of fusion was observed to be -28.26 mJ, predicted crystalline drug nature whereas that of PMs also depicted the same, as shown in Figure 3. Studies indicated no change in peak characteristics for pure drug and formulation; thus, no interactions between drug and excipients were inferred in the present study.

Micromeritic studies

Table 4 enlists micrometric properties of lyophilized PNs, where the angle of repose is 27.96±1.5 degrees and % moisture content is 2.8±0.4, respectively. Based on these micrometric properties, Run-16 was selected to be the best formulation with better flow properties.

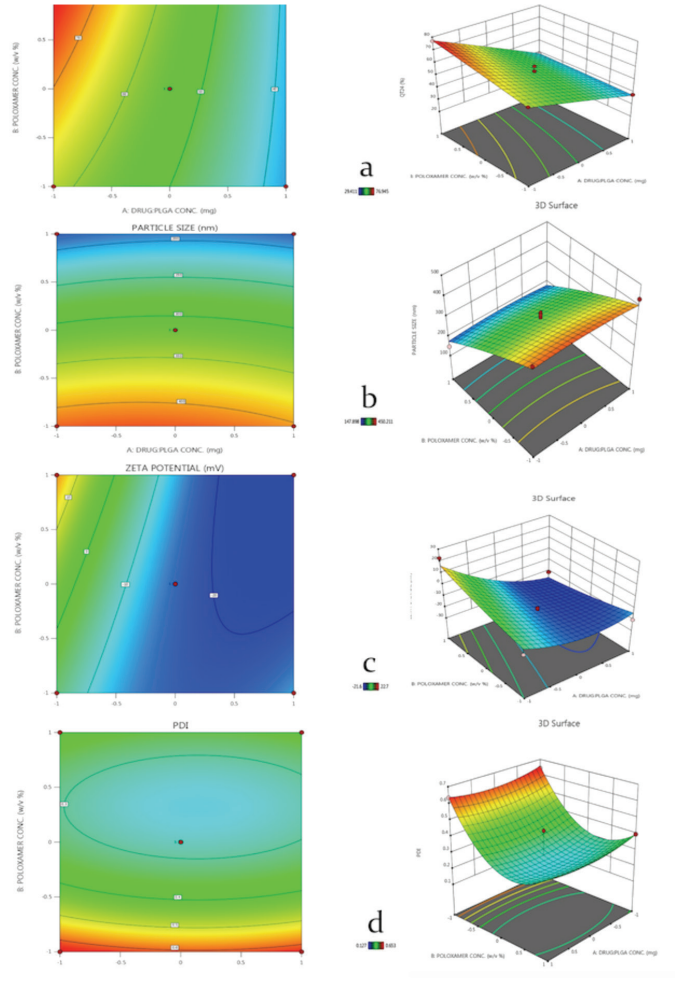

Figure 1. Contour plots (2D) and response surface plots (3D) of selected independent factors on selected dependant factors: QT24% (a); particle size (b); zeta potential (c), and polydispersibility index (d)

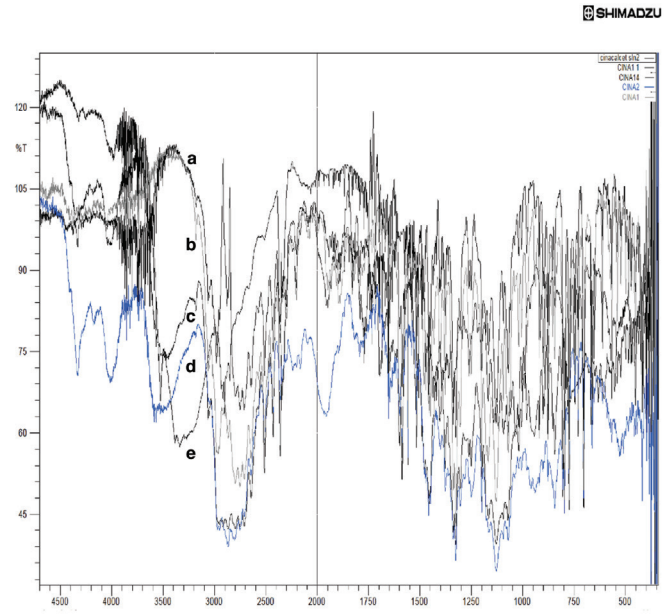

Figure 2. FT-IR spectra of pure drug (a); physical mixture of drug with PLGA polymer (b); physical mixture of drug with polaxomer-188 (c); polaxomer-188 (d) and, PLGA polymer (e)

FT-IR: Fourier-transform infrared spectroscopy, PLGA: Poly-lactic-co-glycolic acid

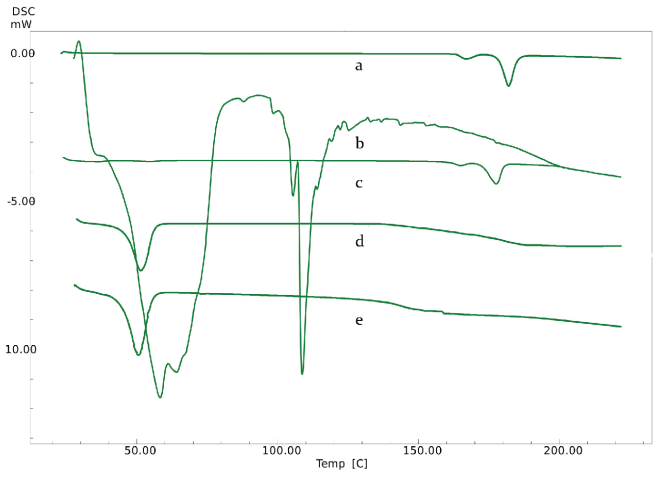

Figure 3. DSC thermogram of pure drug (a); PLGA polymer (b); drug with PLGA polymer (c); drug with polaxomer-188 (d), and polaxomer-188 (e)
DSC: Differential scanning calorimetry, PLGA: Poly-lactic-co-glycolic acid

EE

Among all the trials Run-16 (i.e., Drug:PLGA concentration 30:30 mg), poloxamer-188 1.5% w/v at stirring speed of 10000 rpm was found to have higher EE (69.56%).

Particle size and ZP determination

The zeta-sizer instrument analyzed the particle size of all formulations. The optimized size range for the PNs of CIH was 147.8 nm [i.e., for Run-16 (Figure 4a)]. The developed CIH loaded PLGA-NPs formulation showed spherical surface morphology and uniform particle size distribution of <200 nm. The increase in PLGA concentration had a potential behavior on the particle size, which produced a hazy appearance (i.e., due to the increased aggregation). The ZP results for the respective formulation were 22.7 mV for Run-16. (Figure 4b).

P-XRD

The X-RD patterns of optimized PNs of CIH and pure-drug CIH are depicted in Figure 5a and Figure 5b. Pure-drug CIH showed

Table 3. Composition of various PNs of CIH as per BBD along with the obtained CQAs responses and their coded levels QT24% cumulative % drug release at 24h

Runs	Factor 1 A:X1 PLGA:Drug ratio (mg)	Factor 2 B:X2 polaxomer-188 concentration (%w/v)	Factor 3 C:X3 stirring speed (rpm)	Response Y1 QT24%	Response Y2 Particle size (nm)	Response Y3 Zeta potential (mV)	Response Y4 PDI
1	-1	0	-1	60.345	390.311	13.23	0.453
2	1	0	-1	35.692	348.781	-21.21	0.432
3	0	0	0	48.824	345.453	-18.28	0.428
4	1	1	0	38.567	168.312	-21.6	0.389
5	-1	-1	0	62.542	432.367	-10.324	0.642
6	0	1	1	60.321	232.345	-18.674	0.299
7	0	1	-1	45.432	236.544	-19.421	0.349
8	0	-1	-1	42.871	450.211	-11.984	0.653
9	0	0	0	53.567	334.021	-15.27	0.257
10	0	0	0	54.987	323.237	-15.311	0.234
11	0	0	0	55.342	293.245	-16.322	0.231
12	-1	0	1	67.311	290.312	-6.321	0.171
13	1	-1	0	37.985	432.211	-20.3	0.634
14	1	0	1	29.411	286.768	-21.24	0.127
15	0	0	0	59.093	290.578	-18.431	0.231
16	-1	1	0	76.945	147.898	22.7	0.398
17	0	-1	1	44.252	403.231	-12.234	0.543

Independent variables	Levels		
	Low level (-1)	Middle level (0)	High level (+1)
X1: DRUG:PLGA ratio (mg)	1:1(30 mg)	1: 1.5 (45 mg)	1:2 (60 mg)
X2: Polaxomer-188 concentration (%)	0.5%	1%	1.5%
X3: Stirring speed (rpm)	5000	10000	15000

PNs: Polymeric nanoparticles, CIH: Cinacalcet hydrochloride, BBD: Box-Behnken Design, CQAs: Critical quality attributes, PDI: Polydispersity index, PLGA: Poly-lactic-co-glycolic acid

sharp peaks at the diffraction angles, such as 11.9°, 15.3°, 16.9°, 19.3°, 22.4°, 23.6°, and 25.2°, indicating a typical crystalline pattern. Optimized PNs of CIH showed a reduction (i.e., the minimal peak intensity at those angles), indicating amorphous form and confinement of the drug at the molecular level in the freeze-dried form.

SEM and TEM

Figure 6a and Figure 6b illustrate the scanning electron microscopic pictures of pure-drug CIH and optimized PNs of CIH. The SEM of pure-drug CIH appears to be a rough surface with crystalline structures. However, the TEM studies of the optimized PNs of CIH predict the amorphous structure with spherical smooth-surfaced particles (Figure 7).

TGA

The TGA curve of pure-drug CIH exhibits that at an initial temperature of 23°C, the weight loss is found to be 0.045 mg, with % weight loss of 2.76, which observed a straight line up to a temperature of 280°C with 1.42 mg with % weight loss of 93.42. The TGA curve of optimized PNs of CIH exhibited at 24°C temperature, weight loss was found to be 0.24 mg (% weight loss of 8.22), followed by a sharp decrease of curve observed at 180°C with weight loss of 1.70 mg (57.58%), as depicted in Figure 8a and 8b, and its decline up to 480°C; however, later on, it showed a straight line up to 800°C. This curve indicates that the optimized formulation seems to be significant and thermo-stable concerning % weight loss compared to CIH's pure drug.

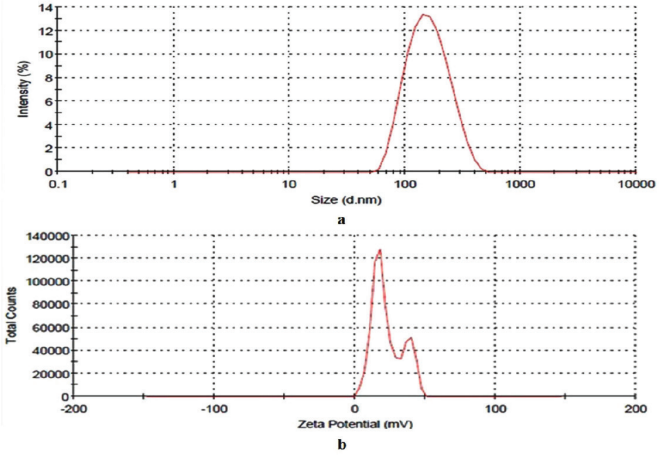

Figure 4. Particle size distribution and zeta potential curves of optimized formulation batch

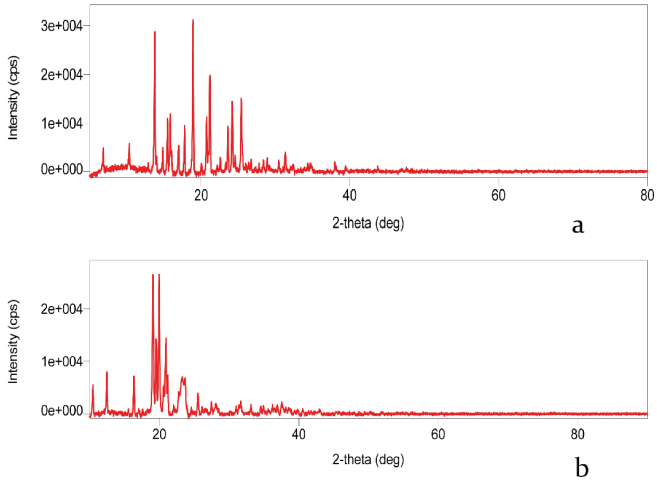

Figure 5. X-RD curves of pure drug (a) and optimized formulation batch (b)
X-RD: X-ray diffraction

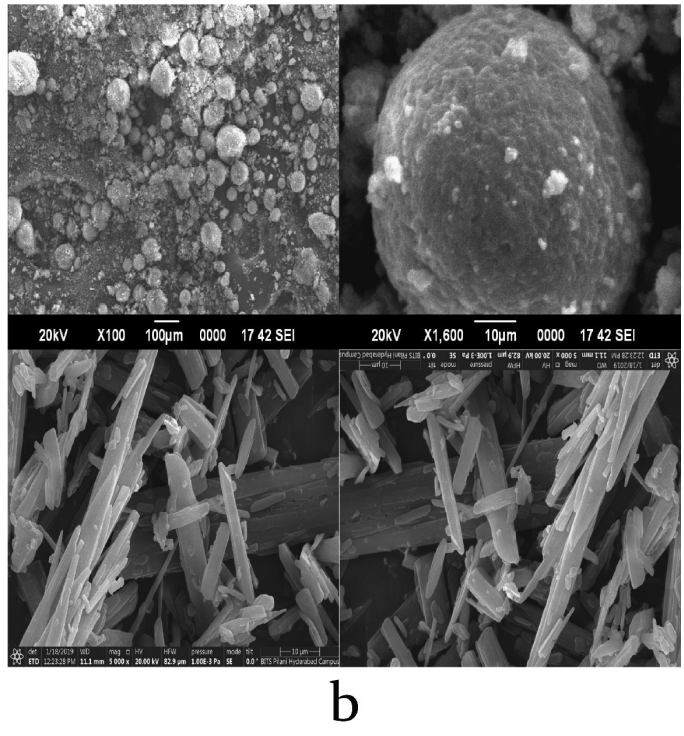

Figure 6. SEM images of optimized formulation batch (a) and pure drug (b)
SEM: Scanning electron microscopy

Table 4. Carr's index, angle of repose, moisture content, and *in vivo* pharmacokinetic parameters of pure drug and optimized formulation batch

Formulations	Carr's index	Angle of repose (Θ)	Moisture content (%)	C_{max} (µg/mL)	T_{max} (h)	K_e	AUC^{∞} 0 (µg/h)/m L	$t_{1/2}$
Pure drug (CIH)	16.66±1.08	35.5±1.98	3.2±0.31	0.671	4	190.773	10.457	0.0036
Optimized formulation	12.20±0.98	27.96±1.5	2.8±0.4	1.945	6	192.737	31.558	0.0035

CIH: Cinacalcet hydrochloride, AUC: Area under curve

DTA

The DTA curve of CIH exhibited melting point at 181°C, a significant decrease in intensity of peak, which signifies an endothermic reaction with respect to the change in the melting point. Similarly, in the case of optimized PNs showed melting point at 226°C, that means sharp change in peak of curvature in case of optimized batch due to the change in melting point at enthalpy of 348.6 mJ. Finally the onset of peaks for the optimized batch showed at 21°C and 67.31°C with the endset enthalpy at 67.31 and 13.5 J respectively. The details of DTA thermograms of optimized PNs formulations and its pure drug of CIH are depicted in Figure 9a and 9b.

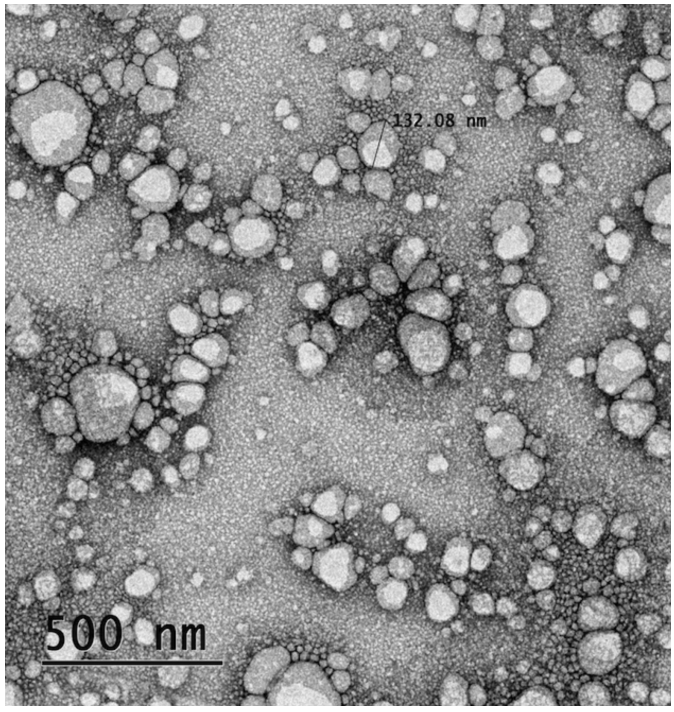

Figure 7. TEM image of optimized formulation batch
TEM: Transmission electron microscopy

In vitro diffusion studies

The behavior pattern of drug release for the optimized PNs of CIH and pure-drug of CIH is illustrated in Figure 10. The pattern of drug release was observed from the *in vitro* diffusion studies for the optimized drug loaded PNs and pure drug as shown in Figure 10. The graph indicated the optimized batch showed a substantial improvement drug release or nearly two times drug release than compared to pure drug after performing 6 h study. Hence, an optimum combination of Drug:PLGA and poloxamer-188 provides a better dissolution profile than the pure drug. For the better understanding about the drug release mechanism and fitting kinetic models, different kinetic model equations are applied such as zero-order, first order and Higuich models respectively. After applying such models, the R^2 values for each kinetic model were calculated separately for pure drug as well as for drug loaded PNs. The obtained R^2 values for pure drug, 0.921 in case of zero-order, 0.934 for first-order and 0.940 Higuchi model, and similarly the optimized drug loaded PNs R^2 values was found to be 0.835, 0.868, and 0.944, respectively. The R^2 obtained for different kinetic models suggested that Higuchi model for pure-drug CIH and optimized PNs of CIH were highest fit. The value of release exponent (n) for the pure-drug CH and optimized PNs of CIH formulation

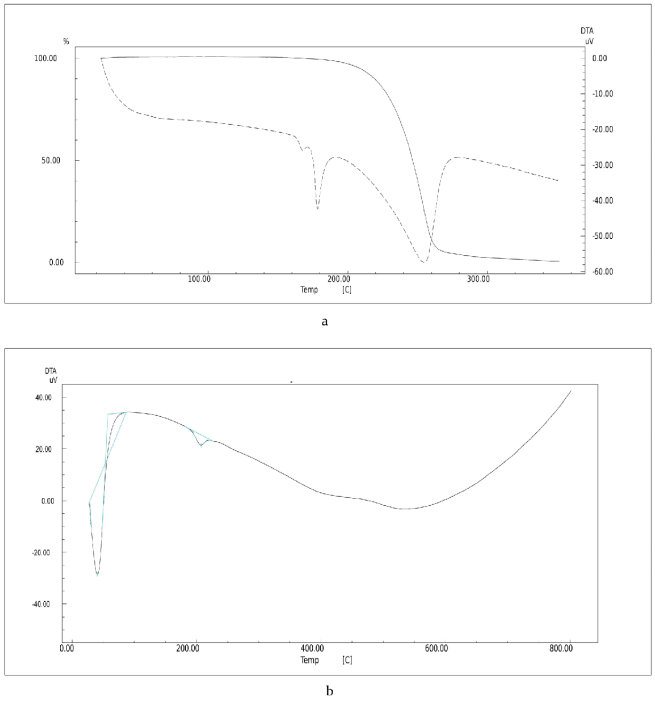

Figure 8. TGA plot of pure drug (a) and optimized formulation batch (b)
TGA: Thermogravimetric analysis

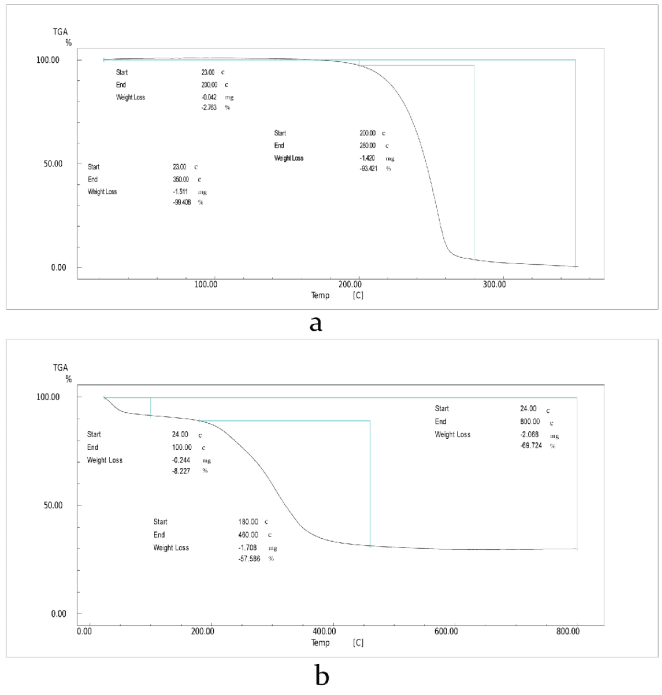

Figure 9. DTA plot of pure drug (a) and optimized formulation batch (b)
DTA: Differential thermal analysis

was 0.689 and 0.478. Hence, the drug release from pure drug follows Fickian diffusion kinetics, whereas optimized PNs of CIH follow non-Fickian diffusion kinetics.

In vivo pharmacokinetic study

From the *in vivo* pharmacokinetic study data table (Table 4) and mean plasma concentrations vs. the time curve (Figure 11) showed that T_{max} was achieved at 6 h in case of optimized PNs and at 4 h in case of pure drug, which indicated sustained release time of the drug. C_{max} of optimized PNs of CIH was 1.945 mcg/mL, whereas compared to the pure drug of CIH, it is 0.671 µg/mL. AUC of optimized PNs of CIH 31.558 (µg/h/mL) was revealed as a more than three-fold increase as compared

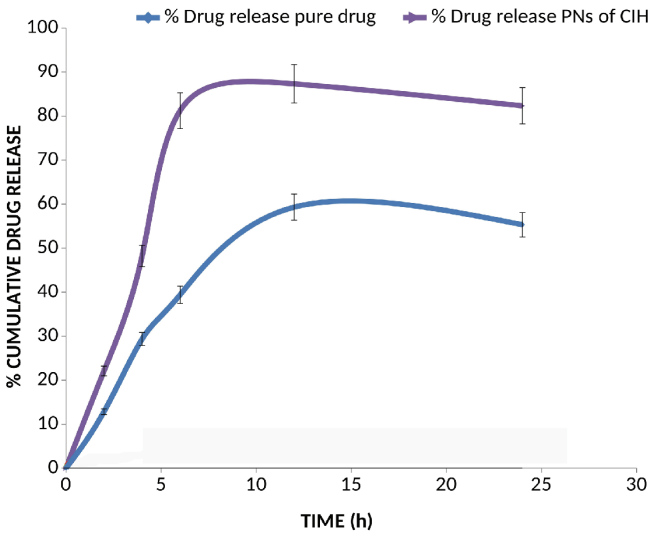

Figure 10. *In vitro* drug release curve of pure drug vs. optimized formulation batch

PNs: Polymeric nanoparticles, CIH: Cinacalcet hydrochloride

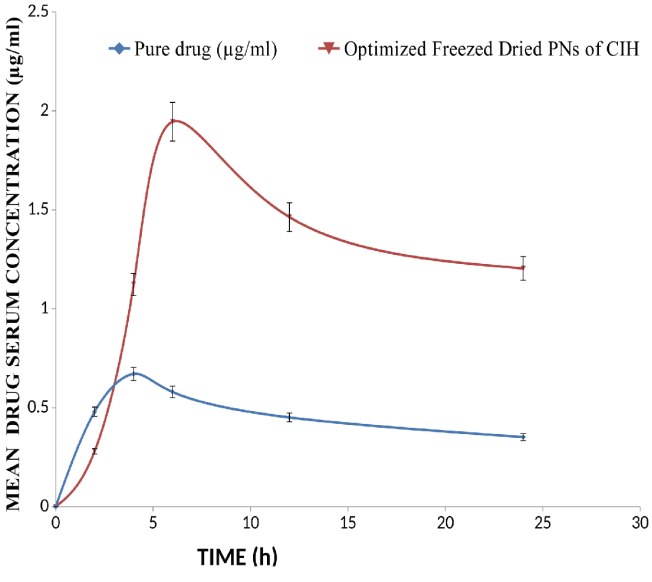

Figure 11. Serum concentration (µg/mL) vs. time (h) curve of optimized formulation batch vs. pure-drug suspension

PNs: Polymeric nanoparticles, CIH: Cinacalcet hydrochloride

to the AUC of the pure CIH 10.457 (µg/h/mL). The rationale for the boosting up in bioavailability is its improvement in the dissolution and absorption profile of drugs through the gastrointestinal membrane. *In vivo* studies proved a significant elevation in the drug CIH absorption and permeation profile concerning optimized PNs of CIH, which is evident from the distinctly superior pharmacokinetic parameter in contrast to pure drug.

Accelerated stability outcomes

The p values of the design obtained during accelerated stability studies are stated in Supplement 1. The p value was more than 0.05 for all the CQAs, indicating no significant change. Hence, the optimized freeze-dried PNs of CIH were found to satisfy the stability criteria as minimal substantial alterations in CQAs throughout the stability period.

CONCLUSION

This research instigates a systematized elaboration of PNs of a novel therapeutic for hyperparathyroidism-CIH-using a quality-by-design approach to improve drug bioavailability and sustained drug release. In the process of QbD, the first QTTPs and CQAs were identified with proper justification. Taguchi screening resulted in primary screening, followed by orderly optimization using the BBD. The regression equation and response surface were analyzed. ANOVA model was applied in the identification of the specific appreciable model term. Optimization of freeze-dried PNs of CIH was taken by coding the high and low-value range for various CQAs. The design space identification was confirmed from the overlay plot. The optimized single dose of freeze-dried PNs of drug obtained using BBD consisted of 30 mg of CIH, 30 mg of PLGA, and 1.5% w/v of poloxamer-188. The optimized freeze-dried PN formulation showed an optimum particle size of 147.89 nm, ZP at 22.7 mV, EE of 69.56%, and *in vitro* drug release of more than 75% after 24h. *In vivo* studies showed 3-folds enhancement in oral bioavailability with increased C_{max} for optimized formulation compared to a pure drug in an aqueous suspension. Accelerated stability study of optimized PNs validates the insubstantial changes in the CQAs during a stored period of 6 months, which was distinct by p values for all CQAs. The conclusive justification of the present study is that an optimum combination of 30 mg of CIH:30 mg of PLGA and 1.5% w/v of poloxamer-188 for the PLGA-based PNs of the drug may effectively be implemented to achieve the desired objective of sustained drug release and enhanced bioavailability.

ACKNOWLEDGMENTS

The authors would also like to sincerely acknowledge Dr. Sanjeeb Kumar Sahoo, Scientist-E, Institute of Life Sciences, Bhubaneswar, for providing technical support for zeta-sizer. The authors are also very thankful to Mr. Naveen Kumar Patro, Lab Technician, Central Instrumentation Facility of Roland Institute of Pharmaceutical Sciences, Berhampur, for his technical support and to Mr. Ashutosh Kumar Behera, Technical

Superintendent, Central Instrumentation Facility, BIT, Mesra, India, for providing the facility to carry out the characterization analysis of SEM, P-XRD, TGA and DTA during our study.

ETHICAL ISSUES

All the animal studies performed in the present work were carried out before the approval of the study protocol. The pharmacokinetic study was permitted by the Animal Care Committee, Roland Institute of Pharmaceutical Sciences, Berhampur, Institutional Animals Ethics (926/PO/Re/5/06/CPCSEA, approval no. 87). All the animal experimentation complied with the ARRIVE guidelines and were performed in association with the UK Animals (Scientific Procedures) Act, 1986 and connected guidelines, EU Directive 2010/63/EU for animal experiments.

Conflict of interest: No conflict of interest was declared by the authors. The authors are solely responsible for the content and writing of this paper.

REFERENCES

1. Peer D, Karp JM, Hong S, Faro Khzad OC, Margalit R, Langer R. Nanocarriers as an emerging platform for cancer therapy. Nat Nanotechnol. 2007;2:751-760.
2. Davis ME,Chen Z, Shin DM. Nanoparticle therapeutics: an emerging treatment modality for cancer. Nat Rev Drug Discov. 2008;7:771-782.
3. Quintanar-Guerrero D, Allemann Fessi EH, Doelker E. Preparation techniques and mechanisms of formation of biodegradable nanoparticles from preformed polymers. Drug Dev Ind Pharm. 1998;24:1113-1128.
4. Bhanoji Rao ME, Swain S, Patra CN, Mund SP. Formulation design, optimization and characterization of eprosartanmesylate nanoparticles. Nanosci Nanotech-Asia. 2018;8:2130-2143.
5. Kreuter J. Nanoparticles-a historical perspective. Int J Pharm. 2007;331:1-10.
6. Soppimath KS, Aminabhavi TM, Kulkarni AR, Rudzinski WE. Biodegradable polymeric nanoparticles as drug delivery devices. J Control Release. 2001;70:1-20.
7. Shenoy DB, Amiji MM. Poly (ethylene oxide)-modified poly-(epsilon-caprolactone) nanoparticles for targeted delivery of tamoxifen in breast cancer. Int J Pharm. 2005;293:261-270.
8. Glen A. The impact of nanotechnology in drug delivery: global developments, Market Analysis Future Prospects, 2005. Last Accessed Date: 31.03.09. Available from: http://www.nanomarkets.com
9. Safra T, Muggia F, Jeffers S, Tsao-Wei DD, Groshen S, Lyass O, Henderson R, Berry G, Gabizon A. Pegylated liposomal doxorubicin (doxil): Reduced clinical cardio toxicity in patients reaching or exceeding cumulative doses of 500 mg/m^2. Ann Oncol. 2000;8:1029-1033.
10. Schroeder U, Sommerfeld P, Ulrich S, Sabel BA. Nanoparticle technology for delivery of drugs across the blood-brain barrier. J Pharm Sci. 1998;87:1305-1307.
11. Raghuvanshi RS, Katare YK, Lalwani K, Ali MM, Singh O, Panda AK. Improved immune response from biodegradable polymer particles entrapping tetanus toxoid by use of different immunization protocol and adjuvants. Int J Pharm. 2002;245:109-121.
12. Kreutera J, Petrov VE, Kharkevich DA, Alyautdin RN. Influence of the type of surfactant on the analgesic effects induced by the peptide dalargin after its delivery across the blood- brain barrier using surfactant-coated nano-particles. J Control Release. 1997;49:81-87.
13. Allemann E, Gurny R, Christophe JL. Biodegradable nanoparticles- from sustained release formulations to improved site specific drug delivery. J Control Release. 1996;39:339.
14. Moffitt M, Khougaz K, Eisenberg A, Micellization of ionic block copolymers. Acc Chem Res. 1996;29:95-102.
15. Sushant SK, Yogesh M, ChoudhariNazma NI, Vishnukant M. Polymeric micelles: authoritative aspects for drug delivery. Designed Monomers and Polymers. 2012;15:465-521.
16. Burt HM, Zhang X, Toleikis P, Embree L, Hunter WL. Development of copolymers of poly (dl-lactide) and methoxypolyethylene glycol as micellar carriers of paclitaxel. Colloids Surf B Biointerfaces. 1999;16:161-171.
17. Xiaoqing XU, Guoguang C, Yaning LI, Jingjing W, Jun Y, Lili R. Enhanced dissolution and oral bioavailbility of cinacalcet hydrochloride nanocrystals with no food effect. Nanotechnol. 2019;30:55-102.
18. Yoo HS, Park TG. Biodegradable polymeric micelles composed of doxorubicin conjugated PLGA-PEG block copolymer. J Control Release. 2001;70:63-70.
19. Jain RK, Stylianopoulos T. Delivering nanomedicine to solid tumors. Nat Rev Clin Oncol. 2010;7:653-654.
20. Lammers T, Kiessling F, Hennink WE, Storm G. Drug targeting to tumors: principles, pitfalls and (pre) clinical progress. J Control Release. 2012;161:175-187.
21. Bae YH, Yin H. Stability issues of polymeric micelles. J Control Release. 2008;131:2-4.
22. Read ES, Armes SP. Recent advances in shell cross-linked micelles. Chem Commun (Camb). 2007:3021-3035.
23. Deng C, Jiang Y, Cheng R, Meng F, Zhong Z. Biodegradable polymeric micelles for targeted and controlled anticancer drug delivery: promises, progress and prospects. Nano Today. 2012;7:467-480.
24. Abdollahi S, Lotfipour F. PLGA-and PLA -based polymeric nanoparticles for antimicrobial drug delivery. Biomed Int. 2012;3:1-11.
25. Burlington MA. 2014 Nurse's drug handbook. (13th ed). Burlington, Massachusetts: Jones & Bartlet Learning; 2014.
26. Yousaf F, Charytan C. Review of cinacalcet hydrochloride in the management of secondary hyperparathyroidism. Ren Fail. 2014;36:131-138.
27. Padhi D, Harris R. Clinical pharmacokinetic and pharmacodynamic profile of cinacalcet hydrochloride. Clin Pharmacokinet. 2009;48:303-311.
28. Swain S, Parhi R, Jena BR, Babu SM. Quality by design: concept to applications. Curr Drug Discov Technol. 2019;16:240-250.
29. Podczeck F. Pharmaceutical Experimental Design. In: Lewis GA, Mathieu D, and R. Phan-Tan-Lu, eds. Boca Raton, Florida: CRC Press; 1999:498.
30. Box GEP, Wilson KB. On the experimental attainment of optimum conditions. J Royal Stat Soc Ser B. 1951;1:1-45.
31. Swain S, Jena BR, Madugula D, Beg S. Application of Quality by Design Paradigms for Development of Solid Dosage Forms. In: Beg S, Hasnain S, eds. Pharmaceutical Quality by Design; Principles and Applications. (1st ed). Cambridge, Massachusetts: Elsevier Academic Press; 2019:109-130.

32. Box GEP, Behnken DW. Some new three level designs for the study of quantitative variables.Technometrics. 1960;2:455-475.
33. Panigrahi KC, Patra CN, Rao MEB. Quality by design enabled development of oral self- nanoemulsifying drug delivery system of a novel calcimimetic cinacalcet HCl using a porous carrier: *in vitro* and *in vivo* characterization. AAPS Pharm Sci Tech. 2019;20:216.
34. Neupane YR, Sabir MD, Ahma N, Ali M, Kohli K. Lipid drug conjugate nanoparticle as a novel lipid nanocarrier for the oral delivery of decitabine: *ex vivo* gut permeation studies. Nanotechnology. 2013;24:415102.
35. Hu C, Rhodes DG. Proniosomes: a novel drug carrier preparation. Int J Pharm.1999;185:23-35.
36. GregorC Mc, Bines E. The use of high-speed differential scanning calorimetry (Hyper- DSC) in the study of pharmaceutical polymorphs. Int J Pharm. 2007;350:48-52.
37. Didem AS, Muharrem S,Johanna GW, Frank S, Thomas S. Nano structured Biomaterials and applications. J of Nanomater. 2016;13.
38. Dynamic Light Scattering Particle Size and Zeta Potential Analyzer. Last Accessed Date: 03.11.2015. Available from: https://www.iitk.ac.in/dordoldn/dynamic-light-scattering-particle-size-and-zeta-potential-analyzer
39. Cruz CN, Tyner KM, Velazquez L, Hyams KC, Jacobs A, Shaw AB, Jiang W, Lionberger R, Hinderling P, Kong Y, Brown PC, Ghosh T, Strasinger C, Suarez-Sharp S, Henry D, Van Uitert M, Sadrieh N, Morefield E. CDER risk assessment exercise to evaluate potential risks from the use of nonmaterial's in drug products. AAPS J. 2013;15:623-628.
40. Langer R. New methods of drug delivery. Science. 1990;249:1527-1533.
41. Arifin DY, Lee LY, Wang CH. Mathematical modeling and simulation of drug release from microspheres: implications to drug delivery systems. Adv Drug Deliv Rev. 2006;58:1274-1325.
42. Siepmann J, Siepmann F. Mathematical modeling of drug delivery. Int J Pharm. 2008;364:328-343.
43. Lin SB, Hwang KS, Tsay SY, Cooper SL. Segmental orientation studies of polyether polyurethane block copolymers with different hard segment lengths and distributions. Colloid Polym Sci. 1985;263:128-140.
44. Carter M, Jennifer S. In Guide to Research Techniques in Neuroscience. (2nd ed). Marcel Dekker Inc; USA; 2015.
45. Peter Christoper GV, Vijaya Raghavan C, Siddharth K, Siva Selva KM, Hari Prasad R. Formulation and optimization of coated PLGA- zidovudine nanoparticles using factorial design and *in-vitro in-vivo* evaluations to determine brain targeting efficiency. Saudi Pharm. J 2014;22:133-140.
46. Haines PJ. Principles of thermal analysis and calorimetry, RSC paperbacks, Royal Soc of Chem. 2002:1-9.
47. Nakashima D, Takama H, Ogasawara Y, Kawakami T, Nishitoba T, Hoshi S, Uchida E, Tanaka H. Effect of cinacalcet hydrochloride, a new calcimimetic agent, on the pharmacokinetics of dextromethorphan: *in vitro* and clinical studies. J Clin Pharmacol. 2007;47:1311-1319.
48. Differential thermal Analysis. Last Accessed Date: 01.12.2018. Available from: https://www.sciencedirect.com/topics/medicine-and-dentistry/differential-thermal-analysis.
49. Janga KY, Jukanti R, Velpula A, Sunkavalli S, Bandari S, Kandadi P, Veerareddy PR. Bioavailability enhancement of zaleplon via proliposomes: role of surface charge. Eur J Pharm Biopharm. 2012;80:347-357.
50. Legrand P, Lesieur S, Bochot A, Gref R, Raatjes W, Barratt G. Influence of polymer behaviour in organic solution on the production of polylactide nanoparticles by nanoprecipitation. Int J Pharm. 2007;344:33-43.
51. Chorny M, Fishbein I, Danenberg HD, Golomb G. Lipophilic drug loaded nanospheres prepared by nanoprecipitation: effect of formulation variables on size, drug recovery and release kinetics. J Conrol Release. 2002;83:389-400.
52. Rostamizadeh AHK, Salari D, Hamidi M. Preparation of biodegradable nanoparticles of tri- block PLA-PEG-PLA copolymer and determination of factors controlling the particle size using artificial neural network. J Microencapsul. 2011; 28:406-416.

Supplement 1. Drug release, particle size, zeta potential, and PDI of optimized PN formulations at accelerated stability conditions

Time (months)	QT24% (cumulative drug release)	Particle size (nm)	Zeta potential (mV)	PDI
0	76.945	147.898	22.7	0.398
1	73.394	168.493	18.342	0.232
2	71.452	182.312	-13.41	0.421
3	68.341	168.301	-12.311	0.311
6	66.311	190.451	-22.212	0.390
P value $\alpha \leq 0.05$=significant	0.072	0.263	0.217	0.481

PDI: Polydispersity index, PN: Polymeric nanoparticle

Turk J Pharm Sci 2021;18(4):465-475
DOI: 10.4274/tjps.galenos.2020.33239

ORIGINAL ARTICLE

Development of an *Aloe vera*-based Emulgel for the Topical Delivery of Desoximetasone

Dezoksimetazonun Topikal Uygulaması İçin *Aloe vera* Bazlı Bir Emüljelin Geliştirilmesi

Jitendra SAINY[1]*, Umesh ATNERIYA[2], Jagjiwan Lal KORI[2], Rahul MAHESHWARI[3]

[1]School of Pharmacy, Devi Ahilya Vishwavidyalaya, Indore (M.P.), India
[2]BM College of Pharmaceutical Education and Research, Indore, Madhya Pradesh, India
[3]SVKM'S NMIMS University Faculty of Pharmacy and Technology Management, Department of Pharmaceutics, Telangana, India

ABSTRACT

Objectives: Desoximetasone (DMS) is a widely recommended drug for the topical treatment of plaque psoriasis. However, low water solubility and short half life of DMS present major obstacles in the development of an effective topical formulation. Thus, there is a demand for the development of a safe and effective topical system to deliver hydrophobic DMS. The present study aimed to develop an *Aloe vera*-based emulgel formulation to ensure enhanced skin deposition of DMS for effective treatment of plaque psoriasis.

Materials and Methods: Different formulations (DE1-DE4) of *Aloe vera* emulgel were prepared using dispersion technique, wherein varying concentrations of propylene glycol (6-14% w/w) and carbopol 934 (0.5-1.0% w/w) were used.

Results: Zetasizer measurements revealed that the globule size of the formulations ranged from 10.34 µm±0.9 to 14.60 µm±1.4 (n=50). Extrudability analysis for the DE3 and DE2 formulations revealed an extrudability of 5.6±0.11 g/cm^2 and 5.8±0.13 g/cm^2, respectively. The pH of the formulations was recorded in the range of 5.8-6.8. Among these formulations, DE3 showed a maximum drug content of 94.64%±0.29 (n=3), and thus was used for further *in vitro* evalutions. A texture analyzer showed that an optimized DE3 formulation was firmer and exhibited optimal spreadability in comparison with the DE2 formulation. For DE3, the mean max force that represented "firmness" was recorded to be 833.37 g, where as the mean area, denoting "work of shear", was 324.230 g.sec. The DE3 formulation exhibited DMS permeation of 95.40±1.6% over a period of 7 h, as detrmined using an in house fabricated Franze diffusion cell. Evaluation of *in vitro* release kinetics revealed that the release of DMS fitted into the Korsmeyer-Peppas model.

Conclusion: Physicochemical characteristics and enhanced *in vitro* permeation of DMS from *Aloe vera* emulgel highlight its suitability to be efficiently employed for the topical treatment of skin ailments.

Key words: *Aloe vera*, desoximetasone, plaque psoriasis, emulgel, skin diseases, kinetic models

ÖZ

Amaç: Desoximetazon (DMS), plak psöriasisin topikal tedavisi için yaygın olarak önerilen bir ilaçtır. Ancak, DMS'nin düşük suda çözünürlüğü ve kısa yarı ömrü, etkili bir topikal formülasyonun geliştirilmesinde büyük engeller oluşturmaktadır. Bu nedenle, hidrofobik DMS vermek için güvenli ve etkili bir topikal sistemin geliştirilmesine yönelik bir talep vardır. Bu çalışma, plak psöriasisin etkili tedavisi için DMS'nin deride daha fazla birikmesini sağlamak için *Aloe vera* bazlı bir emüljel formülasyonu geliştirmeyi amaçlamıştır.

Gereç ve Yöntemler: *Aloe vera* emüljelinin farklı formülasyonları (DE1-DE4), değişen konsantrasyonlarda propilen glikol (%6-14 w/w) ve karbopol 934 (%0,5-%1,0 w/w) içeren dispersiyon tekniği kullanılarak hazırlanmıştır.

Bulgular: Zetasizer ölçümleri, formülasyonların globül boyutunun 10,34 µm±0,9 ila 14,60 µm±1,4 (n=50) arasında değiştiğini ortaya koymuştur. DE3 ve DE2 formülasyonları için ekstrüde edilebilirlik analizi, sırasıyla 5,6±0,11 g/cm^2 ve 5,8±0,13 g/cm^2'lik bir ekstrüde edilebilirlik ortaya koymuştur. Bu formülasyonlar arasında DE3, %94,64±0,29 (n=3) maksimum ilaç içeriği göstermiş ve bu nedenle daha ileri *in vitro* değerlendirmeler için kullanılmıştır. Bir doku analiz cihazı, optimize edilmiş bir DE3 formülasyonunun DE2 formülasyonu ile karşılaştırıldığında daha sıkı olduğunu ve optimal yayılabilirlik sergilediğini göstermiştir. DE3 için, "sertliği" temsil eden ortalama maksimum kuvvet 833,37 g olarak kaydedilirken, "kesme işini" ifade eden ortalama alan 324,230 g sn bulunmuştur. DE3 formülasyonu tarafımızdan üretilmiş bir Franze difüzyon hücresi kullanılarak belirlendiği üzere, 7 saatlik bir süre boyunca %95,40±1,6 DMS geçirgenliği sergilemiştir. *İn vitro* salım kinetiğinin değerlendirilmesi, DMS salımının Korsmeyer-Peppas modeline uyduğunu ortaya çıkarmıştır.

*Correspondence: jsainy24@gmail.com, Phone: 919826230903, ORCID-ID: orcid.org/0000-0002-8611-6666
Received: 16.06.2020, Accepted: 27.10.2020

Sonuç: Fizikokimyasal özellikler ve *Aloe vera* emüljelindeki DMS'nin gelişmiş *in vitro* permeasyonu, deri rahatsızlıklarının topikal tedavisi için verimli bir şekilde kullanılmaya uygunluğunu vurgulamaktadır.

Anahtar kelimeler: *Aloe vera*, desoksimetazon, plak psöriasis, emüljel, deri hastalıkları, kinetik modeller

INTRODUCTION

Plaque psoriasisis the most common form of psoriasis, and it is basically an autoimmune inflammatory skin disease that is challenging to treat. Being ask in disorder, plaques are visible mostly on the skin Stark et al.[1] In particular, plaque psoriasis leads to the formation of red and white plaques of dead skin cell on elbow, knees, scalp, and lower back of the body Grubauer et al.[2] These plaquesare usually irritating and painful, and these can also crack and bleed Kuchekar et al.[3]

Desoximetasone, (11β,16α) 9 fluoro 11,21 dihydroxy 16 methylpregna 1,4 diene 3,20 dione (DMS), is a synthetic fluorinated corticosteroid that is known to exert antipruritic and antiinflammatory effects. In fact, it is one of the most commonly used medication for the treatment of plaque psoriasis Laws and Young.[4] Despite its use in topical skin formulations Imran et al.,[5] low water solubility and short half life of DMS limit its therapeutic efficacy.

In recent years, emulgel has emerged asa promising strategy for effective delivery of drugs, which is usally dependent on the combination of different approaches. In general, emulgel refers to a formulation that contains both gels and emulsions together in the same dosage form Kumar et al.[6] Emulgel formulations have been prepared for several classes of drugs, including antiinflammatory drugs, antifungal agents, antiviral drugs, antibacterial drugs, local anesthetics, and drugs for plaque psoriasis Khunt et al.[7] Currenlty, emulgels are used as a carrier for delivery of various drugs to the skin Susmitha and Gudas.[8] The major components of an emulgel are emulsifying agent, gelling agent, and oil phase Berdey and Voyt.[9] The concentration of these components significantly affects the release of a drug from the formulation, and thereby determines the bioavailability of the drug Kumari et al.[10] One of the advantages of an emulgel is that it easily entraps water-insoluble drugs into a gel base with the help of an oil in water emulsion system Khullar et al.[11] This further enhances the cargo loading capacity, stability, and release of drugsin a controlled manner Vyas and Khar.[12]

The properties of an emulgel that make it a promising option for the treatment of plaque psoriasis include biocompatibility, thixotropic nature, easy spreadability, greaselessness, easy to remove, water solublility, transparency, non staining impact, pleasant appearance, and stability. In addition, the topical application of an emulgel provides softness to the skin Singla et al.[13] The ability of *aloe vera* to enhance the penetration power of drugs and produce an excellent emulsion makes its suitable to be used in the development of an emulgel Thanushree et al.[14]

Several conventional drug delivery systems, including cream, lotion, and gel, have been commercially used for the delivery of DMS. However, the use of these formulations for the treatment of plaque psoriasis is limited, owing to the low contact time and limited localized bioavailability of the drug from these formulations Prajapati.[15] In a previous study, the property of *aloe vera* to stay in contact with skin was explored to develop an emulgel formulation that could be retained for a longer period onto the skin and provide effective and controlled release of drugs Kasliwal et al.[16]

Several previous studies reported the development and evaluation of emulgel formulations for the topical delivery of various drugs. Panwar et al.[17] developed an emulgel formulation of DMS using the incorporation method. Raju et al.[18] utilized *aloe vera* as a gel base for the development of emulgel formulations. Joshi et al.[19] reported that the emulgel formulations they prepared exhibited superior spreadability and consistency. In another study, a physicochemically stable DMS emulgel was prepared, which could significantly release DMS across the cell membrane in a controlled manner with the help of *aloe vera* for a prolong period in the treatment of plaque psoriasis Yapar et al.[20]

Since early decennial of the 21st century, topical delivery of drug has gained immense attention. One of the key benefits of transdermal delivery is that it bypasses metabolism Patel et al.[21] In addition, topical formulations minimize off target effects, such as pH variation, empty stomach time, and presence of enzymes. Thus, topical formulations bypass the difficulty and discomfort associated with an endovenous treatment therapy Sah et al.[22] The present study aimed to developa DMS-loaded emulgel for effective permeation using *aloe vera*.

MATERIALS AND METHODS

Materials

DMS was purchased from Lupin Ltd., Pithampur, Madhya Pradesh, India. Carbapol 934, Tween 20, Span 20, light liquid paraffin, triethanolamine, potassium dihydrogen phosphate, and sodium hydroxide were procurred from Lobachemie Pvt. Ltd., Mumbai, India. Propyl paraben and propylene glycol were obtained from Molychem, Mumbai, India. Methyl paraben was procurred from Merk specialities Pvt. Ltd., Mumbai, India and ethanol from Changshu hongsheng fine chemical Co. Ltd., Changshu city, China.

Methods

Preparation of a gel from aloe vera juice

Central parenchymatous pulp of *aloe vera* was taken out from a fresh leaf using spatula Roy et al.,[23] and it was washed with distilled water several times. Then, the aloe vera pulp was treated with 0.1 N sodium hydroxide toneutralize its acidity Shivhare et al.[24] Further, the treated pulp was blended in a mechanical blender (Secor India research testing instrument, Mumbai, India) at 10,000 rpm for 20 min, and the obtained juice was filtered three times using cotton bed to remove any adhering peel Bharadwaj et al.[25] The prefiltered juice was then subjected to vacuum using a Buchner funnel vacuum suction

filtration apparatus (Zhengzhoukeda machinery and instrument equipment Co., *Ltd*., Zhengzhou city, Henan Province) and clear fluid was collected Bhanja et al.[26] Further, 1% w/w carbapol 934 was added and mixed with the help of a dual-shaft mechanical stirrer at 2.000 rpm (Secor India research testing instrument, Mumbai, India) for 30 min Khullar et al.[11] *Aloe vera* gel was prepared via dispersion technique to ensure that no lumps are formed. During the dispersion of the aloe vera juice, carbapol 934 was assorted with propyl paraben and methyl paraben Baviskar et al.,[27] and gel formation was mediated by the gradual addition of 1 N sodium hydroxide solution Tambe et al.[28]

Formulation of different batches of emulgel containing 0.25% DMS

A 0.25% DMS oil-in-water (o/w) emulgel system was prepared using dispersion method, as described earlier. Various formulations of emulgel (DE1-DE4) were prepared using varying concentrations of carbopol 934 as summarized in Table 1. Briefly, 1% w/w Span 20 was added toliquid paraffin in order to prepare an oil phase, and then 0.25% DMS was dissolved in this oil phase Patwardhan et al.[29] An aqueous phase was prepared via dissolving 0.5% w/w Tween 20 in 10 mL distilled water. Similarly, propyl paraben and methyl paraben were mixed in propylene glycol, and these were finally combined with the aqueous phase. The aqueous phase and oil phase were heated separately at 80˚C in a water bath (Omkar instruments, Bhiwandi, Maharashtra, India) Pakhare et al.[30] Lastly, the emulsion was formulated by mixing the oil phase with the aqueous phase using a mechanical stirrer at 1.500 rpm for 20 min. After stirring, the formulation was cooled to room temperature Martin.[31] The prepared 0.25% DMS emulsion was added to the prepared *aloe vera* gel with continuous stirring on a mechanical stirrer at 1.000 rpm for 60 min. Triethanolamine was used to maintain a pH of 6.4 of the prepared 0.25% DMS emulgel Premjeet et al.[32]

Table 1. Formulation of 0.25% DMS emulgel

S. no.	Name of ingredients (% w/w)	DE1	DE2	DE3	DE4
1	Desoximetasone	0.25	0.25	0.25	0.25
2	Span 20	1	1	1	1
3	Tween 20	0.5	0.5	0.5	0.5
4	Propylene glycol	6	10	14	8
5	Methyl paraben	0.03	0.03	0.03	0.03
6	Ethanol	4	4	4	4
7	Liquid paraffin	16	16	16	16
8	*Aloe vera*	10	15	20	10
9	Carbopol 934	1	0.75	0.5	1
10	Propyl paraben	0.02	0.02	0.02	0.02
11	Distilled water	q.s.	q.s.	q.s.	q.s.
12	Triethanolamine	Adjust pH 5.8 to 6.8			

DE formulation denotes desoximetasone emulgel. DE: Different formulation, DMS: Desoximetasone

Globule size analysis

The globule size of the prepared *aloe vera* emulgel of DMS was studied using a zetasizer (Malvern instrument 3.000 HSA, UK). Size measurements were performed at 25˚C. The samples were diluted before analysis. All measurements were performed in triplicates Khullar et al.[33]

Determination of extrudability

The extrudability was determined in terms of the load applied (grams) to extrude a 0.5 cm strip of emugel from the collapsible tube of lacquered aluminium within 10 seconds Vijaya et al.[34] The scalability of optimized preparation was measured in triplicates. The extrudability was measured using the following equation (1):

$$\text{Extrudability} = \frac{\text{Applied load (g) to extruded emulgel from tube}}{\text{Area (in cm}^2\text{)}}$$

equation (1)

pH studies of DMS emulgel

To measure the pH of emulgel formulations, a digital pH meter (Mettler Toledo India Pvt. Ltd., Mumbai, Maharashtra, India) was used Moghbel and Faghiri[35] All measurements were performed in triplicates.

Determination of drug content in DE1-DE4 emulgel formulations

To determine the drug content in the formulations, approximately 200 mg of emulgel was taken in a petri dish and 5 mL of ethanol (65% v/v) was added. Emulgel was dissolved in ethanol by gentle shaking with a glass rod for 15 min. The resulting solution was transferred to a 10-mL volumetric flaskand sonicated for 10 min. The final volume of the solution was made up to 10 mL using ethanol Kumar et al.[36] Further, the solution was filtered using filter paper grade no. 41 (Whatman) and analyzed spectrophotometrically (Shimadzu 1700, Shimadzu analytical Pvt. Ltd., Mumbai, India) at 242 nm Vladimirov et al.[37] The drug content was calculated using the following equation (I2):

$$\text{Drug content (\%)} = \frac{\text{Actual amount of drug determined in 200 mg emulgel}}{\text{Theoretical amount of drug present in 200 mg emulgel}} \times 100$$

equation (2)

An in vitro release study of the optimized DMS emulgel

An *in vitro* release study for the optimized emulgel formulation was performed using a modified dissolution assembly, as previsously described by Bazigha et al.[38] The filter paper grade no. 41 (Whatman®) was cut into desired size and placed at the bottom and inner wall of the stainless steel basket assembly. The modified basket assembly wasplaced in a 50 mL glass beaker containing 30 mL ofphosphate buffer (pH 7.4) as a drug release medium. The dissolution assembly was placed on a magnetic stirrer and ateflon coated magnetic bead was used for stirring the drug release medium ata temperature of 32˚C±0.5˚C.

Emugel equivalent to 2.5 mg of DMS was weighed and applied as a thin layer in the modified basket assembly. At different time intervals, 3 mL of drug release medium was withdrawn and 3 mL of fresh buffer medium was added. The test sample was filtered through the filter paper, and concentration of the test sample was measured in terms of absorbance at 242 nm using a double beam ultraviolet (UV)/visible spectrophotometer (Shimadzu® 1700) Navya et al.[39]

Assessment of DMS permeation using a Franz diffusion cell

To evaluate the permeation of DMS for the optimized emulgel formulation, a Franz diffusion assembly was used, as previously described by Nayak et al.[40] The Franz diffusion cell consists of donor and receptor chambers. In the present study, the donor chamber was kept in contact with the environment and unclosed at the top, with a diffusion area of 1.43 cm^2. Phosphate buffer (pH 7.4) was used as a dissolution medium, and 0.0025% w/v sodium azide solution was added to prevent microbial growth in the receptor chamber. Arice magnetic bead was placed in the receptor chamber. A cellophane membrane was tied to the donor chamber, and the excised diffusion cellwas placed between the chambers of the diffusion cell and clamped into position. The whole assembly was placed on a magnetic stirrer at 37°C±0.5°C Gupta and Gupta.[41] For hydration, the membrane was placed in the cell for 2 h. Then, the emulgel formulation of DMS (5 mL) was spread onto the surface of membrane. At different time intervals, 1 mL of permeated drug sample was withdrawn and 1 mL of fresh release medium was added to the receptor compartment. The test sample was analyzed using a double beam UV/visible spectrophotometer (Shimadzu® 1700 analytical Pvt. Ltd., Mumbai, India) at 242 nm Dhawan et al.[42]

Consistency of the optimized DMS emulgel formulation

The consistency of the optimized emulgel formulation was determined using a texture analyzer (TA.XT Plus). Prior to the test, distance calibration of the probe was performed by keeping the return distance fixed at 30 mm. The consistency of the formulated emulgel was measured using a standard-sized container (back extrusion 50 mm diameter). The container was filled with 75% emulgel formulation and a 40 mm extrusion disc was placed at the center, over the test container. Care was taken to hold the container firmly in place to prevent it from lifting when prob returns to start position Shah and Desai.[43] The disk was inserted into the deepest part, where active surface was reported, i.e., the point at which the bottom surface of the disc comes into contact with the product. At this point, the probe moved back to its real position when maximum force was applied. The firmness of the formulation was measured at maximum force or peak value. The area under the curve, at this point, was taken as the measurement of consistency, which showed that higher the area, more dense is the consistency of the formulated emulgel. The gripping effect of the optimized emulgel formulation was measured by back extrusion, where in the negative region of the graph presented consistency. A higher cohesiveness value of the emulgel formulation was indicated by maximum negative force or higher negative value. The negative area region of the curve is called work of cohesion. The consistency of the optimized emulgel formulation showed that more is the area of curve, higher is the resistance to withdraw the emulgel formulation Swamy et al.[44]

Spreadability of the optimized DMS emulgel

The spreadability of the DMS emulgel was determined using a texture analyzer (TA.XT Plus). Spreadability fixity is a group of accurately coinciding male and female cones (febricated with Perspex 90). The test required the use of a heavy duty platform to which the female probe containing the sample was attached. The male cone was positioned centrally over the cone containing the sample. Before starting the experiment, the male cone probe was moved downward such that it was installed into the female cone sample holder. The instrument was calibrated for distance using a void female holder prior to the test. The DMS emulgel was loaded into the female holder using a spatula. Upon starting the test, the male cone probe proceeded toward the female cone and penetrated the sample holder surface (depth of 2 mm). At this point, the maximum penetration depth was attained for the given penetration force, and firmness was measured at a specified depth in terms offorce value. A higher area of firmer sample indicated total quantity of the force required to perform shearing process. The male probe was then allowed to return back to its original position from the female probe. Mean maximum force and mean area were calculated from the curve Gupta and Gaud.[45]

In vitro release kinetics

The release profile for sustained release of DMS from the emulgel formulation could be interpreted in several ways, including diffusion, erosion, or osmosis by using different kinetic models. For *in vitro* release kinetics assesment, zero-order models were used for cumulative % drug released vs. time, Higuchi kinetic model represented cumulative % drug release vs. square root of time, first-order kinetic model as log of cumulative % drug left vs. time, Korsmeyer-Peppas model as log of % drug released vs. log time, and Hixson-Crowell cube root model as cube root of % drug remaining vs. time. The desired model was selected on the basis of excellence of fit test Wesley and Gude.[46]

Zero-order model: In this equation, the release data for emulgel containing DMS showed that DMS was released slowly, which was measured by applying the following equation 3:

$$M_0 - M_t = k_0 t \qquad \text{equation (3)}$$

Where, "M_t" denotes the quantity of DMS dissolved in time t, "M_0" denotes the initial quantity of DMS in the release medium (times, M_0=0), and "k_0" is the kinetic zero-order release constant (concentration/time).

First-order model: This equation was used to explain the absorption and/or elimination of DMS. The DMS release profile following the first-order kinetics model was measured using the equation 4:

$$\ln (M_0/M_t) = k_1 t \qquad \text{equation (4)}$$

Krate constant of first order (time^{-1}).

Higuchi model: This model was used to explain DMS release from the matrix, wherein the obtained data were calculated using equation 5:

$M_t = k\sqrt{t}$ equation (5)

Here, k√t is the Higuchi dissolution constant.

Korsmeyer-Peppas model: The proposed equation was used to explain the release of drugs from a polymer system. To find out the release mechanism of DMS, the obtained data were calculated as per the given equation 6:

$M_t/M_\infty = Kt^n$ equation (6)

Where, "M_t/M_∞" denotes the amount of drug released due to friction at time t, "K" is the rate release constant and "n" denotes the release exponent.

Hixson-Crowell model: According to this model, area of the particle is proportional to the cube root of volume, and the obtained data were calculated as per the given equation 7:

$(W_0)\ 1/3 - (W_t)\ 1/3 = kt$ equation (7)

Where, "W_0"represents the initial quantity of DMS, "W_t" denotes the quantity of remaining DMS at time t, and "k" is a constant incorporating surface volume relation.

Stability study of the DE3 emulgel formulation

The stability of the DE3 emulgel formulation was assessed as per the international conference on harmonization guideline for 6 months. The optimized DE3 emulgel formulation was placed at an accelerated temperature of 40˚C±2˚C/75±5% RH. The drug content of the optimized DMS emulgel formulation was measured at an interval of 0 (beginning), 1, 2, 3, and 6 months Kumar and Verma.[47]

Statistical analysis

All results are presented as mean ± standard deviation (SD). The results were analysed using Duncan's multiple range test, wherein mean values were considered to be well seprated at p≤0.05.

RESULTS AND DISCUSSION

Determination of globule size, extrudability, and pH

The average globule size of the DMS emulgel formulation (DE) was found to bein the range of 10.17-14.60 µm. The extrudability of DMS emulgel formulation correlated with the concentration of emollient. Among different formulations, DE3 and DE2 showed good extrudability. In fact, the extrudatbility of DE3 was recorded to be higher than that of other formulations, which was attributed toa higher concentration of emollient in DE3. To determine the pH of DMS emulgel formulations, a calibrated pH meter (Mettler-Toledo India Pvt. Ltd., Mumbai, India) was used. An ideal topical formulation must be compatible with the skin. Measurements for globule size, extrudability, and pH value were performed in triplicates and expressed as mean ± SD (Table 2).

Determination of the drug content informulated batches of emulgel formulations

The percentage of the drug present in the prepared emulgel formulations was measured in terms of absorbance at 242 nm using a UV spectrophotometer (Shimadzu 1700, Shimadzu analytical Pvt. Ltd., Mumbai). The percentage of DMS in the DE2 and DE3 emulgel formulations were recorded to be 92.30±0.21% and 94.06±0.29%, respectively. Importantly, these drug percentages lied within the pharmacopoeia limits (Table 2). The drug content of the formulated batches are graphically presented in Figure 1.

Thus, based on these results, the DE2 and DE3 formulations were selected for further analysis.

In vitro release study of optimized DMS emulgel

An *in vitro* drug release study revealed that the DE3 emulgel formulation showed better drug release than DE2. The release

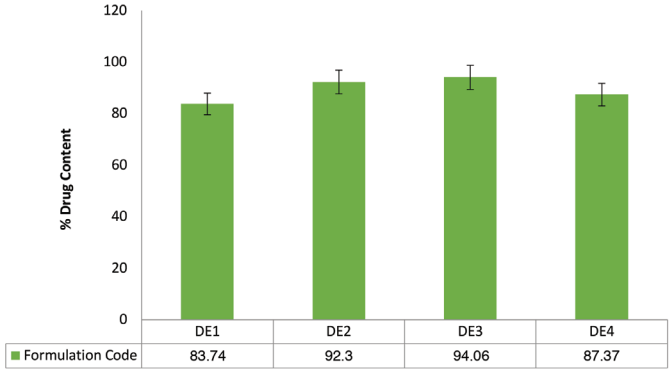

Figure 1. Drug content of the prepared emulgelformulations. DE3 displayed the highest drug content as compared with other formulations, but with non-significant differences (p<0.01)

DE: Different formulation

Table 2. Globule size, extrudability, pH, and drug contents of the developed emulgel formulation

S. no.	Formulation code	Globule size (µm) (n=50)	Extrudability (g/cm^2)	pH	Drug content (%) (n=3)
1	DE1	12.21±1.3	5.4±0.15	5.8	83.74±0.64
2	DE2	10.34±0.9	5.6±0.11	6.4	92.30±0.21
3	DE3	10.17±0.5	5.8±0.13	6.2	94.06±0.29
4	DE4	14.60±1.4	4.4±0.26	6.8	87.37±0.82

Average globule size, extrudability, pH, and drug contents of various formulation codes. The globule size results are presented as mean ± SD (n=50).The extrudability results are presented as mean ± SD (n=3). The recorded pH of all emulgel formulations of DMS was in acceptable range, which is important to avoid the risk of skin irritation. The determination of drug content is important to determine topical dosage form performance. The results are presented as mean ± SD (n=3). DE: Different formulation, DMS: Desoximetasone, SD: Standard deviation

of DMS from emulgel was found to be dependent on the concentrations of *aloe vera* and propylene glycol that were used as gel base and penetration enhancer, respectively. For the DE3 formulation, DMS release of 87.84±2.5% was recorded in 7 h. Thus, the DE3 formulation was selected as an optimized formulation and further used for *in vitro* DMS permeation study. The results for cumulative % DMS released measured using a cellophane membrane are reported in Supplement 1 and graphically presented in Figure 2.

In vitro permeation study usingthe Franz diffusion cell

The DE3 emulgel formulation exhibited higher DMS permeation than the DE2 formulation. For DE3, the drug permeation was found to be 95.40±1.6%, which was consistent over a period of 7 hr. Thus, DE3 was selected as an optimized emulgel formulation for the evaluation of firmness, cohesiveness, consistency, and viscosity. The results of *in vitro* permeation study are summarized in Supplement 2 and graphically presented in Figure 3.

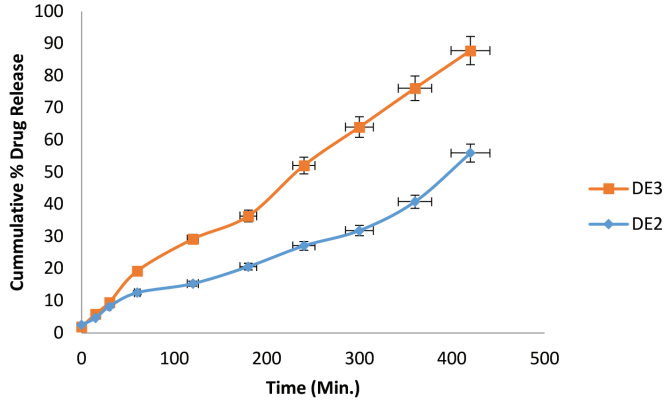

Figure 2. *In vitro* cumulative % drug release evaluated using a modified dissolution assembly. DE3 showed better drug release than DE2. Values are represented as mean ± SD (n=3)

DE: Different formulation, SD: Standard deviation

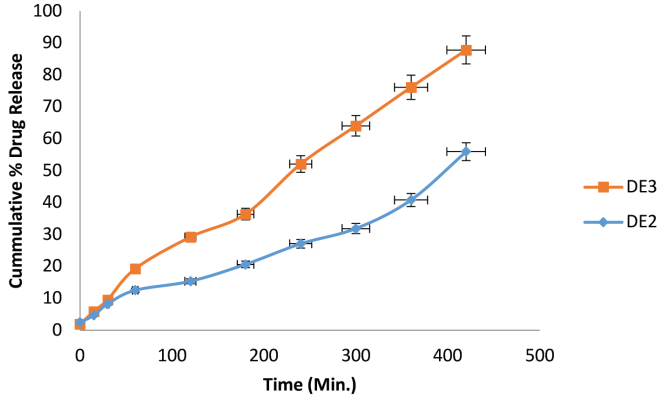

Figure 3. *In vitro* permeation study using a Franz diffusion cell

The permeation rate of DMS for DE3 and DE2 emulgel formulations was assessed using the Franzdiffusion cell. Phosphate buffer (pH 7.4) was selected as a drug diffusion medium. A cellophane membrane was used for permeation study at a temperature of 37°C±0.5°C. The data are presented as mean ± SD (n=3)

DE: Different formulation, DMS: Desoximetasone, SD: Standard deviation

Evaluation of the consistency, cohesiveness, viscosity, and firmness of the optimized emulgel formulation

The consistency, cohesiveness, viscosity, and firmness of the optimized DMS emulgel formulations (DE3 and DE2) were measured using a texture analyzer. The DE3 emulgel formulation was found to be firmer, cohesive, and displayed superior consistency than DE2. For firmness, the maximum positive force was recorded to be 67.604 g. The maximum negative area representing cohesiveness of DMS emulgel was found to be -49.480 g, and the consistency value of DMS emulgel, measured in terms of mean positive area of curve, was recorded to be 591.697 g.sec. The mean area for negative index of viscosity was found to be 450.153 g.sec. The DE3 emulgel formulation displayed superior consistency than the DE2 formulation,as measured using a texture analyzer. All these results are summarized in Table 3 and graphically presented in Figure 4, 5.

Determination of spreadability

The spreadability of the optimized emulgel formulations of DMS (DE3 and DE2) was measured, wherein DE3 was found to be firmer and displayed optimal spreadability, which was superior than that exhibited by DE2. For DE3, a very high value of mean maximum force of 833.37 g was recorded, which represented "firmness", and mean area, representing "work of shear", was observed to be 324.230 g.sec. These results are summarized in Table 4. Graphs of spreadability for the optimized formulations of DMS emulgel are shown in Figure 6, 7.

In vitro release kinetics model for the optimized emulgel formulation

The best model for studying the release kinetics of the optimized emulgel formulation was determined as per the regression data. The zero-order model showed a regression value of 0.996 (Figure 8A). The regression value for first-order model was recorded to be 0.926 (Figure 8B), whereas the Higuchi kinetic model showed a regression value of 0.941 (Figure 8C). The Korsmeyer-Pappas model and Hixon-Crowell model displayed regression values of 0.972 (Figure 8D) and 0.967 (Figure 8E), respectively. For the aforementioned models, regression values were recorded to be <1. Intial release data of 60% of DMS fitted into Korsmeyer-Peppas model, indicating that the release mechanism obeyed the Korsmeyer-Peppas model and confirmed that the release of DMS followed a diffusion mechanism. Release data for DMS emulgel are summarized in Supplement 3.

Stability study ofthe emulgel formulation

The stability data indicated that the emulgel formulation was stable for 6 months. The stability results are summarized in Table 5.

Study limitations

The DMS emulgel formulation showed a higher rate of drug release than that showed by traditional DMS ointment and DMS cream. Despite several benefits of the emulgel, the delivery of water-insoluble drugs poses a great challenge. Thus, the aim of this study was to prepare a DMS emulgel using a conventional

method. The present study aimed to formulate a DMS emulgel using *aloe vera*, which is considered to be safe to use, non sensitive, and non irritant, and displays good spreadability and penetrability across the skin. An emulgel is used to deliver DMS deep into the skin in a better manner. In this way the study limitation further relates to methods for making and using such compositions.

CONCLUSION

In the present study, an aloe vera-based topical emulgel of DMS was optimized, formulated, and characterized as an attractive alternative for the local delivery of DMS into the skin. The developed formulation presented an attractive option for better patient compliance, long contact timeat the target site, and ease of use. Among the different formulations, the DE3 formulation

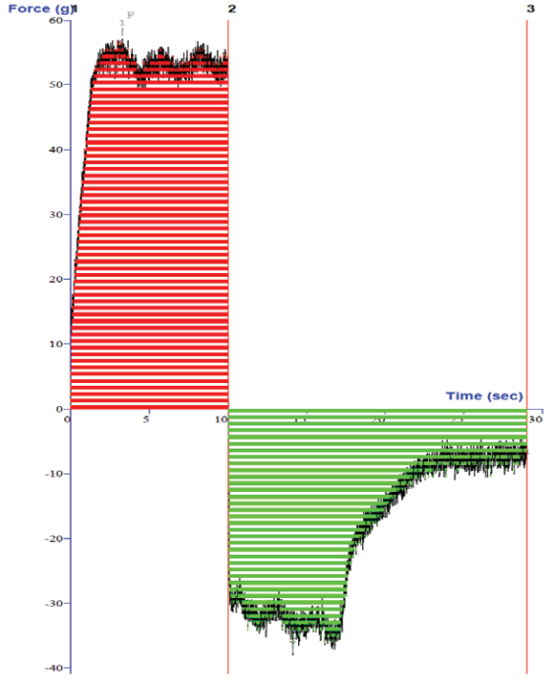

Figure 4. Consistency graph ofa DMS emulgel formulation (formulation code DE3)

DE: Different formulation, DMS: Desoximetasone

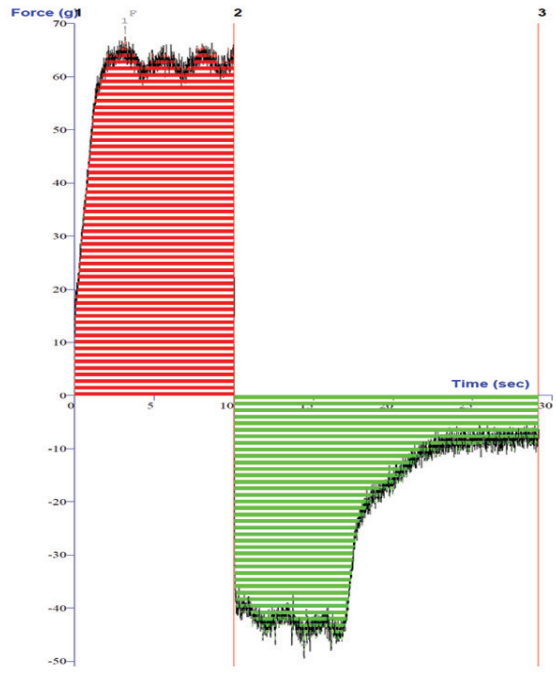

Figure 5. Consistency graph ofan optimized DMS emulgel formulation (formulation code DE2)

DE: Different formulation, DMS: Desoximetasone

Table 3. Results of consistency study ofoptimized emulgel formulations of DMS

S. no.	Formulation code	Mean maximum positive force "firmness" (g)	Mean positive area "consistency" (g.sec)	Mean maximum negative force "cohesiveness" (g)	Mean negative area "index of viscosity" (g.sec)
1	DE2	57.152	504.173	-38.027	-364.294
2	DE3	67.604	591.697	-49.480	-450.153

DMS: Desoximetasone

Table 4. Results of spreadability study ofoptimized emulgel formulations of DMS

S. no.	Formulation code	Mean max force "firmness" (g)	Mean area "work of shear" (g.sec)
1	DE2	734.522	276.821
2	DE3	833.37	324.230

DMS: Desoximetasone, DE: Different formulation, max: Maximum

Table 5. Preliminary results ofstability study ofthe emulgel formulation of DMS (formulation code DE3) (n=3)

Storage condition	Assay (%)				
	0 day	First month	Second month	Third month	Sixth month
40±2°C/75±5% RH	98.86±0.57	97.68±0.37	96.74±1.3	96.03±0.04	94.73±0.5

DMS: Desoximetasone, DE: Different formulation, RH: Relative humidity

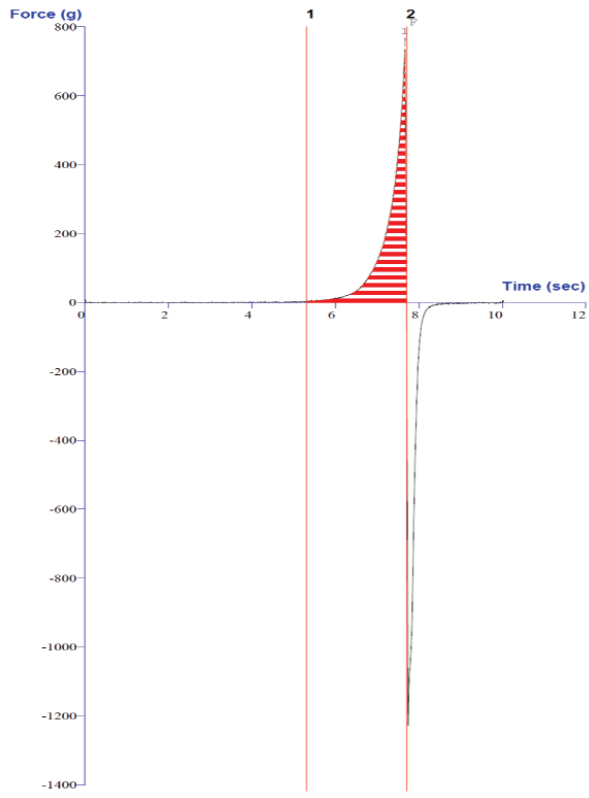

Figure 6. Spreadability graph ofan optimized DMS emulgel formulation (formulation code DE2)

DE: Different formulation, DMS: Desoximetasone

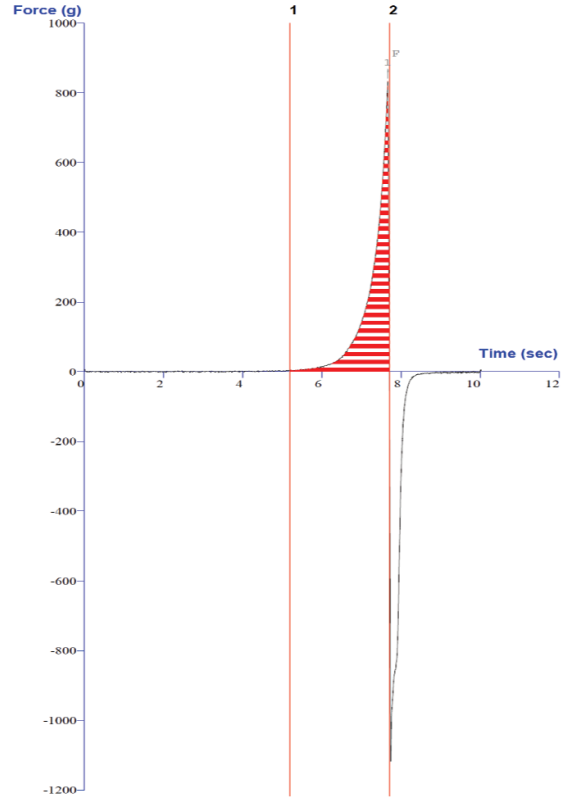

Figure 7. Spreadability graphof an optimized DMS emulgel formulation (formulation code DE3)

DE: Different formulation, DMS: Desoximetasone

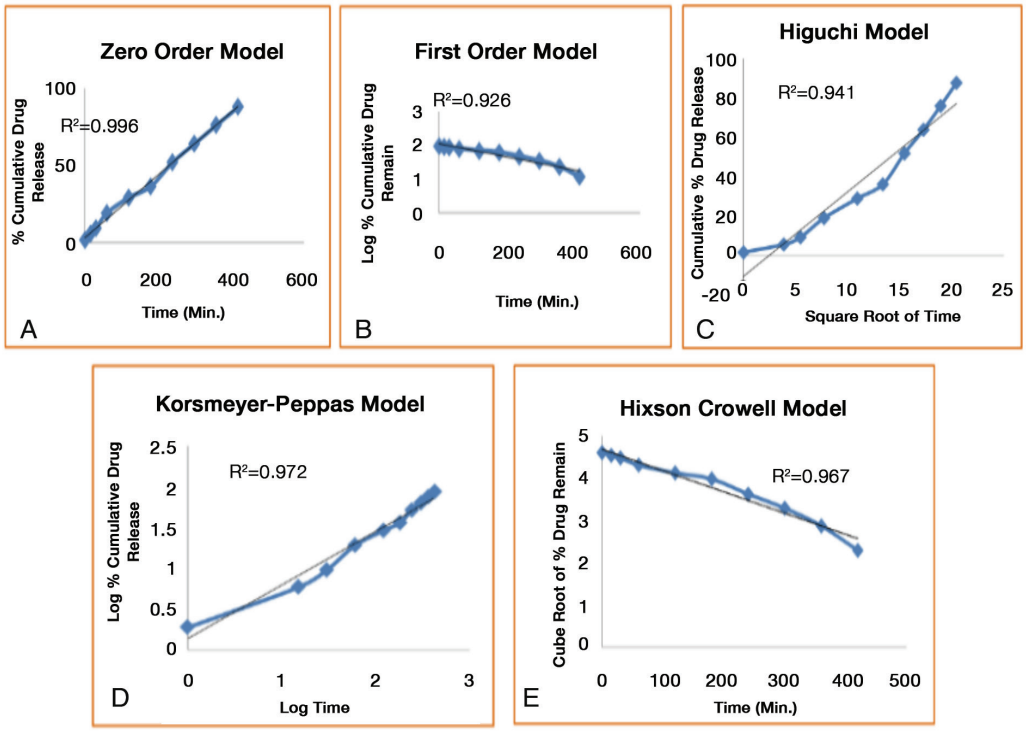

Figure 8. *In vitro* release kinetics model. A) Zero-order model, B) first-order model, C) Higuchi, D) Korsmeyer-Peppas model, and E) Hixson-Crowell model. For *in vitro* release study, a modified dissolution assembly was employed. Values are represented as mean ± SD (n=3)

SD: Standard deviation

was found to adhere to biological membrane for an extended period of time and provided an optimum drug release for the effective treatment of plaque psoriasis. The DE3 formulation displayed a better contact time than traditional formulations, including ointmentand cream. These results highlighted the suitability of an aloe vera-based emulgel formulation of DMS to overcome the skin barriers for the effective treatment of plaque psoriasis. However, *in vivo* and clinical studies are further required to validate its suitability for commercial development.

ACKNOWLEDGMENTS

Author Umesh Atneriya is grateful to the Dr. Vimukta Sharma for carrying out the research at BM College of Pharmaceutical Education and Research, Indore (Madhya Pradesh) India.

Conflict of interest: No conflict of interest was declared by the authors. The authors are solely responsible for the content and writing of this paper.

REFERENCES

1. Stark HJ, Boehnke K, Mirancea N, Willhauck MJ, Pavesio A, Fusenig NE, Boukamp P. Epidermal homeostasis in long-term scaffold-enforced skin equivalents. J Investig Dermatol Symp Proc. 2006;11:93-105.
2. Grubauer G, Feingold KR, Elias PM. Relationship of epidermal lipogenesis to cutaneous barrier function. J Lipid Res. 1987;28:746-752.
3. Kuchekar BA, Pujari RR, Kuchekar SB, Dhole SN, Mule PM. Psoriasis a comprehensive. Int J Pharm Life Sci. 2011;2:857-877.
4. Laws PM, Young HS. Topical treatment of psoriasis. Expert Opin Pharmacother. 2010;11:1999-2009.
5. Imran KT, Gore S, Giradkar P. A review advances in topical drug delivery system. Int J Pharm Res Allied Sci. 2011:1:14-23.
6. Kumar V, Mahant S, Rao R, Nanda S. Emulgel based topical delivery system for loratadine. ADMET DMPK. 2015;2:254-271.
7. Khunt DM, Mishra AD, Shah DR. Formulation design & development of piroxicam emulgel. Int J PharmTech Res. 2012;4:1332-1344.
8. Susmitha A, Gudas GK. Formulation and evalaution of chlorzoxazone transdermal emulgel by using natural penetration enhancer. Int J Phar Anal Res. 2019;8:38-44.
9. Berdey II, Voyt OI. Rheological properties of emulgel formulations based on different gelling agent. The Pharma Innovation. 2016;5:76-79.
10. Kumari A, Singh A, Saurabh SS, Rathore KS, Issarani R. Formulation and evaluation of lycopene emulgel. Indo Am J Pharm Sci. 2015;2:1013-1027.
11. Khullar, R, Kumar D, Seth N, Saini S. Formulation and evaluation of mefenamic acid emulgel for topical delivery. Saudi Pharm J. 2012;20:63-67.
12. Vyas SP, Khar RK. Controlled drug delivery: Concepts and advances Vallabh Prakashan; pp. 2002;418-422.
13. Singla V, Saini S, Joshi B, Rana AC. Emulgel: a new platform for topical drug delivery. Int J Pharm Bio Sci. 2012;3:485-498.
14. Thanushree HR, Kumar GBK, Acharya A. Formulation development of diclofenac sodium emulgel using aloe vera gel for transdermal drug delivery system. Int J Pharm Sci Technol. 2017;10:3858-3865.
15. Prajapati MN. Emulgels: A novel approach to topical drug delivery. Int J Univ Pharm Biosci 2013;2134-2148.
16. Kasliwal N, Derele D, Negi J, Gohil K. Effect of permeation enhancer an the release and pharmacokinetics of meloxicam gel formulation through rat skin. Asian J Pharm Sci. 2008;3:193-199.
17. Panwar AS, Upadhyay N, Bairagi M, Gujar S, Darwhekar GN, Jain DK. Emulgel: A review. Asian J Pharm Life Sci. 2011;1:333-343.
18. Raju YP, Haritha K, Satyanarayana RP, Vandana KR, Bindu DT, Vinesha V, Chowdary VH. Formulation and characterization of aceclofenac -aloe vera transemulgel. Curr Drug Deliv. 2015;12:703-708.
19. Joshi V, Singh G, Rana AC, Saini S. Development and characterization of clarithromycin emulgel for topical delivery. Int J Drug Dev Res. 2012;4:310-323.
20. Yapar EA, Ynal O, Erdal MS. Design and in vivo evaluation of emulgel formulations including green tea extract and rose oil. Acta Pharm. 2013;63:531-544.
21. Patel CJ, Tyagi S, Gupta AK, Sharma P, Prajapati PM, Potdar MB. Emulgel: a combination of emulsion and gel. J Drug Discov Ther. 2013;1;72-76.
22. Sah S, Badola A, Nayak VK. Emulgel: magnifying the application of topical drug delivery. Indian J Pharm Biol Res. 2018;5:25-33.
23. Roy CS, Singh DH, Gupta R, Masih D. A review on pharmaceutical gel. Int J Pharm Res Biosci. 2012;1:21-36.
24. Shivhare DU, Jain BK, Mathur BV, Bhusari PK, Roy AA. Formulation development and evaluation of diclofenac sodium gel water soluble polyacrylamide polymer. Dig J Nanomater Biostrectures. 2009;4:285-290.
25. Bharadwaj S, Gupta GD, Sharma VK. Topical Gel: A Novel approach for drug delivery. J Chem Bio Phy Sci Sec. 2012;2:856-867.
26. Bhanja S, Kumar PK, Sudhakar M, Das AK. A Research Formulation and Evaluation of Diclofenac Transdermal Gel. J Adv Pharm Educ Res. 2013;3:248-259.
27. Baviskar DT, Biranwar YK, Bare KR, Parik VB, Sapte MK, Jain DK. A research, *in vitro* and *in vivo* evaluation of diclofenac sodium gel prepared with cellulose ether and carbopol 934P. Tropical J Pharm Res. 2013;12:489-494.
28. Tambe R, Kulkarni M, Joice A, Gilani I. Formulation and evaluation of aloe vera gel. J Pharm Res. 2009;2:1588-1590.
29. Patwardhan N, De A, Kulkarni KR, Dey A, Jain R. Desoximetasone 0.25% cream and ointment - an updated review of its pharmacological properties and therapeutic efficacy in the treatment of steroid responsive dermatoses. Int J Health Sci Res. 2017;7:290-298.
30. Pakhare AV, Deshmane SV, Deshmane SS, Biyani KR. Development of emulgel. Asian J Pharm. 2017;11:S712-S716.
31. Martin A. 1994 physical pharmacy. (50th ed). New Delhi: Wolters Kluwer; 469-491.
32. Premjeet S, Bilandi A, Kumar S, Kapoor B, Katariya S, Rathore D, Bhardwaj S. Review article additives in topical dosase forms. Int J Pharm Chem Biol Sci. 2012;2:78-96.
33. Khullar R, Saini S, Seth N, Rana AC. Emulgel: a surrogate approach for topical used hydrophobic drugs. Int J Pharm Biol Sci. 2011;1:117-128.
34. Vijaya PB, Shanmugam V, Lakshmi PK. Development and optimization of novel diclofenec emulgel for topical drug delivery. Int J Comprehens Pham. 2011;9:1-4.
35. Moghbel A, Faghiri A. Influence of dimethyl sulfoxide as a penetration enhancer of piroxicam gel through biological skin. Iran J Pharm Sci. 2006;2:177-184.

36. Kumar AJ, Pullaknandam N, Prabu SL, Gopal V. Transdermal drug delivery system: an overview. Int J Pharm Sci Rev Res. 2010;3:49-54.
37. Vladimirov S, Čudina O, Danica A, Jovanović M, Stakic D. Spectrophotometric determination of desoximetasone in ointment using 1,4-dihydrazinophthalazine. J Pharm Biomed Anal. 1996;14:947-950.
38. Bazigha KAR, Eman FAG, Sahar AF, Heyam SS, Khan SA. Development and evaluation of ibuprofen transdermal gel formulations. Topical J Pharm Res. 2010;9:355-363.
39. Navya M, Yadav HKS, Kumar HS, Tashi CK, Kumar NS. Design and evaluation of a lyophillized liposomal gel of an anti viral drug for intravaginal delivery. J Appl Polym Sci. 2014;131:1-4.
40. Nayak AK, Mohanty B, Sen KK. A Review Comparative Evaluation of *in vitro* diclofenac sodium permeability across excised mouse skin from different common pharmaceutical vehicles. International Journal of PharmTech Research. 2010;2:920-930.
41. Gupta R, Gupta GD. A review formulation development and evaluation of ant- inflammatory potential of cordial obliqua topical gel on animal model. Pharmacognj. 2017;9:93-98.
42. Dhawan S, Medhi B, Chopra S. Formulation and evaluation of diltiazim hydrochloride gels for the treatment of anal fissures. Sci Pharm. 2010;77:465-482.
43. Shah VK, Desai TR. Formulation and evaluation of wheatgrass topical gel. Pharma Science Monitor. 2012;3:3010-3015.
44. Swamy NGN, Mazhar P, Zaheer A. Formulation and evaluation of diclofenac sodium gels using sodium carboxy methyl hydroxy propyl guar and hydroxy methyl propyl methyl cellulose. Indian J Pharm Educ Res. 2010;44:310-314.
45. Gupta GD, Gaud RS. Release Rate of Tenoxicam From Acrypol Gels. Ind Pharm. 2005:69-76.
46. Wesley Z, Gude R. Formulation, design, development and evaluation of emulgel for topical delivery of meloxicam in the treatment of rheumatoid arthritis. Indo Am J Pharm Res. 2015;5:1271-1276.
47. Kumar L, Verma R. Chemical stability studies of bioadhesive topical gel. Int J Pharm Pharm Sci. 2011;3:101-104.

Supplement 1. *In vitro* drug release from optimized emulgel formulations of DMS

Time (min)	Cumulative percentage drug release	
	Formulation code	
	DE2	DE3
0	2.496±0.010	1.89±0.5
15	4.68±0.1	5.906±2.1
30	8.237±0.5	9.545±4.8
60	12.532±1.8	19.27±6.3
120	15.347±3.6	29.21±8.1
180	20.647±4.8	36.40±5.8
240	27.094±6.2	52.09±6.7
300	31.866±0.7	64.06±1.1
360	40.82±1.3	76.13±0.7
420	55.96±4.0	87.84±2.5

For *in vitro* drug release of emulgel formulations containing DMS, dissolution of DE2 and DE3 formulations was performed using amodified dissolution assembly at a temperature of 32˚C±0.5˚C. Phosphate buffer (pH 7.4) was used as a release medium. The results are presented as mean ± SD (n=3). DE: Different formulation, DMS: Desoximetasone, SD: Standard deviation

Supplement 2. *In vitro* drug permeation of emulgel formulations of DMS

Time (min)	Cumulative percentage drug release	
	Formulation code	
	DE2	DE3
0	0	0
15	4.68±0.4	8.90±0.9
30	8.23±0.8	16.54±1.3
60	12.53±1.1	32.27±1.1
120	15.34±1.6	46.21±1.6
180	20.64±1.4	58.40±0.9
240	27.09±1.7	64.06±1.4
300	31.86±0.9	76.62±0.8
360	40.82±1.8	88.29±0.7
420	55.96±0.3	95.40±1.6

Values are represented as mean ± SD (n=3). DE: Different formulation, DMS: Desoximetasone, SD: Standard deviation

Supplement 3. Percentage drug release valuescalculated using different kinetic models. Data was fitted in zero-order model, first-order model, Higuchi matrix, and Hixon-Crowell model

Time (min)	√t	Log time	Cumulative % drug release	Log of cumulative % drug released	Cumulative % drug remaining	Cube root of % drug remaining	Log of cumulative % drug remaining
0	0	0	1.89	0.276	98.11	4.612	1.991
15	3.872	1.176	5.906	0.771	94.09	4.548	1.973
30	5.477	1.477	9.545	0.979	90.45	4.488	1.956
60	7.745	1.778	19.27	1.284	80.73	4.321	1.907
120	10.95	2.079	29.21	1.465	70.79	4.136	1.849
180	13.41	2.255	36.40	1.561	63.60	3.991	1.803
240	15.49	2.380	52.09	1.716	47.91	3.631	1.680
300	17.32	2.477	64.06	1.806	35.94	3.300	1.555
360	18.97	2.556	76.13	1.881	23.87	2.879	1.377
420	20.49	2.623	87.84	1.943	12.16	2.299	1.084

The best model for release pattern of DMS was determined as per the regression data. For release study, a modified dissolution assembly was employed. Values are presented as mean ± SD (n=3). DMS: Desoximetasone, SD: Standard deviation

Turk J Pharm Sci 2021;18(4):476-482
DOI: 10.4274/tjps.galenos.2020.42966

ORIGINAL ARTICLE

Physicochemical Evaluation and Antibacterial Activity of *Massularia acuminata* Herbal Toothpaste

Massularia acuminata Herbal Diş Macununun Antibakteriyel Aktivitesi ve Fizikokimyasal Değerlendirmesi

Olutayo Ademola ADELEYE[1]*, Oluyemisi BAMIRO[1], Mark AKPOTU[2], Modupe ADEBOWALE[3], John DAODU[4], Mariam Adeola SODEINDE[3]

[1]Federal University Oye-Ekiti, Department of Pharmaceutics and Pharmaceutical Technology, Ekiti State, Nigeria
[2]Olabisi Onabanjo University, Department of Pharmaceutical Microbiology, Ago Iwoye, Nigeria
[3]Olabisi Onabanjo University, Department of Pharmacognosy, Ago Iwoye, Nigeria
[4]Olabisi Onabanjo University, Department of Pharmaceutical Chemistry, Ago Iwoye, Nigeria

ABSTRACT

Objectives: Oral hygiene, an integral part of the body's general well-being, should be maintained to prevent dental problems. This study was conducted to incorporate the ethanol extract of *Massularia acuminata* twigs in a formulation of herbal toothpaste and evaluate its antibacterial activity compared with a commercially available herbal toothpaste against two dental pathogens, namely, *Staphylococcus aureus* and *Streptococcus mutans*.

Materials and Methods: The content of dried *M. acuminata* twig was extracted using ethanol and used in the formulation of toothpaste containing 1%, 2%, 3%, 4%, and 5% *M. acuminata* extract. The sensory and physicochemical properties of the toothpaste were evaluated. The agar well diffusion method was used to evaluate the antibacterial susceptibility of the toothpaste against *S. aureus* and *S. mutans*. Data were analyzed using One-Way analysis of variance and Student's t-test.

Results: All toothpastes were smooth and sweet and smelled pleasant. They all had good retention ability on the bristles of toothbrush and had a pH range of 7.18-7.83. The toothpastes of the extracts of different concentration demonstrated antibacterial activities against the test organisms. The antibacterial activity of the formulated toothpastes increased significantly with an increase in the extract concentration. F5 that contained 5% extract showed the highest activity, with an inhibition zone of 19.30±0.17 mm and 12.60±0.52 mm against *S. aureus* and *S. mutans*, respectively, even when compared with the commercially available herbal toothpaste.

Conclusion: The incorporation of the *M. acuminata* extract in the formulation of herbal toothpaste prevented the growth of *S. aureus* and *S. mutans*. Incorporating this extract in toothpaste formulation will satisfactorily maintain oral hygiene, which is desirable to prevent dental caries and periodontal diseases.

Key words: Toothpaste, *Staphylococcus aureus*, *Streptococcus mutans*, dental caries, antibacterial

ÖZ

Amaç: Vücudun genel iyilik halinin bir bileşeni olan oral hijyenin dental sorunları önlemek için idamesi sağlanmalıdır. Bu çalışma *Massularia acuminata* dallarının etanol ekstresinin bir bitkisel diş macunu formülasyonuna dahil etmek ve iki dental patojen olan *Staphylococcus aureus* and *Streptococcus mutans*'a karşı antibakteriyel aktivetisini ticari olarak var olan bir diş macunuyla karşılaştırarak değerlendirmek için yapılmıştır.

Gereç ve Yöntemler: Kurutulmuş *M. acuminata* dalının içeriği etanol kullanılarak ekstre edilmiştir ve %1, %2, %3, %4 ve %5 *M. acuminata* ekstresi içeren diş macunu formülasyonlarında kullanılmıştır. Diş macununun duyusal ve fizikokimyasal özellikleri değerlendirilmiştir. Diş macununun *S. aureus* ve *S. mutans*'a karşı antibakteriyel duyarlılığını değerlendirmek için agar kuyusu difüzyon yöntemi kullanılmıştır. Veriler One-Way analizi ve Student t-testi kullanılarak analiz edilmiştir.

Bulgular: Tüm diş macunları pürüzsüz ve tatlıydı ve hoş kokuyordu. Hepsinin diş fırçası kılları üzerinde iyi bir tutma kabiliyeti vardı ve pH aralığı 7,18-7,83 idi. Farklı konsantrasyondaki ekstraktların diş macunları, test organizmalarına karşı antibakteriyel aktivite göstermiştir. Formüle edilmiş diş macunlarının antibakteriyel aktivitesi, ekstrakt konsantrasyonundaki artışla önemli ölçüde artmıştır. %5 ekstrakt içeren F5, ticari olarak satılan bitkisel diş macunu ile karşılaştırıldığında bile, sırasıyla *S. aureus* ve *S. mutans*'a karşı 19,30±0,17 mm ve 12,60±0,52 mm'lik bir inhibisyon bölgesi ile en yüksek aktiviteyi göstermiştir.

***Correspondence:** olutayoadeleye@yahoo.com, **Phone:** +234 8056112885, **ORCID-ID:** orcid.org/0000-0001-8716-4064

Received: 09.06.2020, **Accepted:** 28.10.2020

Sonuç: *M. acuminata* özütünün bitkisel diş macunu formülasyonuna katılması *S. aureus* ve *S. mutans*'ın büyümesini engellemiştir. Bu ekstreyi diş macunu formülasyonuna dahil etmek, diş çürüklerini ve periodontal hastalıkları önlemek için arzu edilen ağız hijyenini tatmin edici bir şekilde koruyacaktır.

Anahtar kelimeler: Diş macunu, *Staphylococcus aureus*, *Streptococcus mutans*, diş çürüğü, antibakteriyel

INTRODUCTION

Oral hygiene is an integral part of the body's general well-being, which begins with clean teeth. The cleaning of one's teeth is a cultural habit that is followed from generation to generation and is usually performed as a daily morning routine. It is regarded as an indispensable component of oral health.[1] Different populations employ various techniques when cleaning the teeth. Modern conventional techniques involve the use of toothpaste and toothbrush, which have been in use for decades,[2,3] whereas traditional techniques primarily involve the use of chewing sticks and local toothpaste.[4] Other traditional methods of teeth cleaning involve the use of one's finger to rub various substances, including natural powders, bark of plants, ash, charcoal, oil, and salt, onto the teeth[5,6] (Josefine Hirschfeld, not all cultures use toothbrushes. But how effective are alternative methods? The Conversation 7 July 2019).

Poor oral hygiene could lead to dental caries and periodontal diseases. Dental caries, commonly known as tooth decay, is an infectious disease caused primarily by *Streptococcus mutans*.[7,8] Periodontal disease, also known as gum disease, is an inflammatory condition of the gum (known as gingivitis) or the bone and tissues of the teeth (known as periodontitis).[9] Bacteria that cause periodontal diseases include *Aggregatibacter actinomycetemcomitans*, *S. mutans*, *Bacteroides forsythus, Staphylococcus intermedius*, *Lactobacillus acidophilus*, *Porphyromonas gingivalis*, *Prevotella nigrescens*, and *Treponema denticola*.[10,11]

Chewing sticks, a traditional method of cleaning the teeth to maintain oral hygiene, has been practiced for thousands of years and is still being widely used in Africa, Asia, and the Middle East.[12,13] Some studies have reported that the effectiveness of chewing stick lies in the presence of antibacterial bioactive compounds in these sticks that help remove dental plaque, thereby preventing dental caries and periodontal diseases.[14,15] Some of the chewing sticks that have been investigated include *Terminalia glaucescens*, *Sorindeia warneckei*, *Vitex doniana*, *Vernonia amygdalina*, *Fagara zanthoxyloides*, *Xanthoxylum zanthoxyloides*, *Massularia acuminata*, *Pseudocedrela kotschyi*, *Anogeissus schimperi*, *Anogeissus leiocarpus*, and *Azadirachta indica*.[16-18]

M. acuminata (G. Don) Bullock ex Hoyle is a shrub (Figure 1) that belongs to the family Rubiaceae and is widely distributed in West Africa. It is commonly known as the chewing stick tree. Its root, leaf, bark, and twig have several medicinal values, and it is used traditionally in some West African regions for treating diarrhea, dysentery, muscular pains, and venereal diseases and as an aphrodisiac.[19] Pharmacological studies have shown the plant to possess a strong antibacterial property against oral pathogens.[20-22]

Figure 1. *Massularia acuminata* plant

The present study was conducted to incorporate the extract of *M. acuminata* in a formulation of herbal toothpaste and evaluate its antibacterial activity against two pathogens associated with dental caries and periodontal diseases.

MATERIALS AND METHODS

Plant collection

M. acuminata twigs were collected from Onigambari Forest, Ibadan, Oyo State, in the month of February 2019 and authenticated at the Forestry Research Institute of Nigeria, Ibadan, Oyo State, Ogun State, by Mr. Odewo (Voucher no. FHI. 112857).

Test organisms

The clinical isolates of *Staphylococcus aureus* and *S. mutans* were obtained from the Microbiology Laboratory of Olabisi Onabanjo University Teaching Hospital, Sagamu, Ogun State, and used for antibacterial study.

Extract preparation

Twigs were cut into pieces and air dried for 30 days. The dried twig pieces were then ground into powder. Approximately 150 g of the powdered sample was macerated in 750 mL 95% ethanol (BHD Chemicals, Poole, England) for 72 h at room temperature with intermittent agitation, as per the protocol described by Tedwins et al.[21] Thereafter, the sample was filtered through Whatman's filter paper. The filtrate was concentrated to a dry powder using a rotary evaporator and stored in a refrigerator prior to use.

Phytochemical screening

Phytochemical screening of the extract was performed to determine the bioactive compounds present in the extract, as per the procedure described by Trease and Evans.[23]

Antibacterial screening

The antibacterial activity of 100 mg/mL *M. acuminata* extract in distilled water was determined by the agar diffusion method. A suspension of an overnight culture of *S. aureus* and *S. mutans* in nutrient broth was standardized to 0.5 McFarland standards (10^6 colony forming units mL^{-1}). Nutrient agar plates were prepared in a Petri dish by inoculating with 0.2 mL of the standardized culture of the test organisms and allowed to settle. Wells of 6.0 mm were bored in nutrient agar, and each well was filled with 0.5 mL of the extracts; the positive control was gentamicin and the negative control was distilled water. The plates were allowed to stand for 30 min for the proper diffusion of the extract before incubating at 37˚C for 24 h. The diameters of the zones of growth inhibition were then measured in millimeters. The experiments were performed in triplicate.

Preparation of M. acuminata extract herbal toothpaste

The quantity of the ingredients required to prepare 100 g toothpaste is shown in Table 1. To prepare a paste, tragacanth gum was mixed with about 10 mL of distilled water in a mortar and pestle. Glycerin was added and triturated vigorously, followed by the slow addition of calcium carbonate with continuous trituration. *M. acuminata* extract was then added to the content in the mortar and thoroughly mixed for even distribution. Sodium lauryl sulfate (SLS) was added with slow stirring to prevent foaming. Saccharine and peppermint oil were added, and the paste was then adjusted to the required weight by adding distilled water.

Evaluation of M. acuminata extract herbal toothpaste

Determination of organoleptic properties

The color, appearance, texture, odor, and taste of each formulation were determined by sensory and physical evaluations.

Determination of pH

In this step, 1 g of each toothpaste formulation was dispersed in 10 mL of purified water (pH 6.98), and the pH was measured in triplicate with a digital pH meter (pH 600, Milwaukee).[24]

Table 1. Composition of toothpaste formulation (100 g)

Ingredients (g)	F0	F1	F2	F3	F4	F5
Massularia acuminata	0.0	1.0	2.0	3.0	4.0	5.0
Calcium carbonate	20.0	0.0	20.0	20.0	20.0	20.0
Sodium lauryl sulfate	1.5	1.5	1.5	1.5	1.5	1.5
Glycerin	30.0	30.0	30.0	30.0	30.0	30.0
Tragacanth gum	1.2	1.2	1.2	1.2	1.2	1.2
Saccharine	0.5	0.5	0.5	0.5	0.5	0.5
Peppermint oil	1.0	1.0	1.0	1.0	1.0	1.0
Distilled water	45.8	44.8	43.8	42.8	41.8	40.8

Determination of foaming ability

Next, 5 g of toothpaste formulation was dispersed in 10 mL of water in a 100 mL glass beaker. The beaker was covered with a watch glass and allowed to stand for 30 min. The mixture was stirred with a glass rod to break up lumps and transferred into a 250 mL graduated measuring cylinder while ensuring that no foams >2 mL were formed. The beaker was rinsed with 5-6 mL of water into the measuring cylinder. The cylinder was filled with up to 50 mL of water, covered with a stopper, maintained at 30˚C, and shaken for about 20 seconds. The cylinder was then allowed to stand for 5 min. The volume of foam with water (V_1) and water only (V) was recorded.[25]

Foaming ability was calculated as V_1-V_2. The experiments were performed in triplicate.

Determination of moisture

The moisture content was determined by accurately weighing 5 g (W_0) each of the formulation into an evaporating dish of 6-8 cm in diameter and 2-4 cm in depth. The formulation was then dried in an oven at 105˚C±2˚C until the weight remained constant and was noted as W_1.[25]

Percentage loss by mass: $(W_0 - W_1 / W_0) \times 100\%$

The mean of three values obtained was calculated.

Determination of spreadability

In this process, 1 g of toothpaste was placed on a glass plate of 10x10 cm size and covered with another glass plate of the same size. A weight of 1 kg was placed on the top glass plate and allowed to stand for 10 min, after which it was removed. The diameter of the spread on the plate was measured, and the mean of three values was taken.[25]

Determination of viscosity

The viscosities of the formulations were measured at 20, 50, and 100 rpm at 25˚C using a Brookfield viscometer (Model DV-II+Pro, Brookfield Eng. Labs Inc., Middleboro, MA, USA) with spindle number 4.

Antibacterial screening of toothpastes

The antibacterial activities of a commercially available toothpaste and the formulated *M. acuminata* toothpaste in different concentrations were determined by the agar diffusion method. The method used for the screening of the *M. acuminata* extract against *S. aureus* and *S. mutans* was adopted.

Statistical analyses

Statistical analyses of the data were performed by Student's t-test and One-Way ANOVA using GraphPad Prism (version 5.01) software. P values <0.05 were considered significant.

RESULTS

The phytochemical constituents present in the ethanol extract of the *M. acuminata* twig (Table 2) included anthraquinones, saponins, flavonoids, alkaloids, tannins, and flavonoids.

The antibacterial activity of the ethanol extract of the *M. acuminata* twig (100 mg/mL) is presented in Table 3. The extract and positive control (gentamicin) demonstrated high antibacterial activities against *S. aureus* and *S. mutans*, whereas the negative control (distilled water) did not show any antibacterial activity.

The results of the sensory and physical evaluation as well as pH measurement of the formulated toothpaste without herbal extract (F0), formulated herbal toothpaste containing different concentrations of the *M. acuminata* twig extract (F1-F5), and the commercially available herbal toothpaste (F6) are presented in Table 4. F0 was off white in color, F1-F5 varied between light brown and brown, and F6 appeared green. All formulations had a pleasant odor and a sweet taste. They were all smooth in texture and paste-like in appearance. The moisture content of F0-F5 ranged from 24.22% to 28.25%, whereas that of F6 was 31.36%. The spreadability and foaming ability of all toothpastes ranged from 5.7 cm to 7.2 cm and from 51.0 cm to 63.0 cm, respectively. The pH of the toothpastes ranged from 7.18 to 7.83.

The viscosity of the toothpastes as measured by different spindle speeds at 25°C is shown in Figure 2. The results showed that viscosity significantly decreased as the spindle speed increased.

All toothpastes demonstrated high antibacterial activities against both *S. aureus* and *S. mutans*, except F0 and F1 (Table 5). F0 and F1 did not show any antibacterial activity against *S. mutans.*

Table 2. Phytochemical screening of extracts

Phytochemical	Result
Anthraquinones	+
Saponins	+
Flavonoids	+
Alkaloids	+
Tannins	+
Flavonoids	+

+: Present

Table 3. Antibacterial activity of extract

Test organisms	Zones of inhibition (mm)		
	Extract	Positive control	Negative control
Staphylococcus aureus	25.50±0.10	33.00±0.37	-
Streptococcus mutans	20.20±0.28	29.50±0.81	-

Mean ± standard deviation, n=3, extract, *Massularia acuminata* 100 mg/mL, positive control, gentamicin 80 mg/2 mL, negative control, distilled water. -: Absent

DISCUSSION

The phytochemical constituents of plants are secondary metabolites; these metabolites are bioactive components that possess pharmacological activity in plants. The phytochemical constituents of the ethanol extract of *M. acuminata* twig are anthraquinones, saponins, flavonoids, alkaloids, tannins, and flavonoids. This finding is similar to those of some previous studies.[20-22] Tannins, saponins, and flavonoids in herbs are bioactive compounds that have been reported to possess antibacterial activities.[26,27]

In this study, the test organisms employed were *S. aureus* and *S. mutans*, which are among the main organisms associated

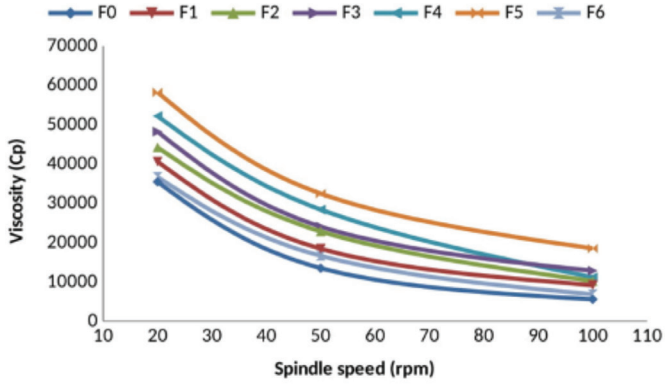

Figure 2. Viscosity of toothpaste formulations at 25°C

Table 4. Physical evaluation and pH of formulations

Parameters	F0	F1	F2	F3	F4	F5	F6
Color	Off white	Light brown	Light brown	Brown	Brown	Brown	Green
Appearance	Paste-like	Paste-like	Paste-like	Paste-like	Paste-like	Paste-like	Paste-like
Texture	Smooth	Smooth	Smooth	Smooth	Smooth	Smooth	Smooth
Odor	Pleasant	Pleasant	Pleasant	Pleasant	Pleasant	Pleasant	Pleasant
Taste	Sweet	Sweet	Sweet	Sweet	Slightly sweet	Slightly sweet	Sweet
Moisture content (%)	28.25±1.23	26.94±0.75	26.15±0.13	25.66±1.90	24.81±2.06	24.22±0.11	31.36±1.83
Spreadability (cm)	6.9±0.06	6.5±0.02	6.5±0.15	6.2±0.04	6.0±0.11	5.7±0.61	7.2±0.12
Foaming ability (cm)	51±0.22	55±0.20	56±0.06	60±0.13	62±0.10	63±0.24	58±0.22
pH	7.18±0.04	7.32±0.12	7.34±0.10	7.41±0.22	7.44±0.43	7.57±0.25	7.83±0.54

Mean ± standard deviation, n=3, F0: Formulated toothpaste without herbal extract, F1-F5: Formulated herbal toothpaste containing 1%, 2%, 3%, 4%, and 5% *Massularia acuminata* extract, respectively, F6: Commercially available herbal toothpaste

with dental caries and periodontal diseases, respectively.[11,28-32] The antibacterial activity of the ethanol extract demonstrated a strong activity against these organisms. This result corroborates with those of several other studies.[20-22] The ethanol extract demonstrated a significantly higher antibacterial activity against *S. aureus* than against *S. mutans*; however, the activity of the positive control (gentamicin) was significantly higher against the test organisms. The antibacterial activity of the extract could be attributed to the presence of bioactive components, including tannins, saponins, and flavonoids.

With respect to the sensory and physical evaluation of the toothpastes (Table 4), all were smooth, smelled pleasant, and tasted sweet but were of different colors. The pleasant odor and sweet taste can be attributed to the presence of flavoring agent (peppermint oil) and sweetener (saccharin), respectively, in all toothpastes, including the commercially available one. Despite the high concentration of *M. acuminata* extract in F4 and F5, the sweetener was able to mask the bitter taste of the extract. The formulated toothpaste without herbal extract (F0) was off white in color because it did not contain the herbal extract. Formulated herbal toothpaste (F1-F5) had colors varying from light brown to brown; the color intensity deepened with the increasing concentration of the extract. The commercially available herbal toothpaste (F6) was green. All these parameters may enhance the consumer acceptability of the product. F6 had the highest moisture content (28.25%); the moisture content was ranked in the following order: F6 > F0 > F1 > F2 > F3 > F4 > F5. This is reflected in the level of water content in the formulations, as shown in Table 1. This property could, in turn, affect the spreadability, foaming ability, and viscosity of the toothpaste. While the spreadability of the formulated toothpastes decreased with increased concentration of the extract (F0 > F1 > F2 > F3 > F4 > F5), foaming ability and viscosity increased (F0 < F1 < F2 < F3 < F4 < F5).

Viscosity is a factor that determines the spreadability, thickness, and ability of the toothpaste to retain its ribbon shape when extruded from the tube on the toothbrush.[33] Ribbon shape retention is defined as the ability of the toothpaste to retain its ribbon shape on the bristles of a toothbrush without collapsing.[34] All toothpastes had good retention ability. Spreadability measures the extent of the area that the toothpaste can spread, such as on the teeth, gum, gum lines, and other areas, and the extent of penetration into the infected tooth and gum. The spreadability of commercially available toothpaste was significantly higher than that of the formulated toothpastes. Foaming ability is the measure of the cleansing power of toothpastes, which is affected by the presence of surfactants (i.e., SLS). SLS produces foam that lowers the surface tension of the surface film on the tooth, thereby suspending and removing debris. Toothpaste with good foaming ability will provide a good cleansing action of the teeth. A significant difference was found in the foaming ability of the toothpastes, with F5 having the greatest cleansing action. The presence of the extract progressively increased the foaming ability of the formulated toothpastes. This may be because of the frothing properties of saponin present in the extract.[35]

Table 5. Antibacterial activity of toothpaste formulations

Test organisms	Zones of inhibition (mm)	
	Staphylococcus aureus	*Streptococcus mutans*
F0	3.10±0.23	-
F1	7.50±0.55	-
F2	11.00±0.61	6.70±0.40
F3	13.60±0.22	9.20±0.32
F4	17.70±0.19	10.60±0.20
F5	19.30±0.17	12.60±0.52
F6	11.50±0.42	7.80±0.72

Mean ± standard deviation, n=3, F0: Formulated toothpaste without herbal extract, F1-F5: Formulated herbal toothpaste containing 1%, 2%, 3%, 4%, and 5% *Massularia acuminata* extract, respectively, F6: Commercially available herbal toothpaste, -: Absent

The oral microbial flora when compromised, usually by reduction in pH due to the carbohydrate metabolism of the organisms, could cause dental caries, other periodontal diseases, and dental plaque.[31,36,37] Maintaining the microbial flora is desirable for the well-being of individuals; this can be achieved by proper oral hygiene, such as by cleaning of one's teeth. Keeping the pH of the teeth at an alkaline range may prevent the development of these dental problems. In this study, the pH of all toothpastes was in the alkaline range.

This study evaluated the antibacterial activity of the toothpastes against *S. aureus* and *S. mutans*. These bacteria are among the most implicated pathogens in dental caries and periodontal diseases, respectively. The results revealed that the toothpastes demonstrated antibacterial activities against the test organisms at all extract concentrations and antibacterial activities increased significantly with an increase in extract concentration ($p<0.05$). F5 containing 5% extract exhibited the highest antibacterial activity, with an inhibition zone of 19.30±0.17 and 12.60±0.52 against *S. aureus* and *S. mutans*, respectively, even when compared with the commercially available herbal toothpaste. The increase in antibacterial activity could be attributed to the increase in the concentration of the bioactive phytochemical component of the extract, which was similar to the trend observed with the antibacterial evaluation of the crude extract during preformulation. The antibacterial activity against *S. aureus* was significantly higher than that against *S. mutans* ($p<0.05$). F0 showed little antibacterial activity because SLS and peppermint oil contained in the composition of the paste are known to possess antibacterial activity against *S. aureus* and *S. mutans*.[38-40] The antibacterial activities of the formulated toothpastes with >2% concentration of *M. acuminata* extract were significantly higher than those of the commercially available herbal toothpaste against both test organisms ($p<0.05$). However, further investigation is required to isolate

the bioactive compound in the extract responsible for the antibacterial activity of this plant.

CONCLUSION

Poor oral hygiene is associated with the development of dental caries and periodontal diseases. However, the use of toothpastes plays a role in maintaining oral hygiene and otherwise prevents the consequences of poor oral hygiene. This study demonstrated that fortifying toothpastes with herbal antibacterial agents, such as the ethanolic extract of *M. acuminata*, provides higher antibacterial activities against some of the pathogens implicated in the development of dental caries and periodontal diseases *in vitro*. The use of the *M. acuminata* extract as an ingredient in toothpaste formulation will improve the maintenance of oral hygiene to prevent dental caries and periodontal diseases.

Conflict of interest: No conflict of interest was declared by the authors. The authors are solely responsible for the content and writing of this paper.

REFERENCES

1. Ersoy M, Tanalp J, Ozel E, Cengizlier R, Soyman M. The allergy of toothpaste: a case report. Allergol Immunopathol (Madr). 2008;36:368-370.
2. Horseman RE. The her-story of toothpaste. J Calif Dent Assoc. 2006;34:769-770.
3. Jardim JJ, Alves LS, Maltz M. The history and global market of oral home-care products. Braz Oral Res. 2009;(Suppl 1):17-22.
4. Oke GA, Bankole OO, Denloye OO, Danfillo IS, Enwonwu CO. Traditional and emerging oral health practices in parts of Nigeria. Odontostomatol Trop. 2011;34:35-46.
5. Shah N, Mathur VP, Jain V, Logani A. Association between traditional oral hygiene methods with tooth wear, gingival bleeding, and recession: A descriptive cross-sectional study. Indian J Dent Res. 2018;29:150-154.
6. Gupta P, Shetty H. Use of natural products for oral hygiene maintenance: revisiting traditional medicine. J Complement Integr Med. 2018 Mar 27;15:/j/jcim.2018.15.issue-3/jcim-2015-0103/jcim-2015-0103.xml.
7. Bowen WH, Koo H. Biology of *Streptococcus mutans*-derived glucosyltransferases: role in extracellular matrix formation of cariogenic biofilms. Caries Res. 2011;45:69-86.
8. Fejerskov O, Nyvad B, Kidd E. Dental caries, what is it? In: Fejerskov O, Nyvad B, Kidd E, eds. Dental caries: The disease and its clinical management. Oxford, UK; Wiley Blackwell;2015:7-10.
9. Chapple IL, Van der Weijden F, Doerfer C, Herrera D, Shapira L, Polak D, Madianos P, Louropoulou A, Machtei E, Donos N, Greenwell H, Van Winkelhoff AJ, Eren Kuru B, Arweiler N, Teughels W, Aimetti M, Molina A, Montero E, Graziani F. Primary prevention of periodontitis: managing gingivitis. J Clin Periodontol. 2015;(Suppl 16):S71-S76.
10. Popova C, Dosseva-Panova V, Panov V. Microbiology of periodontal diseases. A review. Biotechnol Biotechnol Equip. 2013;27:3754-3759.
11. Silva N, Abusleme L, Bravo D, Dutzan N, Garcia-Sesnich J, Vernal R, Hernández M, Gamonal J. Host response mechanisms in periodontal diseases. J Appl Oral Sci. 2015;23:329-355.
12. Darout IA, Christy AA, Skaug N, Egeberg PK. Identification and quantification of some potentially antibacterial anionic components in miswak extract. Indian J Pharmacol. 2000;32:11-14.
13. al-Otaibi M. The miswak (chewing stick) and oral health. Studies on oral hygiene practices of urban Saudi Arabians. Swed Dent J Suppl. 2004;2-75.
14. Almas K, Al-Zeid Z. The immediate antimicrobial effect of a toothbrush and miswak on cariogenic bacteria: a clinical study. J Contemp Dent Pract. 2004;5:105-114.
15. Saha S, Mohammad S, Saha S, Samadi F. Efficiency of traditional chewing stick (miswak) as an oral hygiene aid among Muslim school children in Lucknow: A cross-sectional study. J Oral Biol Craniofac Res. 2012;2:176-180.
16. Taiwo O, Xu HX, Lee SF. Antibacterial activities of extracts from Nigerian chewing sticks. Phytother Res. 1999;13:675-679.
17. Ogundiya MO, Okunade MB, Kolapo AL. Antibacterial activities of some Nigerian chewing sticks. Ethnobot Leaflets. 2006;10:265-271.
18. Oloke J, Odelade K. Oladeji O. Characterization and antibacterial analysis of flavonoids in vernonia amygdalina: a common chewing stick in south-western Nigeria. Bull Pharm Res. 2017;7:149-158.
19. Iwu MM. Pharmacognostical profile of selected medicinal plants: Handbook of African medicinal plants CRC Press, 2014.
20. Bankole PO, Adekunle AA, Oyedele RT, Faparusi F, Adewole A. Antibacterial activities and phytochemical screening of two tropical Nigerian chewing sticks. Int J Applied Sci Tech. 2012;2:131-138.
21. Tedwins EJO, Benjamin OUU, Ayobola ED, Goodies ME, Oghenesuvwe EE. A comparative study on the effect of Massularia acuminata and mouthwash against isolates from the oral cavity. J Res Dent. 2016;4:64-68.
22. Odeleye OF, Okunye OL, Kesi C, Abatan TO. A Study of the anticaries activity of three common chewing sticks and two brands of toothpaste in south west Nigeria. Bri J Pharm Res. 2016;11:1-7.
23. Trease A, Evans WC. Pharmacognosy (13th ed). London; Balliene Tindiall; 1989.
24. Ali HS, Abdul-Rasool BK. Propolis buccal paste in treatment of aphthous ulceration: formulation and clinical evaluation. Asian J Pharm Clin Res. 2011;4;29-33.
25. Mangilal T, Ravikumar M. Preparation and evaluation of herbal toothpaste and compared with commercial herbal toothpastes: An *invitro* study. Int J Ayu Her Med. 2016;6:2266-2251.
26. Muinat AA, Mbang FON, Lateef BG, Esther TO, Oluyemisi BA. Antimicrobial studies of the leaf extract of Argemone mexicana and its ointment formulation. West Afr J Pharm. 2015;26:33-40.
27. Adeleye OA, Babalola CO, Femi-Oyewo MN, Balogun GY. Antimicrobial activity and stability of Andrographis paniculata cream containing shea butter. Nig J Pharm Res. 2019;15:9-18.
28. Antwi-Boasiako C, Abubakari A. Antimicrobial and phytochemical properties of crude extracts of Garcina kola heckle stems used for oral health. Res J Pharmacol. 2011;5:68-76.
29. Maripandi A, Arun KT, Al Salamah AA. Prevalence of dental caries bacterial pathogens and evaluation of inhibitory concentration effect on different tooth pastes against *Streptococcus* spp. Afri J Microbio Res. 2011;5:1778-1783.
30. Daniyan S, Abalaka M. Prevalence and sceptibility pattern of bacterial isolates of dental caries in a secondary health care institution, Nigeria. Shiraz E-Med J. 2012;12:135-139.

31. Dige I, Baelum V, Nyvad B, Schlafer S. Monitoring of extracellular pH in young dental biofilms grown *in vivo* in the presence and absence of sucrose. J Oral Microbiol. 2016;8:30390.

32. Adeoti OM, Adedoja SA, Adedokun EO, Olaoye OJ, Abiola AO, Okesipe FO. Efficacy of chewing sticks extract on the agent of dental carries isolates. Arch Clin Microbiol. 2020;11:101-104.

33. Oladimeji F, Akinkunmi EO, Raheem A, Abiodun G, Bankole V. Evaluation of topical antimicrobial ointment formulations of essential oil of lippia multiflora moldenke. Afr J Tradit Complement Altern Med. 2015;12:135-144.

34. Ahuja A, Potanin A. Rheological and sensory properties of toothpastes. Rheol Acta. 2018;57:459-471.

35. Moghimipour E, Handali S. Saponin: properties, methods of evaluation and applications. Annu Res Rev Bio. 2014;5:207-220.

36. Welin-Neilands J, Svensater G. Acid tolerance of biofilm cells of *Streptococcus mutans*. Appl Environ Microbiol. 2007;73:5633-5638.

37. Sanz M, Bäumer A, Buduneli N, Dommisch H, Farina R, Kononen E, Linden G, Meyle J, Preshaw PM, Quirynen M, Roldan S, Sanchez N, Sculean A, Slot DE, Trombelli L, West N, Winkel E. Effect of professional mechanical plaque removal on secondary prevention of periodontitis and the complications of gingival and periodontal preventive measures: consensus report of group 4 of the 11th European Workshop on Periodontology on effective prevention of periodontal and peri-implant diseases. J Clin Periodontol. 2015;(Suppl 16):S214-S220.

38. Chaudhari LK, Jawale BA, Sharma S, Sharma H, Kumar CD, Kulkarni PA. Antimicrobial activity of commercially available essential oils against *Streptococcus mutans*. J Contemp Dent Pract. 2012;13:71-74.

39. Liang R, Xu S, Shoemaker CF, Li Y, Zhong F, Huang Q. Physical and antimicrobial properties of peppermint oil nanoemulsions. J Agric Food Chem. 2012;60:7548-7555.

40. Shen Y, Li P, Chen X, Zou Y, Li H, Yuan G, Hu H. Activity of Sodium Lauryl Sulfate, Rhamnolipids, and *N*-Acetylcysteine Against Biofilms of Five Common Pathogens. Microb Drug Resist. 2020;26:290-299.

Turk J Pharm Sci 2021;18(4):483-491
DOI: 10.4274/tjps.galenos.2020.44452

ORIGINAL ARTICLE

Development and Characterization of Conducting-Polymer-Based Hydrogel Dressing for Wound Healing

Yara İyileştirme için İletken Polimer Esaslı Hidrojel Sargının Geliştirilmesi ve Karakterizasyonu

Ravindra V. BADHE[1]*, Anagha GODSE[1], Ankita SHINKAR[1], Avinash KHARAT[2], Vikrant PATIL[2], Archana GUPTA[2], Supriya KHEUR[2]

[1]Dr. D. Y. Patil Institute of Pharmaceutical Sciences and Research, Department of Pharmaceutical Chemistry, Pune, India
[2]Regenerative Medicine Laboratory, Dr. D. Y. Patil Dental College and Hospital, Dr. D. Y. Patil Vidyapeeth, Pune, India

ABSTRACT

Objectives: Normal and chronic wound healing is a global challenge. Electrotherapy has emerged as a novel and efficient technique for treating such wounds in recent decades. Hydrogel applied to the wound to uniformly distribute the electric current is an important component in wound healing electrotherapy. This study reports the development and wound healing efficacy testing of vitamin D entrapped polyaniline (PANI)-chitosan composite hydrogel for electrotherapy.

Materials and Methods: To determine the morphological and physicochemical properties, techniques like scanning electron microscopy (SEM); differential scanning calorimetry; X-ray diffraction; fourier-transform infrared spectroscopy were used. Moreover, pH, conductance, viscosity, and porosity were measured to optimize and characterize the vitamin D entrapped PANI-chitosan composite hydrogel. The biodegradation was studied using lysozyme, whereas the water uptake ability was studied using phosphate buffer. Ethanolic phosphate buffer was used to perform the vitamin D entrapment and release study. Cell adhesion, proliferation, and electrical stimulation experiments were conducted by seeding dental pulp stem cells (DPSC) into the scaffolds and performing (3-[4,5-dimethylthiazol-2-yl]-2,5 diphenyl tetrazolium bromide) assay; SEM images were taken to corroborated the proliferation results. The wound healing efficacy of electrotherapy and the developed hydrogel were studied on excision wound healing model in rats, and the scarfree wound healing was further validated by histopathology analysis.

Results: The composition of the developed hydrogel was optimized to include 1% w/v PANI and 2% w/v of chitosan composite. This hydrogel showed 1455 µA conduction, 98.97% entrapment efficiency and 99.12% release of vitamin D in 48 hrs. The optimized hydrogel formulation showed neutral pH of 6.96 and had 2198 CP viscosity at 26˚C. The hydrogel showed 652.4% swelling index and 100% degradation in 4 weeks. The *in vitro* cell culture studies performed on hydrogel scaffolds using DPSC and electric stimulation strongly suggested that electrical stimulation enhances the cell proliferation in a three-dimensional (3D) scaffold environment. The *in vivo* excision wound healing studies also supported the *in vitro* results suggesting that electrical stimulation of the wound in the presence of the conducting hydrogel and growth factors like vitamin D heals the wound much faster (within 12 days) compared to non-treated control wounds (requires 21 days for complete healing).

Conclusion: The results strongly suggested that the developed PANI-chitosan composite conducting hydrogel acts effectively as an electric current carrier to distribute the current uniformly across the wound surface. It also acted as a drug delivery vehicle for delivering vitamin D to the wound. The hydrogel provided a moist environment, a 3D matrix for free migration of the cells, and antimicrobial activity due to chitosan, all of which contributed to the electrotherapy's faster wound healing mechanism, confirmed through the *in vitro* and *in vivo* experiments.

Key words: Polyaniline, chitosan, composite hydrogel, wound healing, electrical stimulation, vitamin D

ÖZ

Amaç: Normal ve kronik yara iyileşmesi küresel bir zorluktur. Elektroterapi, son yıllarda bu tür yaraların tedavisi için yeni ve etkili bir hidrojel tekniği olarak ortaya çıkmıştır. Elektrik akımını eşit olarak dağıtmak için yaraya uygulanan hidrojel, yara iyileşmesi elektroterapisinde önemli bir bileşendir. Bu çalışma, elektroterapi için D vitamini içeren polianilin (PANI)-kitosan kompozit hidrojelin geliştirilmesini ve yara iyileştirme etkinlik testini bildirmektedir.

Gereç ve Yöntemler: Morfolojik ve fizikokimyasal özellikleri belirlemek için taramalı elektron mikroskobu (SEM); diferansiyel tarama kalorimetrisi; X-ışını kırınımı; fourier dönüşümü kızılötesi spektroskopisi gibi teknikler kullanılmıştır. Ayrıca, D vitamini hapsedilmiş PANI-kitosan kompozit hidrojeli geliştirmek ve karakterize etmek için pH, iletkenlik, viskozite ve gözeneklilik ölçülmüştür. Biyobozunma, lizozim kullanılarak ve su alma yeteneği

*Correspondence: badheravi2@gmail.com, Phone: +9422432038, ORCID-ID: orcid.org/0000-0002-9919-8154
Received: 10.05.2020, Accepted: 02.11.2020

ise fosfat tamponu kullanılarak incelenmiştir. D vitamini tutma ve salma çalışmasını gerçekleştirmek için etanoik fosfat tamponu kullanılmıştır. Hücre adhezyonu, çoğalması ve elektrik stimülasyonu, diş özü kök hücrelerinin (DPSC) yapı iskelelerine ekilmesi ve (3-[4,5-dimetil-tiyazolil-]2,5-difeniltetrazolyum bromür yöntemi, kullanılarak gerçekleştirilmiştir. Proliferasyon sonuçlarını doğrulamak için SEM görüntüleri alınmıştır. Elektroterapinin yara iyileştirme etkinliği ve geliştirilen hidrojel, sıçanlarda eksizyon yara iyileştirme modelinde incelenmiş ve skarsız yara iyileşmesi histopatoloji analizi ile de doğrulanmıştır.

Bulgular: Geliştirilen hidrojelin bileşimi, %1 a/h PANI ve %2 a/h kitosan kompozit içerecek şekilde optimize edilmiştir. Hidrojel 48 saat içinde, bu hidrojel 1455 µA iletim, %98,97 tutma verimliliği ve %99,12 D vitamini salınımı gösterdi. Optimize edilmiş hidrojel formülasyonu, 6,96 nötr pH göstermiş ve 26˚C'de 2198 CP viskoziteye sahip olarak bulunmuştur. Hidrojel, 4 haftada %652,4 şişme indeksi ve %100 bozunma göstermiştir. DPSC ve elektrik stimülasyonu kullanılarak hidrojel yapı iskeleleri üzerinde gerçekleştirilen *in vitro* hücre kültürü çalışmaları, elektrik stimülasyonunun üç boyutlu (3D) bir iskele ortamında hücre proliferasyonunu artırdığını kuvvetle önermiştir. *İn vivo* eksizyon yara iyileştirme çalışmaları, iletken hidrojel ve D vitamini gibi büyüme faktörlerinin varlığında yaranın elektrikle uyarılmasının, tedavi edilmeyen kontrol yaralarına kıyasla yarayı çok daha hızlı (12 gün içinde) iyileştirdiğini öne süren *in vitro* sonuçları desteklemiştir (tam iyileşme için 21 gün).

Sonuç: Sonuçlar, geliştirilmiş PANI-kitosan kompozit iletken hidrojelin, akımı yara yüzeyi boyunca düzgün bir şekilde dağıtmak için bir elektrik akımı taşıyıcısı olarak etkili bir şekilde hareket ettiğini kuvvetle önermiştir. Ayrıca yaraya D vitamini vermek için bir ilaç taşıyıcısı görevi görmüştür. Hidrojel, nemli bir ortam sağlayarak hücrelerin serbest migrasyonu için 3 boyutlu bir matris ve kitosan kaynaklı antimikrobiyal aktivite sağlamıştır ki bunların tümü, elektroterapinin daha hızlı yara iyileştirme mekanizmasına katkıda bulunmuş ve bu bilgiler *in vitro* ve *in vivo* deneylerle doğrulanmıştır.

Anahtar kelimeler: Polianilin, kitosan, kompozit hidrojel, yara iyileşmesi, elektrik stimülasyonu, D vitamini

INTRODUCTION

According to the World Health Organization (WHO), injuries are becoming a more widespread public health issue. It is one of the leading causes of death across the globe annually. According to a WHO survey, about 5.7 million deaths are reported annually due to injuries, accounting for 9% of the total global annual deaths. These deaths represent a very small portion of the injured patients. Millions of people suffer from injuries that require hospitalization, emergency treatments, and consultation of a general practitioner or home remedies.[1] An injury is caused by a wound, which is defined as the disruption of the dermis layer and cellular continuity due to an external impact on the skin. Generally, there are five kinds of wounds: Abrasion, puncture, burn, avulsion and laceration. The normal wound healing is slow, and it takes a minimum of 21 days to complete the four phases of wound healing, including hemostasis, inflammatory/defensive phase, proliferative phase, and maturation/remodeling phase.[2]

Chitosan is an N-de-acetylated derivative of chitin. It is the most abundant biopolymer found in the exoskeleton of crustaceans, mollusks, and insects.[3] Chitosan is non-irritant, biodegradable, and biocompatible, and it exhibits high mechanical strength, good film-forming properties, adequate adhesionnon.[4,5] Chitosan based hydrogel can be made using various crosslinking agents like genipin, glutaraldehyde, and sodium tripolyphosphate.[6] Hydrogels are three-dimensional (3D) swollen structures that contain more than 90% of water. They can swell and retain the volume of the absorbed aqueous medium in their 3D swollen network when placed in an aqueous medium.[7] Conducting polymer hydrogels are gels composed of a conducting polymer and a supporting polymer, and they are swollen with water or electrolyte solution. The most widely used conducting polymer are polyaniline (PANI), poly-pyrrole, or poly(3,4-ethylene-dioxythiophene), representing the conducting moiety, while crosslinked water-soluble polymers make up the other part of hydrogel.[8]

PANI is the most widely used conducting polymer with various applications in molecular sensors, protection of metals from corrosion, gas separating membranes, and rechargeable batteries.[9-11] PANI exhibits the desired conductivity range; it is easy to synthesize, requires low operational voltage, offers thermal and chemical stability, and is a pH-responsive polymer with different chemical forms, based on acidic/basic treatment.[12,13] Despite these advantages, PANI has some drawbacks, including poor solubility in common organic solvents, poor infusibility, and poor mechanical properties.[14,15] Various attempts have been made to circumvent these drawbacks, including doping PANI using specific doping techniques like additives or forming a composite of PANI with another polymer matrix.[16,17] The PANI-polymer matrix composite enhances its solubility, mechanical properties, and PANI supplies the conducting properties to the PANI/polymer composite making it stimuli-responsive (pH and external electrical stimuli). Such PANI/polymer matrix is widely employed in sustained drug delivery if the polymer matrix exhibits properties of hydrogel. Its water uptake ability allows the entrapment of drugs or actives inside a 3D matrix and releases them in a controlled manner, making it an advanced candidate for biomedical applications.[18]

Recent studies have reported on the synthesis of chitosan blends with PANI or its derivatives[19-21] and using chitosan as a steric stabilizer for stimuli-responsive PANI colloids. In this study, chitosan-PANI composite hydrogel with good mechanical properties and electrical conductivity was developed.[22,23] The PANI was initially synthesized using oxidative polymerization reaction followed by formulating chitosan-PANI hydrogel with vitamin D (as a growth factor) in a controlled 3D matrix. PANI was distributed uniformly throughout the chitosan network in these composite hydrogels, and the concentration of the PANI was optimized by considering the conduction requirement for wound healing applications. Chitosan was selected for its biodegradable, hemostatic, antimicrobial, film-forming properties and its structure. Chitosan enhances the conductivity of PANI due to the presence of hydrogen bonds between hydrogelthe hydrogel network and PANI. The formulated hydrogel was lyophilized to get scaffolds of chitosan-PANI to highlight the significance of vitamin-D-loaded matrix in wound healing and for ease of cell line studieshydrogel. These

composites' preliminary application in *in vivo* wound healing was further demonstrated.

MATERIALS AND METHODS

Materials

Chitosan (cell culture tested-Low molecular weight grade 50,000-190,000, degree of deacetylation 90%) was procured from Sigma-Aldrich, United States. Ammonium persulfate and aniline were purchased from Loba Chemicals, India. Alfa Aesar in India provided the vitamin D. All other chemicals utilized were of the highest purity and analytical grade.

Synthesis of polyaniline

PANI was synthesized using the method reported by, Marcasuzaa et al.[24] In a nutshell, 5 mL of aniline was mixed with 100 mL 1M HCl. A 100 mL of 1 M ammonium persulfate solution was added into the mixture as a polymerization initiator. The solution was stirred for 24 hours at 1200 rpm on a magnetic stirrer until a dark green precipitate was formed. The precipitate was washed with distilled water three times to remove free aniline monomers before being recrystallized with methanol. The precipitate was then dried for 24 hours to get fibrous powder.

Preparation of conducting polymer-based hydrogel (conducting hydrogel)

Chitosan was slowly added to 1% acetic acid solution, under constant stirring, using a homogenizer. Vitamin D (dissolved in 6:4 v/v water:ethanol ratio) and PANI were added after the chitosan is dissolved completely, and the mixture was continuously stirred to uniformly distribute the PANI.[25] Vitamin D was used as a growth factor (drug) because it has previously been reported to improve wound healing.[26] Furthermore, a sodium TPP solution was added dropwise and stirred for 30 minutes to get a homogenized gel. The hydrogel was used for characterization and animal study. Hydrogel was lyophilized to form scaffolds for cell line studies.

Experimental section

Physicochemical characterization

The appearance and color of the hydrogel was determined by visual observation. A digital pH meter (ELICO LI-120, India) was utilized to measure the pH of the optimized batch and the blank hydrogel.

Conductivity

The conductivity of the blank and optimized batch of hydrogel was determined using a two probe conductivity meter (Labman-EQ-650, India).[27]

Viscosity

The viscosity of the conducting hydrogel and the blank hydrogel was verified using Brookfield viscometer (DV PRO-II, USA). The torque and viscosity were recorded at 26˚C with a spindle no: 18 fitted on a small sample adapter at different rpm (10-40), and the Newtonian behavior of the hydrogels was predicted.[28]

Scanning electron microscopy (SEM)

The porosity and morphology of the lyophilized hydrogels were studied using a SEM (FEI Nova Nano SEM 450, India) machine. The samples were first coated using a gold sputter coater (SPI module sputter coater, USA). The samples were then randomly scanned, and photomicrographs were taken at the acceleration voltage of 10 kV.[29]

Fourier-transform infrared spectrophotometer (FTIR)

The lyophilized blank and the conducting hydrogel powders were characterized by FTIR. The FTIR spectra were recorded using a FTIR (Shimadzu scientific instruments, model no 8400s, Japan) using KBr pellets.[30] The spectra were recorded and compared from 600 to 4500 cm^{-1}.

Differential scanning calorimetry (DSC)

The DSC study was carried out using (Mettler-Toledo DSC-I, USA) for the lyophilized blank and conductive polymer hydrogels. The samples were heated from 40˚C to 300˚C at the rate of 10˚C/min. For accurate results, an inert atmosphere was maintained throughout the experiment by purging nitrogen gas at the rate of 50-70 mL/min using a crimped aluminum pan.[29]

X-ray diffraction (XRD)

The XRD study was carried out for the blank hydrogel and the conducting hydrogel, using a Rigaku Miniflex-600 instrument from a scanning range of 2θ to 80θ.[30]

Drug entrapment efficiency

The drug (vitamin D) loaded crosslinked hydrogel (5 g) was added to 50 mL of ethanolic phosphate buffer (pH 7.4) at 26˚C for 2 hours with frequent sonication (at every 20 min) to release all the drug entrapped in the crosslinked matrix. The amount of free drug (vitamin D) was determined by collecting clear supernatant using ultraviolet spectroscopy at 262 nm. The supernatant from the empty hydrogel (without crosslinker) was taken as a blank,[31] and the drug entrapments of the crosslinked and normal matrix were compared.

Drug diffusion study

In vitro diffusion studies of the prepared hydrogel were carried out in a Franz-diffusion cell using a 25 mL ethanolic phosphate buffer (pH 7.4) with the temperature maintained at 37±1˚C. The acceptor compartment of the cell was filled with the 25 mL ethanolic phosphate buffer 7.4 and stirred continuously with a small magnetic bead. The donor compartment was filled with the hydrogel (equivalent to 50 mg of vitamin D). The 100 µL sample was withdrawn at specific time intervals to assess the release of vitamin D from the hydrogel in the donor compartment. The sink condition due to sample withdrawal was maintained by replenishing the receiver compartment with an equal amount of ethanolic phosphate buffer.[32]

Water uptake ability swelling behavior

Pre-weighed scaffold was immersed in the swelling medium (phosphate buffer pH: 7.4).[33,34] Scaffolds were removed using a spatula at various intervals and placed on filter paper to remove excess water and immediately weighed. The procedure was repeated and continued until no weight increase was observed.

The swelling percent was calculated using equation (1)

$$Q = (Ms - Md) / Md \times 100 \quad \text{equation (1)}$$

where, Q=is the swelling ratio; Ms=is the mass in the swollen state; Md=is the mass in the dried state.

Biodegradation study

The scaffolds degradation was performed in a phosphate buffer saline solution (phosphate buffered saline, pH: 7.4), containing 800 mg/L of lysozyme, at 37°C in an orbital shaker at 50 rpm for four weeks. The lysozyme solution was replaced with a fresh one after every three days. The samples were analyzed at a predetermined time (1, 2, 3, and 4 weeks, respectively). The samples were removed from the medium, rinsed with distilled water, and dried in an oven at 50°C until a constant mass is reached.[35] The degradation degree (Δm) was determined as the weight loss percent with respect to the initial weight of the sample and calculated using equation (2).

$$\Delta m\ (\%) = m1 - m2 / m1 \times 100 \quad \text{equation (2)}$$

where, Δm is the degree of biodegradation; m1 is the initial weight of the scaffold; m2 is the weight of the scaffolds after the predetermined rate.

Cell proliferation studies

The effect of electric current (1 mA supplied using BioRad power supply) on the cell survival and proliferation was studied using stem cells isolated from dental pulp stem cell (DPSC). The DPSC were selected for this study as they easily undergo differentiation under the influence of growth factors like vitamin D to give the multiple differentiated cells required for better angiogenesis and neurogenesis. Angiogenesis and neurogenesis are the rate-limiting stages in the wound healing process. As a result, using DPSC can effectively address this issue in wound healing leading to faster healing. The *in vitro* cell proliferation studies were conducted to prove that the DPSCs can significantly survive in the developed conducting hydrogel. The cell proliferation and viability of the DPSCs seeded in the conducting scaffold treated and not treated with a small electric current (1 mA) were assessed using (3-[4,5-dimethylthiazol-2-yl]-2,5 diphenyl tetrazolium bromide) (MTT) assay.

The cells were sub-cultured in 20% fetal bovine serum-Dulbecco's Modified Eagle Medium-F12 with 1% penicillin-streptomycin medium to determine the proliferation of DPSCs. When the cells were 90% confluent, 1×10^4 cells / mL were seeded into two 24-well culture plates separately containing blank and conducting hydrogel scaffolds (5 mm height and 4 mm diameter cylindrical scaffold). The plates were incubated at 37°C in a humidified CO_2 incubator.

The MTT assay was performed (N=6 samples each) every 5 days for the scaffolds, with and without electrical stimulation for a total of 15 days, with absorbance readings recorded at 570 nm.[36] The population doubling times (PDT) was then calculated using equation (3).

$$PDT = T \log^2 / \log FCC - \log ICC \quad \text{equation (3)}$$

where, ICC is the initial cell count, FCC is the final cell count, and T is the incubation time (in hours).

In vivo wound healing study

Excision wound healing using Wistar albino rats model was carried out after CPCSEA Clearance (approval no: DYPIPSR/IAEC/Nov./18-19/P-09 Date 25/11/2019). The animals were placed into four groups (n=6) in this study; group 1 was treated as a control group (not treated with anything), group 2 as a standard group (treated with cipladine), group 3 as a blank hydrogel, and group 4 as a CP-based hydrogel. In all the groups, a full-thickness excision wound was created on the back of the Wister rats. Wound healing was monitored by measuring the wound area. Equation (4) was employed to calculate the wound area and the % wound contraction.

$$\%\ \text{Wound Contraction} = (A0 - At) / A0 \times 100 \quad \text{equation (4)}$$

where, A*0* and A*t* are the initial wound area and wound area after a time interval *t,* respectively.

Histopathology

Following a 15-day *in vivo* wound healing study, a patch of 1 cm×1 cm skin sample from the healed wound was excised for histopathological studies. Healed skin of the rat was fixed in neutral buffered formalin, and a standard histopathology procedure was conducted. The tissues were trimmed longitudinally and routinely processed in ascending grades of alcohol to dehydrate them, cleared in xylene, and embedded in paraffin wax. Paraffin wax embedded tissue blocks were sectioned at 3 µm thickness with the Rotary Microtome. All the slides of the skin were stained with hematoxylin and eosin stain. The prepared slides were examined under a microscope to note histopathological lesions like angiogenesis, inflammatory cell (neutrophilic/lymphocytic) infiltration, edema and fibroblast, necrosis, and scar tissue formation. The severity of the observed lesions was recorded as minimal (<1%), mild (1-25%), moderate (26-50%), moderately severe (51-75%), severe (76-100%), respectively, and the distribution was recorded as colored arrows.[36]

RESULTS AND DISCUSSION

Appearance

The color, odor, and appearance of the prepared formulation were visually inspected. The blank hydrogel appeared to be a slight yellowish translucent gel (Figure 1a), and the conducting hydrogel appeared as a dark green colored translucent gel (Figure 1b). The blank scaffolds were white, porous 3D matrix (Figure 1c), and the conductive scaffolds were slightly greenish 3D structures (Figure 1d).

pH Measurement

The pH of the conducting hydrogel was 6.94, which is neutral. It was compared to the pH of the blank hydrogel, which was found to be 6.4. In the *in vivo* animal studies, this increased pH permitted the direct application of formulation on the wound and did not cause any redness or irritation at the wound site.

Conductivity

The conducting hydrogel showed better conductivity of 1455 µA when compared to the conductivity of the blank hydrogel (0.098 µA). The previously reported results for poly-pyrrole-based conducting hydrogel with the same concentration was 1849 µA, which is quite close to our findings.[37,38]

Viscosity

The viscosity of the blank hydrogel and the conducting hydrogel was determined using a Brookfield viscometer. It was observed that hydrogels showed a shear-thinning behavior, as the viscosity decreased with increase stress from 3.198 to 2.198 CP for the blank hydrogel and from 3.280 to 2.208 for the CP-based hydrogel. Similar results were reported by Mawad et al.[39] for single component CP-based hydrogel using an in-situ approach.

SEM analysis

The SEM images of non-crosslinked (blank) and crosslinked (conducting) hydrogels are shown in Figure 1e, f, respectively. When observed at 500×, the obtained scaffolds revealed irregular pore sizes ranging from 100-230 µm. The crosslinked batch was more porous than the batch without crosslinking, which might be due to the higher interaction with TPP.

IR spectra spectral analysis

Figure 2 shows the IR spectra of chitosan and the conducting hydrogel. The observed frequencies for the blank hydrogel (Figure 2a) OH stretching, N-H bending, CH stretching of CH3 and CH2 groups, and NH-C=O amide bending were observed at 3.628, 3.379, 3.000, and 1.705 cm^{-1}, respectively. The obtained values are consistent with the previously reported results by Kodama et al.[40] Hydrogel the frequencies for C-H stretching, O-H stretching, C-O stretching, C=O stretching, and C-N stretching in the IR spectra of the conducting hydrogel scaffold (Figure 2) are depicted at 2.864, 3.495, 1.022, 1.649, and 1.270 cm^{-1}, respectively. The obtained values closely matched the previously reported results by Oka et al.[41]

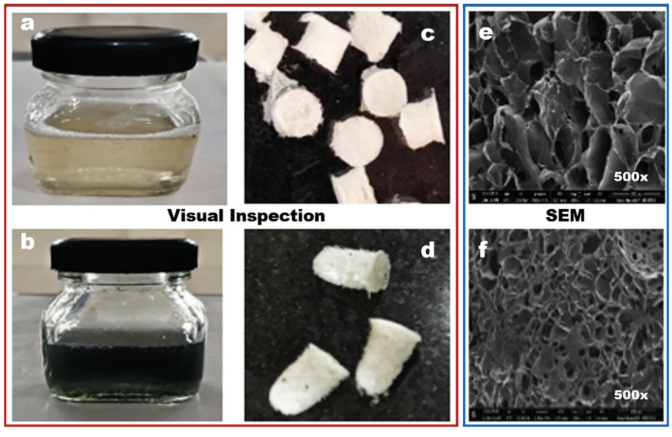

Figure 1. Appearance and morphology of the gel and scaffolds: a) and b) blank and conducting hydrogel respectively; c) and d) blank and conducting hydrogel scaffolds respectively; e) and f) SEM images of blank and conducting hydrogel scaffolds respectively

SEM: Scanning electron microscopy

DSC thermogram analysis

DSC spectra are illustrated in Figure 3a. The DSC spectra of the blank hydrogel revealed a sharp endothermic peak at 82.24°C, which was owing to water loss, and a broad endothermic peak at 268°C followed by a broad exothermic peak at 288°C, which indicates chitosan decomposition. These values are consistent with previously reported values by Martins et al.[20] The conducting hydrogel's DSC thermogram hydrogelshowed a peak at 90°C, which was linked to moisture loss. The sharp endothermic peak at 117.53°C indicated the peak degradation of vitamin D, a broad endothermic peak at 133.69°C followed by a broad exothermic peak at 144.69°C indicated PANI decomposition. The endothermic peak at 270°C followed by the exothermic peak at 292°C confirmed the chitosan degradation, and the obtained results were quite similar to those previously reported by Thanpitcha et al.[42]

XRD spectral analysis

The blank hydrogel and conducting hydrogel's diffractogram hydrogel is shown in Figure 3b. Broad characteristic peaks of the blank hydrogel were observed at 13 and 17 degrees 2θ in crystallographic planes, suggesting amorphous natured chitosan. The obtained values were consistent with those of Badhe et al.[43] The conducting hydrogel is comprised of a dense network structure of interpenetrating polymer chains crosslinked to each other by TPP. Thus, the vitamin-D-loaded conducting hydrogel's diffractogram sharp peaks at 13θ, and 17θ represent chitosan, 25θ represents vitamin D, and the broad peak at 43θ represents the amorphous nature of PANI. The obtained results are comparable to previously reported results by Sultana et al.[44]

Drug entrapment efficiency/drug diffusion study

The entrapment efficiency for the conducting hydrogel was found to be 98.97%. The reported standard drug entrapment efficiency for chitosan scaffolds was 97-100%. Through the Franz diffusion cell using dialysis membrane, the *in vitro*

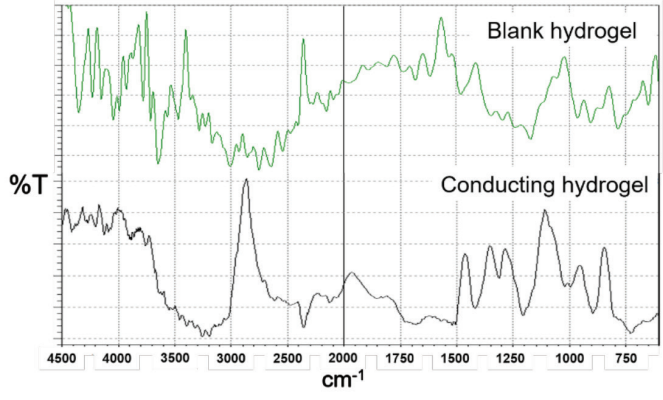

Figure 2. IR spectra of blank hydrogel and conducting hydrogel

IR: Infrared spectrophotometer

release profile of vitamin D was found to be 99.12% in 48 hours, as depicted in Figure 4a. After 52 hours, the release of vitamin D was reported to be 99% for poly-pyrrole-based hydrogel. Crosslinking can be predicted to increase the release time.[45]

Water uptake ability swelling behavior

The medium water uptake ability, which was about 652.4%, was assessed by determining the swelling index of scaffolds in the phosphate buffer at 37˚C. Figure 4b revealed that after 70 minutes, there was no significant increase in the water uptake ability of the scaffolds. Previous reports by Mawad et al.,[39] suggested a 787.69% water uptake ability for poly-pyrrole-based scaffolds, which aligns closely with previously reported results.

Biodegradation study

The research was carried out until the scaffolds were completely removed. The results (Figure 4c) revealed that the scaffolds showed gradual weight loss until the fourth week after which they were completely degraded. Biodegradation was shown to be 91-94% after the seventh week in some previous reports hydrogel. The conducting hydrogel scaffold degraded in 4 weeks, which might be attributed to the chitosan molecular weight.[44]

Cell proliferation study

DPSC isolated from dental pulp were employed for the cell proliferation studies. The scaffolds were electrically stimulated for 15 days during these studies (Figure 5a). It was observed that electrical stimulation helps in the faster proliferation of the cells compared to non-electrical stimulated scaffolds (Figure 5b). Some previously reported studies have shown an over 21 days stem cells proliferation when seeded in scaffolds (significance **p≤0.01 and ***p≤0.005), respectively.[46,47] Figure 5c shows the SEM images demonstrating improved proliferation with electrical stimulation; it was concluded that electric current supports the cell proliferation.

In vivo wound healing study

Figure 6a shows the results of wound healing animal studies using electrical stimulation. The % wound contraction results were statistically analyzed by One-Way ANOVA (n=6), **p<0.01, *p<0.05. Compared to the control and blank hydrogels, wound healing in the animals treated with conducting hydrogel was found to be significantly faster hydrogel (Figure 6b). Thus, the study backs up the observations that electrical stimulation of the wound with the conducting hydrogel speeds up wound healing (within 12 days) compared to the control hydrogel (which took 21 days to heal completely).[48]

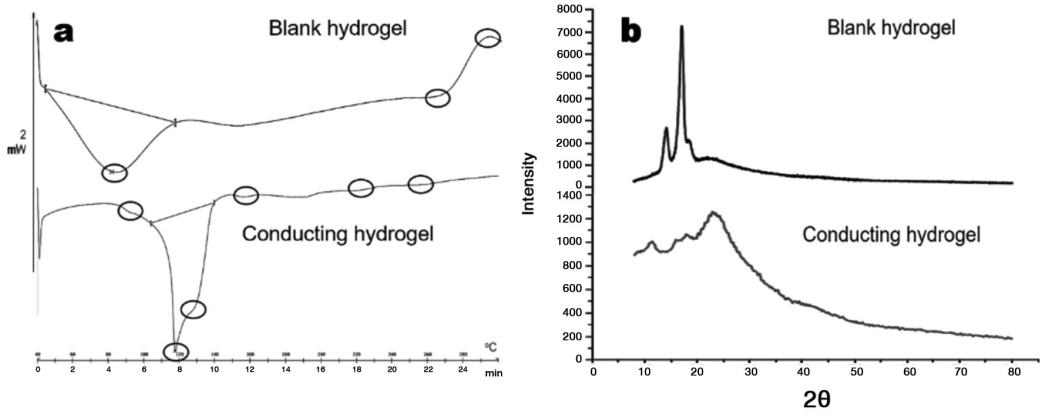

Figure 3. a) DSC spectra of blank and conducting hydrogel; b) XRD spectra of blank and conducting hydrogel
DSC: Differential scanning calorimetry, XRD: X-ray diffraction

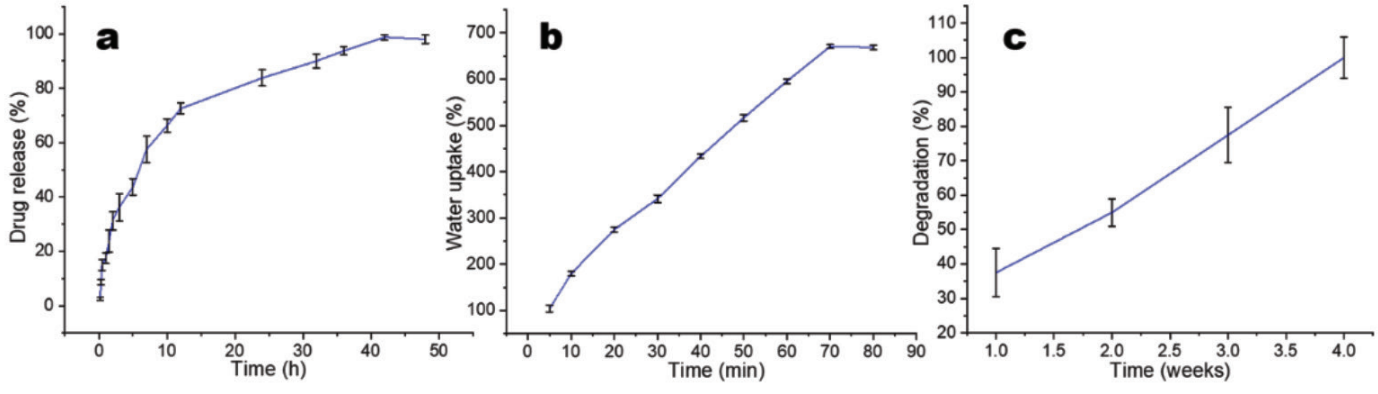

Figure 4. a) Drug release (of vitamin D); b) water uptake; and c) degradation studies of conducting hydrogel

Histopathology

Microscopic examination of the skin revealed mild epidermal hyperplasia with fibrosis in animals belonging to the control group; whereas other groups showed normal epidermis and dermis. The results are shown in Figure 6c. Collagen synthesis, fibroblast migration, and epithelization are seen in group III (blank hydrogel) and group IV (conducting hydrogel), implying the generation of healthy and flexible skin tissue without scar tissue. On the other hand, group II (marketed formulation) only showed epithelization, fibroblast migration, and necrosis, indicating scar tissue formation. Thus, it can be concluded that both the blank and the conducting hydrogels helped in scar-free wound healing, and the electrical stimulation of the conducting hydrogel helped in faster wound healing without scar tissue formation. The same phenomenon is observed in the healed skin images of the animals in Figure 6c.

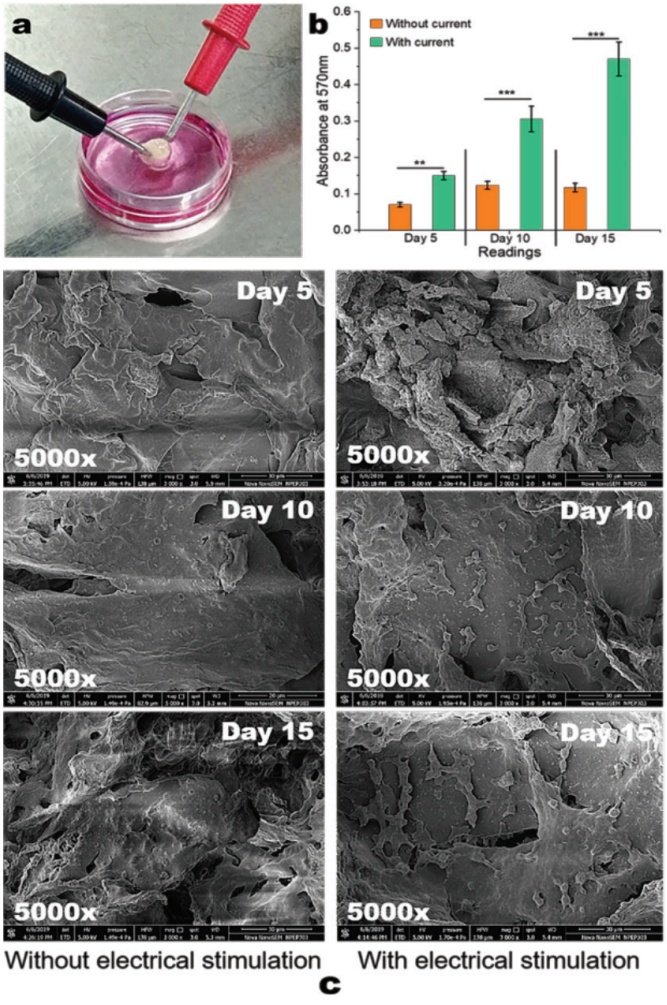

Figure 5. a) Scaffolds electrical stimulation; b) graph of cell proliferation studies performed using MTT assay (**p≤0.01 and ***p≤0.005); c) SEM images of cells seeded scaffolds with and without electrical stimulation

MTT: (3-[4,5-dimethylthiazol-2-yl]-2,5 diphenyl tetrazolium bromide), SEM: Scanning electron microscopy

DISCUSSION

Injuries and wounds are among the most prevalent health concerns we face daily. Generally, small injuries like abrasion or cuts heal naturally without infection and with little care. Emergency medical help is required for large wounds, like laceration, avulsion, incision, or amputation. Many of these wounds heal at a slower rate due to infections and patient health/age conditions. Non-responding or chronic injuries are a distinct class of injuries that is mainly observed in burns, diabetic and obese patients. These types of injuries pose a potential burden on our healthcare system and patients' finances. There are various treatments available for these types of wounds, including hyperbaric oxygen therapy, plastic surgeries, grafts, negative pressure therapy, and electrotherapy. These techniques have their advantages and disadvantages, but electrotherapy has proven to be more useful and cost-effective.

Electrotherapy treatment applies a small electric current (200-800 µA) to help the wound heal faster by mimicking the current of an injury. However, an equally effective hydrogel

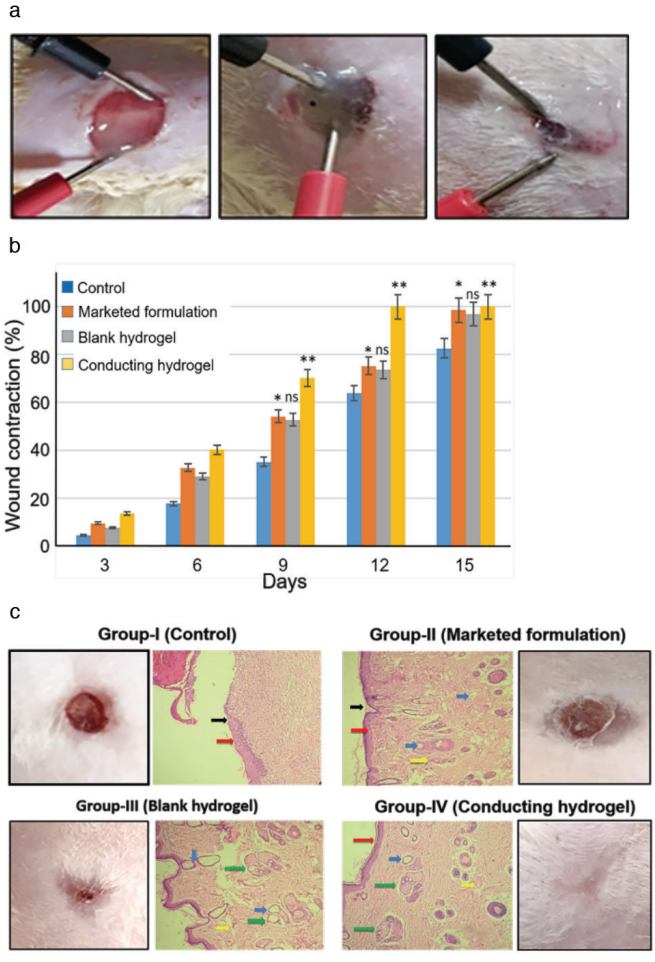

Figure 6. a) % wound contraction graph (**p≤0.01 and *p≤0.05); b) application of conducting hydrogel and electrical current at different time intervals (every 3 days); c) histopathology results (black arrows indicates scar tissue formation, red arrows indicates healing wound/initiation of re- epithelization, blue arrows indicates edema and fibroblasts and yellow arrow indicates necrosis, green arrows in group III and IV indicated initiation of collagen regrowth at wound site)

that can distribute the applied electric current throughout the wound is required to get the maximum benefit from the therapy.[49] This research work focused on developing optimized conducting hydrogel, which can uniformly distribute electric current throughout the wound. In addition to the electric current distribution, the developed hydrogel also serves as a drug delivery vehicle delivering vitamin D as a growth factor. Furthermore, the PANI-chitosan hydrogel base also acts as an antimicrobial wound closure to protect the wound from secondary infection. The hydrogel's highly biocompatible and biodegradable nature provides a moist 3D environment to the wound allowing the cells (fibroblast, keratinocyte) to migrate in a 3D environment to heal the wound faster. The daily electrical stimulation helps the wound heal with normal healthy skin without scar tissue by enhancing the migration of the cells and providing a moist environment with vitamin D (supporting angiogenesis and neurogenesis).

Though the study reported here showed very promising results with the developed hydrogel, there are certain limitations.

CONCLUSION

The study was performed using a 1 mA current, which is slightly higher than the actual current of an injury; optimizing the current will produce better results. This study establishes the biodegradation of the hydrogel but the non-degradable PANI (though in small amounts) needs to be addressed. Understanding these limitations will allow for further modifications of the hydrogel with novel biodegradable and effective conducting materials. Further studies with new drug entity immobilization in hydrogel for the same application are also planned.

ACKNOWLEDGMENTS

Authors are very thankful to Dr. D. Y. Patil Institute of Pharmaceutical Sciences and Research for providing the lab space and animal house to carry out the research work.

Conflict of interest: No conflict of interest was declared by the authors. The authors are solely responsible for the content and writing of this paper.

REFERENCES

1. Caló E, Khutoryanskiy VV. Biomedical applications of hydrogels: a review of patents and commercial products. Eur Polym J. 2015;65:252-267.
2. Swarbrick J. Encyclopedia of pharmaceutics. (4th ed). Boca Raton, FL: Taylor & Francis Group; 2013.
3. Hoare TR, Kohane DS. Hydrogels in drug delivery: progress and challenges. Polymer 2008;49:1993-2007.
4. De France KJ, Xu F, Hoare T. Structured macroporous hydrogels: progress, challenges, and opportunities. Adv Healthc Mater. 2018;7.
5. Larrañeta E, Stewart S, Ervine M, Al-Kasasbeh R, Donnelly RF. Hydrogels for hydrophobic drug delivery. classification, synthesis and applications. J Funct Biomater. 2018;9:13.
6. Robinson J, Lee V. Controlled drug delivery, fundamentals and applications. 2nd ed. New York; Informa Healthcare USA Inc; 2009.
7. Mishra S, Rani P, Sen G, Dey KP. Preparation, properties and application of hydrogels: a Review. Singapore: Springer; 2018:145-173.
8. Qiu Y, Park K. Environment-sensitive hydrogels for drug delivery. Adv Drug Deliv Rev. 2001;53:321-339.
9. Gupta P, Vermani K, Garg S. Hydrogels: from controlled release to pH-responsive drug delivery. Drug Discov Today. 2002;7:569-579.
10. Kamath KR, Par K. Biodegradable hydrogels in drug delivery. Adv Drug Deliv Rev. 1993;11:59-84.
11. Chien Y. Novel drug delivery systems. 2nd ed. New York: Informa Healthcare USA Inc; 2009.
12. Bhattarai N, Gunn J, Zhang M. Chitosan-based hydrogels for controlled, localized drug delivery. J Adv Drug Deliv. 2010;62:83-99.
13. Carterall William A. Molecular mechanisms of gating and drug block of sodium channels. Sodium Channels and Neuronal Hyperexcitability. Novartis Foundation Symposia. 2001.
14. Hudson SM, Smith C. Polysaccharide: chitin and chitosan: chemistry and technology of their use as structural materials. In: Kaplan DL, ed. Biopolymers from renewable resources. New York: Springer-Verlag; 1998:96-118.
15. Dutta PK, Ravikumar MNV, Dutta J. Chitin and chitosan for versatile applications, JMS Polym Rev. 2002;42:307-354.
16. Verma R, Gupta PP, Satapathy T, Roy A. A review of wound healing activity on different wound models. J Appl Pharm Res. 2019;7:1-7.
17. Jayakumar R, Prabaharan M, Sudheesh Kumar PT, Nair SV, Tamura H. Biomaterials based on chitin and chitosan in wound dressing applications. Biotechnol Adv. 2011;29:322-337.
18. Berger J, Reist M, Mayer JM, Felt O, Peppas NA, Gurny R. Structure and interactions in covalently and ionically crosslinked chitosan hydrogels for biomedical applications. Eur J Pharm Biopharm. 2004;57:19-34.
19. Tran PA, Zhang L, Webster TJ. Carbon nanofibers and carbon nanotubes in regenerative medicine. Adv Drug Deliv Rev. 2009;61:1097-1114.
20. Martins AM, Eng G, Caridade SG, Mano JF, Reis RL, Vunjak-Novakovic G. Electrically conductive chitosan/carbon scaffolds for cardiac tissue engineering. Biomacromolecules. 2014;15:635-643.
21. Zhao M. Electrical fields in wound healing-An overriding signal that directs cell migration. Semin Cell Dev Biol. 2009;20:674-682.
22. Wedmore I, McManus JG, Pusateri AE, Holcomb JB. A special report on the chitosan-based hemostatic dressing: experience in current combat operations. J Trauma. 2006;60:655-658.
23. Anithaa A, Sowmyaa S, Sudheesh KPT, Deepthi S, Chennazhi KP. Chitin and chitosan in selected biomedical applications. Prog Polym Sci. 2014;39:1644-1667.
24. Marcasuzaa P, Reynaud S, Ehrenfeld F, Khoukh A, Desbrieres J. Chitosan-graft-polyaniline-based hydrogels: elaboration and properties. Biomacromolecules. 2010;11:1684-1691.
25. Diarrassouba F, Remondetto G, Liang L, Garrait G, Beyssac E, Subirade M. Effects of gastrointestinal pH conditions on the stability of the β-lactoglobulin/vitamin D3 complex and on the solubility of vitamin D3. Food Res Int. 2013;52:515-521.
26. Burkiewicz CJ, Guadagnin FA, Skare TL, do Nascimento MM, Servin SC, de Souza GD. Vitamin D and skin repair: a prospective, double-blind and placebo controlled study in the healing of leg ulcers. Rev Col Bras Cir. 2012;39:401-407.

27. Shahini A, Yazdimamaghani M, Walker KJ, Eastman MA, Hatami-Marbini H, Smith BJ, Ricci JL, Madihally SV, Vashaee D, Tayebi L. 3D conductive nanocomposite scaffold for bone tissue engineering. Int J Nanomedicine. 2014;9:167-181.

28. Lira LM, de Torresi SI. Conducting polymer–hydrogel composites for electrochemical release devices: synthesis and characterization of semi-interpenetrating polyaniline–polyacrylamide networks. Electrochem Commun. 2005;7:717-723.

29. Green RA, Baek S, Poole-Warren LA, Martens PJ. Conducting polymer-hydrogels for medical electrode applications. Sci Technol Adv Mater. 2010;11:014107.

30. Barthus RC, Lira LM, Torresi SI. Conducting polymer-hydrogel blends for electrochemically controlled drug release devices. J Brazil Chem Soc. 2008;19:630-636.

31. Stejskal J, Bober P. Conducting polymer colloids, hydrogels, and cryogels: common start to various destinations. Colloid Polym Sci. 2018;296:989-994.

32. Hardy JG, Lee JY, Schmidt CE. Biomimetic conducting polymer-based tissue scaffolds. Curr Opin Biotechnol. 2013;24:847-854.

33. Zhao F, Shi Y, Pan L, Yu G. Multifunctional nanostructured conductive polymer gels: synthesis, properties, and applications. Acc Chem Res. 2017;50:1734-1743.

34. Lee JY. Electrically conducting polymer-based nanofibrous scaffolds for tissue engineering applications. Polym Rev. 2013;53:443-459.

35. Yang J, Choe G, Yang S, Jo H, Lee JY. Polypyrrole-incorporated conductive hyaluronic acid hydrogels. Biomater Res. 2016;20:31.

36. Salehi M, Ehterami A, Farzamfar S, Vaez A, Ebrahimi-Barough S. Accelerating healing of excisional wound with alginate hydrogel containing naringenin in rat model. Drug Deliv Transl Res. 2021;11:142-153.

37. Ramadan A, Elsaidy M, Zyada R. Effect of low-intensity direct current on the healing of chronic wounds: a literature review. J Wound Care. 2008;17:292-296.

38. Hunckler J, de Mel A. A current affair: electrotherapy in wound healing. J Multidiscip Healthc. 2017;10:179-194.

39. Mawad D, Stewart E, Officer DL, Romeo T, Wagner P, Wagner K, Wallace GG. Conducting polymer hydrogels: a single component conducting polymer hydrogel as a scaffold for tissue engineering. Adv Funct Mater. 2012;22:2691.

40. Kodama H, Inoue T, Watanabe R, Yasuoka H, Kawakami Y, Ogawa S, Ikeda Y, Mikoshiba K, Kuwana M. Cardiomyogenic potential of mesenchymal progenitors derived from human circulating CD14+ monocytes. Stem Cells Dev. 2005;14:676-686.

41. Oka T, Maillet M, Watt AJ, Schwartz RJ. Aronow BJ, Duncan SA, Molkentin JD. Cardiac-specific deletion of Gata4 reveals its requirement for hypertrophy, compensation, and myocyte viability. Circ Res. 2006;98:837-845.

42. Thanpitcha T, Sirivat A, Jamieson AM, Rujiravanit R. Preparation and characterization of polyaniline/chitosan blend film. Carbohydr Polym. 2006;64:560-568.

43. Badhe RV, Bijukumar D, Chejara DR, Mabrouk M, Choonara YE, Kumar P, du Toit LC, Kondiah PPD, Pillay V. A composite chitosan-gelatin bi-layered, biomimetic macroporous scaffold for blood vessel tissue engineering. Carbohydr Polym. 2017;157:1215-1225.

44. Sultana S, Ahmad N, Faisal SM, Owais M, Sabir S. Synthesis, characterisation and potential applications of polyaniline/chitosan-Ag-nano-biocomposite. IET Nanobiotechnol. 2017;11:835-842.

45. Iida ASL, Luz KN, Barros-Alexandrino TT, Fávaro-Trindade CS, de Pinho SC, Assis OBG, Martelli-Tosi M. Investigation of TPP-Chitosomes particles structure and stability as encapsulating agent of cholecalciferol. Polímeros. 2019;29:e2019049.

46. Bakopoulou A, Georgopoulou A, Grivas I, Bekiari C, Prymak O, Loza K, Epple M, Papadopoulos GC, Koidis P, Chatzinikolaidou M. Dental pulp stem cells in chitosan/gelatin scaffolds for enhanced orofacial bone regeneration. Dent Mater. 2019;35:310-327.

47. Moutsatsou P, Coopman K, Georgiadou S. Biocompatibility assessment of conducting pani/chitosan nanofibers for wound healing applications. Polymers (Basel). 2017;9:687.

48. Chen X, Zhang M, Wang X, Chen Y, Yan Y, Zhang L, Zhang L. Peptide-modified chitosan hydrogels promote skin wound healing by enhancing wound angiogenesis and inhibiting inflammation. Am J Transl Res. 2017;9:2352-2362.

49. Badhe RV, Nipate SS. Low-intensity current (LIC) stimulation of subcutaneous adipose derived stem cells (ADSCs) - A missing link in the course of LIC based wound healing. Med Hypotheses. 2019;125:79-83.

Turk J Pharm Sci 2021;18(4):492-497
DOI: 10.4274/tjps.galenos.2020.33254

ORIGINAL ARTICLE

Preparation and Characterization of Mucoadhesive Loratadine Nanoliposomes for Intranasal Administration

İntranazal Uygulama için Mukoadhesif Loratadin Nanolipozomlarının Hazırlanması ve Karakterizasyonu

Lena TAMADDON[1], Negar MOHAMADI[1], Neda BAVARSAD[1,2]*

[1]Department of Pharmaceutics, Faculty of Pharmacy, Ahvaz Jundishapur University of Medical Sciences, Ahvaz, Iran
[2]Nanotechnology Research Center, Ahvaz Jundishapur University of Medical Sciences, Ahvaz, Iran

ABSTRACT

Objectives: The present study aimed to formulate and characterize mucoadhesive liposomes for intranasal delivery of loratadine. In particular, the formulation was aimed to improve the drug bioavailability and efficacy.

Materials and Methods: Liposomes were prepared by thin-film hydration method, with soybean phosphatidylcholine and cholesterol as main components. Liposomes were coated with chitosan solution at a concentration of 0.05% and 0.1%, w/v. The formulations were assessed for particle size, polydispersity index (PDI), encapsulation efficiency (EE), thermodynamic behavior, *in vitro* drug release, mucoadhesiveness, and stability.

Results: Particle size analysis showed that the vesicles of uncoated and coated liposomes with 0.05% and 0.1% chitosan were characterized by size of 193±3.3 nm, 345±4.6, and 438±7.3 nm, respectively. Size distribution for developed formulations was in the acceptable range (PDI <0.7). EE was recorded to be approximately 80%. Chitosan-coated liposomes demonstrated slower release rate as compared to uncoated liposomes. Drug release kinetics profile for all the formulations followed a zero-order model. Chitosan coating improved mucoadhesiveness by more than 3-fold as compared to uncoated liposomes. However, no significant differences were recorded between mucin adsorption behavior of 0.05% and 0.1% chitosan-coated liposomes ($p>0.05$). For stability studies, liposomes were stored at 4˚C for 3 months, and changes in particle diameter, PDI, and EE % were recorded. No significant alternations were reported in particles size, PDI, and drug leakage of coated liposomes.

Conclusion: Liposomes coated with 0.05% chitosan were chosen as the optimum formulation, which demonstrated a significant potential for overcoming the nasal drug delivery limits for short residence time and mucociliary clearance.

Key words: Liposomes, loratadine, mucoadhesive, chitosan, intranasal

ÖZ

Amaç: Bu çalışma, ilaç biyoyararlanımını ve etkinliğini artırmak için loratadin mukoadhesif burun içi lipozomlarını formüle etmek ve değerlendirmeyi amaçlamaktadır. Özellikle, formülasyon ilaç biyoyararlanımını ve efikasitesini geliştirmeyi hedeflemiştir.

Gereç ve Yöntemler: Lipozomlar, ana bileşenler olarak soya fasulyesi fosfatidilekolin ve kolesterol kullanılarak ince film hidrasyon yöntemiyle hazırlanmıştır. Lipozomlar, %0,05 ve %0,1 a/h konsantrasyonda kitosan çözeltisi ile kaplanmıştır. Formülasyonlar partikül boyutu, polidispersite indeksi (PDI), kapsülleme etkinliği (EE), termodinamik davranışları, *in vitro* ilaç salımı, mukoadhesiviteleri ve stabilite açısından değerlendirilmiştir.

Bulgular: Parçacık boyutu analizi veziküllerin kaplanmamış ve sırasıyla; %0,05 ve %0,1 kitosan kaplı lipozomlar için sırasıyla 193±3,3 nm, 345±4,6 ve 438±7,3 nm boyutlarında elde edildiğini göstermiştir. Geliştirilen tüm formülasyonlar için boyut dağılımı için kabul edilebilir ranjda bulunmuştur (PDI <0,7). EE yaklaşık %80 civarında kaydedilmiştir. Kitosan kaplanmış aplanmış lipozomlar, kaplanmamış olanlara kıyasla daha yavaş salım oranı göstermiştir. İlaç salım kinetik modeli, tüm formülasyonlar için sıfır derece modeli göstermiştir. Kitosan kaplama, kaplanmamış lipozomlara kıyasla mukoadhesiviteyi 3 kattan fazla artırmıştır. Ancak, %0,05 ve %0,1 kitosan kaplama müsin adsorpsiyon davranışında arasında anlamlı bir fark kadedilmemiştir ($p>0,05$). Stabilite çalışmaları için, lipozomlae 4˚C'de üç aylık depolanmış ve partikül boyutu, PDI ve %EE'deki değişiklikler kaydedilmiştir. Partikül boyutu, PDI ve kaplı lipozomlardan ilaç sızıntısı konularında belirgin değişiklikler olmadığı raporlanmıştır.

Sonuç: %0,05 ile kaplanan lipozomlar kısa kalma süresinin ve mukosiliyer klerensinin nazal ilaç verme sınırlarının üstesinden gelmek için önemli bir potansiyel gösterebilen optimum formülasyon olarak seçilmiştir.

Anahtar kelimeler: Lipozomlar, loratadin, mukoadhesif, kitosan, intranazal

***Correspondence:** nbavarsad@ajums.ac.ir, **Phone:** 00989163054055, **ORCID-ID:** orcid.org/0000-0002-7872-0273

Received: 05.08.2020, **Accepted:** 09.11.2020

INTRODUCTION

Allergic rhinitis (AR) is an inflammation of the nasal mucosa, caused by the exposure to allergens. Generally, it involves four primary symptoms, namely sneezing, rhinorrhea, nasal congestion, and nasal itching.[1,2] Most commonly prescribed medications for the treatment of AR include antihistamines, corticosteroids, and decongestants.

Loratadine is a long lasting second generation antihistamine, which is widely used in the treatment and management of various allergic disorders, such as rhinitis, urticarial, and upper respiratory tract infections.[3] Despite its fast absorption post oral administration, loratadine suffers from issue of poor oral bioavailability (40%), primarily owing to first-pass metabolism. In addition to this, loratadine has been previously shown to induce certain systemic side effects in the body, after oral administration. In particular, loratadine is associated with allergic reactions that involve rash, itching, difficulty in breathing, tightness in the chest, swelling of the mouth or face, and dizziness.[4] Thus, it is important to explore and utilize another route of administration to bypass the liver metabolism and overcome these systemic side effects.

Intranasal drug delivery appears to be a convenient and interesting route as it confers several advantages. In particular, it provides ample applicable area for improving the systemic absorption of drugs with low solubility.[5] The presence of highly vascularized sub-epithelial layer in the nasal membrane allows rapid onset of drug action. Additionally, this route bypasses first-pass metabolism, and ensures higher bioavailability of drugs even at lower doses.[6,7] However, the process of mucociliary clearance in this area as a defense mechanism against foreign particles acts as the major limitation of the intranasal route. In particular, this phenomena can lead to complete removal of the drug delivery system from the nasal cavity.[8]

Among the various nasal drug delivery systems, liposomes have been widely explored for both local and systemic purposes. Liposomes are phospholipid bilayer vehicles that confer several advantages, including biocompatibility, biodegradability, and targeted drug delivery. Additionally, liposomal drug delivery prevents enzymatic or chemical degradation of drugs.[9,10] Interestingly, coating of liposomes using mucoadhesive polymers might increase their drug residence time in the nasal cavity, and thus improve drug bioavailability.

Chitosan, a natural cationic polymer produced by deacetylation of chitin, can act as a mucoadhesive agent for drug delivery systems, which is mediated via electrostatic interactions with the negative charge of mucin in the nasal cavity. Thus, the use of chitosan assists in improving the overall residence time of the liposomes that further leads to an enhancement in drug bioavailability and permeation.[11]

The present study aimed to formulate mucoadhesive liposomes for intranasal delivery of loratadine, which could circumvent the first-pass hepatic metabolism and enhance the drug bioavailability.

MATERIALS AND METHODS

Materials

Loratadine was received as a kind gift from Shafa® Pharmaceutical Co. (Tahran, Iran). Cholesterol, chitosan, periodic acid, Schiff reagent, and dialysis tubing cellulose membrane were procured from Sigma-Aldrich (St. Louis, Missouri, United States of America). Soybean phosphatidylcholine was purchased from Lipoid GmbH (Ludwigshafen, Germany). Chloroform, methanol, acetic acid, sodium acetate tri-hydrate, and sodium monobasic and dibasic phosphate were acquired from Merck Co. (Darmstadt, Germany). All the chemicals used in the study were of analytical grade.

Preparation of liposomes

Liposomes were prepared using a thin film hydration method. Briefly, soybean phosphatidylcholine and cholesterol at a molar ratio of 7:4 and 100 mg loratadine were dissolved in 20 mL mixture of chloroform:methanol (volume ratio 2:1). Following this, the solvent was evaporated at 50°C, using a rotary evaporator (IKA RV05), until a thin film was formed. The resulting film was incubated at 4°C for 24 h in a refrigerator, to ensure complete evaporation of the solvent. After 24 h, the thin film was hydrated using 20 mL phosphate buffer (pH: 6.5) and agitated using ultrasonic bath (ELMA, t-710 DH) for 30 min at 50°C. For the production of chitosan-coated liposomes, chitosan solutions at the concentrations of 0.1% and 0.05% w/v (in 0.1% v/v acetic acid) were added drop wise into the liposomal suspension with continuous stirring for 1 h. Further, the mixtures were centrifuged at 15,000 rpm for 45 min at 20°C and the sediments were resuspended in phosphate buffer (pH: 6.5) at room temperature using a vortex, to achieve a homogeneous preparation.[12]

Loratadine encapsulation efficiency (EE)

For the calculation of EE, the liposomal suspension was centrifuged at 15,000 rpm for 30 min, at 20°C. Further, the resulting supernatant was analyzed using ultraviolet (UV) spectroscopy (WPA biowave2) at 249 nm. EE was determined using following equation:[13]

% Encapsulation = (Total amount of loratadine - amount of loratadine in the supernatant) × 100% / (total amount of loratadine)

Particle size and polydispersity index (PDI) analysis

The average particle size of the formulation was determined using Scatterscope 1, Qudix (Seoul, South Korea). Prior to the measurement, the liposomal suspension was diluted using filtered deionized water (1 to 20). Each sample was read in triplicates.

Differential scanning calorimetry (DSC)

DSC thermogram was recorded for lipids, chitosan, and the drug using DSC 1 METTLER TOLEDO Co. Certain amount of the samples was placed in an aluminum pan and scanned from 20°C-200°C, at a scanning rate of 10°C min^{-1}.

In vitro drug release studies

In vitro release profile for loratadine was evaluated using dialysis bag diffusion technique, in a dissolution apparatus dt800 ERWEKA Co. (Germany). Briefly, dialysis bags (cut-off: 12 KDa) containing the formulations were placed in baskets, and immersed into the flasks containing 300 mL of the release medium. The release medium comprised of a mixture of acetate buffer (pH: 5.5) and methanol at a ratio of 50:50, v/v. The temperature and rotation speed for the baskets were set at 37˚C and 100 rpm, respectively. The sample collection was performed at pre-defined time intervals of 0.5, 1, 2, 3, 4, 5, 6, and 24 h. At each time point, 1 mL of sample was collected and replaced with 1 mL of fresh medium. Following this, amount of loratadine in the collected samples was analyzed using UV spectroscopy at 249 nm. This test was performed in triplicates for each formulation.[14]

Mucoadhesion test

Mucoadhesive potential of the generated formulations was measured in terms of the adsorption of mucin (porcine stomach type II) by periodic acid/Schiff colorimetric method.[15,16]

Standard mucin solutions at the concentrations of 12.5, 6.25, 3.125, and 1.625 mg per 100 mL of phosphate buffer (pH: 5.5) were prepared. Further, 200 µL of periodic acid (10%) was added to 2 mL of each sample. The samples were incubated at 37˚C for 2 h. Post incubation, 200 µL of Schiff reagent was added to the mixtures, and UV absorbance was measured after 30 min at 555 nm.

For samples, 1 mL of mucin solution (0.125 mg/mL) was added to 1 mL of the liposomal suspensions. Further, liposomes were stirred for 1 h at 37˚C at 300 rpm. To determine the amount of free mucin, the samples were centrifuged at 15,000 rpm for 45 min at 20˚C. Further, 200 µL of periodic acid was added to the supernatants, and the samples were incubated at 37˚C for 2 h. Following this, 200 µL of Schiff reagent was added. After 30 min of incubation, the absorbance was measured at 555 nm using a spectrophotometer.

Stability study

For the assessment of stability, the formulations were stored at 4˚C for 3 months. The stability of the formulations was investigated in terms of particle size, PDI, and EE.

Statistical analyses

One-Way analysis of variance was used to compare the developed formulations. The multiple-comparison Tukey test was used to compare the mean values for different groups, and $p<0.05$ was considered statistically significant.

RESULTS

Characterization of the liposomes

In the present study, chitosan coated liposomal formulations were prepared and assessed for EE, particle size, and PDI. The results for all these parameters are summarized in Table 1. As shown in Table 1, the average size of nanoliposomes prior to the coating was recorded to be 193±3.3 nm. The addition of chitosan as a coating on liposomes resulted in particles with increased size, wherein coating with 0.05% and 0.1% chitosan resulted in particles with size 345±4.6 nm and 438±7.3 nm, respectively. Thus, coating process caused a significant increase in size of the particles ($p<0.05$). Further, EE of ~80% was recorded for uncoated and coated formulations, which confirmed the suitability of preparation method and coating process.

DSC thermogram

The DSC thermograms for loratadine, cholesterol, chitosan, soybean phosphatidylcholine, uncoated liposomes, and liposomes with 0.05% chitosan were recorded (Figure 1a-f, respectively). For loratadine, an endothermic peak was observed at 136˚C in the DSC curve (Figure 1a), whereas two peaks were recorded at 46.30˚C and 148.56˚C for cholesterol (Figure 1b). In comparison to this, a broad endothermic peak was observed at 54.27˚C for chitosan (Figure 1c). For phosphatidylcholine, an endothermic peak was recorded at 131˚C (Figure 1d). The thermograms for uncoated (Figure 1e) and coated liposomes (Figure 1f) exhibited broad endothermic peak at 80˚C-100˚C.

In vitro drug release

In vitro drug release profiles for the prepared liposomal formulations are shown in Figure 2. The drug release from the formulations was evaluated over a period of 24 h. After 24 h, maximum drug release of 99±0.03% was recorded for uncoated liposomes. For coated liposomes, a comparatively slow release rate was recorded, wherein liposomes coated with 0.05% and 0.1% chitosan displayed drug release of 94±0.05% and 81±0.02%, respectively. Therefore, coating of liposomes provided a controllable drug release rate. The values for kinetics parameters and their regression are listed in Table 2. The selection of kinetics model was based on the higher value of r^2. In particular, zero-order model was found to be the most suitable kinetics model for all formulations, and chitosan coating showed no effect on kinetics model.

Stability of formulations

The results for stability study for the formulations, after 3 months of storage, are shown in Table 3. Interestingly, significant changes were recorded in case of uncoated liposomal formulation. Particularly, the size of the particles increased from 193 nm to 426 nm, and PDI increased from 0.41 to 0.65. In addition to this, EE reduced from 83% to 49%. Importantly,

Table 1. Characteristics of different formulations (mean ± SD, n=3)

Formulations	Encapsulation efficiency (%)	Particle size (nm)	PDI
Uncoated liposomes	83±4.3	193±3.3	0.41±0.05
0.05% chitosan-coated liposomes	78±4.6	345±4.6	0.54±0.08
0.1% chitosan-coated liposomes	81±3.9	438±7.3	0.69±0.03

SD: Standard deviation, PDI: Polydispersity index

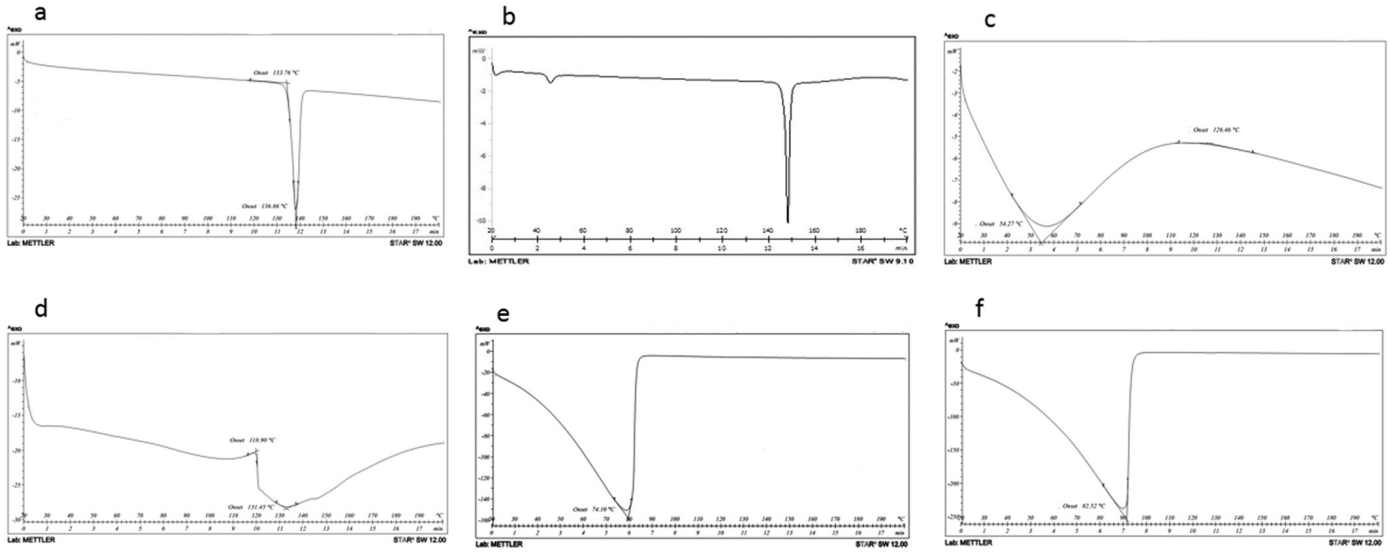

Figure 1. Differential scanning calorimetry thermograms for a) loratadine, b) cholesterol, c) chitosan, d) phosphatidylcholine, e) uncoated liposomes, and f) coated liposomes

coated formulations displayed no significant changes in the values of these parameters ($p>0.05$).

Mucin adsorption study

Chitosan is a polycationic polymer that interacts via electrostatic interactions with anionic groups present in the mucus layer, such as mucin. In particular, mucin is the most important component of mucus layer. The flexibility of chitosan backbone ensures ease of interaction between chitosan molecules and the mucus layer.[17] Thus, the present study assessed mucin adsorption by nanoliposomes (uncoated and coated). As shown in Figure 3, chitosan-coated liposomes exhibited a higher mucin adsorption, which was >3-folds higher as compared to uncoated liposomes. Interestingly, no significant differences were recorded for mucin adsorption behavior of the formulations coated with 0.05% and 0.1% chitosan ($p>0.05$).

DISCUSSION

Loratadine is a long lasting second-generation antihistamine. It is lipophilic nature and belongs to class II Biopharmaceutical Classification System. Thus, it is characterized by low

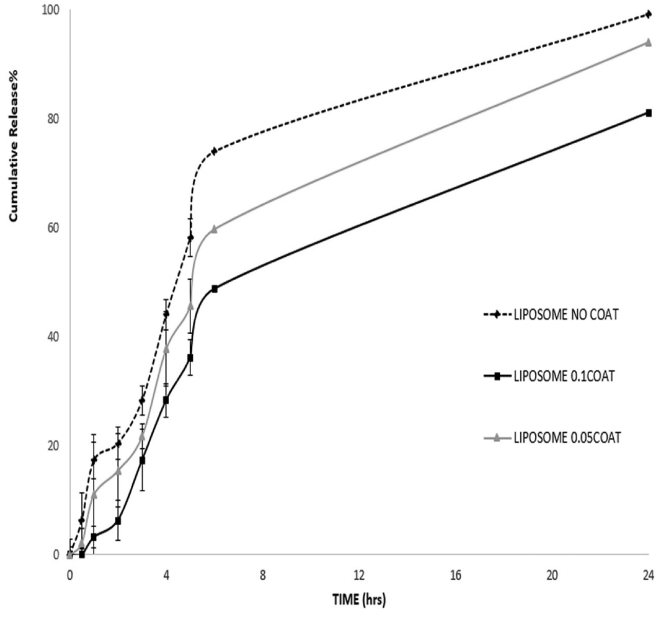

Figure 2. In vitro cumulative percentage of drug release expressed as a function of time (mean ± SD, n=3)

SD: Standard deviation

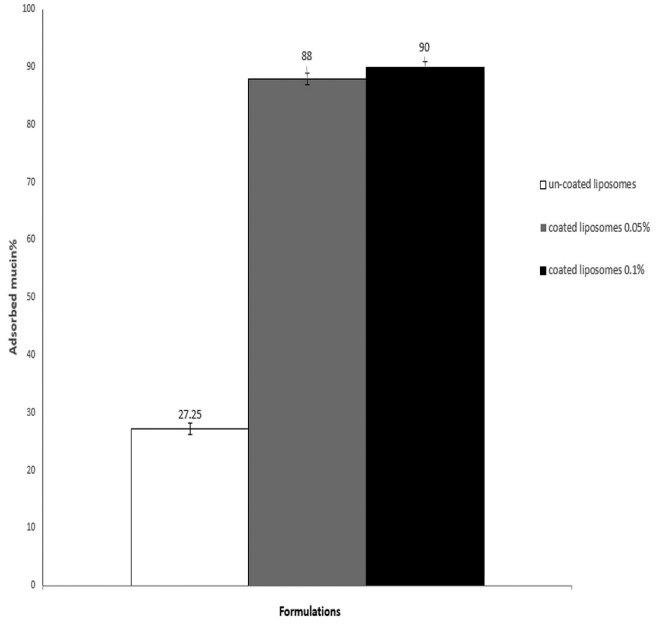

Figure 3. Mucoadhesive capacity of the formulations (expressed as percentage of mucin adsorbed, mean ± SD, n=3)

SD: Standard deviation

Table 2. Drug release kinetics for the generated formulations

		Liposomal formulations		
Kinetic model	**Parameters**	**Uncoated**	**0.05% chitosan coated**	**0.1% chitosan coated**
Zero order	R^2	0.977	0.994	0.98
	K_0 (mg h^{-1})	1.3994	1.1771	1.1398
Higuchi	R^2	0.8785	0.9113	0.9212
	K_H (mg cm^2 h^{-1})	3.4836	3.0972	3.5243
First order	R^2	0.9069	0.8326	0.9384
	K_1 (h^{-1})	-0.3905	0.4496	0.5556
Korsmeyer-Peppas	R^2	0.9566	0.976	0.9798
	K	1.546	1.0787	1.6027
	N	0.9061	1.0997	1.6027

Table 3. Characteristics of the formulations after 3 months of storage at 4˚C (mean ± SD, n=3)

Formulations	Encapsulation efficiency (%)	Particle size (nm)	PDI
Uncoated liposomes	49±6.6	426±6.7	0.65±0.06
0.05% chitosan-coated liposomes	71±3.8	360±4.7	0.59±0.09
0.1% chitosan-coated liposomes	72±8.1	450±2.7	0.73±0.07

SD: Standard deviation, PDI: Polydispersity index

solubility and high permeability.[18] In the present study, different formulations of uncoated and coated liposomes loaded with loratadine were developed, and evaluated for intranasal administration. The results of the study showed that thin film hydration method provided a suitable method for successful preparation of liposomal preparation. All the developed formulations were characterized by submicron-sized vesicles, which exhibited acceptable stability and high EE. Importantly, coating of liposomes with chitosan resulted in a significant increase in the size of the particles.

The interaction between chitosan and liposomes could be attributed to a combination of adsorption coagulation and bridging between them. Interestingly, previous studies have provided evidences for hydrogen bonding between chitosan and the phospholipid head groups, and hydrophobic interaction between hydrophobic segments of chitosan and soybean phosphatidylcholine.[19,20] The coating of liposomes with chitosan resulted in an increase in the mucoadhesive potential by more than 3-folds, which is suggestive of a significant potential for overcoming the nasal drug delivery limits for shorter residence time and mucociliary clearance. Mucoadhesive potential of chitosan-based delivery systems are mostly contributed by the presence of ionic interactions between the cationic primary amino groups of chitosan and the anionic substructures of the mucus. In addition to this, the hydrophobic interactions might also act as a contributing factor for this mucoadhesive potential.[21]

To study the interactions between various components and thermal events, DSC was performed. The DSC thermogram for loratadine showed an endothermic peak at 136˚C that correlated with the melting point of the crystals. The thermogram for cholesterol first displayed a shallow endothermic peak at 46.30˚C and an endothermic sharp peak at 148.56˚C, which are attributed to its melting point. Chitosan exhibited broad endothermic peak at 54.27˚C, which is related to the polymer phase transition from glassy to rubbery state. Phosphatidylcholine thermogram displayed a broad endothermic peak at 131˚C that might be attributed to its physical change. In case of uncoated and coated liposomes, only a broad endothermic peak was observed at 80˚C-100˚C, which was associated with evaporation of water.[22] The disappearance of the components peak can be related to the interaction between the ingredients of liposome to form liposomal bilayer and appropriate encapsulation of loratadine inside this lipid bilayer.[23] The results of the present study are consistent with the findings of previous studies. Alshweiat et al.[24] investigated the nasal delivery of loratadine in a nanosuspension form, wherein DSC thermograms depicted a single endothermic peak at 135˚C for loratadine. In comparison to this, the formulated loratadine showed a shifted peak with a reduced intensity, toward the lower melting point of loratadine.[24] In another study, Singh et al.[25] investigated the nasal delivery of mucoadhesive *in situ* gel of loratadine, and the disappearance of characteristic endothermic peak of loratadine in this formulation was described in terms of inclusion of loratadine into the formulated preparation. Similar to present study, only a broad peak for water loss was detected in case of this complex.

The coating of liposomes with chitosan showed a significant effect on the drug release rate from liposomes, at different time intervals. As shown in Figure 2, the percentage of drug release from coated liposomes was lower as compared to uncoated liposomes, at all examined time intervals. This effect might be attributed chitosan mediated stabilization of the liposomal membrane by adherence to the surface, and formation of a coated layer that acts as a barrier against the release of drug from the surface. The data were analyzed using different fitting models for controlled release mechanisms. Interestingly, the models of controlled release mechanisms for liposomes coated with chitosan were found to be in agreement with the release behavior of uncoated liposomes.[20,26]

Stability studies for the formulations showed that coated liposomes exhibited little but non-significant changes in the size and PDI, over a period of 3 months. Therefore, in addition to mucoadhesiveness, coating of the liposomes improved their shelf life also.

In the view of insignificant effects of high concentration of chitosan coating on the mucoadhesiveness of the loratadine loaded liposomes and negative effects of high concentration of chitosan on particle size and PDI of the formulations, liposomes coated with lower percentage of chitosan (0.05%) was selected as the optimum formulation, intended to be used for the treatment of AR. To establish the efficacy of selected preparation, *in vivo* studies would be performed in future.

CONCLUSION

The present study reported the development of chitosan-coated liposomes, and the developed formulation was found to be a suitable delivery system for intranasal administration of loratadine. Chitosan-coated liposomes exhibited suitable release profile and improved mucoadhesiveness. In future, *in vivo* studies would be conducted to further establish the therapeutic efficacy of the developed formulation.

ACKNOWLEDGMENTS

This paper is issued from Pharm D thesis of Negar Mohamadi and financial support was provided by a grant (N-9608) from vice chancellor of research of Ahvaz Jundishapur University of Medical Sciences, Ahvaz, Iran.

Conflict of interest: The authors have no conflicts of interest to declare. The experiments were conducted in full compliance with local regulatory principles of ethics committee of Ahvaz Jundishapur University of Medical Sciences (Ethics code: IR.AJUMS.REC.1396.770).

REFERENCES

1. Greiner AN, Hellings PW, Rotiroti G, Scadding GK. Allergic rhinitis. Lancet. 2011;378:2112-2122.
2. Bousquet J, Khaltaev N, Cruz AA, Denburg J, Fokkens W, Togias A, Zuberbier T, Baena-Cagnani C, Canonica G, Van Weel C. Allergic rhinitis and its impact on asthma (aria). Allergy. 2008;63:8-160.
3. Kroll V, Nothofer B, Werdermann K. Allergic bronchial asthma treated with loratadine. Fortschr Med. 1993;111:76-78.
4. Borgaonkar P, Virsen T, Hariprasanna R, Najmuddin M. Formulation and *in vitro* evaluation of buccal tablets of loratadine for effective treatment of allergy. Int J Res Pharm Chem. 2011;1:551-559.
5. Üner M, Karaman EF, Aydoğmuş Z. Solid lipid nanoparticles and nanostructured lipid carriers of loratadine for topical application: Physicochemical stability and drug penetration through rat skin. Trop J Pharm Res. 2014;13:653-660.
6. Bitter C, Suter-Zimmermann K, Surber C. Nasal drug delivery in humans. In: C Surber, P Elsner, MA Farage, eds. Topical applications and the mucosa. Karger Publishers; 2011:20-35.
7. Davis SS. Delivery of peptide and non-peptide drugs through the respiratory tract. Pharm Sci Technol Today. 1999;2:450-456.
8. Singh AK, Singh A, Madhv NS. Nasal cavity, a promising transmucosal platform for drug delivery and research approaches from nasal to brain targetting. J Drug Deliv Ther. 2012;2:22-33.
9. Marttin E, Schipper NG, Verhoef JC, Merkus FW. Nasal mucociliary clearance as a factor in nasal drug delivery. Adv Drug Del Rev. 1998;29:13-38.
10. Romeo V, DeMeireles J, Sileno A, Pimplaskar H, Behl C. Effects of physicochemical properties and other factors on systemic nasal drug delivery. Adv Drug Del Rev. 1998;29:89-116.
11. Sharma A, Sharma US. Liposomes in drug delivery: Progress and limitations. Int J Pharm. 1997;154:123-140.
12. Mombeini M, Saki G, Khorsandi L, Bavarsad N. Effects of silymarin-loaded nanoparticles on ht-29 human colon cancer cells. Medicina (Kaunas). 2018;54:1-9.
13. Kouchak M, Malekahmadi M, Bavarsad N, Saki Malehi A, Andishmand L. Dorzolamide nanoliposome as a long action ophthalmic delivery system in open angle glaucoma and ocular hypertension patients. Drug Dev Ind Pharm. 2018;44:1239-1242.
14. Bavarsad N, Kouchak M, Mohamadipour P, Sadeghi-Nejad B. Preparation and physicochemical characterization of topical chitosan-based film containing griseofulvin-loaded liposomes. J Adv Pharm Technol Res. 2016;7:91-98.
15. Kisel M, Kulik L, Tsybovsky I, Vlasov A, Vorob'Yov M, Kholodova E, Zabarovskaya Z. Liposomes with phosphatidylethanol as a carrier for oral delivery of insulin: studies in the rat. Int J Pharm. 2001;216:105-114.
16. Saladini B, Bigucci F, Cerchiara T, Gallucci MC, Luppi B. Microparticles based on chitosan/pectin polyelectrolyte complexes for nasal delivery of tacrine hydrochloride. Drug Deliv Trans Res. 2013;3:33-41.
17. Takeuchi H, Yamamoto H, Niwa T, Hino T, Kawashima Y. Enteral absorption of insulin in rats from mucoadhesive chitosan-coated liposomes. Pharm Res. 1996;13:896-901.
18. Rodriguez Amado JR, Prada AL, Duarte JL, Keita H, da Silva HR, Ferreira AM, Sosa EH, Carvalho JCT. Development, stability and *in vitro* delivery profile of new loratadine-loaded nanoparticles. Saudi Pharm J. 2017;25:1158-1168.
19. Refai H, Hassan D, Abdelmonem R. Development and characterization of polymer-coated liposomes for vaginal delivery of sildenafil citrate. Drug Deliv. 2017;24:278-288.
20. Mady MM, Darwish MM. Effect of chitosan coating on the characteristics of dppc liposomes. J Adv Res. 2010;1:187-191.
21. Jøraholmen MW, Vanić Ž, Tho I, Škalko-Basnet N. Chitosan-coated liposomes for topical vaginal therapy: Assuring localized drug effect. Int J Pharm. 2014;472:94-101.
22. Merlusca IP, Matiut DS, Lisa G, Silion M, Gradinaru L, Oprea S, Popa IM. Preparation and characterization of chitosan-poly(vinyl alcohol)-neomycin sulfate films. Polym Bull. 2018;75:3971-3986.
23. Zhai B, Wu Q, Wang W, Zhang M, Han X, Li Q, Chen P, Chen X, Huang X, Li G, Zhang Q, Zhang R, Xiang Y, Liu S, Duan T, Lou J, Xie T, Sui X. Preparation, characterization, pharmacokinetics and anticancer effects of pegylated β-elemene liposomes. Cancer Biol Med. 2020;17:60-75.
24. Alshweiat A, Csóka I, Tömösi F, Janáky T, Kovács A, Gáspár R, Sztojkov-Ivanov A, Ducza E, Márki Á, Szabó-Révész P, Ambrus R. Nasal delivery of nanosuspension-based mucoadhesive formulation with improved bioavailability of loratadine: preparation, characterization, and *in vivo* evaluation. Int J Pharm. 2020;579:119166.
25. Singh RM, Kumar A, Pathak K. Thermally triggered mucoadhesive in situ gel of loratadine: Β-cyclodextrin complex for nasal delivery. AAPS PharmSciTech. 2013;14:412-424.
26. Gibis M, Ruedt C, Weiss J. *In vitro* release of grape-seed polyphenols encapsulated from uncoated and chitosan-coated liposomes. Food Res Int. 2016;88:105-113.

Turk J Pharm Sci 2021;18(4):498-509
DOI: 10.4274/tjps.galenos.2020.03443

ORIGINAL ARTICLE

Formulation and Evaluation of Enteric Coated Elementary Osmotic Tablets of Aceclofenac

Aseklofenak Enterik Kaplı Elementer Ozmotik Tabletlerin Formülasyonu ve Değerlendirilmesi

Shankhadip NANDI[1]*, Ayan BANERJEE[2], Khandekar Hussan REZA[2]

[1]Eminent College of Pharmaceutical Technology, Department of Pharmaceutics, Kolkata, India
[2]Bengal School of Technology, Department of Pharmaceutics, Chinsurah, India

ABSTRACT

Objectives: This study aimed to develop a controlled drug delivery device for aceclofenac, a non-steroidal anti-inflammatory drug. Therefore, the agent was projected to develop an osmotic pump with enteric coating. The strength of the semipermeable membrane was improved by optimizing the formulation of the device, which can control the drug release over a prolonged period of time.

Materials and Methods: The formulations were designed and optimized by using the statistical design of experiment followed by 3^2 factorial design to discover the best formulation. Several evaluation tests were performed to assess the physical parameters of the formulations. The percentage drug release of the formulations was observed for up to 9 h.

Results: The model 3D graph analysis indicated that as an osmogen, a higher percentage of potassium chloride was utilized more effectively than mannitol for the rapid dissolution of osmotic tablets. The optimized formulation can release 88.60±0.02% up to 9 h. The accelerated stability study confirmed that the optimized formulation was stable.

Conclusion: The formulated osmotic tablets of aceclofenac were therapeutically safe and effective and did not release any drug content in the simulated gastric medium for a predetermined time.

Key words: Statistical design of experiment, 3^2 factorial design, 3D graph analysis, osmotic tablet

ÖZ

Amaç: Bu çalışma, bir non-steroidal antienflamatuvar ilaç olan aseklofenakın kontrollü bir ilaç verme cihazını formüle etmeyi hedeflemiştir. Bu amaçla, enterik kaplamalı bir ozmotik pompa geliştirmesi öngörülmüştür. Yarı geçirgen zarın kuvveti ilacın uzun bir süre boyunca salımını kontrol edebilen cihazın formülasyonunu optimize ederek geliştirilmiştir.

Gereç ve Yöntemler: Formülasyonlar, en iyi formülasyonu bulmak için deneyin istatistiksel tasarımı ve ardından 3^2 faktörlü tasarım kullanılarak tasarlanmış ve optimize edilmiştir. Formülasyonların fiziksel parametrelerini değerlendirmek için çeşitli değerlendirme testleri yapılmıştır. Formülasyonların yüzde ilaç salımı 9 saate kadar gözlenmiştir.

Bulgular: Model 3D grafik analizi, ozmotik tabletlerin hızlı çözünmesi için bir ozmojen olarak mannitolden daha yüksek bir potasyum klorür yüzdesinin daha etkili bir şekilde kullanıldığını göstermiştir. Optimize edilmiş formülasyon, 9 saate kadar ilacın 88,60±%0,02'sini salabilmektedir. Hızlandırılmış stabilite çalışması, optimize edilmiş formülasyonun stabil olduğunu doğrulamıştır.

Sonuç: Aseklofenakın formüle edilmiş ozmotik tabletleri terapötik olarak güvenli ve etkili bulunmuş ve önceden belirlenmiş bir süre boyunca simüle edilmiş gastrik ortamda herhangi bir ilaç içeriği salmamıştır.

Anahtar kelimeler: Deneyin istatistiksel tasarımı, 3^2 faktör tasarımı, 3D grafik analizi, ozmotik tablet

***Correspondence:** shankhadipnandi@gmail.com, **Phone:** +91-9804344736, **ORCID-ID:** orcid.org/0000-0002-7673-7645

Received: 26.05.2020, **Accepted:** 16.11.2020

INTRODUCTION

Drug delivery refers to the methods, formulations, skills, and systems for carrying drug substances in the human body used to attain the desired therapeutic outcomes safely.[1] Novel drug delivery systems can diminish the related difficulties by improving the efficacy, safety, product shelf life, and patient compliance.[2] Ideal oral drug delivery systems uninterruptedly convey a measurable and duplicable amount of drugs over a prolonged period. Controlled release dosage form include systems that can furnish a drug for its absorption at zero-order magnitude.[3,4]

The osmotic drug delivery systems utilized for controlled delivery of drugs are now well recognized in human and veterinary medication.[5] Osmotically controlled oral drug delivery systems apply osmotic pressure, which is developed in the system for the controlled delivery of drugs.[6] These osmotic systems can deliver drugs in to a large extent, and the delivery is independent of the physiological factors of the gastrointestinal tract and drug concentration.[7] The drug release from these devices is dependent on the coating thickness of the device, drug's solubility in the core tablet, level of leachable constituents in the coating, and changes in the osmotic pressure across the semipermeable membrane.

Oral osmotic pump tablets became popular for their numerous advantages, such as simple operation, easy formulation, zero-order delivery rate, and reduced dosing frequency with improved patient compliance.[8,9]

Aceclofenac (2-[2-[2-(2,6-dichloroanilino)phenyl]acetyl]oxyacetic acid) is a phenylacetic acid derivative belonging to the category of non-steroidal anti-inflammatory drugs (NSAIDs).[10,11] Aceclofenac inhibits the enzyme cyclo-oxygenase in the body. This enzyme is engaged in the production of prostaglandins, which results in inflammation and pain.[12,13] Aceclofenac can be used as an antirheumatic, anti-inflammatory, and analgesic (effective pain killer for the lower backache and dental). This compound is also used in the treatment of osteoarthritis, rheumatoid arthritis, gynecological pain, and alkylosing spondylitis in an oral dose of 200 mg daily.[14,15] Reduced doses should be used in patients with hepatic impairment.[16,17] Aceclofenac possesses higher antipyretic, analgesic, and anti-inflammatory action than any other NSAIDs, thus achieving better patient compliance.[18]

The long-term use of NSAIDs associated with different treatments causes heart burn, vertigo, hepatic toxicity, epigastric discomfort, dyspepsia, and abdominal pain.[19] However, aceclofenac offers enhanced gastric tolerance compared with indomethacin, naproxen, and diclofenac, which is required for chronic treatment.[18] Aceclofenac is practically insoluble in water and has a molecular weight of 354.19 g/mol, pK_a value of 4.7, partition coefficient of 1.86, and biological half-life of 4 h.[18,20,21] Aceclofenac meets all the criteria for being an ideal drug candidate for designing osmotic drug delivery systems.[8]

Literature survey showed that the marketed products of osmotic tablets for any NSAIDs are unavailable, whereas such type of products are available for antihistamine, anti-hypertensive, anti-diabetic, and anticonvulsant drugs; however, none of these tablets are enteric coated.[8,22] Aceclo, Aceclo SR, Acenac SR, Hifenac, Hifenac SR tablets, etc., are the currently available marketed film-coated preparations of aceclofenac. Hence, this study aimed to formulate enteric coated elementary osmotic tablets of aceclofenac as a NSAID to explore its novel opportunities.

Given that the osmotic tablet was fabricated with enteric coating, any drug content was not released from the osmotic tablet in stomach. Hence, the most common adverse effects and contradictions related to aceclofenac for its gastric impairment can be prevented.

MATERIALS AND METHODS

Aceclofenac and cellulose acetate were purchased from Simson Pharma (Mumbai, India). Micro-crystalline cellulose, mannitol (MANN), polyvinyl pyrrolidone K30, sodium lauryl sulfate, magnesium stearate, talc, and ethyl cellulose were procured from Loba Chemie Pvt. Ltd. (Mumbai, India). Potassium chloride (KCl) was acquired from Merck Specialities Pvt. Ltd. (Mumbai, India). Cellulose acetate phthalate was obtained from Spectrochem Pvt. Ltd. (Mumbai, India). Changshu Hongsheng Fine Chemicals (Changshu City) provided the ethanol. Acetone and methanol were supplied by Qualigens Fine Chemicals (Mumbai, India). All the chemicals, reagents, and solvents used were of analytical grade. Hifenac Tablets (100 mg) were obtained from a retail pharmacy store.

Statistical analysis by design of experiment (DOE)

It can be only attained by a statistical approach that supports the optimization of the product within a defined range.[23] Using the Design-Expert software, enteric coated osmotic tablets were developed and optimized. The statistical design used for the formulation development and optimization was proceeded by 3^2 factorial design.

Two factors were selected considering three levels of concentration. Two osmogens, namely, MANN and KCl (Table 1), were mixed at different ratios in accordance with the design requirement to produce nine formulations (Table 2). The rationality for osmogen selection was aimed at the development of a composition comprising high and low osmotic pressures. Literature had reported sodium chloride, KCl, and MANN are the most commonly used osmogens.[22] Sodium chloride was avoided due to its capability to elevate cardiogenic problems.

Table 1. Factors and levels considered for analysis

Levels (mg/tablet)	Factors for osmogens	
	Mannitol	Potassium chloride
Lower (-1)	50 mg	50 mg
Middle (0)	150 mg	150 mg
Upper (+1)	250 mg	250 mg

Drug identification

The drug (aceclofenac) used for this work was identified through several monographic tests and fourier transform infrared spectroscopy (FT-IR) study.

Compatibility of drug with excipients

The compatibility between drug and excipients was checked using a FT-IR spectrophotometer. The spectrum was recorded in the wavelength region of 4000 cm^{-1} to 400 cm^{-1}.

Pre-compression studies

The angle of repose, Carr's index, and Hausner's ratio were determined to access the flow property of the mixed powder blends and granules formed.

Fabrication of core aceclofenac tablets

The core tablets were fabricated by the moist granulation technique. The drug and excipients, apart from talc and magnesium stearate, were separately weighed. The weighed ingredients were methodically triturated in a porcelain mortar. Then, the mixture was passed through a sieve no: 60. Polyvinyl pyrrolidone K30 in warm water as a binder solution was added to the resultant powder to form a coherent mass. Granules were formed by passing the cohesive mass through a 12-mesh screen. The wet granules were then dried at 60˚C-70˚C for about 3 h. The completely dried granules were sieved through a 22-mesh screen to break down the lumps, and uniform, fine particles of granules were obtained. Talc and magnesium stearate were passed through a sieve no: 40 and mixed with the dried granules. The lubricated granules were then compacted into round-shaped core tablets using a single-punch compression machine.[24] Altering the ratio of excipients nine batches (F1-F9) of aceclofenac core tablets were prepared (Table 3).

Table 2. Interaction of the factor levels for formulation development

Formulation code	A: MANN (mg/tablet)	B: KCl (mg/tablet)	Interaction of levels	
			A: MANN	B: KCl
F1	50	50	-1	-1
F2	150	50	0	-1
F3	250	50	+1	-1
F4	50	150	-1	0
F5	150	150	0	0
F6	250	150	+1	0
F7	50	250	-1	+1
F8	150	250	0	+1
F9	250	250	+1	+1

MANN: Mannitol, KCl: Potassium chloride

Designing the coating composition for osmotic tablets

The maximal rupturing time of the coating membrane was determined by combining ethyl cellulose and cellulose acetate in three different ratios. Glycerol was employed as a plasticizer, and ethanol was used as the solvent. The coating solutions were applied to dummy tablet batches.

Optimization of the plasticizer for osmotic tablets

Glycerol was added as a plasticizer to the designated coating solution in various proportions to enhance the flexibility of osmotic device.

Coating of the core aceclofenac tablets

The compressed core tablets were coated using an optimized coating composition (Table 4) with the aid of dip coating technology. After coating, the tablets were dried for about 1-2 h at temperature of 40˚C-50˚C to eliminate the residual solvent.[24]

Designing an orifice

Using an insulin syringe needle (gauge 31 or 0.226 mm or 226 µm), an orifice was fashioned on the surface of each coated tablet.

Enteric coating of the tablets

Using a suitable enteric coating solution of cellulose acetate phthalate (Table 5), the tablets were finally prepared as enteric

Table 3. Composition of core aceclofenac tablets

S. no.	Ingredients	Amount (mg/tablet) present in core formulation								
		F1	F2	F3	F4	F5	F6	F7	F8	F9
1	Aceclofenac	100	100	100	100	100	100	100	100	100
2	Micro-crystalline cellulose	357	257	157	257	157	57	157	57	7
3	Mannitol	50	150	250	50	150	250	50	150	250
4	Potassium chloride	50	50	50	150	150	150	250	250	250
5	Polyvinyl pyrrolidone K30	25	25	25	25	25	25	25	25	25
6	Sodium lauryl sulfate	10	10	10	10	10	10	10	10	10
7	Magnesium stearate	5	5.5	5	4.5	5	5	5	4.5	5
8	Talc	3	2.5	3	3.5	3	3	3	3.5	3
9	Warm water	q.s.	q.s.	q.s.	q.s.	q.s.	q.s.	q.s.	q.s.	q.s.
Total weight (mg)		600	600	600	600	600	600	600	600	650

coated. After the enteric coating of the tablets, they were dried for about 1-1.5 h at a temperature of 50˚C-60˚C to eliminate the residual solvent.

Evaluation of enteric coated elementary osmotic tablets

The formulated tablets were evaluated by performing several tests, such as uniformity of weight, diameter and thickness, hardness, friability, percentage drug content, etc.

In vitro dissolution studies

In vitro dissolution studies of the formulated enteric coated osmotic tablets were carried out using USP type II dissolution apparatus (paddle type). The tablets were placed in the dissolution medium, and the dissolution process was started. Then, 5 mL samples were withdrawn at 0, 30, 60, 90, and 120 min from the dissolution medium containing 0.1 N HCl (pH 1.2), and after completion of 120 min, the tablets were immediately transferred to alkaline medium from the acidic medium. 5 mL samples were withdrawn at 150, 180, 210, 240, 270, 300, 330, 360, 390, 420, 450, 480, and 540 min from the dissolution medium containing phosphate buffer (pH 6.8). After sampling, an equal volume of fresh dissolution medium was replaced each time in the dissolution vessel to maintain the sink condition. The samples were diluted with the respective dissolution medium and filtered through a Whatman filter paper. Small aliquots of the filtrate were obtained in a cuvette, and the absorbance was measured by a ultraviolet-visible spectrophotometer at a wavelength 273.0 nm.[25,26] The percentage cumulative drug release was calculated.

Study of drug release kinetics

To explain the drug release kinetics, we fitted the *in vitro* drug release data of the optimized formulation to different mathematical models, such as zero-order, first order, Korsmeyer-Peppas, Higuchi, and Hixson-Crowell release kinetics.[27-29]

Comparative analysis of drug release with a marketed formulation

This study was performed to compare the drug release profile of the optimized formulation with a controlled release marketed formulation (Hifenac Tablet 100 mg).

Table 4. Composition of coating solution

S. no.	Ingredients	Quantity
1	Ethyl cellulose	3.45 g
2	Cellulose acetate	1.15 g
3	Glycerol	0.75 mL
4	Ethanol	q.s. to 50 mL

Table 5. Composition of the enteric coating solution

S. no.	Ingredients	Quantity
1	Cellulose acetate phthalate	10 g
2	Ethanol:acetone (1:3)	q.s. to 50 mL

Accelerated stability study

Stability studies were performed only for osmotic tablets from the best optimized batch. The osmotic tablets were quarantined and stored at a temperature 40˚C±2˚C and RH 75%±5% for a period of one month. Upon completion of the specific time period, the samples were withdrawn from the storage condition and evaluated for numerous parameters, such as loss on drying, visual appearance, and *in vitro* dissolution study.[30]

Given the limited time, a stability study was employed for a period of one month only. However, future work is projected to carry out 6 months of accelerated and 6 months of long-term analysis for this current study.

This study did not require any approval from the ethics committee nor any other patient informed consent because it did not focus on any clinical parameter nor utilize any human volunteer and animals for research development.

RESULTS AND DISCUSSION

Identification of aceclofenac

A number of monographic tests were performed (Table 6) to assess the identity of aceclofenac. The results obtained from particular tests were compared with the specifications required. All the results matched with their corresponding specifications, thus confirming the identity of aceclofenac.

FT-IR

The identification of aceclofenac and the compatibility study between the drug and excipients were performed using a FT-IR spectrophotometer. Physical compatibility was also checked visually. The results showed that the drug and excipients were physically compatible with each other.

The FT-IR characteristics of aceclofenac are almost identical to the spectra of genuine sample of aceclofenac (Figure 1). By scrutinizing the FT-IR spectra, the physical mixtures of aceclofenac with the different excipients exhibited the existence of aceclofenac characteristics bands at their similar wavenumbers (Figure 2, Table 7). This result specified that the drug was pure, and no chemical interaction occurred between the drug and excipients.

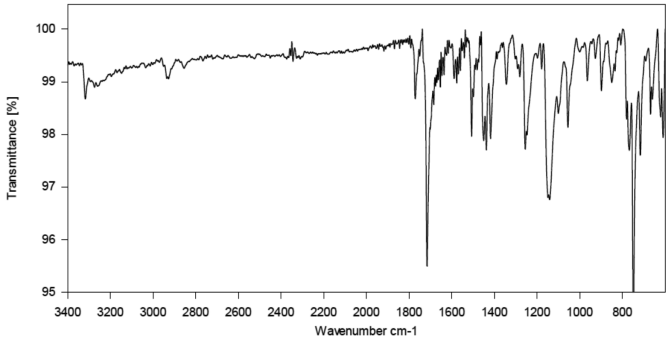

Figure 1. FT-IR spectrum of aceclofenac

FT-IR: Fourier transform infrared spectroscopy

Table 6. Identification of aceclofenac by performing numerous monographic tests

Tests	Expected result	Obtained result
About 10 mg aceclofenac was dissolved in 10 mL ethanol. To 1.0 mL of the solution, 0.2 mL mixture of equal volumes of a 0.6% (w/v) solution of potassium ferricyanide and a 0.9% (w/v) solution of ferric chloride (both were freshly prepared) were added. The resultant solution was allowed to stand and was protected from light for about 5 min. Then, 3.0 mL 1.0% (v/v) solution of hydrochloric acid was added	A blue color will develop, and a precipitate will be formed.	Blue color was developed and a precipitate was formed
Appearance of solution: A 5.0% (w/v) solution of aceclofenac in methanol	Clear	Clear
pH of 1.0% (w/v) solution of aceclofenac	6.5-8.5	7.25
Loss on drying: A total of 1.0 g aceclofenac was dried in a hot-air oven at 105°C for 3 h	Not more than 0.5%	0.4%
Assay: About 0.3 g aceclofenac was weighed accurately and dissolved in 40 mL methanol. The solution was titrated with 0.1 M sodium hydroxide. The end point was determined by the indicator method. A blank titration was also carried out (1 mL 0.1 M sodium hydroxide is equivalent to 0.03542 g aceclofenac)	-	95.21%

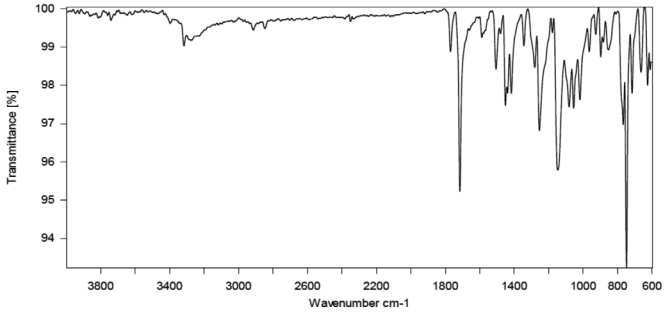

Figure 2. FT-IR spectrum of aceclofenac along with all excipients used
FT-IR: Fourier transform infrared spectroscopy

Table 7. Interpretation of FT-IR spectrum

Wave number of aceclofenac (cm^{-1})	Wave number of aceclofenac along with excipients (cm^{-1})	Interpretation
3317.60	3316.83	O-H stretching
1715.88	1715.49	C=O stretching (aromatic)
1619.84	1588.30	N-H bending
1456.27	1451.05	C-C stretching
1241.26	1253.97	C=C stretching
939.06	923.92	O-H bending

FT-IR: Fourier transform infrared spectroscopy

Pre-compression studies

Pre-compression studies were performed to check the parameters for aceclofenac, mixed powder blends, and granules formed. The results showed that value of all the pre-compression parameters, i.e., Carr's index, Hausner's ratio, and angle of repose were relatively less for granules compared with aceclofenac and powder blends formed (Table 8). Hence, as per the flow property of powders, aceclofenac and mixed powder blends exhibited a good flow property, whereas the formulated granules manifested an excellent flow property.[31,32]

Designing the coating composition of osmotic tablets

Compared with other coating compositions, ethyl cellulose:cellulose acetate (3:1) in solvent ethanol (100 mL) displayed the highest rupturing time of 4.5 h and can tolerate an osmotic pressure for a prolonged period (Table 9). Thus, the C3 coating solution was used in the coating of core aceclofenac tablets.

Optimization of the plasticizer amount for osmotic tablets

The maximum rupturing time of 4 h was determined when 0.75 mL glycerol was used as a plasticizer in the C3 coating solution (Table 10). Glycerol can provide elasticity for expansion and the maximum mechanical strength of the membrane. Thus, 0.75 mL glycerol was added to the optimized coating composition.

Evaluation of enteric coated elementary osmotic tablets

Post-compression parameters

Table 11 shows that the formulated tablets (F1-F8) were almost uniform in their weight, diameter, and thickness. The weight of the core tablets for batch F9 was higher (Table 3) compared with those of F1-F8 batches. Hence, batch F9 was not compared with other batches for these parameters.

The tablets from each batch exhibited adequate hardness and strength to withstand sufficient mechanical shocks during handling in manufacture, packaging, shipping, transport, etc. All the batches contained a satisfactory percentage of drug content in the formulated osmotic tablets (Table 11).

In vitro dissolution studies

The data obtained from *in vitro* dissolution studies (Table 12, 13) showed that any drug content was not released from the osmotic tablets in acidic medium (Figure 3-5). This finding proved the successful demonstration of enteric coating. It helped the device to control its drug release over a prolonged period of time and prevented gastric degradation by aceclofenac.

Table 8. Pre-compression studies of aceclofenac, mixed powder blends, and granules formed

Sample		Bulk density (g/cm^3)	Tapped density (g/cm^3)	Carr's index (%)	Hausner's ratio	Angle of repose (θ)
Aceclofenac		0.625	0.733	14.73	1.16	31.32
Powder blends	F1	0.622	0.730	14.79	1.17	35.44
	F2	0.610	0.718	13.15	1.17	35.10
	F3	0.618	0.722	14.95	1.16	34.21
	F4	0.640	0.731	15.18	1.14	34.08
	F5	0.605	0.711	14.90	1.175	35.80
	F6	0.621	0.742	14.95	1.19	37.21
	F7	0.635	0.750	15.23	1.18	37.01
	F8	0.627	0.734	14.57	1.14	33.90
	F9	0.621	0.755	17.74	1.21	40.09
Granules	F1	0.479	0.534	10.29	1.11	25.43
	F2	0.468	0.522	10.34	1.115	25.48
	F3	0.457	0.519	11.94	1.13	27.40
	F4	0.449	0.508	11.61	1.129	26.92
	F5	0.458	0.520	11.92	1.135	22.65
	F6	0.464	0.531	12.61	1.14	28.54
	F7	0.476	0.530	10.18	1.113	29.45
	F8	0.482	0.541	10.90	1.12	27.65
	F9	0.467	0.532	12.21	1.139	27.96

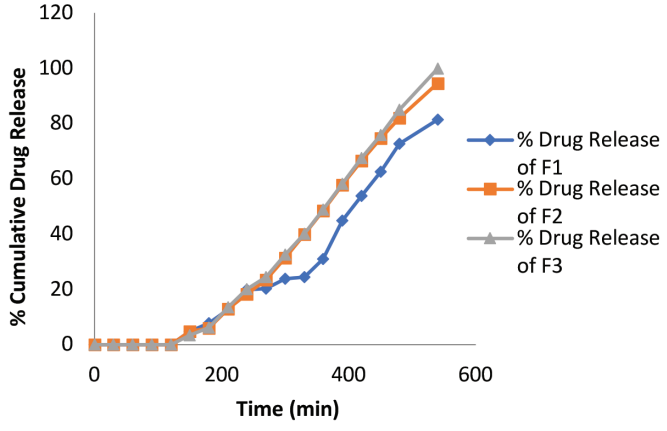

Figure 3. *In vitro* drug release study of osmotic tablets (F1-F3)

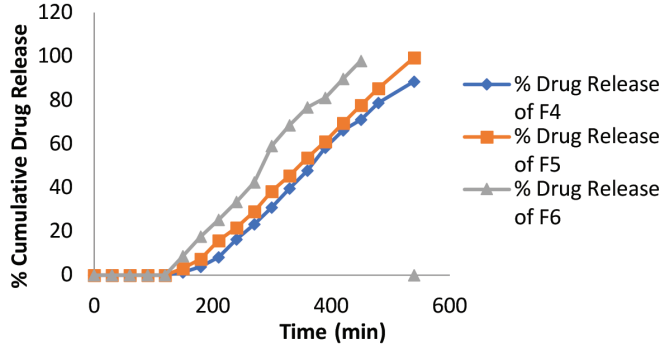

Figure 4. *In vitro* drug release study of osmotic tablets (F4-F6)

Statistical analysis

Statistical analysis by DOE using Design-Expert software

By analyzing the multiple regression analysis equation, dissolution times were reported to be linear type, thus proving that the factors did not interact. The equation obtained is demonstrated below:

Percentage drug release ($T_{80\%}$)= +440.92-46.00×MANN-63.00×KCl.

In the above case of percentage drug release (Table 14), KCl had a more negative effect than MANN. Thus, the increase in the concentration of KCl resulted in the increased time of drug release. On the other hand, MANN had a lesser effect because KCl has a greater osmotic pressure compared with MANN.[22] The drug was forced out of the orifice at a high release rate, reducing the time for 80% drug release ($T_{80\%}$). In this study, the drug release rate was controlled by optimizing the concentration of both osmogens.

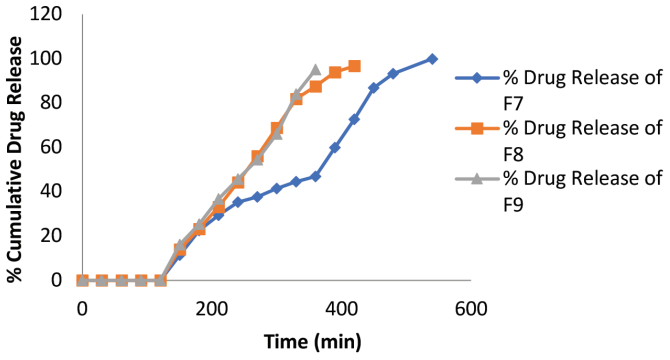

Figure 5. *In vitro* drug release study of osmotic tablets (F7-F9)

Table 9. Optimization of the coating composition

S. no.	Code	Coating materials	Rupturing time
1	C1	Ethyl cellulose:cellulose acetate (1:1) in ethanol	3.5 h
2	C2	Ethyl cellulose:cellulose acetate (1:3) in ethanol	2.0 h
3	C3	Ethyl cellulose:cellulose acetate (3:1) in ethanol	4.5 h

h: Hour

Table 10. Optimization of plasticizer amount

S. no.	Code	Amount of glycerol	Rupturing time
1	P1	0.35 mL	3.0 h
2	P2	0.50 mL	3.5 h
3	P3	0.60 mL	3.5 h
4	P4	0.75 mL	4.0 h
5	P5	0.90 mL	3.5 h

h: Hour

The model 3D graph analysis and contour plot analysis demonstrated that KCl had a greater effect on the dissolution time than MANN (Figure 6, 7). The dissolution time ($T_{80\%}$) was more diminished when the concentration of KCl increased compared with that of MANN. This result proved that the above consideration stated.

During the optimization study, the dissolution time was considered as a reference criterion within the range limits of the maximum and minimum values of dissolution time. The optimized ratio for using osmotic agents (MANN:KCl) was 81.91:111.65 (Figure 8). Among the various formulations, F4 had the ratio nearest to the desirability.

Drug release kinetics study

The drug release kinetics study for the optimized formulation (F4) showed that drug release from the device was independent of the drug concentration, following zero-order kinetics because it had the highest regression value (Figure 9, Table 15). Therefore, the drug release did not depend on the amount

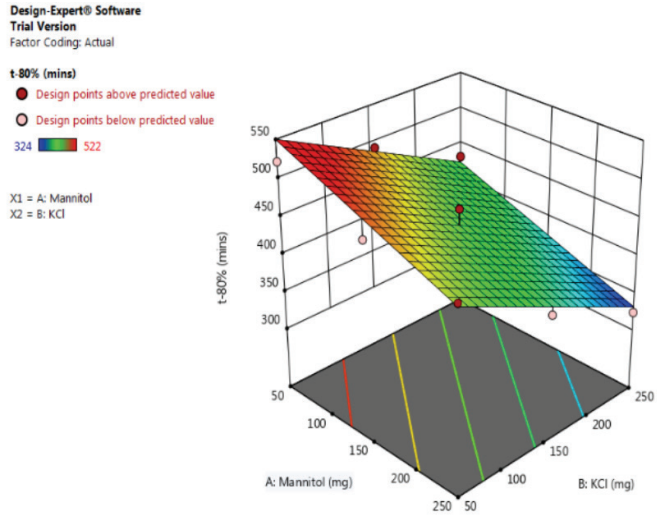

Figure 6. Model 3D graph analysis

Table 11. Post-compressive parameters of formulations

Formulation code	Average weight (mg)[b] ± SD	Diameter (mm)[a] ± SD	Thickness (mm)[a] ± SD	Hardness (kg/cm²)[a] ± SD	Friability (% w/w)[a] ± SD	Drug content (%)[a] ± SD
F1	672±0.05	12.04±0.05	3.11±0.12	5.8±0.14	0.75±0.04	98.58±0.627
F2	675±0.04	12.06±0.04	3.14±0.15	6.0±0.11	0.68±0.07	96.03±0.372
F3	671±0.01	12.00±0.06	3.19±0.11	6.5±0.14	0.52±0.01	99.86±0.672
F4	670±0.03	12.10±0.09	3.30±0.04	6.0±0.12	0.65±0.05	97.55±0.711
F5	671±0.06	12.10±0.03	3.58±0.12	5.9±0.13	0.71±0.06	100.12±0.12
F6	676±0.04	12.01±0.02	3.47±0.06	6.1±0.11	0.64±0.07	94.06±0.185
F7	675±0.10	12.05±0.02	3.28±0.04	6.5±0.13	0.50±0.04	95.16±0.188
F8	673±0.05	12.04±0.04	3.15±0.04	7.0±0.16	0.38±0.01	99.49±0.281
F9	706±0.09	12.07±0.03	3.48±0.02	6.0±0.15	0.65±0.06	98.20±0.418

All values are expressed as mean SD, [a]n=10, [b]n=20, SD: Standard deviation

present in the system, but it was completely dependent on the nature of the delivery device.

Comparative analysis of drug release with a marketed product

Given that the marketed product was film-coated, the drug was also released in an acidic medium (Table 16) which can often cause gastric impairment. The rate of drug release from the optimized formulation (F4) followed a constant linear trend compared with the marketed formulation in which the drug release was initially slow. However, it was superimposed at the later stage (Figure 10). The *in vitro* drug release data of optimized formulation (F4) was more closely fitted to the zero-order release kinetics model compared with the same of the marketed product (Figure 10).

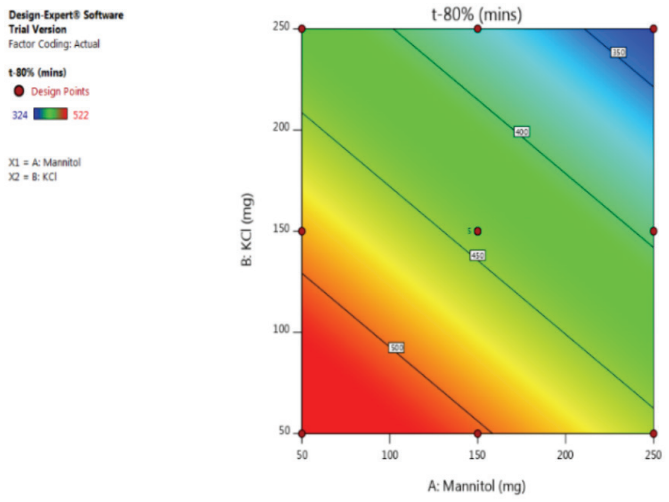

Figure 7. Contour plot analysis

Therefore, the optimized formulation (F4) was comparatively suited for controlled release of drug over a prolonged period of time and better patient compliance.

Accelerated stability study

Any significant degradation was not observed within the specified period in the accelerated stability study employed for the optimized batch (F4) of formulated osmotic tablets (Table 17). The study confirmed about the stability of optimized formulation (F4).

CONCLUSION

The *in vitro* drug release rate from the optimized batch (F4) of formulated osmotic tablets was 88.60%±0.02% in 9 h, and no evidence of drug release the from the device in acidic medium was observed, which justified the primary aim of the present study. The semipermeable membrane developed was extremely flexible and proficient to withstand satisfactory osmotic pressure. Thus, the formulated device

Table 12. Tabulation of % cumulative drug release from *in vitro* dissolution studies (F1-F5)

Dissolution media	Time (min)	Cumulative drug release (%)[a] ± SD				
		F1	F2	F3	F4	F5
0.1 N HCl (pH 1.2)	0	0	0	0	0	0
	30	0	0	0	0	0
	60	0	0	0	0	0
	90	0	0	0	0	0
	120	0	0	0	0	0
Phosphate buffer (pH 6.8)	150	4.84±0.04	4.69±0.05	3.32±0.02	1.19±0.04	3.19±0.01
	180	7.74±0.03	5.96±0.012	6.249±0.02	3.99±0.04	7.55±0.58
	210	12.79±0.04	12.85±0.25	13.56±0.58	8.24±0.27	15.86±0.24
	240	19.90±0.02	18.25±0.02	20.14±0.04	16.35±0.09	21.84±0.08
	270	20.35±0.04	23.40±0.38	24.47±0.04	23.40±0.025	29.17±0.02
	300	23.88±0.04	31.47±0.04	32.50±0.05	30.97±0.47	38.50±0.03
	330	24.47±0.05	39.87±0.05	40.21±0.08	39.76±0.05	45.61±0.01
	360	30.95±0.01	48.53±0.04	48.83±0.07	47.93±0.007	53.83±0.05
	390	44.92±0.02	57.88±0.47	58.12±0.01	58.28±0.02	61.12±0.02
	420	53.79±0.05	66.57±0.02	67.44±0.25	66.17±0.03	69.47±0.04
	450	62.62±0.01	74.69±0.04	75.80±0.03	71.19±0.07	77.86±0.05
	480	72.71±0.02	82.05±0.05	84.91±0.07	78.80±0.07	85.31±0.34
	540	81.40±0.04	94.59±0.25	99.89±0.09	88.60±0.02	99.51±0.14

All values are expressed as mean SD, [a]n=3, SD: Standard deviation

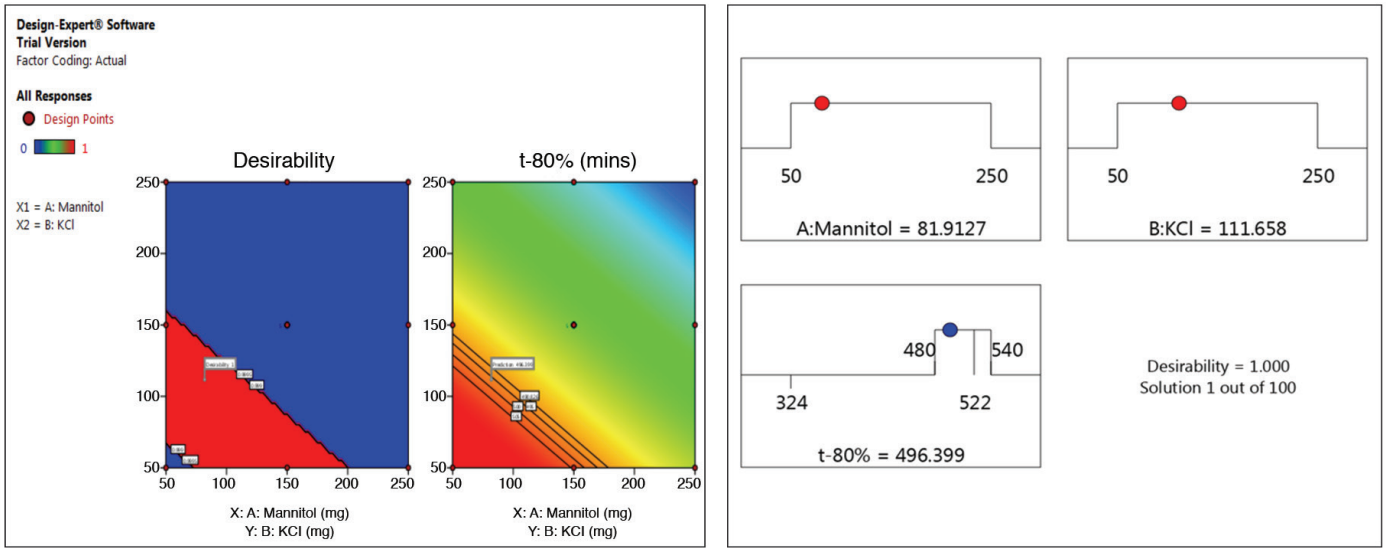

Figure 8. Optimized formulation with maximum desirability and design points

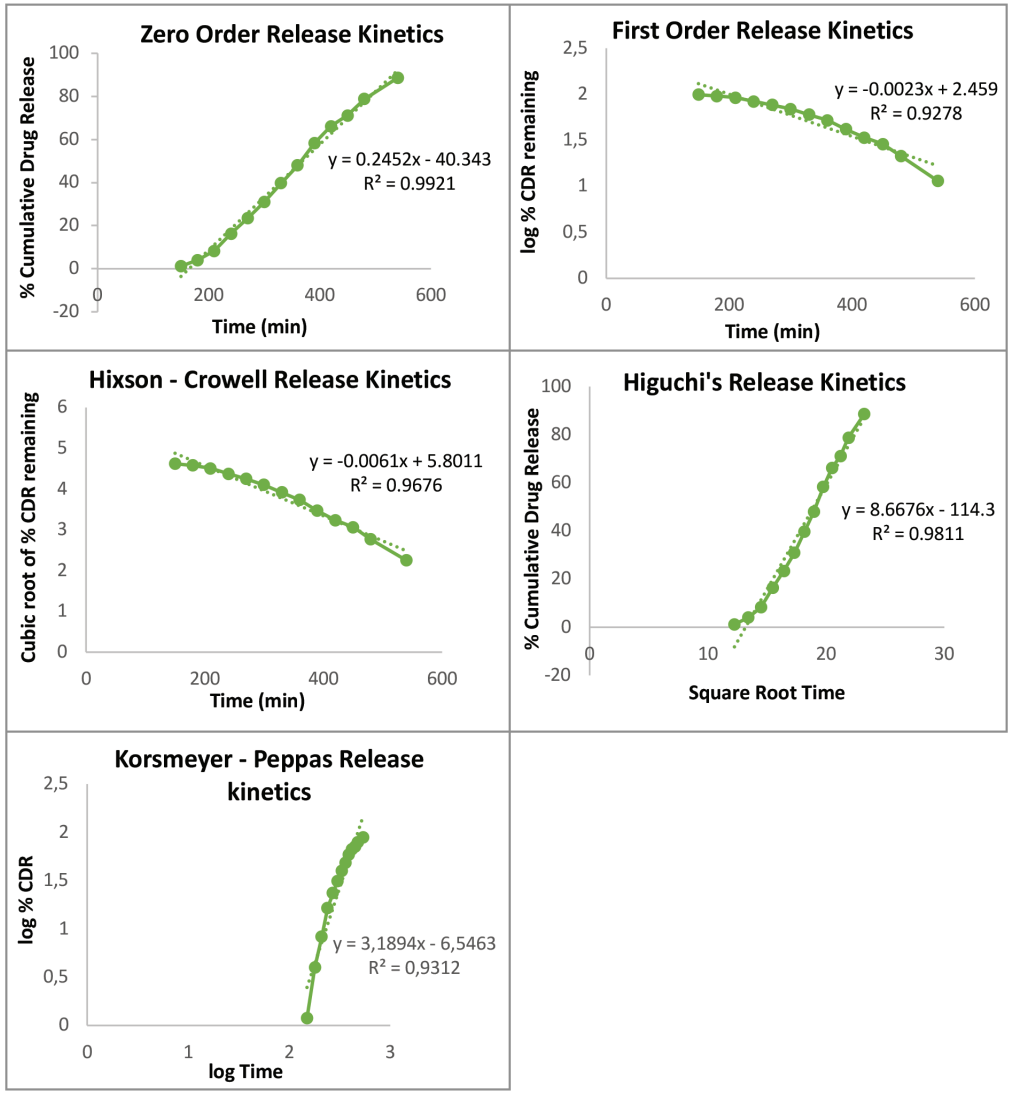

Figure 9. Fitting *in vitro* drug release data of optimized formulation (F4) in different release kinetics models

Table 13. Tabulation of % cumulative drug release from *in vitro* dissolution studies (F6-F9)

Dissolution media	Time (min)	Cumulative drug release (%)[a] ± SD			
		F6	F7	F8	F9
0.1 N HCl (pH 1.2)	0	0	0	0	0
	30	0	0	0	0
	60	0	0	0	0
	90	0	0	0	0
	120	0	0	0	0
Phosphate buffer (pH 6.8)	150	8.65±0.025	11.42±0.25	13.94±0.05	16.08±0.02
	180	17.66±0.07	22.55±0.025	23.28±0.02	25.34±0.27
	210	25.27±0.71	29.32±0.05	33.17±0.04	36.66±0.03
	240	33.53±0.07	35.20±0.05	44.30±0.17	45.75±0.14
	270	42.44±0.07	37.70±0.04	56.21±0.04	54.47±0.05
	300	59.13±0.07	41.33±0.08	68.81±0.02	66.02±0.07
	330	68.57±0.02	44.51±0.87	81.90±0.82	84.05±0.18
	360	76.62±0.02	46.78±0.14	87.47±0.05	95.10±0.24
	390	81.04±0.025	59.89±0.02	94.04±0.002	-
	420	89.77±0.05	72.59±0.58	96.67±0.05	-
	450	98.05±0.08	86.80±0.07	-	-
	480	-	93.25±0.08	-	-
	540	-	99.94±0.02	-	-

All values are expressed as mean SD, [a]n=3, SD: Standard deviation

Table 14. Time required to release a minimum of 80% drug from the formulations

Formulation code	F1	F2	F3	F4	F5	F6	F7	F8	F9
$T_{80\%}$ (min)	522	478	462	492	462	384	432	328	324

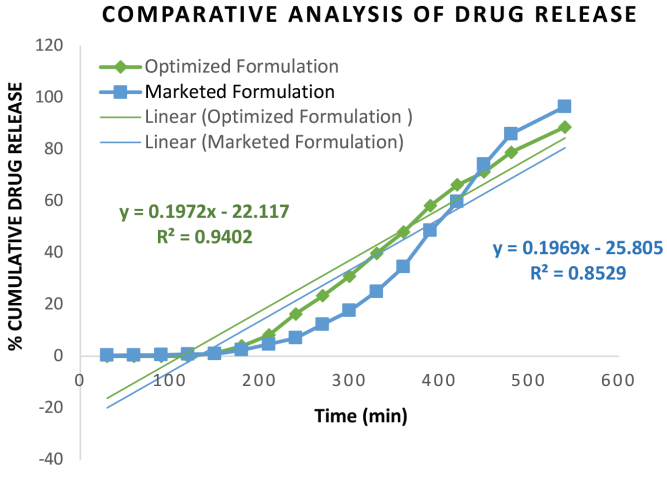

Figure 10. Comparison of drug release between optimized and marketed formulation

Table 15. Drug release kinetics study for optimized formulation (F4)

S. no.	Release kinetics	Regression equation	Regression value (R^2)
1	Zero order	y=0.2452x-40.343	0.9921
2	First order	y=-0.0023x+2.459	0.9278
3	Higuchi	y=8.6676x-114.3	0.9811
4	Korsmeyer-Peppas	y=3.1894x-6.5463	0.9312
5	Hixson-Crowell	y=-0.0061x+5.8011	0.9676

Table 16. Tabulation of % cumulative drug release from the optimized and marketed formulation

Dissolution media	Time (min)	Cumulative drug release (%)[a] ± SD	
		Optimized formulation (F4)	Marketed formulation (Hifenac tablet 100 mg)
0.1 N HCl (pH 1.2)	30	0	0.329±0.06
	60	0	0.397±0.01
	90	0	0.481±0.63
	120	0	0.763±0.72
Phosphate buffer (pH 6.8)	150	1.19±0.04	0.921±0.05
	180	3.99±0.04	2.43±0.07
	210	8.24±0.27	4.60±0.021
	240	16.35±0.09	7.06±0.58
	270	23.40±0.025	12.28±0.84
	300	30.97±0.47	17.61±0.01
	330	39.76±0.05	25.03±0.06
	360	47.93±0.007	34.53±0.05
	390	58.28±0.02	48.51±0.01
	420	66.17±0.03	59.64±0.14
	450	71.19±0.07	74.08±0.08
	480	78.80±0.07	85.88±0.04
	540	88.60±0.02	96.45±0.77

All values are expressed as mean SD, [a]n=3, SD: Standard deviation

Table 17. Accelerated stability study for optimized formulation (F4)

S. no.	Parameters	On 1st day	On 15th day	On 30th day
1	Visual appearance	White round-shaped tablets with smooth surface	White round-shaped tablets with smooth surface	White round-shaped tablets with smooth surface
2	Loss on drying (% w/w)[a] ± SD	0.51±0.04	0.51±0.04	0.52±0.03
3	Microbial or fungal growth	Absent	Absent	Absent
4	Average weight (mg)[b] ± SD	670±0.03	670±0.03	670±0.02
5	Diameter (mg)[b] ± SD	12.10±0.09	12.10±0.09	12.10±0.09
6	Thickness (mg)[b] ± SD	3.30±0.04	3.30±0.04	3.30±0.04
7	Hardness (kg/cm^2)[b] ± SD	6.0±0.12	6.0±0.12	6.0±0.10
8	Friability (% w/w)[b] ± SD	0.65±0.05	0.65±0.05	0.65±0.05
9	Drug content (%)[b] ± SD	97.55±0.711	97.55±0.711	97.55±0.711
10	*In vitro* drug release (%)[a] ± SD up to 9 h	88.60±0.02	88.60±0.02	88.60±0.03

All values are expressed as mean SD, [a]n=3, [b]n=10, SD: Standard deviation, h: Hour

can drug control the release over a prolonged period of time. The model 3D graph analysis engaged for the optimized device proved the greater effectiveness of KCl than MANN as an osmogen.

ACKNOWLEDGEMENTS

The authors would like to thank the laboratory facility of Bengal School of Technology, West Bengal for carrying out necessary research work and providing the compulsory requirements for successful completion of the research work.

Conflict of interest: No conflict of interest was declared by the authors. The authors are solely responsible for the content and writing of this paper.

REFERENCES

1. Mothilal M, Swati PS, Nelofar S, Damodharan N, Manimaran V, Lakshmi KS. Formulation and evaluation of aceclofenac compression coated tablets for colon drug delivery. Res J Pharm Biol Chem Sci. 2012;3:1062-1071.
2. Roco MC, Bainbridge WS. Societal implications of nanoscience and nanotechnology: maximizing human benefit. J Nanoparticle Res. 2005;7:1-13.
3. Ahuja N, Kumar V, Rathee P. Osmotic-controlled release oral delivery system: An advanced oral delivery form. Pharm Innov. 2012;1:116-124.
4. Rathore GS, Gupta RN. Formulation development and evaluation of controlled porosity osmotic pump delivery system for oral delivery of atenolol. Asian J Pharm. 2012;6:151-160.
5. Dasankoppa FS, Ningangowdar M, Sholapur H. Formulation and evaluation of controlled porosity osmotic pump for oral delivery of ketorolac. J Basic Clin Pharm. 2012;4:2-9.
6. Venkateswarlu BS, Pasupathi C, Pasupathi A, Jaykar B, Chandira RM, Palanisamy P. Osmotic drug delivery system: A review. J Drug Deliv and Ther. 2019;9:611-616.
7. Rastogi V, Shukla S, Singh R, Lal N, Yadav P. Microspheres: A Promising Drug Carrier. J Drug Deliv Ther. 2016;6:18-26.
8. Mathur M, Mishra R. A review on osmotic pump drug delivery system. Int J Pharm Sci Res. 2016;7:453-471.
9. Lachman L, Lieberman HA. The theory and practice of industrial pharmacy. (4th ed). New Delhi; CBS Publishers and Distributors; 2013:872-876.
10. Tripathi KD. Essentials of medical pharmacology. (7th ed). New Delhi; Jaypee Brothers Medical Publishers Pvt. Ltd; 2013:192-204.
11. Raza K, Kumar M, Kumar P, Malik R, Sharma G, Kaur M, Katare OP. Topical delivery of aceclofenac: challenges and promises of novel drug delivery systems. Biomed Res Int. 2014;2014:1-11.

12. Ashok CH, Bhaskar NV, Prakash PR. Design and characterization of press coated tablets of Aceclofenac for pulsatile delivery. Int J Pharm Sci Res. 2015;6:2902-2912.
13. Shivkant S, Roshan I, Prakash NB. Evaluation of formulation parameters for development of aceclofenac nanosuspension using Doe statistical tool. International J Drug Deliv Technol. 2016;6:142-150.
14. Ragidi A, Madhuri J, Anusha P, Venkateswara RT. Formulation and *in-vitro* evaluation of compression coated tablets of Aceclofenac for controlled release. World J Pharm Pharm Sci. 2012;2:216-222.
15. Patel PB, Patel TK. Efficacy and safety of aceclofenac in osteoarthritis: a meta-analysis of randomized controlled trials. Eur J Rheumatol. 2017;4:11-18.
16. Vohra F, Raut A. Comparative efficacy, safety, and tolerability of diclofenac and aceclofenac in musculoskeletal pain management: a systematic review. Indian J Pain. 2016;30:3-6.
17. Kamal AH, Malla SFE, Hammad SF. A review on uv spectrophotometric methods for simultaneous multicomponent analysis. Eur J Pharm Med Res. 2016;3:348-360.
18. Dave V, Paliwal S. A novel approach to formulation factor of aceclofenac eye drops efficiency evaluation based on physicochemical characteristics of *in vitro* and *in vivo* permeation. Saudi Pharm J. 2014;22:240-245.
19. Shaikh AC, Nazim S, Siraj S, Khan T, Patel MS, Zameeruddin M, Shaikh A. Formulation and evaluation of sustained release tablets of aceclofenac using hydrophilic matrix system. Int J Pharm Pharm Sci. 2011;3:145-148.
20. Jayanthi B, Madhusudhan S, Mohanta GP, Manna PK. Preformulation characterisation, designing and formulation of aceclofenac loaded microparticles. International J Drug Dev Res. 2012;4:186-196.
21. Kala S, Juyal D. Preformulation and characterization studies of aceclofenac active ingredient. Pharm Innov J. 2016;5:110-119.
22. Keraliya RA, Patel C, Patel P, Keraliya V, Soni TG, Patel RC, Patel MM. Osmotic drug delivery system as a part of modified release dosage form. ISRN Pharm. 2012;2012:528079.
23. Politis SN, Colombo P, Colombo G, Rekkas DM. Design of experiments (DoE) in pharmaceutical development. Drug Dev Ind Pharm. 2017;43:889-901.
24. Reza KH, Vikram NS, Kumaravelrajan R. Formulation and optimization of aceclofenac monolithic osmotic pump. Int J Pharm Sci Rev Res. 2011;6:42-47.
25. Attimarad M, Narayanswamy VK, Aldhubaib BE, SreeHarsha N, Nair AB. Development of UV spectrophotometry methods for concurrent quantification of amlodipine and celecoxib by manipulation of ratio spectra in pure and pharmaceutical formulation. PLoS One. 2019;14:1-15.
26. Sultana T, Sohel D, Kawsar H, Banoo R. *In-vitro* dissolution study and assay of diclofenac sodium from marketed solid dosage form in Bangladesh. J Bioanal Biomed. 2017;9:118-122.
27. Zhan S, Wang J, Wang W, Cui L, Zhao Q. Preparation and in vitro release kinetics of nitrendipine-loaded PLLA-PEG-PLLA microparticles by supercritical solution impregnation process. Royal Soc Chem. 2019;9:16167-16175.
28. Higuchi T. Mechanism of sustained-action medication. Theoretical analysis of rate of release of solid drugs dispersed in solid matrices. J Pharm Sci. 1963;51:1145-1149.
29. Peppas NA. Analysis of Fickian and non-Fickian drug release from polymers. Pharm Acta Helv. 1985;60:110-111.
30. Yasmeen A, Sofi G. A review of regulatory guidelines on stability studies. J Phytopharmacol. 2019;8:147-151.
31. Purushothaman M, Kalvimoorthi V. Formulation and evaluation of colon targeted drug delivery system of flurbiprofen using HPMC and K4M sodium alginate as polymeric carrier. Int J Chemtech Res. 2017;10:156-168.
32. Bolmal UB, Subhod RP, Gadad AP, Patill AS. Formulation and evaluation of carbamazepine tablets using biosurfactant in ternary solid dispersion system. Indian J Pharm Educ Res. 2020;54:302-309.

Turk J Pharm Sci 2021;18(4):510-516
DOI: 10.4274/tjps.galenos.2020.09623

ORIGINAL ARTICLE

Development of Metronidazole-loaded *In situ* Thermosensitive Hydrogel for Periodontitis Treatment

Periodontit Tedavisi için Metronidazol Yüklü Yerinde Termosensitif Hidrojel Geliştirilmesi

Duy Toan PHAM[1], Premchirakorn PHEWCHAN[2], Kanchana NAVESIT[2], Athittaya CHOKAMONSIRIKUN[2], Thatawee KHEMWONG[3], Waree TIYABOONCHAI[2,4]*

[1]Can Tho University College of Natural Sciences, Department of Chemistry, Can Tho, Vietnam
[2]Naresuan University Faculty of Pharmaceutical Sciences, Department of Pharmaceutical Technology, Phitsanulok, Thailand
[3]Naresuan University Faculty of Dentistry, Department of Diagnostic Dentistry, Phitsanulok, Thailand
[4]Mahidol University Faculty of Science, Department of Chemistry and Center of Excellence for Innovation in Chemistry, Nakhon Pathom, Thailand

ABSTRACT

Objectives: Periodontal treatment focuses on the thorough removal of specific periodontal pathogens, mainly anaerobic Gram-negative bacteria, by mechanical scaling and root planning. In case the periodontal abscess is detected after treatment, a high dose of antimicrobial agents is commonly applied via oral administration. However, this approach increases the risk of antibiotic resistance and systemic side effects and decreases efficacy. To overcome the aforementioned issues, this study focused on the development of thermosensitive hydrogel to deliver the antibiotic drug metronidazole (MTZ) directly and locally to the oral infection site.

Materials and Methods: The thermosensitive hydrogels were prepared by blending 28% w/v Pluronic F127 with various concentrations of methylcellulose (MC) and silk fibroin (SF). The gel properties, such as sol-gel transition time, viscosity, and gel strength, were investigated. The drug dissolution profiles, together with their theoretical models and gel dissolution characteristics, were also determined.

Results: All hydrogel formulations exhibited sol-gel transitions at 37˚C within 1 min. An increase in MC content proportionally increased the viscosity but decreased the gel strength of the hydrogel. By contrast, the SF content did not significantly affect the viscosity but increased the gel strength of the hydrogel. The thermosensitive hydrogels also showed prolonged MTZ release characteristics for 10 days in phosphate-buffered saline (PBS) at pH 6.6, which followed the Higuchi diffusion model. Moreover, MTZ-thermosensitive hydrogel exhibited delayed dissolution in PBS at 37˚C for more than 9 days.

Conclusion: MTZ-thermosensitive hydrogels could be considered a prospective local oral drug delivery system to achieve efficient sustained release and improve the drug pharmacological properties in periodontitis treatment.

Key words: Thermosensitive hydrogel, metronidazole, silk fibroin, sol-gel transition, periodontitis

ÖZ

Amaç: Periodontal tedavi, özellikle anaerobik Gram-negatif bakteriler olmak üzere spesifik periodontal patojenlerin mekanik ölçekleme ve kök planlaması ile tamamen ortadan kaldırılmasına odaklanmaktadır. Tedaviden sonra periodontal apse saptanması durumunda, oral yoldan yüksek dozda antimikrobiyal ajanlar yaygın olarak uygulanır. Ancak, bu yaklaşım antibiyotik direnci ve sistemik yan etki riskini artırmakta ve etkinliği azaltmaktadır. Bu çalışma, bahsedilen bu sorunların üstesinden gelmek için antibiyotik ilaç metronidazolün (MTZ) doğrudan ve lokal olarak oral enfeksiyon bölgesine verilmesi için ısıya duyarlı hidrojel geliştirilmesine odaklanmıştır.

Gereç ve Yöntemler: Isıya duyarlı hidrojeller, %28 a/h Pluronic F127'nin çeşitli konsantrasyonlarda metilselüloz (MC) ve ipek fibroin (SF) ile karıştırılmasıyla hazırlanmıştır. Sol-jel geçiş süresi, viskozite ve jel kuvveti gibi jel özellikleri araştırılmıştır. Teorik modelleri ve jel çözünme özellikleri ile birlikte ilaç çözünme profilleri de belirlenmiştir.

Bulgular: Tüm hidrojel formülasyonları, 1 dakika içinde 37˚C'de sol-jel geçişleri sergilemiştir. MC içeriğindeki bir artış, orantılı olarak viskoziteyi artırmış, ancak hidrojelin jel gücünü azaltmıştır.

*Correspondence: wareet@nu.ac.th, Phone: 66814211464, ORCID-ID: orcid.org/0000-0002-8570-0465
Received: 18.08.2020, Accepted: 27.11.2020

Sonuç: MTZ-ısıya duyarlı hidrojeller, periodontit tedavisinde verimli sürekli salım sağlamak ve ilaç farmakolojik özelliklerini geliştirmek için olası bir yerel oral ilaç dağıtım sistemi olarak düşünülebilir.

Anahtar kelimeler: Isıya duyarlı hidrojel, metronidazol, ipek fibroin, sol-jel geçişi, periodontit

INTRODUCTION

Periodontitis is a pathological inflammatory condition of periodontal tissues, including gingiva, periodontal ligament, cementum, and alveolar bone. The major cause of this condition relates to the dysbiosis condition, which is mainly associated with anaerobic Gram-negative bacterial loads.[1] Thus, periodontitis treatment mainly focuses on the reduction or eradication of periodontal pathogens.[2] The first step of periodontal treatment involves scaling and root planing through the elimination of subgingival calculus by mechanical removal.[3] However, in some cases, conventional therapy alone is insufficient because bacterial endotoxin has penetrated the root surface.[4] Therefore, combined treatment with antimicrobial agents, such as local antiseptic agents or systemic antibiotics, is essentially administered to increase treatment efficiency. Presently, metronidazole (MTZ) is one of the most widely used antibacterial compounds, which efficiently inhibits anaerobic microorganisms, in periodontal treatment.[5,6] However, oral administration of MTZ to deliver antibiotics directly to the infected site is difficult, thus leading to an insufficient concentration of the drug within the periodontal pocket. Moreover, the use of high doses of MTZ causes various side effects, such as gastrointestinal disorders, development of resistant bacterial strains, and supra-infection.[7] To this end, novel approaches for advanced periodontal treatments are necessary.

Local drug delivery administration to the oral cavity is a potential approach to overcome the aforementioned challenges. This route provides a high concentration of antimicrobial compounds directly to the infected site and minimizes their potential systemic side effects. Nevertheless, for the local route to be effective, the capability to precisely control drug release at the target site is crucial. For this issue, a drug delivery system, such as thermosensitive hydrogel that can favorably carry, protect, and release the drug, proves its benefits.

In the recent decade, thermosensitive hydrogels have been increasingly utilized as carriers for the local delivery of drugs to the sites of action. An ideal thermosensitive hydrogel should exhibit a suitable sol-gel transition behavior, in which the hydrogel remains in the solution state below body temperature and forms a gel at body temperature.[8] One of the most commonly used materials for sol-gel reversible hydrogels is Poloxamer 407 with the registered trademark of Pluronic F127 (PF127). PF127 is considered a biocompatible polymer and has been approved by the US Food and Drug Administration (FDA).[9] PF127 is a triblock copolymer of poly(ethylene oxide)-poly(propylene oxide)-poly(ethylene oxide) (PEO-PPO-PEO) that exhibits a phase transition temperature of approximately 25˚C-32˚C[9] during micellization or micelle aggregation.[10] However, because of their low mechanical strength and low molecular weight (MW), PF127 hydrogels are prone to rapid erosion, thus exhibiting low stability under physiological conditions. Consequently, burst and uncontrolled drug release occur, which further reduces system efficiency.[10,11] To overcome these, we proposed a novel approach of co-incorporating methylcellulose (MC) and silk fibroin (SF) into the PF127 thermosensitive hydrogels to improve their properties.

MC, a water-soluble cellulose derivative, has the potential characteristic to induce reversible sol-gel transitions through hydrophobic interactions in an aqueous solution with increasing temperature.[12] MC is recognized by the US FDA as a highly biocompatible material.[13] MC has been used for biomedical applications, including dermal wound repair, regenerative medicine, cell sheet engineering, and bone regeneration.[12,14] SF from *Bombyx mori* silkworms has also been widely investigated as a biomaterial because of its unique properties, including excellent mechanical properties, controllable degradability, and biocompatibility.[15-21] SF can generate sol-gel transition through β-sheet assembly under physiological conditions,[22] such as ionic surfactant, pH, concentration, and temperature.[23,24] Therefore, we hypothesized that MTZ-thermosensitive hydrogel based on PF127 with SF and MC could improve the properties of hydrogels, including increased gel strength, slow erosion, and sustained drug release, to complement periodontitis treatment.

This study aimed to develop MTZ-thermosensitive hydrogels composed of the combination of PF127, MC, and SF, at various ratios and concentrations, for intraperiodontal pocket local drug administration. The hydrogels were prepared using the physical mixing method. The hydrogel gelation time was investigated by sol-gel transition at different temperatures. The hydrogel viscosity was determined at storage temperature to ensure that the hydrogel can be administered after long-term storage. Furthermore, the gel strength was investigated at 37˚C to determine its suitability for application to the oral cavity. Finally, the drug dissolution profiles were investigated in phosphate-buffered saline (PBS) at pH 6.6 to determine the effect of biocompatible polymer content on the drug release rates from hydrogels.

MATERIALS AND METHODS

Materials

Silk yarns of *B. mori* were obtained from Bodin Thai Silk Khorat Co., Ltd. (Khorat, Thailand). PF127 (MW: 12.500 g/mol) was purchased from BASF Corporation (Bangkok, Thailand). MC (M0512; viscosity: 4.000 cP, MW: 88.000 g/mol, and DS: 1.5-1.9) was obtained from Sigma-Aldrich (St. Louis, MO, USA). MTZ injection (5 mg/mL) was purchased from Utopan Co., Ltd. (Samutprakan, Thailand). Sterile water for injection was obtained from A.N.B. Laboratories Co., Ltd. (Bangkok, Thailand). Methanol [high-performance liquid chromatography (HPLC) grade] was purchased from Sigma-Aldrich (St. Louis, MO,

USA). Triethylamine [(TEA); DNA and peptide synthesis grade] was purchased from Loba Chemie Pvt. Ltd. (Mumbai, India). Potassium phosphate monobasic (KH_2PO_4) ReagentPlus® was purchased from Elago Enterprises Pty. Ltd. (Cherrybrook, NSW, Australia).

SF extraction

SF was extracted and characterized following a previous report.[15] Briefly, degummed silk cocoon (5 g) was cut into small pieces, added to a mixed solution of $CaCl_2/H_2O/Ca(NO_3)_2$/EtOH at a weight ratio of 30:45:5:20, and heated until a clear solution was obtained. To remove the residual salts, the SF solution was dialyzed against distilled water using a SnakeSkin pleated dialysis tube (10.000 MWCO) for 3 days. Then, the SF solution was centrifuged at 10.000 rpm, 4˚C, for 30 min to eliminate the silk aggregates. To obtain SF in a dry powder form, the SF solution was subjected to a freeze dryer (Heto PowerDry LL3000, Thermo Fisher Scientific, Waltham, MA, USA) at $1x10^{-4}$ $1x10^{-4}$ Torr and -55˚C. Finally, the lyophilized SF powder was preserved in a plastic bag at -20˚C.

Preparation of MTZ-thermosensitive hydrogel

The polymer solutions were separately prepared before hydrogel preparation. The SF solution was prepared by dissolving the freeze-dried SF in sterile water. The MC and PF127 solutions were prepared by separately dispersing the powders in water with gentle mixing, followed by storing them in a refrigerator until the solutions were clear.

The MTZ-thermosensitive hydrogel was prepared using the physical mixing method. MTZ was mixed with the SF solution under gentle stirring at room temperature for 10 min. Then, the MC and PF127 solutions were added to the mixture with gentle stirring for 5 min. The final volume was adjusted with sterile water and further stirred for 30 min. Hydrogels were prepared by varying the concentrations of SF and MC. Meanwhile, the concentrations of PF127 and MTZ were kept constant at 28% and 0.05% w/v, respectively (Table 1).

Table 1. Metronidazole-loaded thermosensitive hydrogel formulations with different amounts of silk fibroin and methylcellulose with 28% Pluronic F127 and 0.05% metronidazole

Formulation		MC (% w/v)	SF (% w/v)
PF/MC	PF/MC 0.25	0.25	-
	PF/MC 0.5	0.5	-
	PF/MC 0.75	0.75	-
PF/SF	PF/SF 0.25	-	0.25
	PF/SF 0.5	-	0.5
	PF/SF 0.75	-	0.75
PF/MC/SF	PF/MC/SF 0.25	0.25	0.25
	PF/MC/SF 0.5	0.25	0.5
	PF/MC/SF 0.75	0.25	0.75

PF: Pluronic F127, MC: Methylcellulose, SF: Silk fibroin

Determination of the sol-gel transition of MTZ-thermosensitive hydrogel

The vial inversion method was employed to determine the occurrence of sol-gel transition. Sol formation was observed as flowing liquid and gel formation was observed as a non-flowing gel when the vial was inverted. Then, 1 mL of the thermosensitive hydrogel solution was transferred to a sealed test tube, which was subsequently immersed in a water bath at 4˚C±0.5˚C, 25˚C±0.5˚C, and 37˚C±0.5˚C. The gelation time of thermosensitive hydrogel was determined as the initial time point that the solution did not move when the vial was inverted.

Viscosity test of MTZ-thermosensitive hydrogel

The viscosity of MTZ-thermosensitive hydrogel solution was measured at 4˚C±0.5˚C by a Brookfield rotational rheometer model DV-III (Brookfield Engineering Labs, Middleborough, MA, USA) fitted with a parallel plate configuration (40 mm in diameter) with a rotation rate of 6 rpm. The sample (i.e., 0.5 mL of the hydrogel) was placed on the parallel plate with a temperature controller and subjected to the viscosity test.

Gel strength test of MTZ-thermosensitive hydrogel

The gel strength of the samples was analyzed by a texture analyzer (TA.XT.Plus, Charpa Techcenter Co., Ltd., Bangkok, Thailand). Then, 1 mL of the hydrogel solution was placed in a 5-mL vial to prevent air from coming in contact with the samples and ensure the generation of a smooth upper surface. Subsequently, the hydrogel solution was incubated at 37˚C±0.5˚C for 15 min to form a hydrogel. The hemispherical probe P/0.5 HS (50 mm in diameter) was compressed into the hydrogel sample to a defined depth of 4 mm. Three replicate analyses were performed at 37˚C±0.5˚C for each formulation under the same conditions.

MTZ dissolution test and hydrogel erosion study

The drug dissolution profiles were evaluated by the *in vitro* dissolution method at 37˚C±0.5˚C. Then, 1 mL of the MTZ-thermosensitive hydrogel was transferred to a 10-mL vial and kept at 37˚C for 15 min to form a hydrogel. Subsequently, 1 mL PBS pH 6.6 was added to the vial as a dissolution medium (sink condition, as MTZ aqueous solubility is 10 mg/mL at pH 2.5-8) and the temperature was kept at 37˚C in an incubator with shaking at 50 rpm. At a predetermined time point, 0.5 mL of the sample was withdrawn and replaced immediately with the same amount of free medium pre-warmed to 37˚C±0.5˚C. The amount of MTZ in the sample was analyzed by HPLC, modified from Trivedi et al.[25] Briefly, the samples were diluted with a mobile phase (20 mM KH_2PO_4/methanol at a ratio of 70:30 (v/v) with TEA 0.1% v/v) and subjected to HPLC (Shimadzu, Tokyo, Japan) equipped with an SPD-20A ultraviolet-visible detector. The separation was done with a VertiSep C18 column (5 µm, 4.6 mm×250 mm; Sigma-Aldrich, St. Louis, MO, USA) at a flow rate of 1.0 mL/min and a detection wavelength of 364 nm. The standard curve was constructed in the range of 5-100 µg/mL with a regression equation of y: 10.706x-2.950.1 and a correlation coefficient (R^2) of 0.9997. The amount of MTZ was calculated based on the calibration curve, and the results were

reported as the average cumulative drug release percentage of three determinations.

To elucidate the drug release mechanism, the correlation coefficients (R^2) for various models, such as zero-order, first-order, and Higuchi models, were tested for all samples using Microsoft Excel 2018. The release model having the highest R^2 value was considered the fitted model to assess the drug release kinetics.

In terms of hydrogel erosion study, the dissolution study was conducted with the same experimental settings. At a predetermined time point, 0.5 mL of the sample was withdrawn and replaced with a fresh sample. The remaining hydrogels after erosion were collected and photographed.

Statistical analysis

Experiments were performed in triplicate, and the data were expressed as the mean ± standard deviation. Analysis of variance followed by Tukey's post hoc test was used to determine the differences between groups, with $p<0.05$ for statistically significant comparisons.

RESULTS AND DISCUSSION

Sol-gel transition time of MTZ-thermosensitive hydrogels

To determine the suitability for in situ application, as well as the storage conditions, of the formulations, the sol-gel transition tests were conducted at three different temperatures, namely, the storage temperature of 4°C, room temperature of 25°C, and application periodontal pocket site temperature of 37°C.

In our preliminary study, by varying the PF127 concentrations from 10% to 30% w/v, we observed that the 28% PF127+0.05% MTZ solution transformed into a hydrogel within 1 min at 37°C. At a lower PF127 concentration of 18%, only the blank PF127 solution transformed into a hydrogel, whereas the PF127+0.05% MTZ solution remained in the solution form. This finding indicates that PF127 and the drug MTZ might interact via non-covalent bonds, consequently disrupting the hydrophobic interaction during the PF127 gelation process and resulting in the increased sol-gel transition temperature of PF127.[26] Therefore, 28% PF127 was selected for further studies. However, the PF127 hydrogel had low mechanical properties, which might result in hydrogel leaking from the periodontal pocket after administration, as well as rapid drug release. Therefore, to increase the mechanical properties of PF127 hydrogels, MC and SF were used as gel strength enhancers.

To this end, three groups of formulations, namely, PF/MC, PF/SF, and PF/MC/SF, at three different concentrations (i.e., 0.25%, 0.5%, and 0.75% w/v) of the enhancer were prepared (Table 1). Then, the gelation time at 4°C (storage temperature), 25°C (room temperature), and 37°C (body temperature) was determined (Table 2). At 4°C, all samples remained in low-viscosity liquid form for at least 6 months, indicating their stability for long-term storage. At 25°C, the gel was formed after at least 15 min, allowing adequate time for periodontal administration. After being administered to the site of action, at 37°C, the solutions formed a gel almost immediately within less than 1 min (Figure 1), which further stick to the dental cavity for a longer time. Thus, the drug could perform its action without being washed down to the gastrointestinal tract, consequently enhancing its efficacy and reducing the systemic side effects. Ultimately, the thermosensitive hydrogel should be stored at 4°C (solution form) and quickly applied (i.e., not more than 15 min) to the periodontal pocket site after retrieving it from the fridge.

The mechanism of sol-gel transition of thermosensitive hydrogel is shown in Figure 2. First, at a concentration higher than the PF127 critical micelle concentration [(CMC); 1-7 g/L][27], the polymer formed polymeric micelles consisting of a PPO hydrophobic core enclosed by hydrophilic PEO blocks. MTZ mostly resided in the PPO hydrophobic core. When the temperature increased to a higher value (37°C in our case) than the PF127 lower critical solution temperature, the polymer solubility decreases through partial dehydration, leading to the decrease in PF127 CMC (0.09 g/L at 37°C). Consequently, more micelles were formed, leading to the formation of a packed micellar structure because of enhanced particle contact and, ultimately, the formation of a gel. The MC and SF molecules could entangle with the hydrophilic PEO shell of the PF127 micelles

Table 2. Sol-gel transition time of thermosensitive hydrogels at 4°C, 25°C, and 37°C. The results are expressed as the mean ± standard deviation (n=3). The time unit at 25°C and 37°C is minute and second, respectively

Formulation[a,c]	Gelation time		
	4°C[b]	25°C (min)	37°C (s)
PF/MC 0.25	N/A	17±1	33±2
PF/MC 0.5	N/A	39±2	48±3
PF/MC 0.75	N/A	>120	61±3
PF/SF 0.25	N/A	26±1	35±2
PF/SF 0.5	N/A	20±2	28±2
PF/SF 0.75	N/A	16±1	25±2
PF/MC/SF 0.25	N/A	19±1	35±2
PF/MC/SF 0.5	N/A	28±2	30±2
PF/MC/SF 0.75	N/A	40±2	29±1

[a]Thermosensitive hydrogel composed of 28% PF127 and 0.05% w/v MTZ, [b]N/A: Could not form a hydrogel for at least 6 months, [c]For PF/MC/SF formulations, the MC concentration was fixed at 0.25% w/v. PF: Pluronic F127, MC: Methylcellulose, SF: Silk fibroin, MTZ: Metronidazole

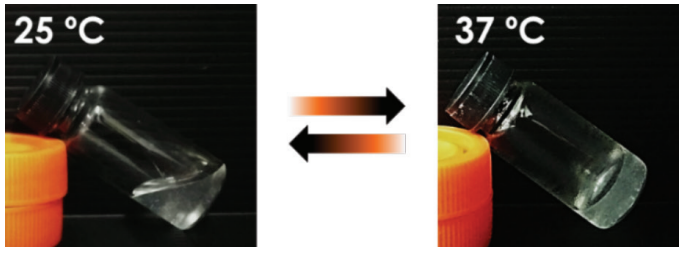

Figure 1. Sol-gel transition images of metronidazole-thermosensitive hydrogel composed of silk fibroin, methylcellulose, and Pluronic F127 by vial inversion method at 25°C and 37°C

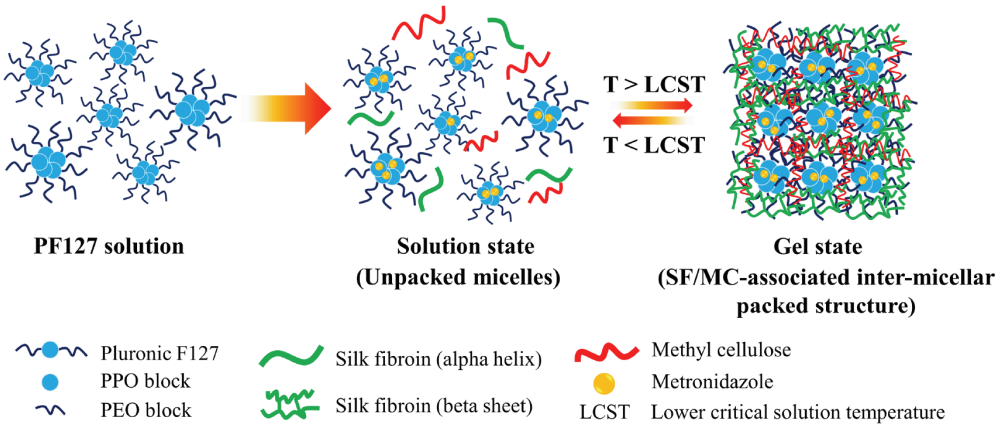

Figure 2. Mechanism of the formation of a packed micellar structure of MTZ-thermosensitive hydrogel

MTZ: Metronidazole, PPP: Poly propylene oxide, PEO: Poly ethylene oxide, PF127: PF: Pluronic F127, MC: Methylcellulose, SF: Silk fibroin, LCST: Lower critical solution temperature

by intercellular packing, thus leading to the enhancement of the gel properties.[10]

Viscosity of MTZ-thermosensitive hydrogel

The viscosity of all hydrogels in solution form was determined at 4˚C to ensure that the hydrogels can be applied to the periodontal infection site (Figure 3). All hydrogel formulations had a viscosity of less than 500 cP, indicating a low viscosity, which ensures easy administration to the lesion site. Moreover, the MC content could influence the viscosity of the hydrogel. When the MC content increased from 0.25% to 0.75% w/v, the viscosity of PF/MC dramatically increased from 158.00 cP to 476.17 cP. Meanwhile, with an increase in SF content, both PF/SF and PF/MC/SF hydrogels showed no observable changes in viscosity. This finding can be explained by the inherent hydrophilicity of MC and SF. MC can form hydrogen bondings with water and PF127, consequently increasing the gel connecting networks and resulting in enhanced viscosity. By contrast, less hydrophilic SF might have limited interactions with the polymer compared with MC, thus not affecting the gel viscosity.

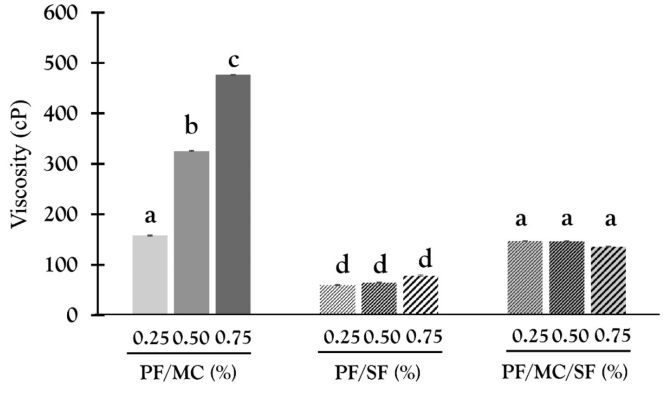

Figure 3. Viscosity of MTZ-thermosensitive hydrogel at 4˚C. The data are expressed as the mean ± standard deviation (n=3). Different letters (a, b, c, d) denote the statistical differences, $p<0.05$

MTZ: Metronidazole, PF: Pluronic F127, MC: Methylcellulose, SF: Silk fibroin

Gel strength of MTZ-thermosensitive hydrogel

The gel strength of all hydrogels was determined at 37˚C, and the results are shown in Figure 4. When increasing the MC concentration from 0.25% to 0.75%, the PF/MC hydrogel gel strength proportionally decreased from 2,234.97 g to 1,143.70 g. By contrast, the PF/SF hydrogel gel strength slightly increased from 1,809.20 g to 2,196.17 g when the SF concentration increased from 0.25% to 0.75%. Thus, the hydrophobic SF possibly enhanced the mechanical strength of the hydrogels by forming a rigid β-sheet, which is induced by heat at 37˚C. Meanwhile, the hydrophilic MC increased hydrogel flexibility by forming hydrogen bondings with water and hydrophilic PEO shell of polymeric micelles.

Notably, when combining both MC and SF in the formulations, the gel strength of PF/MC/SF decreased slightly with the increase in SF concentrations. This phenomenon can be explained by the interactions between MC and SF, as MC could swell and coat the SF surfaces, altering its properties. Nevertheless, more experiments are needed to explain this issue.

Drug dissolution study and erosion behavior of MTZ-thermosensitive hydrogels

To mimic the conditions of periodontal infection, a sink condition with PBS at pH 6.6 and 37˚C was selected to be the medium for analyzing the dissolution behavior of MTZ-thermosensitive hydrogels. Notably, all PF/SF formulations were dissolved rapidly in the dissolution medium, and all PF/MC formulations were not strong/rigid enough for the experiments. Thus, both MC and SF are necessary to improve the gel properties, as MC enhances gel viscosity and SF increases gel strength. Figure 5A shows the cumulative release percentages of MTZ over time from PF/MC/SF formulations at different SF concentrations of 0.25%, 0.5%, and 0.75% w/v. With no significant differences, all formulations showed a sustained dissolution profile of MTZ up to 80% within 10 days. Furthermore, these dissolution data were fitted nicely with the Higuchi model (Table 3), with R^2 values of >0.98, indicating that the drug was released via the diffusion-controlled mechanism.

As expected, hydrogel erosion in the dissolution medium was observed. As shown in Figure 5B, the hydrogels were dissolved sustainably, with a remaining weight of approximately 40% after 9 days of the dissolution study (data not showed). This finding can be attributed to the hydrophilicity of both PF127 and MC, which are subjected to dissolution in an aqueous medium.[28,29] Because the drug MTZ mostly resided in the PPO hydrophobic core of PF127 micelles, its diffusion-controlled release profile is governed by the dissolution of PF127 and/or MC.[28] Therefore, this fact benefits periodontitis treatment, as the systems release a high initial dose in the first day (approximately 30%) that is adequate for fast action, followed by a decreasing release rate over the next 9 days that is suitable for maintaining the drug efficacy without the need for readministration.

Table 3. Kinetic release modeling of the metronidazole-thermosensitive hydrogels

Formulation[a]	R^2 value		
	Zero-order model	First-order model	Higuchi model
PF/MC/SF 0.25	0.7139	-0.5380	0.9872
PF/MC/SF 0.5	0.7331	-0.5090	0.9865
PF/MC/SF 0.75	0.7012	-0.5420	0.9811

[a]Thermosensitive hydrogel consisted of 28% PF127, 0.05% w/v MTZ, and 0.25% w/v MC. PF: Pluronic F127, MC: Methylcellulose, SF: Silk fibroin, MTZ: Metronidazole

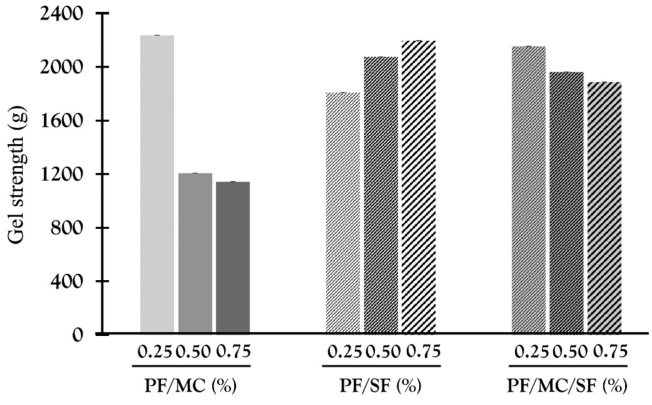

Figure 4. Gel strength of MTZ-thermosensitive hydrogel at 37°C. The data are expressed as the mean ± standard deviation (n=3). All data are significantly different from each other ($p<0.05$)

MTZ: Metronidazole, PF: Pluronic F127, MC: Methylcellulose, SF: Silk fibroin

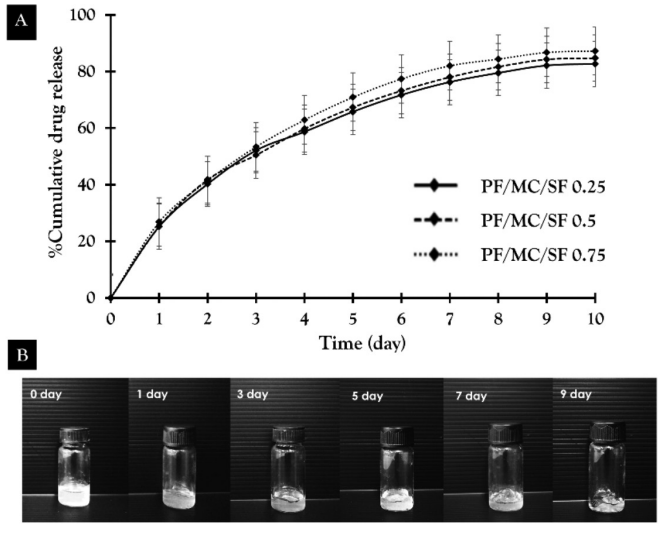

Figure 5. (A) Cumulative release of MTZ from thermosensitive hydrogel in phosphate-buffered saline (PBS) pH 6.6 within 10 days and (B) erosion of MTZ-thermosensitive hydrogel (PF/MC/SF 0.75) in PBS pH 6.6 within 9 days. The data are expressed as the mean ± standard deviation (n=3)

MTZ: Metronidazole, PF: Pluronic F127, MC: Methylcellulose, SF: Silk fibroin

MTZ is commonly used to inhibit infection from anaerobic microorganisms, such as *Porphyromonas gingivalis*. The minimal inhibitory concentration (MIC) of MTZ against this bacteria isolated is in the range of 0.063-0.514 µg/mL.[30,31] From our data, the amount of MTZ release in the first time point (the first day) was approximately 120 µg/mL for all formulations, which was more than 200 times higher than the MIC of MTZ against *P. gingivalis*. Moreover, the amount of MTZ release on the ninth day was approximately 13 µg/mL, which was still more than 20 times higher than the required MIC. Thus, the release amount of the drug reached the therapeutic concentration for at least 9 days

CONCLUSION

This study successfully developed and characterized the novel MTZ-loaded PF/MC/SF thermosensitive hydrogels as in situ drug delivery systems for periodontitis treatment. The hydrogels remained in low-viscosity solution form for at least 6 months at 4°C (storage temperature) and rapidly formed a hydrogel at 37°C within 1 min after injection into the dental pocket. SF significantly enhanced the gel strength, whereas MC increased the gel viscosity. Furthermore, the hydrogels exhibited sustained MTZ release for 10 days, which reduces administration frequency. The drug dissolution profile of PF/MC/SF was governed by two different mechanisms, namely, hydrogel erosion by fluids at the administration site (periodontal pocket) and diffusion of the drug through the hydrogels. In conclusion, these novel thermosensitive hydrogels have considerable potential to control drug release in the periodontal pocket, which might improve its pharmacological properties. Thus, these novel thermosensitive hydrogels could be further investigated *in vitro* and *in vivo* for application to clinical treatment in the future.

ACKNOWLEDGMENTS

This study was financially supported by the Faculty of Pharmaceutical Sciences, Naresuan University, and the National Research Council of Thailand under the Royal Golden Jubilee (RGJ-ASEAN) Ph.D. Programme (PHD/0234/2560). The authors sincerely acknowledge Siam Pharmaceutical Co. Ltd. for the MTZ raw material.

Conflict of interest: No conflict of interest was declared by the authors. The authors are solely responsible for the content and writing of this paper.

REFERENCES

1. Aminu N, Toh SM. Applicability of nanoparticles-hydrogel composite in treating periodontal diseases and beyond. Asian J Pharm Clin Res. 2017;10:65-70.
2. Sato S, Fonseca MJ, Ciampo JO, Jabor JR, Pedrazzi V. Metronidazole-containing gel for the treatment of periodontitis: an *in vivo* evaluation. Braz Oral Res. 2008;22:145-150.
3. Kida D, Karolewicz B, Junka A, Sender-Janeczek A, Dus I, Marciniak D, Szulc M. Metronidazole-loaded porous matrices for local periodontitis treatment: *In vitro* evaluation and *in vivo* pilot study. Appl Sci (Switzerland). 2019;9:1-18.
4. Lee FY, Chen DW, Hu CC, Hsieh YT, Liu SJ, Chan EC. *In vitro* and *in vivo* investigation of drug-eluting implants for the treatment of periodontal disease. AAPS PharmSciTech. 2011;12:1110-1115.
5. Nurul Adha IE, Harry Agusnar. The effectiveness of metronidazole gel based chitosan inhibits the growth of bacteria Aggregatibacter actinomycetemcomitans, *Porphyromonas gingivalis*, Fusobacterium nucleatum (*In vitro*). Int J Appl Dent Sci. 2017;3:30-37.
6. Loesche WJ, Giordano JR, Soehren S, Kaciroti N. The nonsurgical treatment of patients with periodontal disease: Results after five years. J Am Dent Assoc. 2002;133:311-320.
7. Junmahasathien T, Panraksa P, Protiarn P, Hormdee D, Noisombut R, Kantrong N, Jantrawut P. Preparation and evaluation of metronidazole-loaded pectin films for potentially targeting a microbial infection associated with periodontal disease. Polymers (Basel). 2018;10:1021.
8. Gong C, Qi T, Wei X, Qu Y, Wu Q, Luo F, Qian Z. Thermosensitive polymeric hydrogels as drug delivery systems. Curr Med Chem. 2013;20:79-94.
9. Gioffredi E, Boffito M, Calzone S, Giannitelli SM, Rainer A, Trombetta M, Mozetic P, Chiono V. Pluronic F127 hydrogel characterization and biofabrication in cellularized constructs for tissue engineering applications. Procedia CIRP. 2016;49:125-132.
10. Jung YS, Park W, Park H, Lee DK, Na K. Thermo-sensitive injectable hydrogel based on the physical mixing of hyaluronic acid and Pluronic F-127 for sustained NSAID delivery. Carbohydr Polym. 2017;156:403-408.
11. Lee SH, Lee Y, Lee SW, Ji HY, Lee JH, Lee DS, Park TG. Enzyme-mediated cross-linking of Pluronic copolymer micelles for injectable and in situ forming hydrogels. Acta Biomater. 2011;7:1468-1476.
12. Kim MH, Kim BS, Park H, Lee J, Park WH. Injectable methylcellulose hydrogel containing calcium phosphate nanoparticles for bone regeneration. Int J Biol Macromol. 2018;109:57-64.
13. Bain MK, Bhowmick B, Maity D, Mondal D, Mollick MM, Rana D, Chattopadhyay D. Synergistic effect of salt mixture on the gelation temperature and morphology of methylcellulose hydrogel. Int J Biol Macromol. 2012;51:831-836.
14. Contessi N, Altomare L, Filipponi A, Farè S. Thermo-responsive properties of methylcellulose hydrogels for cell sheet engineering. Mater Lett. 2017;207:157-160.
15. Chomchalao P, Nimtrakul P, Pham DT, Tiyaboonchai W. Development of amphotericin B-loaded fibroin nanoparticles: a novel approach for topical ocular application. J Mater Sci. 2020;55:5268-5279.
16. Pham DT, Saelim N, Cornu R, Béduneau A, Tiyaboonchai W. Crosslinked fibroin nanoparticles: investigations on biostability, cytotoxicity, and cellular internalization. Pharmaceuticals (Basel). 2020;13:86.
17. Pham DT, Saelim N, Tiyaboonchai W. Paclitaxel loaded EDC-crosslinked fibroin nanoparticles: a potential approach for colon cancer treatment. Drug Deliv Transl Res. 2020;10:413-424.
18. Pham DT, Saelim N, Tiyaboonchai W. Alpha mangostin loaded crosslinked silk fibroin-based nanoparticles for cancer chemotherapy. Colloids Surf B Biointerfaces. 2019;181:705-713.
19. Pham DT, Tetyczka C, Hartl S, Absenger-Novak M, Fröhlich E, Tiyaboonchai W, Roblegg E. Comprehensive investigations of fibroin and poly(ethylenimine) functionalized fibroin nanoparticles for ulcerative colitis treatment. J Drug Deliv Sci Technol. 2020;57:101484.
20. Pham DT, Saelim N, Tiyaboonchai W. Design of experiments model for the optimization of silk fibroin based nanoparticles. Int J Appl Pharm. 2018;10:195.
21. Pham DT, Tiyaboonchai W. Fibroin nanoparticles: a promising drug delivery system. Drug Deliv. 2020;27:431-448.
22. Pham DT, Saelim N, Tiyaboonchai W. Crosslinked fibroin nanoparticles using EDC or PEI for drug delivery: physicochemical properties, crystallinity and structure. J Mater Sci. 2018;53:14087-14103.
23. Chen D, Yin Z, Wu F, Fu H, Kundu SC, Lu S. Orientational behaviors of silk fibroin hydrogels. J Appl Polym Sci. 2017;134:45050.
24. Matsumoto A, Chen J, Collette AL, Kim UJ, Altman GH, Cebe P, Kaplan DL. Mechanisms of silk fibroin sol-gel transitions. J Phys Chem B. 2006;110:21630-21638.
25. Trivedi KD, Chaudhary AB, Mohan S. Devlopment and validation of RP-HPLC Method for estimation of Metronidazole and Norfloxacin in suspension form. International J Adv Pharm. 2013;2:7.
26. Dumortier G, Grossiord JL, Agnely F, Chaumeil JC. A review of poloxamer 407 pharmaceutical and pharmacological characteristics. Pharm Res. 2006;23:2709-2728.
27. Gyulai G, Magyar A, Rohonczy J, Orosz J, Yamasaki M, Bosze S, Kiss E. Preparation and characterization of cationic Pluronic for surface modification and functionalization of polymeric drug delivery nanoparticles. EXPRESS Poly Lett. 2016;10:216-226.
28. Akash MS, Rehman K. Recent progress in biomedical applications of Pluronic (PF127): Pharmaceutical perspectives. J Control Release. 2015;209:120-138.
29. Fu Y, Kao WJ. Drug release kinetics and transport mechanisms of non-degradable and degradable polymeric delivery systems. Expert Opin Drug Deliv. 2010;7:429-444.
30. Oulia P, Saderi H, Jalali Nadoushan MR. Metronidazol Susceptibility Testing of Porphyromonas Gingivalis Associated With Adult Periodontitis (an Invitro Study). Beheshti Univ Dent J. 2005;22:72-75.
31. Duan D, Wang S, Zhang L, Zhao L, Xu Y. [Susceptibility of porphyromonas gingivalis to metronidazole at different planktonic cell densities and in biofilm]. Hua Xi Kou Qiang Yi Xue Za Zhi. 2011;29:571-575.

Turk J Pharm Sci 2021;18(4):517-526
DOI: 10.4274/tjps.galenos.2020.66735

REVIEW

Impact of Clinical Pharmacist-led Interventions in Turkey

Türkiye'de Klinik Eczacı Tarafından Yapılan Müdahalelerin Etkisi

Emre KARA[1]*, Burcu KELLECİ ÇAKIR[1], Mesut SANCAR[2], Kutay DEMİRKAN[1]

[1]Hacettepe University Faculty of Pharmacy, Department of Clinical Pharmacy, Ankara, Turkey
[2]Marmara University Faculty of Pharmacy, Department of Clinical Pharmacy, İstanbul, Turkey

ABSTRACT

Detecting drug-related problems (DRPs) is important in pharmaceutical care in for better therapeutic outcomes. Clinical pharmacists-led comprehensive medication management plays a crucial role in the rational use of drugs by preventing, identifying, and resolving DRPs. In this review, we aimed to determine the effect of interventions on patient outcomes performed by clinical pharmacists in Turkey. A systematic literature search was performed on PubMed, Google Scholar, EMBASE, Cochrane Library, and Turkish databases (ULAKBIM, Dergipark). The main categories were "clinical pharmacist", "intervention", and "Turkey". Two reviewers reviewed each article independently. Two independent reviewers screened all records and extracted data; disagreements were resolved through a consensus. Randomized controlled studies, pre- to post-intervention comparison studies, and cross-sectional studies including pharmacist-led interventions were included in the review. This review included 15 articles evaluating clinical pharmacist interventions. Ten studies (66.7%) focused on DRPs and pharmacist interventions to these problems, while the remaining 5 (33.3%) studies focused on patient education and adherence issues. Studies were conducted in oncology (33.3%), geriatrics (20.0%), chest diseases (13.3%), psychiatry (6.7%), cardiology (6.7%), and infectious diseases (6.7%) clinics. When results of studies are reviewed, most of the interventions were made at the prescriber level followed by the drug level and patient level. Problems were solved in 54.2-93.2% of DRPs, and adherence, patient knowledge, or skills were improved in most of the studies. Most of the studies were carried out within the scope of a postgraduate or doctorate thesis and yet various positive outcomes such as the prevention of side effects, increased quality of life, and decreased duration of hospital stay were observed with high positive rates of interventions, which indicate that other healthcare workers are ready to collaborate with the clinical pharmacists in Turkey.

Key words: Clinical pharmacy, drug-related problems, pharmaceutical care, clinical pharmacist, Turkey

ÖZ

İlaçla ilgili problemlerin saptanması (İİP), farmasötik bakım kapsamında daha iyi tedavi sonuçlarının sağlanması açısından önemlidir. Klinik eczacı tarafından yapılan kapsamlı ilaç yönetimi, ilaçla ilgili problemleri önleyerek, tanımlayarak ve çözerek ilaçların rasyonel kullanımında önemli bir rol oynamaktadır. Bu derlemede, Türkiye'de klinik eczacı tarafından yapılan müdahalelerin hasta sonuçları üzerindeki etkisinin belirlenmesi amaçlanmıştır. PubMed, Google Akademik, EMBASE, Cochrane Kütüphanesi ve Türk veri tabanlarında (ULAKBIM, Dergipark) sistematik bir literatür taraması yapılmıştır. Ana kategoriler "klinik eczacı", "müdahale" ve "Türkiye" olarak belirlenmiştir. İki araştırmacı her makaleyi bağımsız olarak gözden geçirmiştir. İki bağımsız araştırmacı ise tüm kayıtları taramış ve verileri elde etmiş; anlaşmazlıklar fikir birliği ile çözülmüştür. Eczacılar tarafından yapılan müdahaleleri içeren randomize kontrollü çalışmalar, müdahale öncesi ve sonrası karşılaştırma çalışmaları ve kesitsel çalışmalar derlemeye dahil edilmiştir. Bu derlemeye, klinik eczacı müdahalelerini değerlendiren 15 makale dahil edilmiştir. On çalışma (%66,7) ilaçla ilgili problemler ve bu problemlere eczacı müdahalelerine odaklanırken, geri kalan 5 (%33,3) çalışma hasta eğitimi ve uyunç konularına odaklanmıştır. Çalışmalar, onkoloji (%33,3), geriatri (%20,0), göğüs hastalıkları (%13,3), psikiyatri (%6,7), kardiyoloji (%6,7) ve enfeksiyon hastalıkları (%6,7) kliniklerinde yapılmıştır. Çalışmaların sonuçları incelendiğinde, müdahalelerin çoğu hekim düzeyinde, daha sonrası ise ilaç düzeyi ve hasta düzeyinde yapılmıştır. İİP'lerin %54,2-93,2'sinde problem çözülmüştür ve çalışmaların çoğunda uyunç, hasta bilgisi veya becerileri geliştirilmiştir. Çalışmaların çoğunluğu yüksek lisans veya doktora tezi kapsamında yapılmıştır. Müdahalelerin yüksek kabul oranlarının yanı sıra, yan etkilerin önlenmesi, yaşam kalitesinde artış ve hastanede kalış süresinde azalma gibi çeşitli olumlu sonuçlar gözlenmiştir. Bu sonuçlar Türkiye'deki diğer sağlık çalışanlarının klinik eczacılarla iş birliği yapmaya hazır olduklarını göstermektedir.

Anahtar kelimeler: Klinik eczacılık, ilaçla ilgili problemler, farmasötik bakım, klinik eczacı, Türkiye

***Correspondence:** emrekara@hacettepe.edu.tr, **Phone:** +90 506 051 24 43, **ORCID-ID:** orcid.org/0000-0002-7034-4787

Received: 18.05.2020, **Accepted:** 05.07.2020

INTRODUCTION

A drug-related problem (DRP) is defined as "an event or circumstance involving drug therapy that actually or potentially interferes with desired health outcomes".[1,2] Detecting DRPs is important in pharmaceutical care, as DRPs are related to treatment outcomes. To identify and resolve DRPs in terms of rational drug use, clinical pharmacist-led comprehensive medication management plays a crucial role.[2,3]

Clinical pharmacists beyond the many other duties primarily provide pharmaceutical care to improve treatment adherence and to decrease DRPs.[4-6] The quality of care may be improved by pharmaceutical care services in many diseases like hypertension,[7] asthma,[8] hyperlipidemia,[9] and diabetes.[10] The first step in pharmaceutical care services is identifying patients' pharmaceutical care needs and the second step is developing an individualized pharmaceutical care plan, with respect to the patient's knowledge, attitudes, and motivation. The third step is evaluating the outcomes of the pharmaceutical care plan. Finally, the fourth and fifth steps consist of implementing the care plan and continuous monitoring, respectively.[11]

Clinical pharmacy services, including pharmaceutical care, has developed in the USA in the 1960s. It has changed over time in terms of concept and the variety of practices.[12] It has been linked to proper prescribing, preventing or reducing DRPs, adverse drug events, quality of life (QoL), medication errors, and cost charged during the treatment.[13-18] According to the International Pharmaceutical Federation consensus report in 2009, clinical pharmacy services given should be global, which was established in many developed countries[19] including Turkey.[20]

Clinical pharmacy service is a relatively new and developing concept in Turkey.[21] The first discussions started in 1986.[22] It has been performing since 1991 and was started at Marmara University, which opened the first postgraduate education program. In 1994, clinical pharmacy course was a part of undergraduate education at Hacettepe University. In 1997, Ankara University established the interdisciplinary clinical pharmacy postgraduate education program. In 1998, to promote clinical pharmacy in Turkey, "The Society of Clinical Pharmacy, KED" was established. Since 2003, many continuing education programs were organized by both KED and the "Turkish Pharmacists' Association Academy of Pharmacy" on clinical pharmacy and pharmaceutical care.[21] In Turkey, the first Department of Clinical Pharmacy was established at Hacettepe University in 2013, and thereafter at Marmara University and Inonu University.[23] Although clinical pharmacy was established as a subdivision at Marmara University many years ago (1995) and allowed to open a department throughout Turkey in 2013, it still operates as a subdivision under the pharmacology department in some universities due to a lack of academic staff. Furthermore, in 2014, with the approval of the Grand national assembly of Turkey, clinical pharmacy became a legal specialty supported by "Law on pharmacies and pharmacy". According to this law, pharmacists may take a special exam once a year and based on the scores of this exam, and a limited number of them may start the 3-year postgraduate clinical pharmacy specialty education in selected universities.[24]

As mentioned above, as a member of the multidisciplinary and interdisciplinary team, the clinical pharmacist has a significant role in improving the treatment, patient outcomes, and QoL. The positive impact of clinical pharmacist-led interventions on patient outcomes in terms of reduced hospital visits and mortality was reported in other countries.[25,26] Another impact of clinical pharmacists is on the pharmacoeconomic parameters. Studies show that there is proven evidence on the economic benefits of clinical pharmacy services via reducing the total healthcare costs in various health departments.[13,14]

It is important to show nation-wide results from a developing science to emphasize weak and strong sides and guide complete education. This review aimed to present the impact of interventions performed by clinical pharmacists in Turkey on patient outcomes and shows an inside view of what has been done since the implementation of the clinical pharmacy program in Turkey, and to lead further comprehensive studies.

A systematic literature search (up February 20, 2020) was performed according to PICOS formatting on PubMed, Google Scholar, EMBASE, Cochrane Library, Turkish databases (ULAKBIM, Dergipark) with the headings "clinical pharmacist", "intervention", and "Turkey" with "AND" and "OR" operators. Two reviewers (EK and BKC) reviewed each article independently. The search strategy of PubMed was as per the following: ["pharmacists" (MeSH Terms) OR "pharmacists"(All Fields)] OR ["clinical"(All Fields) AND "pharmacist"(All Fields)] OR "clinical pharmacist" (All Fields) AND ["Turkey"(MeSH Terms) OR "Turkey"(All Fields)].

The general principles recommended in the Preferred Reporting Items for Systematic Reviews and Meta-Analyses (PRISMA) statements were used. Two independent researchers screened records, further extracted data, and disagreements were resolved through a consensus. Extracted data and quality assessment variables were presented in tables with a narrative description. Randomized controlled studies, pre- to post-intervention comparison studies, and cross-sectional studies which included pharmacist-led interventions were included. Even though abstracts, letters, and case reports were also read and evaluated, articles with no full-text, conference reports, reviews, editorials, letters, or case reports were excluded. Articles referring to countries other than Turkey were excluded. First author's name, publication year, study design, the type of clinical pharmacist-led interventions, patient age, patient outcomes, and the acceptance rate of interventions were evaluated. The first author (EK) extracted the data, and another review author (BKC) did the double-checking. If there was any conflict, another author (MS or KD) made the final decision.

To prevent bias in individual studies, every researcher extracted data other than their study. Data extraction was undertaken by one reviewer using a tailored data extraction

framework, developed to explicit data extraction elements related directly to the review question for the qualitative studies. All of the extractions were checked by a second reviewer. No additional analyses were made to combine the data.

This review included 15 articles out of 94 publications evaluating clinical pharmacist interventions in Turkey (Figure 1). The oldest article included in this review was published in 2007 and the latest was published in 2020. The distribution of publishing years of the articles is given in Graphic 1. The majority of the articles were published in Science Citation Index-Expanded indexed journals that were ranked in the third quartile and fourth quartile. The characteristics of the journals in which the articles were published are listed in Table 1. The study design of two (13.3%) of the 13 articles included were retrospective, while the remaining 13 (86.7%) were prospective. Ten studies (86.7%) focused on DRPs and pharmacist interventions to these problems, while the remaining five (33.3%) studies focused on patient education and adherence issues. Different versions of the Pharmaceutical Care Network Europe (PCNE) DRPs classification system was used in seven (46.7%) of the studies. Different tools, such as Beers' criteria, screening tool of older persons' potentially inappropriate prescriptions criteria, screening tool to alert doctors to the right treatment criteria and National Cancer Institute common toxicology criteria for adverse effects version 4, were used in other studies.

Studies were conducted in oncology (n=5, 33.3%), geriatrics (n=3, 20.0%), chest disease (n=2, 13.3%), psychiatry (n=1, 6.7%), cardiology (n=1, 6.7%), infectious diseases (n=1, 6.7%), and in clinical and community pharmacy (n=2, 13.3%). The studies were conducted in the inpatient (n=6, 40.0%), outpatient (n=7, 46.7%), and community pharmacy (n=2, 13.3%) settings. The characteristics of the studies, patients, and interventions are listed as Table 2.

The duration of the studies was between 3 to 11 months, the number of patients in the studies were between 25 and 186, and the average age of the patients included in the studies was between 33 and 80 years.

When the study outcomes were reviewed, most of the interventions were made at the prescriber level, followed by drug level, and patient level. Problems were solved in a median of 86% (54.2-93.2%) of DRPs, and adherence, patient knowledge, or skills were improved in these studies (Table 2).

Table 1. The characteristics of the journals in which articles were published

Journal name	First author and year	Indexing	Impact factor	Quartiles
International Journal of Clinical Pharmacy (formerly Pharmacy World & Science)	Umar et al.[27] (2020)	SCI-expanded	1.941 (5-years)	Q4
Journal of Oncology Pharmacy Practice	Kucuk et al.[28] (2019)	SCI-expanded	1.826 (2018)	Q3
Clinical Interventions in Aging	Ertuna et al.[29] (2019)	SCI-expanded	3.195 (5-years)	Q3
International Clinical Psychopharmacology	Yalcin et al.[30] (2019)	SCI-expanded	2.169 (5-years)	Q4
Journal of Research in Pharmacy (formerly Marmara Pharmaceutical Journal)	Izzettin et al.[31] (2019)	Emerging-SCI	0.14 (2018)	-
Turkish Journal of Medical Sciences	Kara et al.[32] (2019)	SCI-expanded	0.698 (5-years)	Q4
Journal of Oncology Pharmacy Practice	Paksoy et al.[33] (2018)	SCI-expanded	1.826 (2018)	Q3
UHOD-Uluslararasi Hematoloji-Onkoloji Dergisi	Tecen-Yucel et al.[34] (2018)	SCI-expanded	1.667 (5-years)	Q4
Marmara Pharmaceutical Journal	Izzettin et al.[35] (2017)	Emerging-SCI	0.14 (2018)	-
European Journal of Hospital Pharmacy-Science and Practice	Tezcan et al.[36] (2016)	SCI-expanded	0.661 (5-years)	Q4
Respiratory Medicine	Apikoglu-Rabus et al.[37] S. (2016)	SCI-expanded	3.702 (5-years)	Q2
Pharmazie	Selcuk et al.[38] (2015)	SCI-expanded	1.004 (5-years)	Q4
European Journal of Hospital Pharmacy-Science and Practice	Sancar et al.[39] (2015)	SCI-expanded	0.661 (5-years)	Q4
Pharmacy World & Science	Turnacilar et al.[40] (2009)	SCI-expanded	1.429 (5-years)	Q3
American Journal of Health-System Pharmacy	Clark et al.[41] (2007)	SCI-expanded	2.427 (5-years)	Q3

SCI: Science citation index

Table 2. The characteristics of the studies, patients, and interventions

First author and design	Title	Population and monitoring time	Age of population	Clinical pharmacist interventions	Major outcomes
Umar et al.[27] (2020) Prospective study	Significance of a clinical pharmacist-led comprehensive medication management program for hospitalized oncology patients	137 oncology patients 5 months	58±14.60	Identification and classification of DRPs were performed by using the PCNE classification V6.2.	A total of 481 DRPs were identified in 114 patients. The majority (69%, n=332) of interventions were made at the prescriber level, while 29.3% (n=141) interventions were made at the drug level, most of which included beginning a new medication (11.4%, n=55) or stopping a medication (9.6%, n=46). The majority (n=437; 90.9%) of the problems were solved
Kucuk et al.[28] (2019) Descriptive, prospective study	Drug-related problems with targeted/ immunotherapies at an oncology outpatient clinic	54 oncology patients in the outpatient setting 3 months	57±11.98	DRPs were identified by a clinical pharmacist in patients receiving targeted chemotherapy and/or immunotherapy. PCNE classification v.7 was used.	During the study period, a total of 105 DRPs (1.94 per patient, 0.38 per consultation) were identified. A total of 149 planned interventions were recorded by the clinical pharmacist of which 8 (5%) were at the prescriber level, 23 (15%) were at drug level, 92 (62%) were at patient level, and 14 (9%) were other interventions or activities. As a result, 68 (65%) out of 105 DRPs were resolved
Ertuna et al.[29] (2019) Retrospective study	Evaluation of pharmacist interventions and commonly used medications in the geriatric ward of a teaching hospital in Turkey: A retrospective study	91 geriatric patients Weekly order review for about 8 months	80±0.46	Problems were classified according to the PCNE classification system v8.02. PIM use was determined by using Beers and STOPP/ START criteria	A total of 329 possible DRPs were detected in 156 orders, of which 282 (85.71%) interventions were proposed to the prescribers. On 47 (14.28%) occasions, the prescriber was only informed, or the intervention was discussed with the prescriber. The acceptance rate of pharmacist interventions was 85.41% (n=281) and 38 (11.55%) of the proposed interventions were rejected by the physician
Yalcin et al.[30] (2019) Prospective study	Compliance in schizophrenic spectrum disorders: Role of clinical pharmacist	40 patients with schizophrenic spectrum disorder 10 months, during hospitalization and 4-6 weeks following discharge	33±10.99	PANSS, ROMI, UKU, SAS, BARS were used	Twenty-three (57.5%) patients showed poor compliance at the first interview, while only 7 (17.5%) patients recorded with poor compliance at the second interview after drug education (average total MARS scores of the first and second interviews were, respectively, 6.6 (2.23) and 8.6 (1.29); ($p<0.001$). According to ROMI, the number of patients who wanted to use medicaion was detected 35 (87.5%) during the first intervention and 39 (97.5%) during the second intervention

Table 2. Continued

First author and design	Title	Population and monitoring time	Age of population	Clinical pharmacist interventions	Major outcomes
Izzettin et al.[31] (2019) Prospective, cross-sectional randomized study	The role of the clinical pharmacist in patient education and monitoring of patients under warfarin treatment	25 patients diagnosed with venous thromboembolism or prosthetic valve replacement in a cardiology clinic 3 months	53±2.18	Pre- and post-test to evaluate the level of knowledge of the patients on oral anticoagulant. The quality of life was measured by SF-36 and the DASS tests were applied	After three months of the study, the SF-36 Physical Component Score and SF-36 mental component score were increased and results were statistically significant. The number of correct answers of the patients in the pre-test was increased and results were statistically significant after three months of the study ($p < 0.001$). Total DASS scores, DASS "limitation" scores, DASS "burden" scores, and DASS "positive effect" scores were improved ($p<0.05$).
Kara et al.[32] (2019) Prospective, cross-sectional study	Polypharmacy and drug-related problems among people living with HIV/AIDS: A single-center experience	186 PLWHA in an infectious disease outpatient clinic 11 months	40±13.1	Followed by a pharmacist interview with PLWHA, the official recommendation was offered to the attending physician and the participants, which encompassed treatment, drug interactions, and side effects. PCNE classification v7.0 was used	Fifty-eight DRPs were found in 45 patients. Twenty-nine (50%) of the interventions were made to the physicians alone, 25 (43%) to the patients alone, and 4 were made to both the physicians and the patients. Twenty-nine (50%) interventions involved comorbidities or co-medications and 19 (32.8%) of these involved anti-retroviral drugs. In this study, 93.2% of the interventions were accepted by the physicians
Paksoy et al.[33] (2018) Prospective study	Evaluation of potentially inappropriate medication utilization in elderly patients with cancer at outpatient oncology unit	114 elderly patients oncology outpatient clinic 4 months	71.78±5.50	Medication review to determine PIMs and POMs made by using STOPP/START criteria	In 94.73% of the patients, polypharmacy was detected. STOPP criteria were applied to a total of 114 patients and 20 PIM uses in 18 patients were found and interventions were accepted by the clinicians. According to the START criteria, a total of 221 medication omissions in 112 patients were found and interventions were accepted by the clinicians. The number of non-cancer medications and the total number of medications was statistically high according to the presence of STOPP criteria ($p<0.001$)
Tecen-Yucel et al.[34] (2018) Descriptive, cross-sectional, prospective study	Clinical pharmacy practices in oncology patients treated with tyrosine kinase inhibitors	55 medical oncology outpatient clinic patients 3 months	60 (range 28-79)	TKI-related adverse effects were monitored and evaluated by using the NCI-CTCAE version 4.	A total of 92 interactions were detected, and 54 (58.7%) were evaluated as clinically significant and required intervention. A total of 32 recommendations for the management of adverse effects were provided by a clinical pharmacist and 29 (90.6%) were accepted by the consultant physicians. Clinically significant improvements in patients were observed in criteria related to dry skin, diarrhea, fatigue, infection, hematuria, acute kidney injury, vomiting, salivary duct inflammation, and alanine aminotransferase levels between the first and second visits

Table 2. Continued

First author and design	Title	Population and monitoring time	Age of population	Clinical pharmacist interventions	Major outcomes
Izzettin et al.[35] (2017) Prospective study	Influence of pharmacist recommendations for chemotherapy-related problems in diabetic cancer patients	50 diabetic patients with a new diagnosis of diverse types of cancers 8 months	61±8.99	The assessment of DRPs was based on PCNE classification V6.2.	In this study, 69.57% (n=80) of the DRPs were solved due to recommendations by the clinical pharmacist. After clinical pharmacist recommendations and provision of patient education, a significant decrease in the occurrence (first vs. second readings) and severity (mild vs. moderate) of adverse drug effects was observed as a mild urinary frequency (p=0.0001) and mild vomiting (p=0.0001)
Tezcan et al.[36] (2016) Prospective study	Role of clinical oncology pharmacist in the determination of pharmaceutical care needs in patients with colorectal cancer	36 colon cancer patients in the outpatient chemotherapy un 5 months, during three chemotherapy courses	58±12.86	The symptom-based quality of life questionnaires were administered before the first and after the third course of chemotherapy. Potential DRPs were recorded	DRPs decreased within the third course of chemotherapy compared with the first course after interventions. A total of 147 recommendations were given and of those, 52.4% (n=77) were non-pharmacological and 47.6% (n=70) were pharmacological. One hundred and forty-four (98%) recommendations were followed by patients. Of the recommendations followed, 91.7% (=132) were succeeded to solve the DRP, while 8.3% (n= 12) were failed to solve the problem.
Apikoglu-Rabus et al.[37] (2016) Prospective study	Drug-related problems and pharmacist interventions in a cohort of patients with asthma and chronic obstructive pulmonary disease	44 patients with asthma and 37 patients with chronic obstructive pulmonary disease 6 months	Asthma patients: 52.4±1.9 COPD patients: 65.9±10.5	DRPs were identified at the initial visit using the Turkish version of the PCNE Classification scheme for drug-related problems v6.2. In addition, MMAS was used	Only five patients with asthma (11.4%) and four patients with COPD (10.8%) were highly adherent with their medication regimen. Fifty-nine DRPs were identified for 44 patients with asthma, of which 93% were manifested and 7% were potential. A majority of these problems (98%) were identified by the pharmacist. A total of 134 causes were identified for 59 problems. Sixty were identified for 37 patients with COPD, with 88% of the problems manifested, while 12% were potential. A majority (95%) of these problems were identified by the pharmacist. A total of 128 causes were identified for 60 problems. A total of 84 interventions were provided for the patients with asthma, and 95 interventions were provided for the patients with COPD. Most of the interventions were made at the patient level (81% on asthma patients and 80% on COPD patients). Almost half of the problems were solved (54.2% on asthma patients and 63.3% on COPD patients)

Table 2. Continued

First author and design	Title	Population and monitoring time	Age of population	Clinical pharmacist interventions	Major outcomes
Selcuk et al.[38] (2015) Retrospective study	The potential role of clinical pharmacists in elderly patients during hospital admission	133 hospitalized elderly patients 4 months, weekly participation in the ward	77±8.12	Medication discrepancies were determined and divided between intended and unintended discrepancies. All DRPs were determined regarding home and hospital medications according to PCNE classification, v.6.2	The utilization of high alert medications was seen in 77.4% of the patients. The PIM was found in 19.5% of elderly patients. A total of 394 medication discrepancies were detected and classified as either intended or unintended discrepancies. The clinical pharmacist was presented a total of 396 recommendations to the physician on the ward and the physicians were accepted 85.6% of them
Sancar et al.[39] (2015) Prospective, pre- and post-intervention study	The effect of pharmacist-led education on inhaler use skills in hospitalized patients with chronic obstructive pulmonary disease	41 hospitalized patients with COPD 9 months, clinic visit was arranged for a month later from hospital discharge (2 days/week)	64±11.78	The clinical pharmacists used verbal instruction and printed and demonstration materials to educate patients on the correct methods for using each inhaler device according to the GOLD guideline	Patients' inhaler administration skills were found to be improved by pharmacist-led education ($p<0.05$). Statistically significant improvement in patient inhaler use skills were obtained for every scored item except removing the cap before starting to use inhalers following pharmacist-led education. The improvement in appropriate inhaler device usage techniques following pharmacist-led education was also determined when evaluating patients' attitudes toward the different types of inhalers. An increase in the rate of mouth rinsing after corticosteroid inhalation was observed in the following pharmacist-led training (38.2% vs 91.2%)
Turnacilar et al.[40] (2009) Prospective, longitudinal study	Improvement of diabetes indices of care by short pharmaceutical care (PC) program	43 patients with type 2 diabetics visiting community pharmacies 7 months retrospective	62±1.50	Retrospective data of past 3 months were collected using a standard self-administered questionnaire	Nine (20.9%) patients used to perform SMBG before PC; this number increased to 13 (30.2%) patients after PC ($p<0.05$). After PC, this number increased to 95.3% ($p < 0.001$). During the PC period, two out of twelve smoking patients quit smoking and reported being smoke-free until the end of the PC period. The barriers to adherence were identified and managed in the two patients
Clark et al.[41] (2007) Prospective, randomized, case-control study	Effect of pharmacist-led patient education on adherence to tuberculosis (TB) treatment	154 hospitalized, newly diagnosed tuberculosis TB patients 8 months, two months during inpatient clinics, and six months after discharge	Newly diagnosed TB patients: 38±14.0 Multi-drug resistant (MDR) TB patients: 43±2.50	In the first interview, patients' health beliefs and knowledge on their current drugs and doses were assessed through an interviewer-assisted questionnaire. The clinical pharmacist provided standard oral and written patient education to the patients in the education group shortly before the discharge	The effect of pharmacist-directed patient education in terms of improving visit was statistically significant ($p<0.05$). The number of patients who attended all the scheduled visits were higher in the education group than in the non-education group (53.6% vs. 29.3%, respectively). The beneficial effect of patient education on the positive isoniazid test result percentage was statistically significant ($p=0.001$). The drug-related issues were again similar for newly diagnosed TB and MDR-TB patients

PIM: Potentially inadequate medication, STOPP: Screening tool of older people's prescriptions, START: Screening tool to alert to right treatment, PANSS: Positive and negative syndrome scale, MARS: Medication adherence rating scale, ROMI: The rating of medication influences, UKU: Udvalg for Kliniske Undersogelser, SAS: Simpson-Angus, abnormal involuntary movement scale, BARS: Barnes Akathisia rating scale, SF-36: Short form 36, DASS: Depression anxiety stress scales, HIV: Human immunodeficiency virus, AIDS: Acquired immunodeficiency syndrome, PLWHA: People living with HIV/AIDS, POM: Potential prescribing omission, TKI: Tyrosine kinase inhibitors, NCI: National Cancer Institute, CTCAE: Common Terminology Criteria for Adverse Events, COPD: Chronic obstructive pulmonary disease, MMAS: Morisky medication adherence scale, GOLD: The Global Initiative for Chronic Obstructive Lung Disease

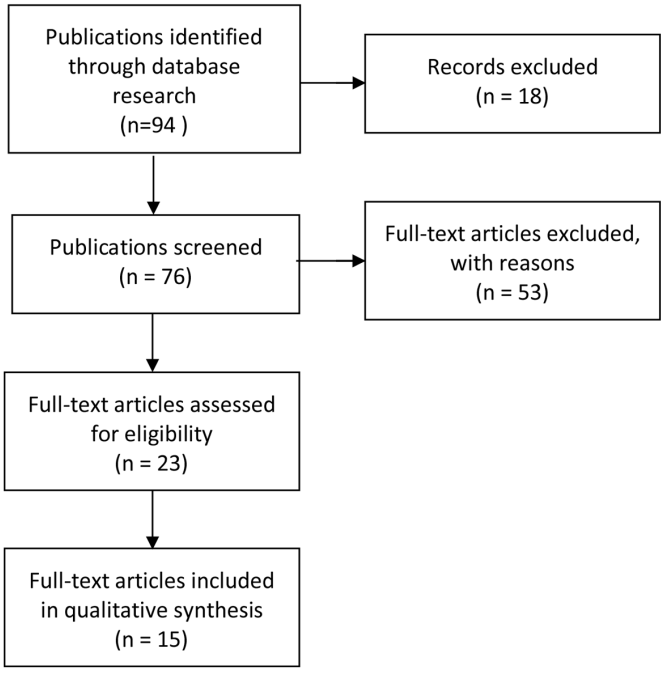

Figure 1. Article selection process

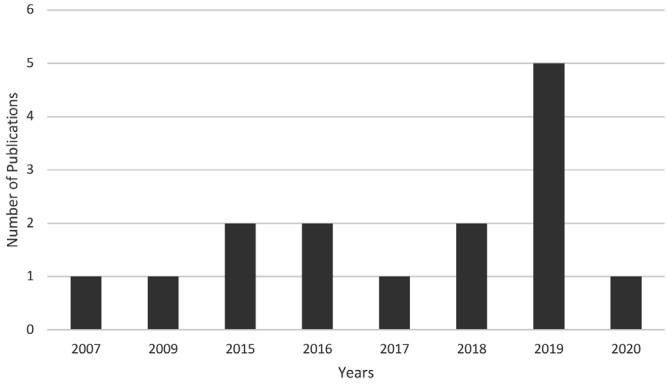

Graphic 1. Distribution of publishing years of the articles

DISCUSSION

According to our perspective, ours is the first study that reviewed the studies in the field of clinical pharmacy in Turkey. Clinical pharmacy services in Turkey still have not entered routine practices. It is thought that it will become a routine practice by 2023.[24] Most of the studies included in this review were carried out within the scope of a postgraduate thesis. Therefore, most of these studies focused on clinical pharmacy services that were offered for the first time to the clinicians or patients. Because clinical pharmacists are still not a routine member of the interdisciplinary team, these studies were unable to address all the identified pharmaceutical care needs, and for the same reason, the duration of studies was limited to few months.

The findings of decreased adverse drug effects, improved appropriate prescribing, shortened length of hospital stay (LoS), and reduced costs were reported in many other studies from outside of Turkey.[13,18,42] The outcomes of the interventions were beneficial in terms of visualizing clinical pharmacy activities and better results in patients. Positive outcomes were observed, such as reduction or prevention of side effects, improvement in QoL, and reduction in LoS in the hospital with the high acceptance rates of interventions by the physicians, which indicate that despite the obstacles that faced in clinical pharmacy services, other healthcare professionals are ready to collaborate with the clinical pharmacists in Turkey.

In China, it was determined that appropriate prescribing and patient knowledge about medications was enhanced with the implementation of clinical pharmacy practices both in inpatient and outpatient settings.[43] Rotta et al.[44] overviewed 49 systematic reviews between 2000-2010 and found that clinical pharmacy practices were focused on certain chronic diseases like blood pressure and glucose control. Due to the variability of methods, interventions about medication adherence and prescription appropriateness caused inconclusive results.

Pehlivanli et al.[45] reviewed 46 articles published between 2006 and 2016 on the role of the clinical pharmacist. They found that the studies were mostly related to cardiovascular diseases (13%), adverse drug events (11%), and infectious diseases (9%). The evaluated studies were generally prospective, observational, or interventional studies.[45] In Turkey, there were also studies conducted within the scope of clinical pharmacy but without pharmacist intervention. Adverse effects and compliance with antidepressants in patients with major depression were evaluated by Sancar et al.[46] Most commonly in 56 patients, side effects such as dizziness, dry mouth, increased sleep were observed, and 73.2% of the patients were found to have low compliance with the treatment. In addition to the routine service they receive from the outpatient clinic, it is concluded that educating and monitoring the side effects and compliance by the pharmacists will contribute to preventing possible DRPs.[46] In another study, the appropriateness of drug treatment was evaluated, and requirements of pharmaceutical care were identified in geriatric patients. A low level of knowledge about drug usage was detected in patients, and they were not informed about the proper drug use.[47] Okuyan et al.[48] aimed to evaluate the knowledge and attitudes of type 2 diabetic patients regarding the use of a disposable insulin pen. As a result of this study, missing or improper usage of the disposable insulin pen was observed in hospitalized patients.[48] The patient risk score was used by Aras et al.[49] to evaluate the risk of febrile neutropenia (FN) and to assess granulocyte colony-stimulating factors use, and its side effects in an outpatient clinic. They found that inadequate or unnecessary treatments should be evaluated for the risk of FN in each chemotherapy cycle and that a routine risk assessment can also be implemented.[49] Abunahlah et al.[50] conducted a study in internal medicine wards to identify DRPs in a teaching and research hospital in Istanbul, Turkey. In this study, 163 DRPs were determined by using the PCNE classification V 7.0 in 100 patients that used a total of 808 drugs. According to their results, age, LoS in hospital, number of drugs, renal impairment, and inflammation correlated with the causes of DRPs, and age, number of drugs, LoS in hospital, renal dysfunction, liver failure, diagnosis, and comorbidities correlated with the number of DRPs.[50]

Another concern is appropriate measures for the effectiveness of pharmacists' services. Hospitalization, mortality, or outpatient visits should be used for the evaluation of effectiveness endpoints; however, an extended duration of follow-up periods is needed to demonstrate a potential input for these endpoints. Thus, intermediate or surrogate indicators may be used to evaluate the short-term effects of interventions. Short-term evaluation methods of the included studies were also explained in this review.

The American College of Clinical Pharmacy (ACCP) defined that clinical pharmacists are a primary source of scientifically valid information and advice regarding the safe, appropriate, cost effective use of medications, and optimizing medication therapy with the background of pharmaceutical care. They routinely provide updated knowledge that contributes to improved health and QoL to patients and healthcare professionals.[51] According to the definition by ACCP, clinical pharmacists in Turkey are also contributing to many research projects in the field of clinical pharmacy and in various other health-related fields. They provide immense knowledge to other healthcare professionals. Since these publications were outside the scope of this study, they were not discussed.

The main limitations of the studies reviewed in this were study setting (one hospital) and the study size (small groups).[28,29,32,34] Other limitations were retrospective evaluations of pharmacist interventions[29,38] and the absence of a control group for comparisons.[28] Additional controlled and prospective studies are also in progress for publication due to ongoing thesis or projects in Turkey. A significant expansion in the number of publications is expected due to the increase in the number of both graduates and special program graduates who were trained in the field of clinical pharmacy in the recent years.

The limitations of this review were that even though a literature search was conducted on different databases, there might have been omitted or overlooked studies. PRISMA checklist items could not be fully followed because the studies included in this review were not homogeneous, and the available studies were few. Future studies are needed to assess the impact of clinical pharmacist interventions on health expenditure in Turkey by using cost-effectiveness or cost-benefit analysis methods.

CONCLUSION

In conclusion, there is a growing practice of clinical pharmacy in Turkey; however, a clear definition of clinical pharmacy services, implementation to the routine healthcare team, and standardized methods that assess the impact of these services on patient health-related outcomes are still needed. It is shown that even with the institutional effort, clinical pharmacy services may make a strong contribution to the Turkish healthcare system, but for providing a trustworthy and sustainable service, governmental and educational support should be developed.

Conflict of interest: No conflict of interest was declared by the authors. The authors are solely responsible for the content and writing of this paper.

REFERENCES

1. van den Bemt PM, Egberts TC, de Jong-van den Berg LT, Brouwers JR. Drug-related problems in hospitalised patients. Drug Saf. 2000;22:321-333.
2. Schlienger RG, Fedson DS, Jick SS, Jick H, Meier CR. Statins and the risk of pneumonia: a population-based, nested case-control study. Pharmacotherapy. 2007;27:325-332.
3. Viktil KK, Blix HS. The impact of clinical pharmacists on drug-related problems and clinical outcomes. Basic Clin Pharmacol Toxicol. 2008;102:275-280.
4. Ellis SL, Billups SJ, Malone DC, Carter BL, Covey D, Mason B, Jue S, Carmichael J, Guthrie K, Sintek CD, Dombrowski R, Geraets DR, Amato M. Types of interventions made by clinical pharmacists in the IMPROVE study. Impact of managed pharmaceutical care on resource utilization and outcomes in veterans affairs medical centers. Pharmacotherapy. 2000;20:429-435.
5. Schumock GT, Michaud J, Guenette AJ. Re-engineering: an opportunity to advance clinical practice in a community hospital. Am J Health Syst Pharm. 1999;56:1945-1949.
6. Gourley DR, Gourley GA, Solomon DK, Portner TS, Bass GE, Holt JM, Braden RL, Rawls N, Wicke WR, Ogden J, Lawrence B. Development, implementation, and evaluation of a multicenter pharmaceutical care outcomes study. J Am Pharm Assoc (Wash). 1998;38:567-573.
7. Garcao JA, Cabrita J. Evaluation of a pharmaceutical care program for hypertensive patients in rural Portugal. J Am Pharm Assoc (Wash). 2002;42:858-864.
8. Gonzalez-Martin G, Joo I, Sanchez I. Evaluation of the impact of a pharmaceutical care program in children with asthma. Patient Educ Couns. 2003;49:13-18.
9. Paulos CP, Nygren CE, Celedon C, Carcamo CA. Impact of a pharmaceutical care program in a community pharmacy on patients with dyslipidemia. Ann Pharmacother. 2005;39:939-943.
10. Anaya JP, Rivera JO, Lawson K, Garcia J, Luna J, Jr., Ortiz M. Evaluation of pharmacist-managed diabetes mellitus under a collaborative drug therapy agreement. Am J Health Syst Pharm. 2008;65:1841-1845.
11. Strand LM, Guerrero RM, Nickman NA, Morley PC. Integrated patient-specific model of pharmacy practice. Am J Hosp Pharm. 1990;47:550-554.
12. Biles JA. The doctor of pharmacy. JAMA. 1983;249:1157-1160.
13. Schumock GT, Butler MG, Meek PD, Vermeulen LC, Arondekar BV, Bauman JL; 2002 Task Force on Economic Evaluation of Clinical Pharmacy Services of the American College of Clinical Pharmacy. Evidence of the economic benefit of clinical pharmacy services: 1996-2000. Pharmacotherapy. 2003;23:113-132.
14. Bond CA, Raehl CL, Franke T. Clinical pharmacy services, pharmacy staffing, and the total cost of care in United States hospitals. Pharmacotherapy. 2000;20:609-621.
15. Bond CA, Raehl CL. Clinical pharmacy services, pharmacy staffing, and hospital mortality rates. Pharmacotherapy. 2007;27:481-493.
16. Kaboli PJ, Hoth AB, McClimon BJ, Schnipper JL. Clinical pharmacists and inpatient medical care: a systematic review. Arch Intern Med. 2006;166:955-964.
17. Pickard AS, Hung SY. An update on evidence of clinical pharmacy services' impact on health-related quality of life. Ann Pharmacother. 2006;40:1623-1634.

18. De Rijdt T, Willems L, Simoens S. Economic effects of clinical pharmacy interventions: a literature review. Am J Health Syst Pharm. 2008;65:1161-1172.
19. Pedersen CA, Schneider PJ, Santell JP. ASHP national survey of pharmacy practice in hospital settings: prescribing and transcribing--2001. Am J Health Syst Pharm. 2001;58:2251-2266.
20. Pande S, Hiller JE, Nkansah N, Bero L. The effect of pharmacist-provided non-dispensing services on patient outcomes, health service utilisation and costs in low- and middle-income countries. Cochrane Database Syst Rev. 2013:CD010398.
21. Sancar M, Okuyan B, Apikoglu-Rabus S, Izzettin F. Opinion and knowledge towards pharmaceutical care of the pharmacists participated in clinical pharmacy and pharmaceutical care continuing education program. Turkish J Pharmaceutical Sci. 2013;10:245-254.
22. Ustel I. Klinik Eczacılık Eğitimi. FABAD J Pharm Sci. 1986;11:270-277.
23. Aypar E, Sancar M, Izzettin FV. New period in pharmacy: place in health system and clinical pharmacy. SD Sağlık Düşüncesi ve Tıp Kültürü Dergisi. 2014;30:48-51.
24. Resmi Gazete (14.11.2014/29175), 6566 sayılı Eczacılar ve Eczaneler Hakkında Kanun ile Bazı Kanun ve Kanun Hükmünde Kararnamelerde Değişiklik Yapılmasına Dair Kanun; 2014. p.3-7.
25. Dawoud DM, Smyth M, Ashe J, Strong T, Wonderling D, Hill J, Varia M, Dyer P, Bion J. Effectiveness and cost effectiveness of pharmacist input at the ward level: a systematic review and meta-analysis. Res Social Adm Pharm. 2019;15:1212-1222.
26. Rodrigues CR, Harrington AR, Murdock N, Holmes JT, Borzadek EZ, Calabro K, Martin J, Slack MK. Effect of pharmacy-supported transition-of-care interventions on 30-day readmissions: a systematic review and meta-analysis. Ann Pharmacother. 2017;51:866-889.
27. Umar RM, Apikoglu-Rabus S, Yumuk PF. Significance of a clinical pharmacist-led comprehensive medication management program for hospitalized oncology patients. Int J Clin Pharm. 2020;42:652-661.
28. Kucuk E, Bayraktar-Ekincioglu A, Erman M, Kilickap S. Drug-related problems with targeted/immunotherapies at an oncology outpatient clinic. J Oncol Pharm Pract. 2020;26:595-602.
29. Ertuna E, Arun MZ, Ay S, Kocak FOK, Gokdemir B, Ispirli G. Evaluation of pharmacist interventions and commonly used medications in the geriatric ward of a teaching hospital in Turkey: a retrospective study. Clin Interv Aging. 2019;14:587-600.
30. Yalcin N, Ak S, Gurel SC, Celiker A. Compliance in schizophrenia spectrum disorders: the role of clinical pharmacist. Int Clin Psychopharmacol. 2019;34:298-304.
31. Izzettin FV, Celik S, Acar RD, Tezcan S, Aksoy N, Bektay MY, Sancar M. The role of the clinical pharmacist in patient education and monitoring of patients under warfarin treatment. J Res Pharm. 2019;23:1057-163.
32. Kara E, İnkaya AÇ, Aydın Haklı D, Demirkan K, Ünal S. Polypharmacy and drug-related problems among people living with HIV/AIDS: a single-center experience. Turk J Med Sci. 2019;49:222-229.
33. Paksoy C, Özkan Ö, Ustaalioğlu BB, Sancar M, Demirtunç R, Izzettin FV, Okuyan B. Evaluation of potentially inappropriate medication utilization in elderly patients with cancer at outpatient oncology unit. J Oncol Pharm Pract. 2019;25:1321-1327.
34. Tecen-Yucel K, Bayraktar-Ekincioglu A, Kilickap S, Erman M. Clinical pharmacy practices in oncology patients treated with tyrosine kinase inhibitors. Int J Hematol Oncol. 2018;28:53-60.
35. Izzettin FV, Al-taie A, Sancar M, Aliustaoğlu M. Influence of pharmacist recommendations for chemotherapy-related problems in diabetic cancer patients. MARMARA Pharm J. 2017;21:603-611.
36. Tezcan S, İzzettin FV, Sancar M, Turhal NS, Yumuk PF. Role of clinical oncology pharmacist in determination of pharmaceutical care needs in patients with colorectal cancer. Eur J Hosp Pharm. 2018;25:e17-e20.
37. Apikoglu-Rabus S, Yesilyaprak G, Izzettin FV. Drug-related problems and pharmacist interventions in a cohort of patients with asthma and chronic obstructive pulmonary disease. Respir Med. 2016;120:109-115.
38. Selcuk A, Sancar M, Okuyan B, Demirtunc R, Izzettin FV. The potential role of clinical pharmacists in elderly patients during hospital admission. Pharmazie. 2015;70:559-562.
39. Sancar M, Sirinoglu Y, Okuyan B, Karagoz T, Izzettin FV. The effect of pharmacist-led education on inhaler use skills in hospitalised patients with chronic obstructive pulmonary disease. Eur J Hosp Pharm. 2015;22:366-368.
40. Turnacilar M, Sancar M, Apikoglu-Rabus S, Hursitoglu M, Izzettin FV. Improvement of diabetes indices of care by a short pharmaceutical care program. Pharm World Sci. 2009;31:689-689.
41. Clark PM, Karagoz T, Apikoglu-Rabus S, Izzettin FV. Effect of pharmacist-led patient education on adherence to tuberculosis treatment. Am J Health Syst Pharm. 2007;64:497-505.
42. Schumock GT, Meek PD, Ploetz PA, Vermeulen LC. Economic evaluations of clinical pharmacy services--1988-1995. The Publications Committee of the American College of Clinical Pharmacy. Pharmacotherapy. 1996;16:1188-1208.
43. Penm J, Li Y, Zhai S, Hu Y, Chaar B, Moles R. The impact of clinical pharmacy services in China on the quality use of medicines: a systematic review in context of China's current healthcare reform. Health Policy Plan. 2014;29:849-872.
44. Rotta I, Salgado TM, Silva ML, Correr CJ, Fernandez-Llimos F. Effectiveness of clinical pharmacy services: an overview of systematic reviews (2000-2010). Int J Clin Pharm. 2015;37:687-697.
45. Pehlivanli A, Akyol B, Ozcelikay G. Evaluation of studies between 2006-2016 years contributions related to treatment of clinical pharmacists. Turkiye Klinikleri J Health Sci. 2018;3:95-112.
46. Sancar M, Duzgun E, Okuyan B, Deniz S, Calıskan M, Coskun K, İzzettin FV. Determination of side effects and medication adherence in major depression patients utilized antidepressants. MARMARA Pharm J. 2017;21:183-189.
47. Sancar M, Mutlu BY, Okuyan B, Izzettin FV. Determination of geriatric patients' drug profile and identify their pharmaceutical care requirements by determining potential risk factors. Eur Geriatr Med. 2011;2:280-283.
48. Okuyan B, Saglam B, Emre E, Demirtunc R, Izzettin F, Sancar M. Attitude and knowledge of hospitalized patients with type 2 diabetes mellitus towards disposable insulin pens utilization. MARMARA Pharm J. 2014;18:159-163.
49. Aras E, Bayraktar-Ekincioglu A, Kilickap S. Risk assessment of febrile neutropenia and evaluation of G-CSF use in patients with cancer: a real-life study. Support Care Cancer. 2020;28:691-699.
50. Abunahlah N, Elawaisi A, Velibeyoglu FM, Sancar M. Drug related problems identified by clinical pharmacist at the Internal Medicine Ward in Turkey. Int J Clin Pharm. 2018;40:360-367.
51. American College of Clinical Pharmacy. The definition of clinical pharmacy. Pharmacotherapy. 2008;28:816-817.

NOTES

NOTES

PUBLICATION NAME	Turkish Journal of Pharmaceutical Sciences
TYPE OF PUBLICATION	Vernacular Publication
PERIOD AND LANGUAGE	Bimonthly-English
OWNER	Erdoğan ÇOLAK on behalf of the Turkish Pharmacists' Association
EDITOR-IN-CHIEF	Prof. Terken BAYDAR, Ph.D.
ADDRESS OF PUBLICATION	Turkish Pharmacists' Association, Mustafa Kemal Mah 2147.Sok No:3 06510 Çankaya/Ankara, TURKEY

TURKISH
JOURNAL OF PHARMACEUTICAL
SCIENCES

Volume: 18, No: 4, Year: 2021

CONTENTS